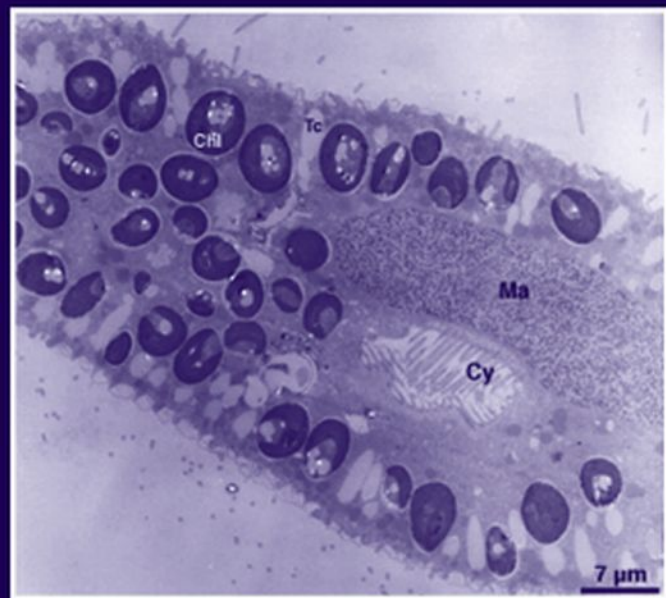


INTERNATIONAL  
REVIEW OF CELL AND  
MOLECULAR BIOLOGY

Edited by  
Kwang W. Jeon



Volume 279





VOLUME TWO SEVENTY NINE

INTERNATIONAL REVIEW OF  
**CELL AND MOLECULAR  
BIOLOGY**

# INTERNATIONAL REVIEW OF CELL AND MOLECULAR BIOLOGY

## *Series Editors*

GEOFFREY H. BOURNE 1949–1988

JAMES F. DANIELLI 1949–1984

KWANG W. JEON 1967–

MARTIN FRIEDLANDER 1984–1992

JONATHAN JARVIK 1993–1995

## *Editorial Advisory Board*

ISAIAH ARKIN

PETER L. BEECH

ROBERT A. BLOODGOOD

DEAN BOK

KEITH BURRIDGE

HIROO FUKUDA

RAY H. GAVIN

MAY GRIFFITH

WILLIAM R. JEFFERY

KEITH LATHAM

WALLACE F. MARSHALL

BRUCE D. MCKEE

MICHAEL MELKONIAN

KEITH E. MOSTOV

ANDREAS OKSCHE

MANFRED SCHLIWA

TERUO SHIMMEN

ROBERT A. SMITH

VOLUME TWO SEVENTY NINE

# INTERNATIONAL REVIEW OF CELL AND MOLECULAR BIOLOGY

*EDITED BY*

**KWANG W. JEON**

*Department of Biochemistry  
University of Tennessee  
Knoxville, Tennessee*



**ELSEVIER**

AMSTERDAM • BOSTON • HEIDELBERG • LONDON  
NEW YORK • OXFORD • PARIS • SAN DIEGO  
SAN FRANCISCO • SINGAPORE • SYDNEY • TOKYO

Academic Press is an imprint of Elsevier



Front Cover Photography: Cover figure by Yuuki Kodama and Masahiro Fujishima

Academic Press is an imprint of Elsevier  
525 B Street, Suite 1900, San Diego, CA 92101-4495, USA  
30 Corporate Drive, Suite 400, Burlington, MA 01803, USA  
32 Jamestown Road, London NW1 7BY, UK  
Radarweg 29, PO Box 211, 1000 AE Amsterdam, The Netherlands

First edition 2010

Copyright © 2010, Elsevier Inc. All Rights Reserved.

No part of this publication may be reproduced, stored in a retrieval system or transmitted in any form or by any means electronic, mechanical, photocopying, recording or otherwise without the prior written permission of the publisher

Permissions may be sought directly from Elsevier's Science & Technology Rights Department in Oxford, UK: phone (+44) (0) 1865 843830; fax (+44) (0) 1865 853333; email: [permissions@elsevier.com](mailto:permissions@elsevier.com). Alternatively you can submit your request online by visiting the Elsevier web site at <http://elsevier.com/locate/permissions>, and selecting *Obtaining permission to use Elsevier material*.

#### Notice

No responsibility is assumed by the publisher for any injury and/or damage to persons or property as a matter of products liability, negligence or otherwise, or from any use or operation of any methods, products, instructions or ideas contained in the material herein. Because of rapid advances in the medical sciences, in particular, independent verification of diagnoses and drug dosages should be made.

#### **British Library Cataloguing in Publication Data**

A catalogue record for this book is available from the British Library

#### **Library of Congress Cataloging-in-Publication Data**

A catalog record for this book is available from the Library of Congress

For information on all Academic Press publications  
visit our website at [elsevierdirect.com](http://elsevierdirect.com)

ISBN: 978-0-12-381011-3

PRINTED AND BOUND IN USA

10 11 12 10 9 8 7 6 5 4 3 2 1

Working together to grow  
libraries in developing countries

[www.elsevier.com](http://www.elsevier.com) | [www.bookaid.org](http://www.bookaid.org) | [www.sabre.org](http://www.sabre.org)

ELSEVIER

BOOK AID  
International

Sabre Foundation

# CONTENTS

*Contributors*

*vii*

<b>1. Functions of Claudin Tight Junction Proteins and Their Complex Interactions in Various Physiological Systems</b>	<b>1</b>
Liron Elkouby-Naor and Tamar Ben-Yosef	
1. Introduction	2
2. Tight Junction Membrane Integral Proteins	4
3. The Claudin Family of Tight Junction Proteins	4
4. Claudin Interactions Within and Between TJ Strands	16
5. Is the Expression Level of Different Claudins Coregulated?	20
6. Claudin-Related Phenotypes	21
7. Concluding Remarks	26
Acknowledgment	27
References	27
<b>2. Secondary Symbiosis Between <i>Paramecium</i> and <i>Chlorella</i> Cells</b>	<b>33</b>
Yuuki Kodama and Masahiro Fujishima	
1. Introduction	34
2. Infection Route	36
3. Different Fates of Infection-Capable and Infection-Incapable <i>Chlorella</i> Species	52
4. Function of PV Membrane	61
5. Host or Algal Changes Induced by Infection	68
6. Concluding Remarks	70
Acknowledgments	72
References	72
<b>3. Molecular Basis of Peroxisome Division and Proliferation in Plants</b>	<b>79</b>
Jianping Hu	
1. Introduction	80
2. Roles of PEROXIN11 Proteins, Dynamin-Related Proteins, and FISSION1	81
3. Other Proteins and Pathways	89

4. Environmental and Nuclear Regulation of Peroxisome Proliferation	91
5. Concluding Remarks	93
Acknowledgments	95
References	95
<b>4. New Insights into the Signal Transmission from Taste Cells to Gustatory Nerve Fibers</b>	<b>101</b>
Ryusuke Yoshida and Yuzo Ninomiya	
1. Introduction	102
2. Diversity of Taste Bud Cells	103
3. Coding of Taste Information	108
4. Mechanisms for the Signal Transmission from Taste Cells to Gustatory Nerve Fibers	118
5. Concluding Remarks	125
Acknowledgments	126
References	126
<b>5. New Insights into the Regulation of Ion Channels by Integrins</b>	<b>135</b>
Andrea Becchetti, Serena Pillozzi, Raffaella Morini, Elisa Nesti, and Annarosa Arcangeli	
1. Introduction	136
2. Main Structural Features of Integrins and Ion Channels	137
3. An Outline of Integrin Signaling	143
4. Integrins and Ion Channels in Normal and Neoplastic Hematopoietic Cells	147
5. Integrins and Ion Channels in Cell Migration	163
6. Integrins and Ion Channels in the Nervous System	166
7. Concluding Remarks	176
Acknowledgments	177
References	178
<i>Index</i>	<i>191</i>

# CONTRIBUTORS

## **Annarosa Arcangeli**

Department of Experimental Pathology and Oncology, University of Firenze, Firenze, Italy

## **Andrea Becchetti**

Department of Biotechnology and Biosciences, University of Milano-Bicocca, Milano, Italy

## **Tamar Ben-Yosef**

Department of Genetics, The Rappaport Family Institute for Research in the Medical Sciences, Technion-Israel Institute of Technology, Haifa, Israel

## **Liron Elkouby-Naor**

Department of Genetics, The Rappaport Family Institute for Research in the Medical Sciences, Technion-Israel Institute of Technology, Haifa, Israel

## **Masahiro Fujishima**

Department of Environmental Science and Engineering, Graduate School of Science and Engineering, Yamaguchi University, Yamaguchi, Japan

## **Jianping Hu**

Department of Energy Plant Research Laboratory, Michigan State University, East Lansing, Michigan, USA

## **Yuuki Kodama**

Department of Environmental Science and Engineering, Graduate School of Science and Engineering, Yamaguchi University, Yamaguchi, Japan

## **Raffaella Morini**

Department of Biotechnology and Biosciences, University of Milano-Bicocca, Milano, Italy

## **Elisa Nesti**

Department of Experimental Pathology and Oncology, University of Firenze, Firenze, Italy



**Yuzo Ninomiya**

Section of Oral Neuroscience, Graduate School of Dental Sciences, Kyushu University, Fukuoka, Japan

**Serena Pillozzi**

Department of Experimental Pathology and Oncology, University of Firenze, Firenze, Italy

**Ryusuke Yoshida**

Section of Oral Neuroscience, Graduate School of Dental Sciences, Kyushu University, Fukuoka, Japan

# FUNCTIONS OF CLAUDIN TIGHT JUNCTION PROTEINS AND THEIR COMPLEX INTERACTIONS IN VARIOUS PHYSIOLOGICAL SYSTEMS

Liron Elkouby-Naor *and* Tamar Ben-Yosef

## Contents

1. Introduction	2
2. Tight Junction Membrane Integral Proteins	4
3. The Claudin Family of Tight Junction Proteins	4
3.1. Claudin protein structure	6
3.2. Claudin electrophysiological properties and generation of the TJ physiological barrier	11
3.3. Claudin expression pattern	11
4. Claudin Interactions Within and Between TJ Strands	16
4.1. All in the family	16
4.2. Dating others	19
5. Is the Expression Level of Different Claudins Coregulated?	20
6. Claudin-Related Phenotypes	21
6.1. Claudin 1	21
6.2. Claudin 6	22
6.3. Claudins 3 and 4	22
6.4. Claudin 5	22
6.5. Claudin 7	23
6.6. Claudin 15	23
6.7. Claudin 16	23
6.8. Claudin 19	24
6.9. Claudin 9	24
6.10. Claudin 14	25
6.11. Claudin 11	25
6.12. Claudin11/claudin 14 double deficient mice	26

Department of Genetics, The Rappaport Family Institute for Research in the Medical Sciences, Technion-Israel Institute of Technology, Haifa, Israel

7. Concluding Remarks	26
Acknowledgment	27
References	27

## Abstract

Members of the claudin family of proteins are the main components of tight junctions (TJs), the major selective barrier of the paracellular pathway between epithelial cells. As such, the claudins have the ability to generate the TJ physiological barrier and to control various physiological processes. Therefore, the importance of this family of proteins is obvious and many efforts were made to reveal different aspects of claudin TJ protein biology. In this review, we discuss recent advances in our understanding of claudin structure and function, as well as their distribution pattern in different organs and tissues. We mainly highlight the complex interactions of claudins in various physiological systems and suggest a possible role for a coregulation mechanism.

**Key Words:** Tight junctions, Tight junction proteins, Membrane proteins, Claudin. © 2010 Elsevier Inc.

## 1. INTRODUCTION

A hallmark in the development of multicellular organisms is the assembly of cellular sheets that separate compartments of different compositions. Maintenance of different compartments is performed by epithelial or endothelial cells, which adhere to each other by forming different types of intercellular junctions (Farquhar and Palade, 1963), including desmosomes (Kowalczyk et al., 1999), adherens junctions (AJs) (Nagafuchi, 2001), gap junctions (Goodenough et al., 1996), and tight junctions (TJs) (Anderson, 2001; Tsukita et al., 2001). The movement of solutes, ions, and water through epithelia occurs both across and between individual cells, and is referred to as the transcellular and the paracellular routes, respectively. Both routes display cell-specific and tissue-specific variations in permeability, and together account for the distinct transport properties of each tissue.

The major barrier in the paracellular pathway is created by TJs, also known as zonula occludens (ZO; “occluding belt”). TJs can be found in various epithelial tissues, in which they form regions of intimate contact between the plasma membranes of adjacent cells (Farquhar and Palade, 1963) (Fig. 1.1A). In freeze-fracture replicas of epithelial cells TJs appear as a band-like network of branching and interconnecting thin ridges or complementary grooves, known as TJ strands (Farquhar and Palade, 1963). There is some evidence that TJs form an intramembrane diffusion barrier that restricts the lateral diffusion of apical and basolateral membrane

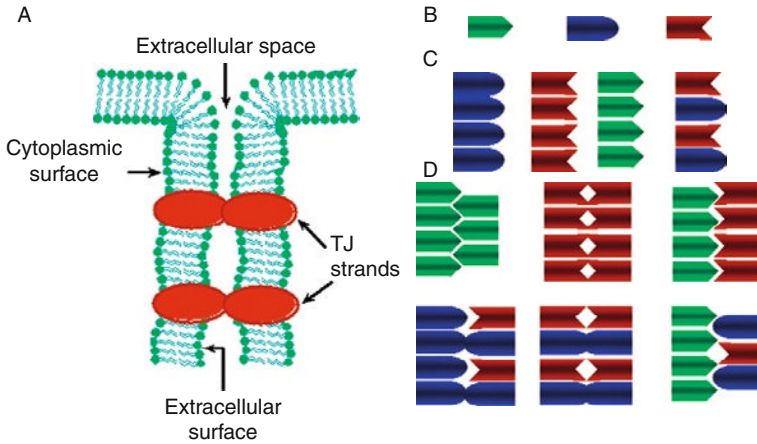


**Figure 1.1** Paired TJ strands are formed by interactions between different claudins. (A) Schematic drawing of TJs that form regions of intimate contact between the plasma membranes of adjacent cells. Illustration of different claudins (B) which can interact with other homo- and heteropolymers within (C) and between (D) TJ strands.

components, thus maintaining cellular polarity (“fence function”) (Cerejido et al., 1998; Dragsten et al., 1981; van Meer and Simons, 1986; van Meer et al., 1986). TJs also close or seal the space between cells and thus set up a semipermeable barrier which prevents or reduces paracellular diffusion (“barrier function”) (Madara, 1998). Depending on the functional requirements of an epithelium, there may be small or large amounts of water and small solutes flowing passively through the TJ (Fromter and Diamond, 1972). The paracellular permeability of different epithelia was found to correlate with the number of TJ strands along the apical–basal axis (Claude and Goodenough, 1973). The morphological pattern of the strands also varies among tissues; however, the physiological correlate of these ultrastructural differences is yet unknown. The actual barrier capacity of TJs can be determined by measurements of the transepithelial electrical resistance (TER) (Fromter and Diamond, 1972).

The main components of TJ strands are over 20 members of the claudin family of proteins. Claudins have various tissue distribution patterns, and many tissues express several different claudins which can interact with each other in both homotypic and heterotypic manners (Furuse et al., 1999; Morita et al., 1999) (Fig. 1.1B–D). Particular combinations and quantities of claudins modulate the charge-selective permeability of the paracellular pathway and, hence, take part in the regulation of the ionic makeup of extracellular fluids (Van Itallie and Anderson, 2006). Here, we review the functions of claudin TJ proteins and the complex interactions between them in various physiological systems.

## 2. TIGHT JUNCTION MEMBRANE INTEGRAL PROTEINS

TJ strands are composed of several types of membrane-spanning proteins: occludin (Furuse et al., 1993), members of the junction adhesion molecule (JAM) family (Mandell and Parkos, 2005), the coxsackievirus and adenovirus receptor (CAR) (Cohen et al., 2001), tricellulin (Ikenouchi et al., 2005; Riazuddin et al., 2006), and more than 20 members of the claudin family (Tsukita and Furuse, 2000; Van Itallie and Anderson, 2006). These strand-associated membrane proteins interact with the actin-based cytoskeleton (Turner, 2000), as well as with membrane-associated proteins that function as adapters and signaling proteins (Gonzalez-Mariscal et al., 2000; Mitic et al., 2000).

Occludin was the first identified TJ protein. It is exclusively localized to TJs of both epithelial and endothelial cells (Furuse et al., 1993). Initially occludin was thought to be the main TJ sealing protein. However, several studies, including gene knockout analyses, revealed that TJ strands can be formed and function normally in the absence of occludin (Hirase et al., 1997; Moroi et al., 1998; Saitou et al., 1998; Wong and Gumbiner, 1997).

JAMs are immunoglobulin superfamily proteins expressed at cell junctions in epithelial and endothelial cells, particularly at the apical-most part of the lateral membrane near the TJ. JAM proteins have been shown to bind to various TJ-associated cytoplasmic proteins. Despite compelling data implicating JAM proteins in formation of intercellular junctions, their direct role in the TJ has not been identified yet (Mandell and Parkos, 2005).

CAR is a 46-kDa integral membrane protein with a typical transmembrane region, a long cytoplasmic domain, and an extracellular region composed of two Ig-like domains. In polarized epithelial cells CAR is expressed at the TJ, where it contributes to the barrier function (Cohen et al., 2001).

Tricellulin is the most recently identified TJ integral membrane protein. It is concentrated at the vertically oriented TJ strands of tricellular contacts. Downregulation of tricellulin expression leads to compromised epithelial barrier function, and both bicellular and tricellular contacts were disorganized (Ikenouchi et al., 2005). Interestingly, in humans tricellulin mutations are associated with nonsyndromic deafness, a surprisingly limited phenotype, given the widespread tissue distribution of tricellulin in epithelial cells (Riazuddin et al., 2006).

## 3. THE CLAUDIN FAMILY OF TIGHT JUNCTION PROTEINS

The claudin family includes more than 20 highly conserved TJ proteins (Table 1.1). Claudins 1 and -2 were discovered first, based on their cofractionation with occludin from isolated chicken liver junctions

**Table 1.1** The claudin family

Protein name	Synonymous names	Gene name	Human chromosome
Claudin 1	SEMP1 (senescence-associated epithelial membrane protein 1)	<i>CLDN1</i>	3q28-29
Claudin 2		<i>CLDN2</i>	Xq22.3-23
Claudin 3	RVP1 (rat ventral prostate 1 protein) CPETR2 ( <i>Clostridium perfringens</i> enterotoxin receptor 2)	<i>CLDN3</i>	7q11.23
Claudin 4	CPE-R, CPER ( <i>Clostridium perfringens</i> enterotoxin receptor) CPETR1 ( <i>Clostridium perfringens</i> enterotoxin receptor 1) WBSCR8 (Williams-Beuren syndrome chromosomal region 8 protein)	<i>CLDN4</i>	7q11.23
Claudin 5	TMVCF (transmembrane protein deleted in velo-cardio-facial syndrome) MBEC (mouse brain endothelial cell 1)	<i>CLDN5</i>	22q11.2
Claudin 6		<i>CLDN6</i>	16p13.3
Claudin 7	CEPTRL2 ( <i>Clostridium perfringens</i> enterotoxin receptor-like 2)	<i>CLDN7</i>	17p13.1
Claudin 8		<i>CLDN8</i>	21q22.1
Claudin 9		<i>CLDN9</i>	16p13.3
Claudin 10	CPETRL3 ( <i>Clostridium perfringens</i> enterotoxin receptor-like 3) OSP-L (oligodendrocyte-specific protein-like)	<i>CLDN10</i>	13q32.1
Claudin 11	OSP (oligodendrocyte-specific protein)	<i>CLDN11</i>	3q26.2
Claudin 12		<i>CLDN12</i>	7q21.13
Claudin 13 <sup>a</sup>		<i>Cldn13</i>	
Claudin 14		<i>CLDN14</i>	21q22.13
Claudin 15		<i>CLDN15</i>	7q22.1

(continued)

**Table 1.1** (continued)

Protein name	Synonymous names	Gene name	Human chromosome
Claudin 16	PCLN1 (Paracellin-1)	<i>CLDN16</i>	3q28
Claudin 17		<i>CLDN17</i>	21q22.1
Claudin 18		<i>CLDN18</i>	3q22.3
Claudin 19		<i>CLDN19</i>	1p34.2
Claudin 20		<i>CLDN20</i>	6q25.3
Claudin 21		<i>CLDN21</i>	4q35.1
Claudin 22		<i>CLDN22</i>	4q35.1
Claudin 23		<i>CLDN23</i>	8p23.1

<sup>a</sup> Found in the mouse, no human orthologue found.

(Furuse et al., 1998a). Immunofluorescence and immunoelectron microscopy revealed that claudins 1 and -2 were both targeted to and incorporated into the TJ strand itself. When each of these proteins was transfected into cells that lack TJs, they were highly concentrated at cell–cell contact sites. In freeze–fracture replicas of these contact sites, well-developed networks of strands were identified that were similar to TJ strand networks *in vivo* (Furuse et al., 1998a). Taken together, the evidence strongly suggests that claudins are the primary proteins responsible for the physiological and structural paracellular barrier function of TJs (Tsukita and Furuse, 2000).

Following the discovery of claudins 1 and -2, additional family members were identified through amino acid sequence similarity searches (Morita et al., 1999), and to date at least 22 claudin paralogs are known in humans (Table 1.1). Similar to claudins 1 and -2, other claudins are also concentrated at preexisting TJs when transfected into MDCK cells. The tissue distribution pattern varies significantly among different claudin family members, and many tissues express multiple claudin species (Morita et al., 1999) (see Section 3.3). These findings suggested that multiple claudin family members are involved in the formation of TJ strands in a tissue-dependent manner. Additional evidence came from the phenotypes of humans and animals with mutations in specific claudin genes (Table 1.2, see Section 6).

### 3.1. Claudin protein structure

All claudins have a similar membrane topology of four transmembrane domains, with cytosolic amino and carboxy termini (Fig. 1.2) (Furuse et al., 1998b). The first extracellular loop of each claudin is longer and more hydrophobic than the second extracellular loop. Multiple sequence alignments carried out for some of the claudin family members revealed that

**Table 1.2** Claudin-related phenotypes

Claudin	Phenotype in humans	Phenotype in animal models	References
Claudin 1	Neonatal ichthyosis and sclerosing cholangitis (NISCH) (MIM 607626)	Neonatal death due to skin barrier defect (knockout mice)	Furuse et al. (2002), Hadj-Rabia et al. (2004)
Claudin 3	Within the region of 7q11 that is commonly deleted in patients with Williams-Beuren syndrome (WBS) (MIM 194050)		Paperna et al. (1998)
Claudin 4	Within the region of 7q11 that is commonly deleted in patients with WBS (MIM 194050)		Paperna et al. (1998)
Claudin 5	Within the region of 22q11 that is commonly deleted in patients with velocardiofacial syndrome (VCFS) (MIM 192430)	Neonatal death, size-selective blood-brain barrier defect (knockout mice)	Sirotkin et al. (1997), Nitta et al. (2003)
Claudin 6		Transgenic mice (overexpression): Homozygotes: neonatal death due to skin barrier defect Heterozygotes: delayed epidermal permeability barrier formation, hair follicle aberrations	Turksen and Troy (2002), Troy et al. (2005)
Claudin 9		Hearing loss (mutant mice)	Nakano et al. (2009)

*(continued)*



**Table 1.2** (continued)

Claudin	Phenotype in humans	Phenotype in animal models	References
Claudin 11		Central nervous system deficits, male sterility, hearing loss (knockout mice)	Gow et al. (1999, 2004), Kitajiri et al. (2004a,b)
Claudin 14	Profound, congenital, recessive deafness DFNB29 (MIM 605608)	Hearing loss (knockout mice)	Wilcox et al. (2001), Ben-Yosef et al. (2003)
Claudin 15		Megaintestine (knockout mice)	Tamura et al. (2008)
Claudin 16	Familial hypomagnesemia with hypercalciuria and nephrocalcinosis (FHHNC) (MIM 248250)	Chronic interstitial nephritis (bovine) Chronic renal wasting of magnesium and calcium and nephrocalcinosis (knock-down mice)	Simon et al. (1999), Hirano et al. (2000, 2002), Hou et al. (2007)
Claudin 19	FHHNC, ocular abnormalities (MIM 248190)	Peripheral nervous system deficits (knockout mice) Chronic renal wasting of magnesium and calcium (knock-down mice)	Miyamoto et al. (2005), Konrad et al. (2006), Hou et al. (2009)
Claudin 11 + claudin 14		Central nervous system deficits, male sterility, hearing loss (double knockout mice)	Elkouby-Naor et al. (2008)
Claudin <sub>j</sub>		Hearing loss, vestibular dysfunction (zebrafish)	Hardison et al. (2005)

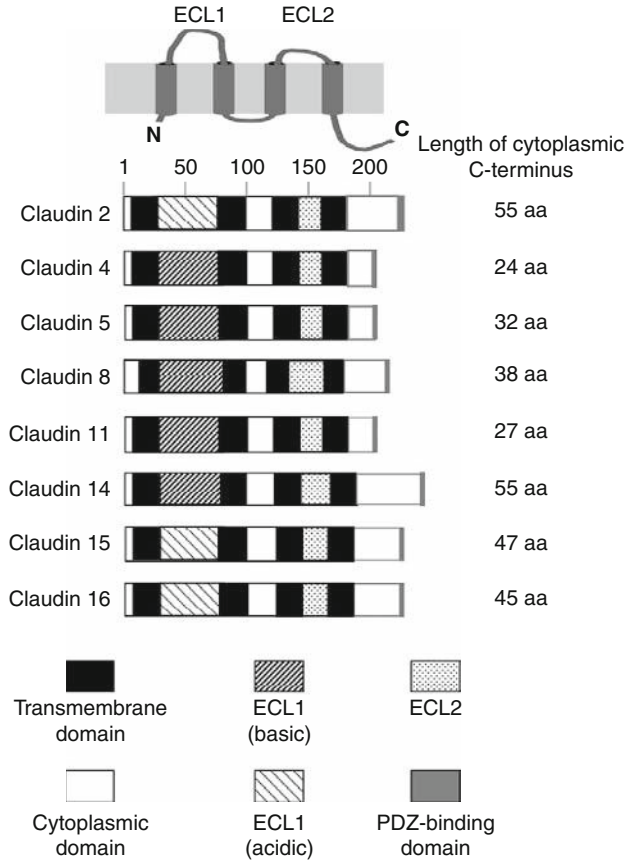


**Figure 1.2** The conserved structural and functional features of claudins. Schematic drawing of claudin main domains and the conservation between several members of the family. ECL1, extracellular loop 1; ECL2, extracellular loop 2.

the amino acid sequence is fairly conserved in the first and fourth transmembrane domains and in the first and second extracellular loops, but diversified in the second and third transmembrane domains (Morita et al., 1999).

### 3.1.1. The first extracellular loop (ECL1)

ECL1 is important for determination of the paracellular charge selectivity of claudins, as demonstrated for claudin 4 in the classic work of Colegio et al. (2003) and Van Itallie et al. (2001), and later for other claudins as well (see Sections 3.2 and 4.1). Using atomic force microscopy, it was recently shown that when a recombinant GST protein fused to the ECL1 of claudin 2 was brought in close contact to a glass cover slip coated with another

GST–ECL1, interaction was measured, in contrast to GST–ECL2 that showed no interaction with another GST–ECL2 (Lim et al., 2008). Thus, ECL1 of claudin 2 is probably sufficient for homophilic interaction of this claudin. Therefore, the ECL1 is one of the more significant domains of claudin proteins, as it affects TJ characters.

### 3.1.2. The second extracellular loop (ECL2)

Structure/function analyses of claudin 3 along with claudin 4 indicated that these proteins act as receptors for the *Clostridium perfringens* enterotoxin (CPE) (Katahira et al., 1997). To determine the region responsible for CPE sensitivity in claudin 3, two chimeric molecules were created, claudin-1/3 (C1/3) and claudin-3/1 (C3/1). Claudin-1/3 contained the ECL1 of claudin 1 and the ECL2 of claudin 3, while claudin-3/1 contained the ECL1 of claudin 3 and the ECL2 of claudin 1. L cells transfected with the C1/3, but not with the C3/1 chimera, showed characteristic sensitivity to CPE, that is, bleb formation and cell death. Moreover, GST-fusion proteins with the ECL2 of claudin 3 bound to CPE on nitrocellulose membranes and were detected by a specific antibody against CPE (Fujita et al., 2000).

CPE cytotoxicity is a multistep process that initiates with CPE binding to ECL2 of a specific claudin (Katahira et al., 1997; Sonoda et al., 1999). This is followed by formation of SDS-resistant complexes, which contain CPE, claudin, and occludin (Singh et al., 2000). These large complexes are thought to represent the cytotoxic pores, which create a hole in the plasma membrane and lead to cell death (Chakrabarti and McClane, 2005). Claudin–CPE binding ability is important in the aspect of drug delivery, since claudins 3 and –4 are overexpressed in some human cancers and, therefore, CPE is also being investigated as a tool for targeted delivery of chemotherapy (Morin, 2005).

### 3.1.3. The cytoplasmic tail

The importance of the cytoplasmic tail was revealed in 1999, shortly after the discovery of the claudin family. The cytoplasmic tail contains a PDZ-binding motif that has the ability to bind other PDZ-containing proteins, including the TJ-associated proteins of the MAGUK family: ZO-1, ZO-2, and ZO-3 (Itoh et al., 1999) (Section 4.2). Interestingly, a missense mutation in the cytoplasmic tail of claudin 16 (p.T233R) inactivates the PDZ-binding motif. This abolishes the interaction of claudin 16 with ZO-1 and leads to its lysosomal mislocalization (Muller et al., 2003). A different mutation of claudin 16, p.L203X, completely deletes the cytosolic domain. Interestingly, expression of the p.L203X mutant claudin 16 is strongly reduced and the protein is found in the endoplasmic reticulum and in the lysosomes (Muller et al., 2006). In contrast to claudin 16, different residues within the cytoplasmic tail, and not the PDZ-binding domain, were shown to be indispensable for correct TJ localization of claudins 1 and –5 (Ruffer

and Gerke, 2004). Therefore, the importance of the PDZ-binding motif for TJ localization may differ between different claudins. Apart from this binding ability, the cytoplasmic tail is also important for stability properties. When chimeric proteins were constructed, by exchanging the cytoplasmic tails of claudins 2 and -4, the tail of claudin 2 stabilized claudin 4 with an increase in both protein level and TER (Van Itallie and Anderson, 2004).

### **3.2. Claudin electrophysiological properties and generation of the TJ physiological barrier**

When examining all the data accumulating on the claudin family of proteins, it is more than obvious that claudins provide the main contribution for the TJ physiological barrier. The growing number of works supporting this declaration is summarized in Table 1.3. In these studies, overexpression or downregulation was used, in order to evaluate the contribution of gain/loss of function of the claudins examined, to the TJ barrier properties. The table also describes some site-directed mutagenesis experiments, in which changes in one amino acid of the examined claudin, influenced ion permeability. This influence of claudins on the TJ barrier properties is so sensitive that even two splice variants of claudin 10 in the kidney create paracellular pores with different ion selectivities (Van Itallie and Anderson, 2006). More evidence for claudins ability to create the TJ physiological barrier came from the mechanism underlying CPE activity. CPE removes specific claudins from TJ strands, causing TJ disintegration and subsequent reduction of the TJ barrier function (Sonoda et al., 1999). In conclusion, it is clear that the influence of claudins on the TJ physiological barrier is crucial for the maintenance of cell homeostasis and, therefore, for the function of the entire organ.

### **3.3. Claudin expression pattern**

Different claudin proteins exhibit diverse tissue-specific patterns of expression, which presumably determine the permeability characteristics of these tissues. There is an increasing number of works dealing with the expression pattern of different claudins in various tissues. Here we chose to present four prominent tissues as an example.

#### **3.3.1. The kidney**

It is not by a coincidence that the kidney is the most investigated model in the research of claudins. It functions as the filtration unit of the body by metabolic waste removal, regulation of extracellular fluid volume, electrolyte balance, and acid base balance. As differential permeability is critic for executing these functions, the kidney is predicted to present a wide variety of claudins. Indeed, at least 15 claudins are expressed in the adult mouse kidney

**Table 1.3** The effects of claudins up- or downregulation on tight junction barrier properties

Claudin	Cell type	Experiment type	TER	P <sub>Na</sub>	P <sub>Cl</sub>	References
Claudin 1	MDCK	Overexpression	↑	ND	ND	Inai et al. (1999)
Claudin 2	MDCK-C7	Overexpression	↓	↑	UC	Amasheh et al. (2002)
	LLC-PK <sub>1</sub>	Overexpression	↓	↑	ND	Van Itallie et al. (2003)
	MDCK	RNAi	↑	↓	UC	Hou et al. (2006)
Claudin 4	MDCK	Overexpression	↑	↓	UC	Van Itallie et al. (2001, 2003)
	LLC-PK <sub>1</sub>	Overexpression	↑	UC	ND	Van Itallie et al. (2003)
	MDCK	S.D.M n → p	ND	↑	ND	Colegio et al. (2002)
	LLC-PK <sub>1</sub>	RNAi	↑	UC	↓	Hou et al. (2006)
Claudin 5	MDCK II	Overexpression	↑	↓	ND	Wen et al. (2004)
	Caco-2	Overexpression	↑	ND	ND	Amasheh et al. (2005)
	bEND.3	RNAi	↓	ND	ND	Koto et al. (2007)
Claudin 6	MDCK II	Overexpression	↑	↓	↓	Sas et al. (2008)
Claudin 7	LLC-PK <sub>1</sub>	Overexpression	↑	↑	↓	Alexandra et al. (2005, 2007)
		S.D.M ECL1 n → p	ND	ND	↑	
	MDCK	RNAi	↓	↑	UC	Hou et al. (2006)
Claudin 8	MDCK II	Overexpression	↑	↓	UC	Yu et al. (2003)
Claudin 9	MDCK II	Overexpression	↑	↓	↓	Sas et al. (2008)
Claudin 11	MDCK II	Overexpression	↑	↓	ND	Van Itallie et al. (2003)
	LLC-PK <sub>1</sub>	Overexpression	↓	UC	ND	
Claudin 15	MDCK	S.D.M n → p	ND	↑	↓	Colegio et al. (2002)
	MDCK II	Overexpression	↑	UC	ND	Van Itallie et al. (2003)
	LLC-PK <sub>1</sub>	Overexpression	↓	↑	ND	
Claudin 16	LLC-PK <sub>1</sub>	Overexpression	ND	↑	UC	Hou et al. (2005)

TER, transepithelial electrical resistance; P<sub>Na</sub>, Na<sup>+</sup> permeability; P<sub>Cl</sub>, Cl<sup>-</sup>, permeability; ND, not detectable; UC, unchanged; RNAi, RNA interference; S.D.M, site-directed mutagenesis; n → p, negative to positive; ECL1, extracellular loop 1.

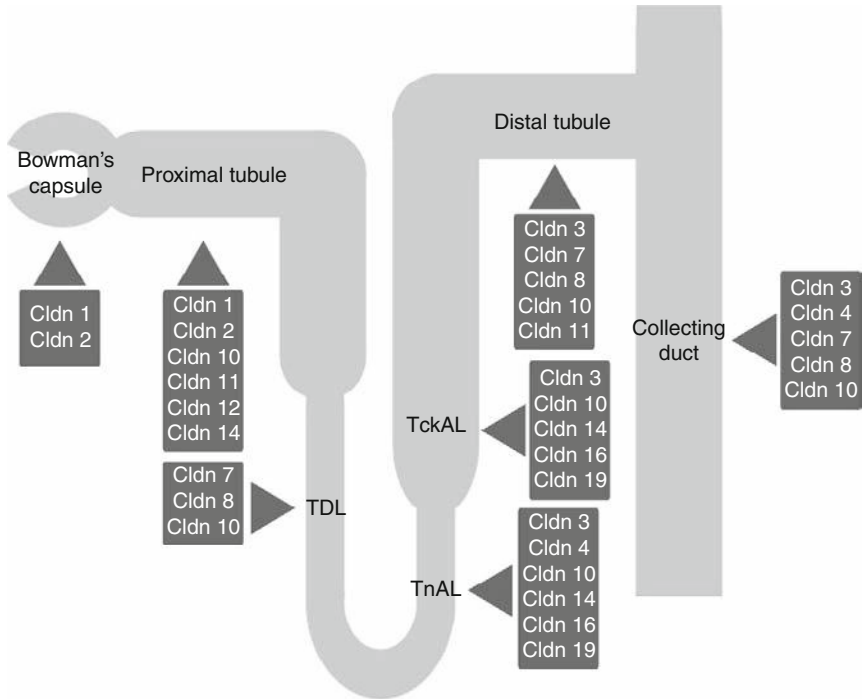


**Figure 1.3** Claudins in the kidney. Schematic drawing summarizing the expression pattern of claudin TJ proteins in the mouse kidney. Localization data were obtained from the following studies: Bowman's capsule (Enck et al., 2001; Kiuchi-Saishin et al., 2002), proximal tubule (Abuazza et al., 2006; Elkouby-Naor et al., 2008; Kiuchi-Saishin et al., 2002), thin descending limb (TDL) (Li et al., 2004; Van Itallie et al., 2006), thin ascending limb (TnAL) (Angelow et al., 2007; Elkouby-Naor et al., 2008; Kiuchi-Saishin et al., 2002; Van Itallie et al., 2006), TAL (Angelow et al., 2007), distal tubule (Angelow et al., 2007; Kiuchi-Saishin et al., 2002; Van Itallie et al., 2006), collecting duct (Kiuchi-Saishin et al., 2002; Li et al., 2004; Van Itallie et al., 2006).

(Angelow et al., 2007; Ben-Yosef et al., 2003; Kiuchi-Saishin et al., 2002; Li et al., 2004). In every segment of the kidney nephron, several claudins are expressed simultaneously (Kiuchi-Saishin et al., 2002) (Fig. 1.3). Claudins 1 and -2 are expressed in Bowman's capsule and the proximal tubule, which also expresses claudins 10, -11, -12, and -14. In the thin descending limb of the loop of Henle, claudin 7 is coexpressed along with claudins 8 and -10, while in the thin ascending limb claudins 3, -4, -10, -14, -16, and -19 are expressed. At least five distinct claudins are located in the thick ascending limb (TAL). These include claudins 3, -10, -14, -16, and -19. Claudins 3, -7, -8, -10, and -11 are expressed in the distal tubule, while claudins 3, -4, -7, -8, and -10 were observed in the collecting duct (Abuazza et al., 2006; Angelow

et al., 2007; Ben-Yosef et al., 2003; Elkouby-Naor et al., 2008; Enck et al., 2001; Kiuchi-Saishin et al., 2002; Li et al., 2004; Van Itallie et al., 2006). Such expression pattern may lead to marked redundancy between claudins, and serve as a backup mechanism. Nevertheless, mutations of either claudin 16 or claudin 19 have been associated with a severe renal phenotype (FHHNC) (Hirano et al., 2000; Hou et al., 2007; Konrad et al., 2006; Simon et al., 1999) (see Sections 6.7 and 6.8). On the other hand, claudin 14-deficiency has no obvious effect on kidney function (Ben-Yosef et al., 2003; Wilcox et al., 2001). Taken together, these observations demonstrate that in certain tissues some claudins appear to be indispensable, while others appear to be functionally redundant.

### 3.3.2. The inner ear

In the inner ear, vibrations are converted into nervous impulses. The special compartmentalization of the cochlea allows this process. The cochlea maintains two compositionally distinct fluid compartments, the scala vestibuli/tympani and the scala media, which are filled with perilymph and endolymph fluids, respectively (reviewed in Ferrary and Sterkers, 1998). These fluids are amazingly different in their chemical composition: the perilymph generally resembles extracellular fluids (Ferrary and Sterkers, 1998), while the endolymph has the characteristics of an intracellular fluid, with high  $K^+$  and low  $Na^+$  concentrations (Sterkers et al., 1988). To maintain the ionic characters of each compartment and other sections of the inner ear, a restrict regulation is needed. This is achieved by the presence of various claudins. At least 10 different claudins are expressed in the inner ear (Fig. 1.4) (Kitajiri et al., 2004b). In the organ of Corti claudins 1, -2, -3, -9, -10, -12, -14, and -18 are expressed. Claudins 1, -2, -3, -8, -9, -10, -12, -14, and -18 are expressed in Rissner's membrane, spiral limbus, and the marginal cells of the stria vascularis. The basal cells of the stria vascularis are exceptional. They only express claudin 11 (Kitajiri et al., 2004b). Claudin 11 knockout mice demonstrate hearing loss due to reduced endocochlear potentials (EP) (Gow et al., 2004; Kitajiri et al., 2004a) (see Section 6.11). Mutations of human *CLDN14* cause profound, congenital deafness DFNB29 (Wilcox et al., 2001). Both *Cldn9*-mutant mice and *Cldn14*-null mice are deaf, due to rapid degeneration of cochlear hair cells shortly after birth (Ben-Yosef et al., 2003; Nakano et al., 2009) (see Sections 6.9 and 6.10). These phenotypes are associated with disturbances of ionic balance within the inner ear.

### 3.3.3. The eye

The mammalian eye is a complex organ containing several distinct tissues (e.g., lens, cornea, retina, and iris), each performing specialized functions to detect a visual image. This kind of structure obligates restrict barriers and, therefore, the expression of a wide variety of claudins. The importance of

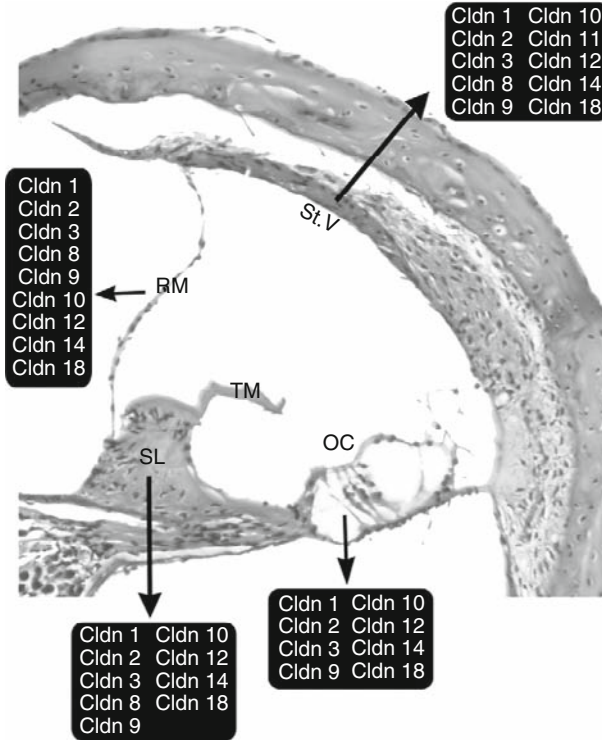


**Figure 1.4** Claudins in the inner ear. Schematic drawing summarizing the expression pattern of claudin TJ proteins in the mouse inner ear. Localization data were obtained from Kitajiri et al. (2004a). RM, Reissner's membrane; St.V, stria vascularis; SL, spiral limbus; TM, tectorial membrane; OC, organ of Corti.

claudins in the eye was demonstrated in humans with severe ocular abnormalities caused by mutations of *CLDN19*, and characterized by macular colobomata, significant myopia, and horizontal nystagmus (Konrad et al., 2006) (see Section 6.8). In the adult mouse eye, claudins 1, -2, -3, -4, -5, -7, -10, -11, -12, -13, -19, and -23 are expressed. The localization of the various claudins was determined by immunofluorescence staining. Claudin 1 is expressed in the retinal pigmented epithelium, the ciliary body, and the cornea. In the cornea, claudins 2 and -4 were also detected. The lens epithelium was positive only for claudin 5, which also localized in the choroid and the optic nerve. The optic nerve was positive for claudin 11 as well, which was also detectable in the retina. At least four other claudins are expressed in the retina. These include claudins 3, -5, -7, and -12 (Fig. 1.5) (L. Elkouby-Naor and T. Ben-Yosef, unpublished data).



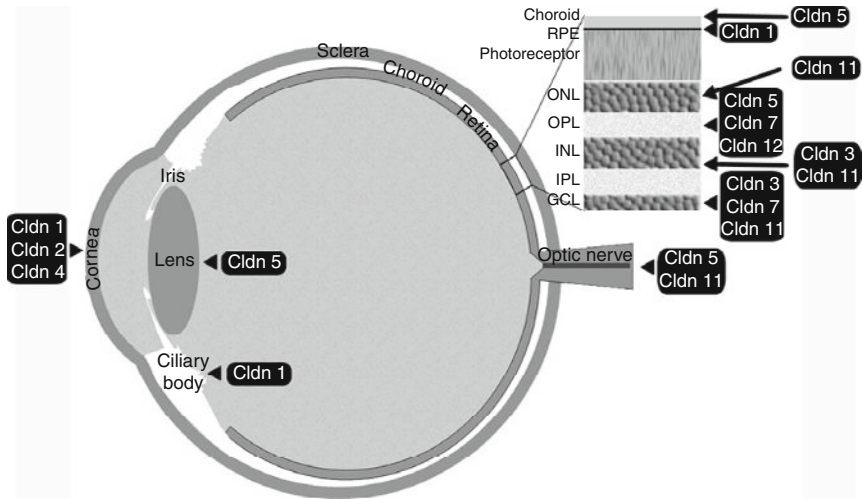


**Figure 1.5** Claudins in the eye. Schematic drawing summarizing the expression pattern of claudin TJ proteins in the mouse eye. GCL, ganglion cell layer; IPL, inner plexiform layer; INL, inner nuclear layer; OPL, outer plexiform layer; ONL, outer nuclear layer; RPE, retinal pigmented epithelium.

### 3.3.4. The skin

The epidermis of the skin is a stratified epithelium that functions as the interface between the human body and the outer environment. Not only that the epidermal layer protects the body from environmental pathogens, but it also acts to prevent water loss. A proof for this claim was provided by claudin 1-null mice and claudin 6-overexpressing mice, which died within 24–48 h after birth because of significant body dehydration (Furuse et al., 2002; Turksen and Troy, 2002). People with mutations of *CLDN1* suffer from ichthyosis (severe dryness of the skin), which is one of the symptoms of their Neonatal ichthyosis and sclerosing cholangitis (NISCH) syndrome (Baala et al., 2002) (see Section 6.1). In addition to claudins 1 and -6, the human epidermal skin also expresses claudins 4, -7, -8, -11, -12, and -17 (Brandner et al., 2002).

## 4. CLAUDIN INTERACTIONS WITHIN AND BETWEEN TJ STRANDS

### 4.1. All in the family

Today it is clear that the combination and the stoichiometry of claudins determine the characteristics of TJ strands. Therefore, it is expected that claudins would have the ability to interact with each other. Indeed, when

claudins 1, -2, and -3 were coexpressed in mouse L fibroblasts in different combinations, different claudins were copolymerized into individual TJ strands (heteropolymers), and when two transfected clones of mouse L fibroblasts separately expressing claudin 1, -2, or -3 were cocultured, it was found that claudin 1- or claudin 2-based strands (homopolymers) laterally associated with claudin 3-based strands but not with each other (Furuse et al., 1999). When L fibroblasts transfected singly expressing claudin 1 were cocultured with transfected cells coexpressing claudins 1 and -2, claudin 1 homopolymers laterally associated with claudins 1 and -2 heteropolymers to form paired strands (Furuse et al., 1998b) (Fig. 1.1B–D). Later it was also shown that claudins 1 and -5, which were heterotypically compatible with claudin 3, did not heterotypically bind to claudin 4. Moreover, a single point mutation in the first extracellular loop of claudin 3 converting Asn<sup>44</sup> to the corresponding amino acid in claudin 4 (Thr) produced a claudin capable of heterotypic binding to claudin 4, while still retaining the ability to bind to claudins 1 and -5. Thus, control of heterotypic claudin–claudin interactions is sensitive to small changes in the extracellular loop domains (Daugherty et al., 2007). Since the claudin family includes more than 20 members, there is a wide number of possible variations within and between TJ strands in different tissues (Fig. 1.1B–D). This mode of assembly of claudins increases both the structural and the functional diversity of TJs in different tissues (Furuse et al., 1999), and may explain the 100,000-fold difference in TER found between “tight” and “leaky” epithelia (Claude and Goodenough, 1973).

The physiological importance of claudin–claudin interactions was clearly demonstrated in the case of claudin 16 and claudin 19. In kidney nephrons both proteins are localized in the TAL of the loop of Henle, and mutations in either one of them lead to a severe kidney disease (see Sections 6.7 and 6.8). *In vitro* data suggested that the interaction between these two claudins may be necessary for cation selectivity of TAL TJs. The two claudins can be coimmunoprecipitated from doubly transfected renal epithelial cells, and their coexpression in renal epithelial cells generates paracellular cation selectivity, whereas expression of either claudin alone does not. Furthermore, mutations that interfere with their ability to interact also abolish the cationic selectivity. Taken together, these data suggested that cooligomerization of claudin 16 and claudin 19 is required for TAL paracellular channel function (Hou et al., 2008). When this hypothesis was tested *in vivo*, in *Cldn19* and *Cldn16* knock-down (KD) mice, it was found that deletion of claudin 19 prohibited assembly of claudin 16 into TAL TJs, whereas deletion of claudin 16 had a similar effect on claudin 19. These findings provided a clear explanation as to why the phenotypes of *Cldn16* and *Cldn19* KD mice are similar: removal of either claudin creates a double deletion at the level of the TJ (Hou et al., 2009).

The molecular mechanism in which claudins interact is yet to be determined. Recently, Piontek et al. (2008) suggested a two-step scenario of claudin 5 polymerization. Due to *cis*-interaction, claudin 5 monomers oligomerize, then, polymerization takes place in the paracellular space via *trans*-interactions, involving the second extracellular loop of claudin 5. In contrast, Lim et al. (2008) have demonstrated that the first extracellular loop is sufficient to promote *trans*-interactions between claudin 2 molecules. The exact reasons for those differences remain ambiguous, but it is clear that the mechanism underlying claudin–claudin interactions is complex and obligates fine detailed analysis.

In order to examine the dynamic behavior of paired claudins, green fluorescent protein (GFP) technology in live fibroblast cells was used. A construct encoding for GFP fused to the carboxy terminus of mouse claudin 1 was introduced into L fibroblasts. The paired claudin strands formed by this GFP–claudin 1 protein, showed a very dynamic behavior, moving in the plane of the membrane, breaking and annealing and associating with each other both in an end-to-side and a side-to-side manner, while at the same time showing a strong stability of the molecular array within the strand (Sasaki et al., 2003).

In a more specific manner, coexpression of claudins 16 and -19, both associated with familial hypomagnesemia with hypercalciuria and nephrocalcinosis (FHHNC), generated a cation-selective TJ complex, acting in a synergistic manner (Hou et al., 2008). The interactions between claudins 1, -3, or -5, which are the claudin components found in the human airway, were studied in NIH/3T3 and human airway (IB3.1) cells. Heterophilic interactions between claudins 1 and -3 and claudins 3 and -5 appear to limit the relative degree of change in solute permeability induced by claudin 5. Moreover, whereas cells expressing claudins 1 or -3 formed unorganized strands, cells expressing both proteins formed strands that appeared to be similar to those associated with polarized epithelia (Coyne et al., 2003). In active Crohn's disease, changes in expression and distribution of claudins 2, -5, and -8 lead to discontinuous TJs and barrier dysfunction (Zeissig et al., 2007). These results demonstrated that different claudin combinations influence not only the characteristics of TJs, but also their ability to form proper strands. On the other hand, the lack of interaction between claudins 11 and -14 in double null mice in tissues expressing both proteins reveals a redundancy mechanism that probably contributes to proper function of these tissues (Elkouby-Naor et al., 2008).

The fascinating field of claudin–claudin interactions is being constantly investigated in the last years. Although there is much more to understand, more and more pieces of the puzzle are being revealed, with the hope that one day the picture will be clear.

## 4.2. Dating others

The most prominent interactions of claudins with other proteins are with members of the MAGUK family of proteins, ZO-1, ZO-2, and ZO-3. The ZOs are scaffolding proteins that are bound to the carboxy-terminal YV sequence of claudins through their PDZ1 domain. This binding ability led to an architecture model in which clusters of YV sequences of claudins are presented toward the cytoplasm and ZO-1, ZO-2, and ZO-3 are recruited to the TJ through their PDZ1 domain (Itoh et al., 1999). Therefore, one can speculate that these proteins are required for the clustering of claudins within the plasma membrane. Indeed, mutation in claudin 16 PDZ domain in which disassociation with ZO-1 occurred resulted in accumulation of claudin 16 in the lysosomes (Muller et al., 2003). These results were consistent with a later finding where the cytoplasmic tail of claudin 16 was expressed as a fusion protein with GST and immobilized on glutathione-sepharose beads. In this case, mutations that resulted in disassociation with ZO-1 also led to mislocalization of the protein. Furthermore, these mutants showed much slower transport of  $\text{Ca}^{2+}$  from apical to basal compartments in comparison with a wild-type (WT) construct transfected into MDCK cells, implicating that the claudin 16/ZO-1 complex may be essential for the reabsorption of divalent cations in renal epithelial cells (Ikari et al., 2004).

A strong tool for finding associations between proteins is the yeast two-hybrid system. By using this method, several proteins were identified as binding partners for the claudin family. One of them is the MUPP1 (multi-PDZ domain protein 1) that binds claudin 1 and claudin 8 through its PDZ9 domain and may function as a scaffold protein that recruits various proteins to TJs (Hamazaki et al., 2002; Jeansonne et al., 2003). MUPP1 was also reported to associate with claudin 5 in Schwann cells (Poliak et al., 2002). The yeast two-hybrid system also revealed another two proteins that associated with claudin 11 through its cytoplasmic tail, Kv3.1 and OAP-1. Kv3.1 is a member of the Kv1 voltage-sensitive  $\text{K}^+$  channels family. In association with claudin 11, it plays a role in proliferation and migration of oligodendrocyte progenitor cells and myelination of axons (Tiwari-Woodruff et al., 2006). OAP-1 is a novel member of the tetraspanin superfamily that is expressed in various tissues including oligodendrocytes. Many members of this family form complexes with integrins. This is also true for OAP-1, as shown by coimmunoprecipitation and confocal immunocytochemistry assays indicating that OAP-1, claudin 11, and  $\beta 1$  integrin form a protein complex. Overexpression of this complex increases proliferation of oligodendrocytes, a finding that may indicate a role for this complex in regulating oligodendrocyte proliferation and migration (Tiwari-Woodruff et al., 2001). Another member of the tetraspanin family that

interacts with claudin 1 is CD9. This interaction was identified by chemical cross-linking and confirmed in multiple cell lines. Interestingly, CD9–claudin 1 complexes were most obvious in cell lines that do not form TJs. Moreover, claudin 1 was distributed very similar to CD9 in sucrose gradients, and like CD9, was released from A431 and A549 cells upon cholesterol depletion (Kovalenko et al., 2007).

A library screening of *Xenopus* embryos revealed that claudin 4 coimmunoprecipitated with ephrin-B1. Using a specific antibody it was also shown that ephrin-B1 was coprecipitated with claudin 1. The association of claudins with ephrin-B1 is required for its phosphorylation on tyrosine residues (Tanaka et al., 2005).

Colocalization of claudins 9 and -6 with canonical AJ proteins, p120ctn,  $\alpha$ - and  $\beta$ -catenins, in the inner ear's organ of Corti, recruits a dense cytoskeletal network. Although this interaction is not physical, it is the first evidence for the existence of a morphological and functional hybrid intercellular junction. This junction, which was designated as tight-AJ, combines critical features of both TJs and AJs into a single large occluding junction (Nunes et al., 2006).

As more proteins that associate with claudins are found, the importance of claudins, not only as structural proteins but also as proteins that play a role in regulation and maintenance, is being revealed. Therefore, it is clear that claudins possess the ability to assemble and act in novel combinations to fulfill specific needs of cells.

## 5. IS THE EXPRESSION LEVEL OF DIFFERENT CLAUDINS COREGULATED?

Selectivity and specificity of paired TJ strands are determined by the type of claudins present and their stoichiometry. Therefore, deregulated expression of a certain claudin may disrupt the delicate balance required for normal physiological function of the TJ. A possible mechanism for maintaining homeostasis within a TJ strand may involve tight coregulation of different claudins, at the mRNA and/or protein level, both temporally and spatially. This hypothesis was tested in several studies.

In the small intestine of *Cldn15*-null mice there was no compensatory upregulation of other claudins at either the RNA or the protein levels (Tamura et al., 2008).

In the epidermis of *Cldn6*-transgenic mice, overexpression of *Cldn6* was associated with downregulation of other claudin genes, including *Cldn3*, *Cldn4*, *Cldn7*, *Cldn8*, *Cldn10*, *Cldn11*, and *Cldn14*. The analysis was performed by RT-PCR, and changes in expression levels were between 1.7- and 2.6-fold. These findings were not tested at the protein level (Turksen and Troy, 2002).

In the cochlea of *Cldn11*-null mice, Northern blot analysis revealed that *Cldn3* expression was approximately fivefold higher than in WT mice, and *Cldn1* expression was slightly diminished. However, these changes could not be confirmed at the protein level, and their meaning remained unclear (Gow et al., 2004).

In claudin11/claudin 14 double deficient mice, the simultaneous elimination of both *Cldn11* and *Cldn14* did not lead to a compensatory upregulation of other types of claudins in the ear, as revealed by RT-PCR. In the kidney, four claudin genes (*Cldn3*, *Cldn5*, *Cldn7*, and *Cldn23*) were slightly upregulated (2.2–2.5-fold increase in expression level) in the double mutants, in comparison to WT mice (Elkouby-Naor et al., 2008).

In conclusion, based on the findings described here it appears that up- or downregulation of certain claudin genes may lead to compensatory changes in expression levels of other claudins expressed within the same tissue. Nevertheless, the meaning of these findings and their putative physiological effects remain to be determined.

## 6. CLAUDIN-RELATED PHENOTYPES

### 6.1. Claudin 1

NISCH is an autosomal recessive syndrome, characterized by scalp hypotrichosis, scarring alopecia, sclerosing cholangitis, and leukocyte vacuolization (Baala et al., 2002). The discovery of *CLDN1* mutations in NISCH patients emphasized the crucial role played by claudin 1 in both liver and skin (Feldmeyer et al., 2006; Hadj-Rabia et al., 2004).

In the liver, TJs separate bile flow from plasma. Bile secretion represents an intricate process reflecting the structural and functional interplay of the two epithelial cells of the liver: hepatocytes and cholangiocytes. In the human liver, claudin 1 is located in both cell types (Hadj-Rabia et al., 2004). Bile duct injury in NISCH patients may be related to altered functional integrity of TJs, which is crucial to prevent paracellular leakage of bile constituents. Unfortunately, the basis for liver dysfunction could not be studied in *Cldn1*-knockout mice due to their early lethality (Furuse et al., 2002).

Claudin 1 is one of several claudins expressed in skin epidermis. The dry ichthyotic skin found in NISCH patients could be ascribed to impaired ionic selectivity. Indeed, an important insight into the role played by claudin 1 in the skin came from *Cldn1*-null mice. These mice presented with severely wrinkled appearance of the skin and died within 24 h after birth because of significant body dehydration. The organization of the epidermis and the morphology of keratinocyte TJs in these mice were normal, except for a more compact and thicker stratum corneum (a feature

also observed in NISCH patients). Nevertheless, the epidermal barrier function was severely affected (Furuse et al., 2002; Hadj-Rabia et al., 2004).

## 6.2. Claudin 6

Like claudin 1, claudin 6 is also expressed in skin epidermis. Homozygous transgenic mice overexpressing *Cldn6* (*Inv-Cldn6* mice) had disrupted epidermal terminal differentiation leading to skin abnormalities. Neonates had a distinct appearance of their skin, which was red, shiny, and sticky to the touch. They suffered from dehydration, which caused the skin to dry up and crack, and resulted in death within 24–48 h. The epidermis was thicker and disorganized, and exhibited an abnormal barrier function (Turksen and Troy, 2002). Heterozygous *Inv-Cldn6* mice were also born with an incomplete epidermal permeability barrier; however, barrier formation continued after birth and normal hydration levels were achieved by postnatal day 12, allowing survival into adulthood. In addition to epidermal abnormalities, there were alterations in hair follicle differentiation (Troy et al., 2005).

## 6.3. Claudins 3 and 4

In humans both *CLDN3* and *CLDN4* genes are within the region of chromosome 7q11 that is commonly deleted in patients with Williams-Beuren syndrome (WBS). WBS is a neurodevelopmental disorder affecting multiple systems. The etiological basis of the disease is probably haploinsufficiency of genes from the commonly deleted interval. Whether claudin 3 and/or claudin 4-deficiencies actually contribute to the WBS phenotype is unknown (Paperna et al., 1998).

## 6.4. Claudin 5

TJs in endothelial cells are thought to determine vascular permeability. Claudin 5 is an endothelial cell-specific component of TJ strands. In blood vessels of the central nervous system (CNS) TJs play a central role in establishing the blood–brain barrier (BBB). *Cldn5*-null mice died shortly after birth. The development and morphology of blood vessels in the brains of these mice were not altered, with any bleeding or edema. However, there was size-selective loosening of the BBB. The causal sequence between BBB impairment and death in *Cldn5*-null mice has not been clarified yet (Nitta et al., 2003).

In humans the *CLDN5* gene is within the region of chromosome 22q11 that is commonly deleted in patients with velocardiofacial syndrome (VCFS). VCFS is characterized by cardiac abnormalities, cleft palate, learning disabilities, and a typical facial dysmorphism. The etiological basis of the disease is probably haploinsufficiency of genes from the

commonly deleted interval. Whether claudin 5-deficiency actually contributes to the VCFS phenotype is unknown (Sirotkin et al., 1997).

## 6.5. Claudin 7

The *Cldn7* gene, encoding for claudin 7, is highly expressed in distal kidney nephrons and has been reported to be involved in the regulation of paracellular  $\text{Cl}^-$  permeability in cell cultures. To investigate the role of claudin 7 *in vivo*, *Cldn7*-null mice were generated. These mice were born viable, but died within 12 days after birth, and exhibited growth retardation. *Cldn7*<sup>-/-</sup> mice showed severe salt wasting, as indicated by elevated urine  $\text{Na}^+$ ,  $\text{Cl}^-$ , and  $\text{K}^+$  levels. Wrinkled skin was evident around 1 week of age, indicating chronic fluid loss. Transepidermal water loss measurements showed no difference between *Cldn7*<sup>+/+</sup> and *Cldn7*<sup>-/-</sup> skin, suggesting that there was no transepidermal water barrier defect in *Cldn7*<sup>-/-</sup> mice. These findings demonstrated that claudin 7 is essential for NaCl homeostasis in distal nephrons and that the paracellular ion transport pathway plays an indispensable role in keeping ionic balance in kidneys (Tatum et al., 2009).

## 6.6. Claudin 15

Claudin 15 is expressed in many organs, in various combinations with other claudins. In *Cldn15*-null mice the upper part of the small intestine was approximately twofold larger in both length and diameter, in comparison to WT mice (megaintestine), due to enhanced proliferation of normal cryptic cells after weaning. Freeze-fracture electron microscopy revealed a decreased number of TJ strands in the small intestine of *Cldn15*-null mice. No differences were detected in the permeability of several different traces between *Cldn15*<sup>+/+</sup> and *Cldn15*<sup>-/-</sup> small intestines. However, in the distal portion of the jejunum of *Cldn15*<sup>-/-</sup> mice, the ion conductance had decreased, suggesting reduced paracellular ion permeability (Tamura et al., 2008).

## 6.7. Claudin 16

Mutations in human *CLDN16* cause FHHNC, due to a defect in paracellular resorption of  $\text{Mg}^{2+}$  and  $\text{Ca}^{2+}$  in the TAL of Henle in the kidney (Simon et al., 1999). Interestingly, two null mutant alleles of bovine *Cldn16* have been identified, both causing chronic interstitial nephritis, which is characterized by failures in selective filtration and absorption in surface renal epithelium, due to dysfunction of paracellular renal transport systems (Hirano et al., 2000, 2002). Histopathological examination of kidneys from mutant animals revealed abnormal development of nephrons (Okada et al., 2005).



Claudin 16-deficient mice were generated by transgenic RNAi depletion of the *Cldn16* gene. *Cldn16* KD mice exhibited chronic renal wasting of magnesium and calcium and nephrocalcinosis. These physiological changes were very similar to those reported in FHHNC patients, providing an accurate animal model of the human disease. Electrophysiological measurements in isolated, perfused renal tubules suggested that claudin 16 forms a nonselective paracellular cation channel, rather than a  $Mg^{2+}/Ca^{2+}$  channel (Hou et al., 2007).

## 6.8. Claudin 19

Mutations of *CLDN19* in humans are also associated with a severe renal disease, FHHNC, which is undistinguishable from the renal phenotype caused by *CLDN16* mutations. In addition, affected individuals also have severe visual impairment, characterized by macular colobomata, significant myopia, and horizontal nystagmus (Konrad et al., 2006). These findings demonstrated the fundamental role of claudin 19 for normal renal function and retinal development. Interestingly, *Cldn19*-null mice presented with peripheral nervous system (PNS) deficits due to the absence of TJs from Schwann cells of peripheral myelinated axons (Miyamoto et al., 2005). Visual impairment, electrolyte imbalance, or renal abnormalities were not reported in these mice. Another strain of claudin 19-deficient mice was generated by transgenic RNAi depletion of the *Cldn19* gene. *Cldn19* KD mice, like *Cldn16* KD mice and FHHNC human patients, exhibited chronic renal wasting of magnesium and calcium (Hou et al., 2009).

## 6.9. Claudin 9

Ethylnitrosourea (ENU) mutagenesis has been a valuable approach for generating new animal models of deafness and discovering previously unrecognized gene functions. The *nmf329* ENU-induced mouse mutant exhibits recessively inherited deafness, due to a widespread loss of sensory hair cells in the organ of Corti after the second week of life. Positional cloning revealed that the *nmf329* strain carries a missense mutation (p.F35L) in the *Cldn9* gene, encoding claudin 9. In an epithelial cell line, heterologous expression of WT claudin 9 reduced the paracellular permeability to  $Na^+$  and  $K^+$ , and the *nmf329* mutation eliminated this ion barrier function without affecting the plasma membrane localization of claudin 9. In the *nmf329* mouse line, the perilymphatic  $K^+$  concentration was found to be elevated, suggesting that the cochlear TJs were dysfunctional. Overall, these findings indicate that claudin 9 is required for the preservation of sensory cells in the organ of Corti because claudin 9-defective TJs fail to shield the basolateral side of hair cells from the  $K^+$ -rich endolymph (Nakano et al., 2009).

In addition to being expressed in the cochlea, *Cldn9* has been detected in the vestibular system, liver, and developing kidney, yet *Cldn9* mutant mice exhibited no signs of vestibular, hepatic, or renal defects. Thus, the ion barrier function of claudin 9 is essential in the cochlea, but appears to be dispensable in other organs (Nakano et al., 2009).

### 6.10. Claudin 14

The DFNB29 locus on chromosome 21q22.1 was defined by two large consanguineous Pakistani families segregating profound, congenital, autosomal recessive deafness. DFNB29 affected individuals in these families showed no signs of vestibular dysfunction or any other symptoms beside deafness. Eventually, these individuals were found to harbor mutations of the *CLDN14* gene, encoding claudin 14 (Wilcox et al., 2001). This finding demonstrated the significant role of claudin 14 in the cochlea and its importance in the hearing process.

*Cldn14* knockout mice are also deaf and, therefore, serve as a valuable model for studying the pathophysiology of autosomal recessive deafness DFNB29. Deafness in these mice is due to rapid degeneration of cochlear outer hair cells (OHC), followed by slower degeneration of the inner hair cells (IHC), during the first 3 weeks of life (Ben-Yosef et al., 2003). The onset of OHC loss in *Cldn14*-null mice, at 8–9 days after birth, coincides with several important developmental processes which occur in inner ears of normal mice, including increase in endolymph  $K^+$  concentration, onset of the EP, and formation of a fluid-filled space between OHCs, referred to as the space of Nuel. We assumed that the process of OHC loss in *Cldn14*-null mice was due to an altered ionic composition within the space of Nuel, which surrounds the basolateral membranes of OHCs. Specifically, we have previously demonstrated that claudin 14 is highly selective against cations. These properties are precisely what would be required to maintain the high cation gradients between perilymph and endolymph. Presumably, in the absence of claudin 14 the ability to maintain the paracellular barrier against cations at the reticular lamina is lost, and perhaps results in elevated  $K^+$  concentration in the space of Nuel. This environment is probably toxic to the basolateral membrane of OHCs (Ben-Yosef et al., 2003).

### 6.11. Claudin 11

Claudin 11 was first identified as a transmembrane protein highly expressed in CNS myelin and testis. *Cldn11*-knockout mice exhibited male sterility and neurological abnormalities, including slowed CNS nerve conduction, fine body tremor, and persistent hindlimb weakness. These findings are explained by the lack of TJs in the CNS myelin and between Sertoli cells in the testis (Gow et al., 1999). In addition, *Cldn11*-knockout mice are deaf,

with markedly reduced EP, due to the lack of TJs from the basal cells of the cochlea's stria vascularis (Gow et al., 2004; Kitajiri et al., 2004a).

### 6.12. Claudin11/claudin 14 double deficient mice

Claudin11/claudin 14 double deficient mice were generated to study the possible cooperation between these two claudin species. These mice exhibited a combination of the phenotypes found in each of the singly deficient mutants, including deafness, neurological deficits, and male sterility. In the kidney, we found that these two claudins have distinct and partially overlapping expression patterns. Claudin 11 is located in both the proximal and the distal convoluted tubules, while claudin 14 is located in both the thin descending and the TALs of the loop of Henle, as well as in the proximal convoluted tubules. Although daily urinary excretion of  $Mg^{2+}$ , and to a lesser extent of  $Ca^{2+}$ , tended to be higher in claudin11/claudin 14 double mutants, these changes did not reach statistical significance comparing to WT animals. These findings suggest that under normal conditions, codeletion of claudin11 and claudin 14 does not affect kidney function or ion balance, and demonstrate that despite the importance of each of these claudins, there is no functional cooperation between them (Elkouby-Naor et al., 2008).



## 7. CONCLUDING REMARKS

When Socrates imprinted the expression, “As for me, all I know is that I know nothing,” it was long before claudins were discovered. However, as more and more data regarding claudins are being accumulated, Socrates's words are becoming more relevant than ever. It is now clear that the role of claudins in biological systems is much wider than previously thought. Their ability to form homo- and heterophilic interactions with each other and with proteins from other families indicates an involvement in cell signaling. Their wide distribution pattern, as well as the great number of members within the family, point to a specific role for each claudin, although data on compensatory mechanisms are also reported. Recent evidence accumulating on changes in expression levels of several claudins as a result of down-regulation of other family members, may demonstrate a coregulative mechanism for the control of claudins coexpression. Therefore, many aspects of the claudin family remain mysterious. Better understanding of the role of each single claudin molecule will be achieved by additional studies of this family of TJ proteins, while integration of the data will hopefully lead to a full understanding of claudin biology as a whole.

## ACKNOWLEDGMENT

This work was supported by the Israel Science Foundation (grant number 24/05) to T. Ben-Yosef.

## REFERENCES

- Abuazza, G., Becker, A., Williams, S.S., Chakravarty, S., Truong, H.T., Lin, F., et al., 2006. Claudins 6, 9, and 13 are developmentally expressed renal tight junction proteins. *Am. J. Physiol. Renal Physiol.* 291, F1132–F1141.
- Alexandra, M.D., Lu, Q., Chen, Y.H., 2005. Overexpression of claudin-7 decreases the paracellular  $\text{Cl}^-$  conductance and increases the paracellular  $\text{Na}^+$  conductance in LLC-PK1 cells. *J. Cell Sci.* 118 (Pt 12), 2683–2693.
- Alexandra, M.D., Jeansonne, B.G., Renegar, R.H., Tatum, R., Chen, Y.H., 2007. The first extracellular domain of claudin-7 affects paracellular  $\text{Cl}^-$  permeability. *Biochem. Biophys. Res. Commun.* 357 (1), 87–91.
- Amasheh, S., Meiri, N., Gitter, A.H., Schoneberg, T., Mankertz, J., Schulzke, J.D., et al., 2002. Claudin-2 expression induces cation-selective channels in tight junctions of epithelial cells. *J. Cell Sci.* 115 (Pt 24), 4969–4976.
- Amasheh, S., Schmidt, T., Mahn, M., Florian, P., Mankertz, J., Tavalali, S., et al., 2005. Contribution of claudin-5 to barrier properties in tight junctions of epithelial cells. *Cell Tissue Res.* 321 (1), 89–96.
- Anderson, J.M., 2001. Molecular structure of tight junctions and their role in epithelial transport. *News Physiol. Sci.* 16, 126–130.
- Angelow, S., El-Husseini, R., Kanzawa, S.A., Yu, A.S., 2007. Renal localization and function of the tight junction protein, claudin-19. *Am. J. Physiol. Renal Physiol.* 293, F166–F177.
- Baala, L., Hadj-Rabia, S., Hamel-Teillac, D., Hadchouel, M., Prost, C., Leal, S.M., et al., 2002. Homozygosity mapping of a locus for a novel syndromic ichthyosis to chromosome 3q27–q28. *J. Invest. Dermatol.* 119, 70–76.
- Ben-Yosef, T., Belyantseva, I.A., Saunders, T.L., Hughes, E.D., Kawamoto, K., Van Itallie, C.M., et al., 2003. Claudin 14 knockout mice, a model for autosomal recessive deafness DFNB29, are deaf due to cochlear hair cell degeneration. *Hum. Mol. Genet.* 12, 2049–2061.
- Brandner, J.M., Kief, S., Grund, C., Rendl, M., Houdek, P., Kuhn, C., et al., 2002. Organization and formation of the tight junction system in human epidermis and cultured keratinocytes. *Eur. J. Cell Biol.* 81, 253–263.
- Cerejido, M., Valdes, J., Shoshani, L., Contreras, R.G., 1998. Role of tight junctions in establishing and maintaining cell polarity. *Annu. Rev. Physiol.* 60, 161–177.
- Chakrabarti, G., McClane, B.A., 2005. The importance of calcium influx, calpain and calmodulin for the activation of CaCo-2 cell death pathways by *Clostridium perfringens* enterotoxin. *Cell. Microbiol.* 7, 129–146.
- Claude, P., Goodenough, D.A., 1973. Fracture faces of zonulae occludentes from “tight” and “leaky” epithelia. *J. Cell Biol.* 58, 390–400.
- Cohen, C.J., Shieh, J.T., Pickles, R.J., Okegawa, T., Hsieh, J.T., Bergelson, J.M., 2001. The coxsackievirus and adenovirus receptor is a transmembrane component of the tight junction. *Proc. Natl. Acad. Sci. USA* 98, 15191–15196.
- Colegio, O.R., Van Itallie, C.M., McCrea, H.J., Rahner, C., Anderson, J.M., 2002. Claudins create charge-selective channels in the paracellular pathway between epithelial cells. *Am. J. Physiol. Cell Physiol.* 283 (1), C142–C147.

- Colegio, O.R., Van Itallie, C., Rahner, C., Anderson, J.M., 2003. Claudin extracellular domains determine paracellular charge selectivity and resistance but not tight junction fibril architecture. *Am. J. Physiol. Cell Physiol.* 284, C1346–C1354.
- Coyne, C.B., Gambling, T.M., Boucher, R.C., Carson, J.L., Johnson, L.G., 2003. Role of claudin interactions in airway tight junctional permeability. *Am. J. Physiol. Lung Cell Mol. Physiol.* 285, L1166–L1178.
- Daugherty, B.L., Ward, C., Smith, T., Ritzenthaler, J.D., Koval, M., 2007. Regulation of heterotypic claudin compatibility. *J. Biol. Chem.* 282, 30005–30013.
- Dragsten, P.R., Blumenthal, R., Handler, J.S., 1981. Membrane asymmetry in epithelia: is the tight junction a barrier to diffusion in the plasma membrane? *Nature* 294, 718–722.
- Elkouby-Naor, L., Abassi, Z., Lagziel, A., Gow, A., Ben-Yosef, T., 2008. Double gene deletion reveals lack of cooperation between claudin 11 and claudin 14 tight junction proteins. *Cell Tissue Res.* 333, 427–438.
- Enck, A.H., Berger, U.V., Yu, A.S., 2001. Claudin-2 is selectively expressed in proximal nephron in mouse kidney. *Am. J. Physiol. Renal Physiol.* 281, F966–F974.
- Farquhar, M.G., Palade, G.E., 1963. Junctional complexes in various epithelia. *J. Cell Biol.* 17, 375–412.
- Feldmeyer, L., Huber, M., Fellmann, F., Beckmann, J.S., Frenk, E., Hohl, D., 2006. Confirmation of the origin of NISCH syndrome. *Hum. Mutat.* 27, 408–410.
- Ferrary, E., Sterkers, O., 1998. Mechanisms of endolymph secretion. *Kidney Int. Suppl.* 65, S98–S103.
- Fromter, E., Diamond, J., 1972. Route of passive ion permeation in epithelia. *Nat. New Biol.* 235, 9–13.
- Fujita, K., Katahira, J., Horiguchi, Y., Sonoda, N., Furuse, M., Tsukita, S., 2000. *Clostridium perfringens* enterotoxin binds to the second extracellular loop of claudin-3, a tight junction integral membrane protein. *FEBS Lett.* 476, 258–261.
- Furuse, M., Hirase, T., Itoh, M., Nagafuchi, A., Yonemura, S., Tsukita, S., et al., 1993. Occludin: a novel integral membrane protein localizing at tight junctions. *J. Cell Biol.* 123, 1777–1788.
- Furuse, M., Fujita, K., Hiiiragi, T., Fujimoto, K., Tsukita, S., 1998a. Claudin-1 and -2: novel integral membrane proteins localizing at tight junctions with no sequence similarity to occludin. *J. Cell Biol.* 141, 1539–1550.
- Furuse, M., Sasaki, H., Fujimoto, K., Tsukita, S., 1998b. A single gene product, claudin-1 or -2, reconstitutes tight junction strands and recruits occludin in fibroblasts. *J. Cell Biol.* 143, 391–401.
- Furuse, M., Sasaki, H., Tsukita, S., 1999. Manner of interaction of heterogeneous claudin species within and between tight junction strands. *J. Cell Biol.* 147, 891–903.
- Furuse, M., Hata, M., Furuse, K., Yoshida, Y., Haratake, A., Sugitani, Y., et al., 2002. Claudin-based tight junctions are crucial for the mammalian epidermal barrier: a lesson from claudin-1-deficient mice. *J. Cell Biol.* 156, 1099–1111.
- Gonzalez-Mariscal, L., Betanzos, A., Avila-Flores, A., 2000. MAGUK proteins: structure and role in the tight junction. *Semin. Cell Dev. Biol.* 11, 315–324.
- Goodenough, D.A., Goliger, J.A., Paul, D.L., 1996. Connexins, connexons, and intercellular communication. *Annu. Rev. Biochem.* 65, 475–502.
- Gow, A., Southwood, C.M., Li, J.S., Pariali, M., Riordan, G.P., Brodie, S.E., et al., 1999. CNS myelin and sertoli cell tight junction strands are absent in *Osp/claudin-11* null mice. *Cell* 99, 649–659.
- Gow, A., Davies, C., Southwood, C.M., Frolenkov, G., Chrustowski, M., Ng, L., et al., 2004. Deafness in Claudin 11-null mice reveals the critical contribution of basal cell tight junctions to stria vascularis function. *J. Neurosci.* 24, 7051–7062.
- Hadj-Rabia, S., Baala, L., Vabres, P., Hamel-Teillac, D., Jacquemin, E., Fabre, M., et al., 2004. Claudin-1 gene mutations in neonatal sclerosing cholangitis associated with ichthyosis: a tight junction disease. *Gastroenterology* 127, 1386–1390.

- Hamazaki, Y., Itoh, M., Sasaki, H., Furuse, M., Tsukita, S., 2002. Multi-PDZ domain protein 1 (MUPP1) is concentrated at tight junctions through its possible interaction with claudin-1 and junctional adhesion molecule. *J. Biol. Chem.* 277, 455–461.
- Hardison, A.L., Lichten, L., Banerjee-Basu, S., Becker, T.S., Burgess, S.M., 2005. The zebrafish gene *claudinj* is essential for normal ear function and important for the formation of the otoliths. *Mech. Dev.* 122, 949–958.
- Hirano, T., Kobayashi, N., Itoh, T., Takasuga, A., Nakamaru, T., Hirotsune, S., et al., 2000. Null mutation of PCLN-1/Claudin-16 results in bovine chronic interstitial nephritis. *Genome Res.* 10, 659–663.
- Hirano, T., Hirotsune, S., Sasaki, S., Kikuchi, T., Sugimoto, Y., 2002. A new deletion mutation in bovine Claudin-16 (CL-16) deficiency and diagnosis. *Anim. Genet.* 33, 118–122.
- Hirase, T., Staddon, J.M., Saitou, M., Ando-Akatsuka, Y., Itoh, M., Furuse, M., et al., 1997. Occludin as a possible determinant of tight junction permeability in endothelial cells. *J. Cell Sci.* 110 (Pt 14), 1603–1613.
- Hou, J., Paul, D.L., Goodenough, D.A., 2005. Paracellin-1 and the modulation of ion selectivity of tight junctions. *J. Cell Sci.* 118 (Pt 21), 5109–5118.
- Hou, J., Gomes, A.S., Paul, D.L., Goodenough, D.A., 2006. Study of claudin function by RNA interference. *J. Biol. Chem.* 281 (47), 36117–36123.
- Hou, J., Shan, Q., Wang, T., Gomes, A.S., Yan, Q., Paul, D.L., et al., 2007. Transgenic RNAi depletion of claudin-16 and the renal handling of magnesium. *J. Biol. Chem.* 282, 17114–17122.
- Hou, J., Renigunta, A., Konrad, M., Gomes, A.S., Schneeberger, E.E., Paul, D.L., et al., 2008. Claudin-16 and claudin-19 interact and form a cation-selective tight junction complex. *J. Clin. Invest.* 118, 619–628.
- Hou, J., Renigunta, A., Gomes, A.S., Hou, M., Paul, D.L., Waldegger, S., et al., 2009. Claudin-16 and claudin-19 interaction is required for their assembly into tight junctions and for renal reabsorption of magnesium. *Proc. Natl. Acad. Sci. USA* 106, 15350–15355.
- Ikari, A., Hirai, N., Shiroma, M., Harada, H., Sakai, H., Hayashi, H., et al., 2004. Association of paracellin-1 with ZO-1 augments the reabsorption of divalent cations in renal epithelial cells. *J. Biol. Chem.* 279, 54826–54832.
- Ikenouchi, J., Furuse, M., Furuse, K., Sasaki, H., Tsukita, S., Tsukita, S., 2005. Tricellulin constitutes a novel barrier at tricellular contacts of epithelial cells. *J. Cell Biol.* 171, 939–945.
- Inai, T., Kobayashi, J., Shibata, Y., 1999. Claudin-1 contributes to the epithelial barrier function in MDCK cells. *Eur. J. Cell Biol.* 78 (12), 849–855.
- Itoh, M., Furuse, M., Morita, K., Kubota, K., Saitou, M., Tsukita, S., 1999. Direct binding of three tight junction-associated MAGUKs, ZO-1, ZO-2, and ZO-3, with the COOH termini of claudins. *J. Cell Biol.* 147, 1351–1363.
- Jeansonne, B., Lu, Q., Goodenough, D.A., Chen, Y.H., 2003. Claudin-8 interacts with multi-PDZ domain protein 1 (MUPP1) and reduces paracellular conductance in epithelial cells. *Cell. Mol. Biol. (Noisy-le-grand)* 49, 13–21.
- Katahira, J., Sugiyama, H., Inoue, N., Horiguchi, Y., Matsuda, M., Sugimoto, N., 1997. *Clostridium perfringens* enterotoxin utilizes two structurally related membrane proteins as functional receptors *in vivo*. *J. Biol. Chem.* 272, 26652–26658.
- Kitajiri, S., Miyamoto, T., Mineharu, A., Sonoda, N., Furuse, K., Hata, M., et al., 2004a. Compartmentalization established by claudin-11-based tight junctions in stria vascularis is required for hearing through generation of endocochlear potential. *J. Cell Sci.* 117, 5087–5096.
- Kitajiri, S.I., Furuse, M., Morita, K., Saishin-Kiuchi, Y., Kido, H., Ito, J., et al., 2004b. Expression patterns of claudins, tight junction adhesion molecules, in the inner ear. *Hear. Res.* 187, 25–34.

- Kiuchi-Saishin, Y., Gotoh, S., Furuse, M., Takasuga, A., Tano, Y., Tsukita, S., 2002. Differential expression patterns of claudins, tight junction membrane proteins, in mouse nephron segments. *J. Am. Soc. Nephrol.* 13, 875–886.
- Konrad, M., Schaller, A., Seelow, D., Pandey, A.V., Waldegger, S., Lesslauer, A., et al., 2006. Mutations in the tight-junction gene claudin 19 (CLDN19) are associated with renal magnesium wasting, renal failure, and severe ocular involvement. *Am. J. Hum. Genet.* 79, 949–957.
- Koto, T., Takubo, K., Ishida, S., Shinoda, H., Inoue, M., Tsubota, K., 2007. Hypoxia disrupts the barrier function of neural blood vessels through changes in the expression of claudin-5 in endothelial cells. *Am. Soc. Investig. Pathol.* 170 (4), 1389–1397.
- Kovalenko, O.V., Yang, X.H., Hemler, M.E., 2007. A novel cysteine cross-linking method reveals a direct association between claudin-1 and tetraspanin CD9. *Mol. Cell. Proteomics* 6, 1855–1867.
- Kowalczyk, A.P., Bornslaeger, E.A., Norvell, S.M., Palka, H.L., Green, K.J., 1999. Desmosomes: intercellular adhesive junctions specialized for attachment of intermediate filaments. *Int. Rev. Cytol.* 185, 237–302.
- Li, W.Y., Huey, C.L., Yu, A.S., 2004. Expression of claudin-7 and -8 along the mouse nephron. *Am. J. Physiol. Renal Physiol.* 286, F1063–F1071.
- Lim, T.S., Vedula, S.R., Hunziker, W., Lim, C.T., 2008. Kinetics of adhesion mediated by extracellular loops of claudin-2 as revealed by single-molecule force spectroscopy. *J. Mol. Biol.* 381, 681–691.
- Madara, J.L., 1998. Regulation of the movement of solutes across tight junctions. *Annu. Rev. Physiol.* 60, 143–159.
- Mandell, K.J., Parkos, C.A., 2005. The JAM family of proteins. *Adv. Drug Deliv. Rev.* 57, 857–867.
- Mitic, L.L., Van Itallie, C.M., Anderson, J.M., 2000. Molecular physiology and pathophysiology of tight junctions I. Tight junction structure and function: lessons from mutant animals and proteins. *Am. J. Physiol. Gastrointest. Liver Physiol.* 279, G250–G254.
- Miyamoto, T., Morita, K., Takemoto, D., Takeuchi, K., Kitano, Y., Miyakawa, T., et al., 2005. Tight junctions in Schwann cells of peripheral myelinated axons: a lesson from claudin-19-deficient mice. *J. Cell Biol.* 169, 527–538.
- Morin, P.J., 2005. Claudin proteins in human cancer: promising new targets for diagnosis and therapy. *Cancer Res.* 65, 9603–9606.
- Morita, K., Furuse, M., Fujimoto, K., Tsukita, S., 1999. Claudin multigene family encoding four-transmembrane domain protein components of tight junction strands. *Proc. Natl. Acad. Sci. USA* 96, 511–516.
- Moroi, S., Saitou, M., Fujimoto, K., Sakakibara, A., Furuse, M., Yoshida, O., et al., 1998. Occludin is concentrated at tight junctions of mouse/rat but not human/guinea pig Sertoli cells in testes. *Am. J. Physiol.* 274, C1708–C1717.
- Muller, D., Kausalya, P.J., Claverie-Martin, F., Meij, I.C., Eggert, P., Garcia-Nieto, V., et al., 2003. A novel claudin 16 mutation associated with childhood hypercalciuria abolishes binding to ZO-1 and results in lysosomal mistargeting. *Am. J. Hum. Genet.* 73, 1293–1301.
- Muller, D., Kausalya, P.J., Bockenbauer, D., Thumfart, J., Meij, I.C., Dillon, M.J., et al., 2006. Unusual clinical presentation and possible rescue of a novel claudin-16 mutation. *J. Clin. Endocrinol. Metab.* 91, 3076–3079.
- Nagafuchi, A., 2001. Molecular architecture of adherens junctions. *Curr. Opin. Cell Biol.* 13, 600–603.
- Nakano, Y., Kim, S.H., Kim, H.M., Sanneman, J.D., Zhang, Y., Smith, R.J., et al., 2009. A claudin-9-based ion permeability barrier is essential for hearing. *PLoS Genet.* 5, e1000610.
- Nitta, T., Hata, M., Gotoh, S., Seo, Y., Sasaki, H., Hashimoto, N., et al., 2003. Size-selective loosening of the blood–brain barrier in claudin-5-deficient mice. *J. Cell Biol.* 161, 653–660.

- Nunes, F.D., Lopez, L.N., Lin, H.W., Davies, C., Azevedo, R.B., Gow, A., et al., 2006. Distinct subdomain organization and molecular composition of a tight junction with adherens junction features. *J. Cell Sci.* 119, 4819–4827.
- Okada, K., Ishikawa, N., Fujimori, K., Goryo, M., Ikeda, M., Sasaki, J., et al., 2005. Abnormal development of nephrons in claudin-16-defective Japanese black cattle. *J. Vet. Med. Sci.* 67, 171–178.
- Paperna, T., Peoples, R., Wang, Y.K., Kaplan, P., Francke, U., 1998. Genes for the CPE receptor (CPETR1) and the human homolog of RVP1 (CPETR2) are localized within the Williams–Beuren syndrome deletion. *Genomics* 54, 453–459.
- Piontek, J., Winkler, L., Wolburg, H., Muller, S.L., Zuleger, N., Piehl, C., et al., 2008. Formation of tight junction: determinants of homophilic interaction between classic claudins. *FASEB J.* 22, 146–158.
- Poliak, S., Matlis, S., Ullmer, C., Scherer, S.S., Peles, E., 2002. Distinct claudins and associated PDZ proteins form different autotypic tight junctions in myelinating Schwann cells. *J. Cell Biol.* 159, 361–372.
- Riazuddin, S., Ahmed, Z.M., Fanning, A.S., Lagziel, A., Kitajiri, S., Ramzan, K., et al., 2006. Tricellulin is a tight-junction protein necessary for hearing. *Am. J. Hum. Genet.* 79, 1040–1051.
- Ruffer, C., Gerke, V., 2004. The C-terminal cytoplasmic tail of claudins 1 and 5 but not its PDZ-binding motif is required for apical localization at epithelial and endothelial tight junctions. *Eur. J. Cell Biol.* 83, 135–144.
- Saitou, M., Fujimoto, K., Doi, Y., Itoh, M., Fujimoto, T., Furuse, M., 1998. Occludin-deficient embryonic stem cells can differentiate into polarized epithelial cells bearing tight junctions. *J. Cell Biol.* 141, 397–408.
- Sas, D., Hu, M., Moe, O.W., Baum, M., 2008. Effect of claudins 6 and 9 on paracellular permeability in MDCK II cells. *Am. J. Physiol. Regul. Integr. Comp. Physiol.* 295, R1713–R1719.
- Sasaki, H., Matsui, C., Furuse, K., Mimori-Kiyosue, Y., Furuse, M., Tsukita, S., 2003. Dynamic behavior of paired claudin strands within apposing plasma membranes. *Proc. Natl. Acad. Sci. USA* 100, 3971–3976.
- Simon, D.B., Lu, Y., Choate, K.A., Velazquez, H., Al-Sabban, E., Praga, M., et al., 1999. Paracellin-1, a renal tight junction protein required for paracellular  $Mg^{2+}$  resorption. *Science* 285, 103–106.
- Singh, U., Van Itallie, C.M., Mitic, L.L., Anderson, J.M., McClane, B.A., 2000. CaCo-2 cells treated with *Clostridium perfringens* enterotoxin form multiple large complex species, one of which contains the tight junction protein occludin. *J. Biol. Chem.* 275, 18407–18417.
- Sirotkin, H., Morrow, B., Saint-Jore, B., Puech, A., Das Gupta, R., Patanjali, S.R., et al., 1997. Identification, characterization, and precise mapping of a human gene encoding a novel membrane-spanning protein from the 22q11 region deleted in velo-cardio-facial syndrome. *Genomics* 42, 245–251.
- Sonoda, N., Furuse, M., Sasaki, H., Yonemura, S., Katahira, J., Horiguchi, Y., et al., 1999. *Clostridium perfringens* enterotoxin fragment removes specific claudins from tight junction strands: evidence for direct involvement of claudins in tight junction barrier. *J. Cell Biol.* 147, 195–204.
- Sterkers, O., Ferrary, E., Amiel, C., 1988. Production of inner ear fluids. *Physiol. Rev.* 68, 1083–1128.
- Tamura, A., Kitano, Y., Hata, M., Katsuno, T., Moriwaki, K., Sasaki, H., et al., 2008. Megaintestine in claudin-15-deficient mice. *Gastroenterology* 134, 523–534.
- Tanaka, M., Kamata, R., Sakai, R., 2005. Phosphorylation of ephrin-B1 via the interaction with claudin following cell–cell contact formation. *EMBO J.* 24, 3700–3711.
- Tatum, R., Zhang, Y., Salleng, K., Lu, Z., Lin, J.J., Lu, Q., et al., 2009. Renal salt wasting and chronic dehydration in claudin-7-deficient mice. *Am. J. Physiol. Renal Physiol.* (in press).



- Tiwari-Woodruff, S.K., Buznikov, A.G., Vu, T.Q., Micevych, P.E., Chen, K., Kornblum, H.I., et al., 2001. OSP/claudin-11 forms a complex with a novel member of the tetraspanin super family and beta1 integrin and regulates proliferation and migration of oligodendrocytes. *J. Cell Biol.* 153, 295–305.
- Tiwari-Woodruff, S., Beltran-Parrazal, L., Charles, A., Keck, T., Vu, T., Bronstein, J., 2006. K<sup>+</sup> channel KV3.1 associates with OSP/claudin-11 and regulates oligodendrocyte development. *Am. J. Physiol. Cell Physiol.* 291, C687–C698.
- Troy, T.C., Rahbar, R., Arabzadeh, A., Cheung, R.M., Turksen, K., 2005. Delayed epidermal permeability barrier formation and hair follicle aberrations in *Inv-Cldn6* mice. *Mech. Dev.* 122, 805–819.
- Tsukita, S., Furuse, M., 2000. Pores in the wall: claudins constitute tight junction strands containing aqueous pores. *J. Cell Biol.* 149, 13–16.
- Tsukita, S., Furuse, M., Itoh, M., 2001. Multifunctional strands in tight junctions. *Nat. Rev. Mol. Cell Biol.* 2, 285–293.
- Turksen, K., Troy, T.C., 2002. Permeability barrier dysfunction in transgenic mice over-expressing claudin 6. *Development* 129, 1775–1784.
- Turner, J.R., 2000. 'Putting the squeeze' on the tight junction: understanding cytoskeletal regulation. *Semin. Cell Dev. Biol.* 11, 301–308.
- Van Itallie, C.M., Anderson, J.M., 2004. The molecular physiology of tight junction pores. *Physiology (Bethesda)* 19, 331–338.
- Van Itallie, C.M., Anderson, J.M., 2006. Claudins and epithelial paracellular transport. *Annu. Rev. Physiol.* 68, 403–429.
- Van Itallie, C., Rahner, C., Anderson, J.M., 2001. Regulated expression of claudin-4 decreases paracellular conductance through a selective decrease in sodium permeability. *J. Clin. Invest.* 107, 1319–1327.
- Van Itallie, C.M., Fanning, A.S., Anderson, J.M., 2003. Reversal of charge selectivity in cation or anion-selective epithelial lines by expression of different claudins. *Am. J. Physiol. Renal Physiol.* 285 (6), F1078–F1084.
- Van Itallie, C.M., Rogan, S., Yu, A., Vidal, L.S., Holmes, J., Anderson, J.M., 2006. Two splice variants of claudin-10 in the kidney create paracellular pores with different ion selectivities. *Am. J. Physiol. Renal Physiol.* 291, F1288–F1299.
- van Meer, G., Simons, K., 1986. The function of tight junctions in maintaining differences in lipid composition between the apical and the basolateral cell surface domains of MDCK cells. *EMBO J.* 5, 1455–1464.
- van Meer, G., Gumbiner, B., Simons, K., 1986. The tight junction does not allow lipid molecules to diffuse from one epithelial cell to the next. *Nature* 322, 639–641.
- Wen, H., Watry, D.D., Marcondes, M.C., Fox, H.S., 2004. Selective decrease in paracellular conductance of tight junctions: role of the first extracellular domain of claudin-5. *Mol. Cell Biol.* 24 (19), 8408–8417.
- Wilcox, E.R., Burton, Q.L., Naz, S., Riazuddin, S., Smith, T.N., Ploplis, B., et al., 2001. Mutations in the gene encoding tight junction claudin-14 cause autosomal recessive deafness DFNB29. *Cell* 104, 165–172.
- Wong, V., Gumbiner, B.M., 1997. A synthetic peptide corresponding to the extracellular domain of occludin perturbs the tight junction permeability barrier. *J. Cell Biol.* 136, 399–409.
- Yu, A.S., Enck, A.H., Lencer, W.I., Schneeberger, E.E., 2003. Claudin-8 expression in Madin-Darby canine kidney cells augments the paracellular barrier to cation permeation. *J. Biol. Chem.* 278 (19), 17350–17359.
- Zeissig, S., Burgel, N., Gunzel, D., Richter, J., Mankertz, J., Wahnschaffe, U., et al., 2007. Changes in expression and distribution of claudin 2, 5 and 8 lead to discontinuous tight junctions and barrier dysfunction in active Crohn's disease. *Gut* 56, 61–72.

## SECONDARY SYMBIOSIS BETWEEN *PARAMECIUM* AND *CHLORELLA* CELLS

Yuuki Kodama *and* Masahiro Fujishima

### Contents

1. Introduction	34
2. Infection Route	36
2.1. Classification of DVs	37
2.2. Timing of acidosomal and lysosomal fusion to DV	38
2.3. Presence of four cytological events needed to establish endosymbiosis	40
2.4. Initiation of algal cell division	51
2.5. Summary of the infection route	52
3. Different Fates of Infection-Capable and Infection-Incapable <i>Chlorella</i> Species	52
3.1. Difference in algal attachment beneath the host cell surface	54
3.2. Relation between sugar residues of the algal cell wall and infectivity	57
3.3. Effects of WGA on the infectivity of <i>C. sorokiniana</i> C-212 to <i>P. bursaria</i>	60
4. Function of PV Membrane	61
4.1. Algal proteins necessary for the PV membrane	62
4.2. The PV membrane can provide protection from host lysosomal fusion	64
5. Host or Algal Changes Induced by Infection	68
6. Concluding Remarks	70
Acknowledgments	72
References	72

### Abstract

Each symbiotic *Chlorella* species of *Paramecium bursaria* is enclosed in a perialgal vacuole (PV) membrane derived from the host digestive vacuole (DV) membrane. Algae-free paramecia and symbiotic algae are capable of growing independently and paramecia can be reinfected experimentally by mixing them.

Department of Environmental Science and Engineering, Graduate School of Science and Engineering, Yamaguchi University, Yamaguchi, Japan

This phenomenon provides an excellent model for studying cell-to-cell interaction and the evolution of eukaryotic cells through secondary endosymbiosis between different protists. However, the detailed algal infection process remains unclear. Using pulse labeling of the algae-free paramecia with the isolated symbiotic algae and chase method, we found four necessary cytological events for establishing endosymbiosis. (1) At about 3 min after mixing, some algae show resistance to the host lysosomal enzymes in the DVs, even if the digested ones are present. (2) At about 30 min after mixing, the alga starts to escape from the DVs as the result of the budding of the DV membrane into the cytoplasm. (3) Within 15 min after the escape, the DV membrane enclosing a single green alga differentiates to the PV membrane, which provides protection from lysosomal fusion. (4) The alga localizes at the primary lysosome-less host cell surface by affinity of the PV to unknown structures of the host. At about 24 h after mixing, the alga multiplies by cell division and establishes endosymbiosis. Infection experiments with infection-capable and infection-incapable algae indicate that the infectivity of algae is based on their ability to localize beneath the host surface after escaping from the DVs. This algal infection process differs from known infection processes of other symbiotic or parasitic organisms to their hosts.

**Key Words:** *Chlorella* spp., Digestive vacuole, Endosymbiosis, Infection, Lysosome, *Paramecium bursaria*, Perialgal vacuole. © 2010 Elsevier Inc.

## 1. INTRODUCTION

Endosymbiosis is a primary force in eukaryotic cell evolution. Recent studies of algal evolution have shown that endosymbiosis has occurred several times and has yielded a variety of eukaryotic cells. Despite the importance of this phenomenon, however, molecular mechanisms for the induction of endosymbiosis between different protists are not well known.

*Paramecium bursaria* cells harbor several hundred symbiotic *Chlorella* spp. in their cytoplasm (Fig. 2.1A). In *P. bursaria*, each symbiotic alga is enclosed in a perialgal vacuole (PV) membrane derived from the host digestive vacuole (DV) membrane, which provides protection from lysosomal fusion (Figs. 2.2B and 2.3B) (Gu et al., 2002; Karakashian and Rudzinska, 1981). Timing of cell divisions of both algae and the host cells is well coordinated (Kadono et al., 2004; Takahashi et al., 2007). For that reason, symbiotic algae can be inherited to the daughter cells. Irrespective of the mutual relations (see Section 5) between *P. bursaria* and symbiotic algae, the algae-free cells and symbiotic algae retain the ability to grow without a partner. Algae-free *P. bursaria* can be produced easily from algae-bearing cells using one of the following methods: rapid fission (Jennings, 1938); cultivation in darkness (Karakashian, 1963; Pado, 1965; Weis, 1969); X-ray

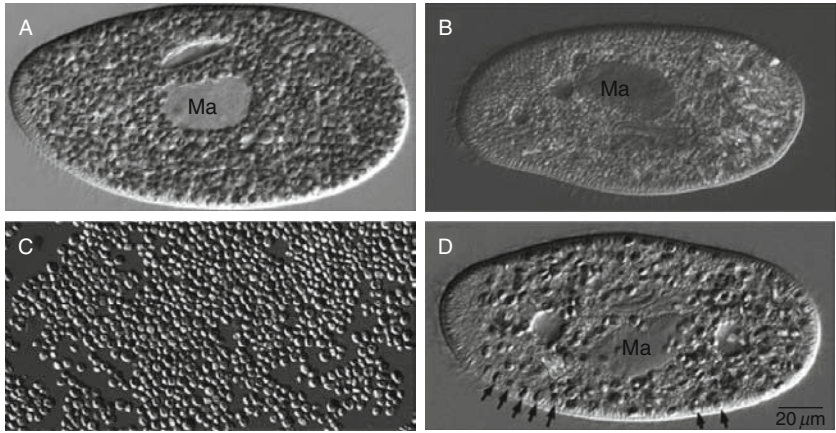


**Figure 2.1** Photomicrographs of *P. bursaria*: (A) algae-bearing strain OS1g1N; (B) algae-free *P. bursaria* strain Yad1w; (C) symbiotic *Chlorella vulgaris* isolated from OS1g1N cells; (D) strain Yad1w cells during the early infection process (4 h after mixing with isolated algae). Ma, macronucleus; Arrow, single green *Chlorella* (SGC), which can establish endosymbiosis. From Kodama and Fujishima (2008b).

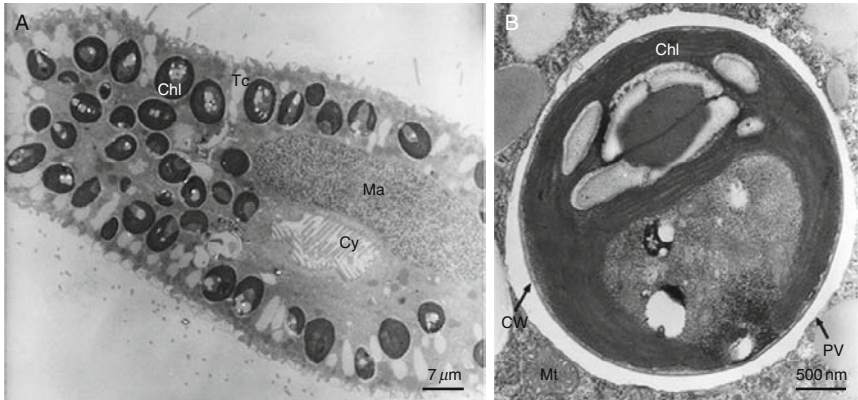


**Figure 2.2** Transmission electron micrographs of *P. bursaria*: (A) algae-bearing strain OS1g1N and (B) symbiotic algae near the host cell surface. Chl, chloroplast; Cy, cytopharynx; CW, cell wall; PV, perialgal vacuole; Ma, macronucleus; Mt, mitochondrion; Tc, trichocyst.

irradiation (Wichterman, 1948); treatment with 3-(3,4-dichlorophenyl)-1,1-dimethylurea (DCMU), a blocker of electron flow in photosystem II (Reisser, 1976); treatment with the herbicide paraquat (Hosoya et al., 1995; Tanaka et al., 2002); or treatment with a protein synthesis inhibitor, cycloheximide (Kodama and Fujishima, 2008a; Kodama et al., 2007; Weis, 1984).

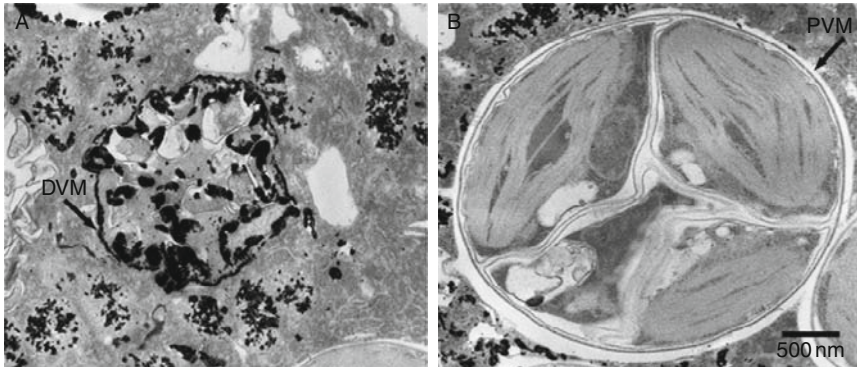


**Figure 2.3** Transmission electron micrographs to show acid phosphatase (AcPase) activity. Positive reaction products of AcPase are shown as black granules by Gomori's staining: (A) DV enclosing food bacteria; (B) PV enclosing symbiotic alga. Inside DV is AcPase-activity positive, but inside PV is activity-negative. DVM, digestive vacuole membrane; PVM, perialgal vacuole membrane.

On the other hand, symbiotic algae can be isolated easily by sonication, homogenization, or treatment with detergents. Furthermore, endosymbiosis between algae-free *P. bursaria* cells and symbiotic algae isolated from algae-bearing *P. bursaria* cells is easily reestablished by mixing them (Karakashian, 1975; Siegel and Karakashian, 1959). In fact, *P. bursaria* can be cultivated easily, producing a mass culture. The reinfection process can be observed easily under a light microscope. An algae-free mutant strain of *P. bursaria* has been collected (Tonooka and Watanabe, 2002, 2007). For these reasons, the symbiotic associations between *P. bursaria* and *Chlorella* spp. are considered an excellent model for studying cell-to-cell interaction and the evolution of eukaryotic cells through secondary endosymbiosis (Gerashchenko et al., 2000; Stoebe and Maier, 2002). However, the mechanisms and timings used by the algae to escape from the host DV and to protect themselves from host lysosomal fusion have long remained unknown. Therefore, in this review, we first introduce the algal reinfection process, as revealed using the pulse label and chase method. Then we review recently reported studies of mutual benefit between *P. bursaria* and symbiotic *Chlorella* spp.

## 2. INFECTION ROUTE

Infection of algae to algae-free *P. bursaria* is conducted through the host's phagocytosis. To investigate the algal infection process, we first examined the differentiation process of the host's DVs in phagocytosis, which has long remained unclear for this species.

## 2.1. Classification of DVs

The DVs of *P. multimicronucleatum* have been classified into four different stages (Fok and Allen, 1982). To classify the DV stages of *P. bursaria* that appear during infection by symbiotic algae and to determine the timing of the appearance of each stage, symbiotic algae and algae-free *P. bursaria* strain OS1w cells were mixed at densities of  $5 \times 10^7$  algae/ml and  $5 \times 10^3$  paramecia/ml under fluorescent lighting (1500 lux) at  $25 \pm 1$  °C and were washed with modified Dryl's solution (MDS) (Dryl, 1959) ( $\text{KH}_2\text{PO}_4$  was used instead of  $\text{NaH}_2\text{PO}_4 \cdot 2\text{H}_2\text{O}$ ). Then they were resuspended in the original density, and fixed with 4% paraformaldehyde at various times after mixing. The experimental procedure is presented in Fig. 2.4. The DVs containing several algae were classified into four stages based on their morphological characteristics and color changes of the algae: DV-I, at which stage the rounded vacuole membrane is clearly visible under a differential-interference-contrast (DIC) microscope and the algae are green; DV-II, where the vacuole is condensed so that the vacuole membrane is hardly visible under a DIC microscope and the algae are green; DV-III, where the vacuole has increased in size and the vacuole membrane is visible again and the algae are discolored as faintly yellow, green, or both. DV-III includes three substages: DV-IIIA contains green algae only; DV-IIIB contains both discolored and green algae; and DV-IIIC contains discolored algae only. In the final stage, DV-IV, the membrane is contracted similar to DV-II, making it difficult to view under a DIC microscope. The algae are green, brown, or both. Unlike DV-II, this vacuole was not observed in cells fixed before 3 min, but was observed 20–30 min after mixing. Furthermore, DV-IV includes three substages: DV-IVa contains green algae only; DV-IVb contains both green and brown algae; and DV-IVc contains brown algae only. The algae in each DV of nonfixed paramecia showed the same colors as those in the fixed paramecia.

To determine the timing of the appearance of each stage of DVs, algae-free *P. bursaria* cells were mixed with isolated symbiotic algae and fixed at 10 s intervals for 60 s. The fixed cells were classified into four stages according to the most advanced stage of DV in the cell (i.e., if DV-I and DV-II were both present in a cell, then the cell was classified as DV-II). Results show that DV-II started to appear in cells fixed at 30 s after mixing.

To determine the timing of DV-III appearance, algae-free cells were pulsed with isolated symbiotic algae for 1.5 min, then washed, chased, and fixed at every 1 min interval for 10 min after mixing. Subsequently, the cells were classified into four stages. As a result, DV-III started to appear in cells fixed at 3 min after mixing (Kodama and Fujishima, 2005).

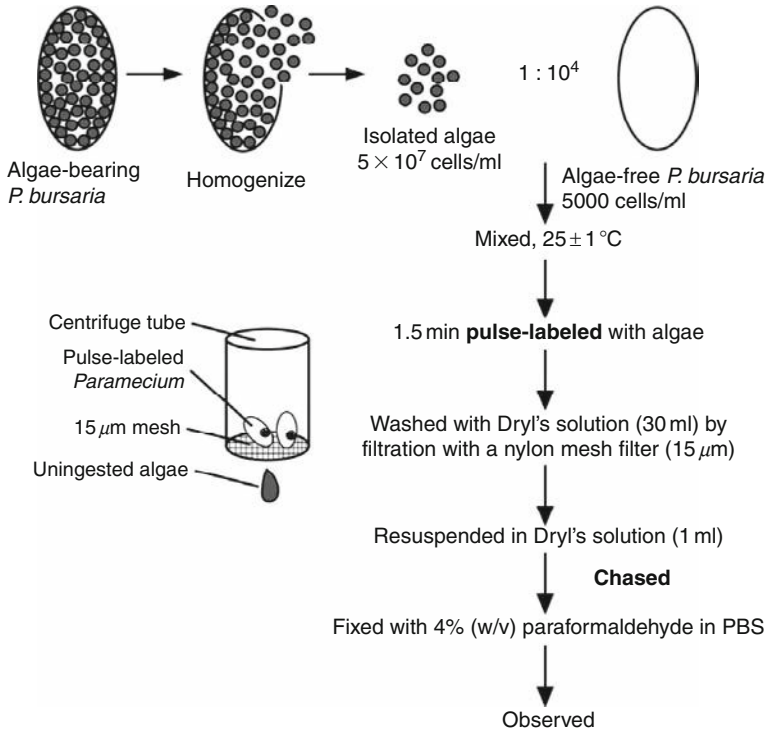


**Figure 2.4** Pulse-labeling and chasing with isolated symbiotic *Chlorella* sp. Algae-free *P. bursaria* cells were mixed at a density of  $5 \times 10^3$  cells/ml with isolated *Chlorella* sp. at  $5 \times 10^7$  algae/ml under fluorescent lighting (1500 lux) for 1.5 min at  $25 \pm 1^\circ\text{C}$ . The ciliate–algae mixture was transferred to a centrifuge tube equipped with a 15- $\mu\text{m}$  pore size nylon mesh and filtered. By pouring fresh modified Dryl's solution (MDS) (Dryl, 1959) ( $\text{KH}_2\text{PO}_4$  was used instead of  $\text{NaH}_2\text{PO}_4 \cdot 2\text{H}_2\text{O}$ ) into the tube, paramecia were washed and algal cells outside paramecia were simultaneously removed through the mesh. Paramecia that were retained in the mesh were transferred to another centrifuge tube and resuspended in MDS, and then chased for various times under fluorescent lighting (1500 lux) at  $25 \pm 1^\circ\text{C}$ . The cell suspension was fixed by mixing it with same volume of 8% (w/v) paraformaldehyde in phosphate-buffered saline (PBS) (137 mM NaCl, 2.68 mM KCl, 8.1 mM  $\text{Na}_2\text{HPO}_4 \cdot 12\text{H}_2\text{O}$ , 1.47 mM  $\text{KH}_2\text{PO}_4$ , pH 7.2) at various times. The cells were observed under a DIC microscope.

## 2.2. Timing of acidosomal and lysosomal fusion to DV

For *P. multimicronucleatum*, it has been reported that intravacuolar pH was changed by the following acidosomal and lysosomal fusion (Fok and Allen, 1982). To determine the timing of the acidosomal and lysosomal fusion to the DVs, we examined the change of the inside pH of *P. bursaria* DVs. Yeast cells were labeled with three kinds of pH indicator dyes, Congo red, bromocresol green (BCG), and bromophenol blue (BPB) and mixed with

algae-free *P. bursaria*. Then the color changes of the ingested yeast cells in the DVs were observed. The color changes of respective dyes occurring in phthalic acid and citric acid buffers are presented in Table 2.1. These changes did not differ between the buffers, but they were dependent on the pH. Figure 2.5 portrays the BCG-labeled yeast cells that were ingested in living paramecia. Figure 2.5A shows that within 0.5 min after mixing, the yeast cells were blue, indicating that the intravacuolar pH was 6.4–7.0.

**Table 2.1** Color of yeast cells labeled with pH indicator dyes in buffers at various pH levels

pH	Color of yeast cells labeled with:		
	Congo red	Bromocresol green (BCG)	Bromophenol blue (BPB)
7.0		Blue	
6.4		Blue	
6.0		Dark blue–green	
5.4		Dark blue–green	
5.0	Red	Blue–green	Blue
4.4	Dark red	Blue–green	Blue
4.0	Dark red	Green	Blue–green
3.4	Dark red	Green	Green
3.0	Purple	Yellow–green	Yellow–green
2.4	Purple	Yellow–green	Yellow–green

From Kodama and Fujishima (2005).

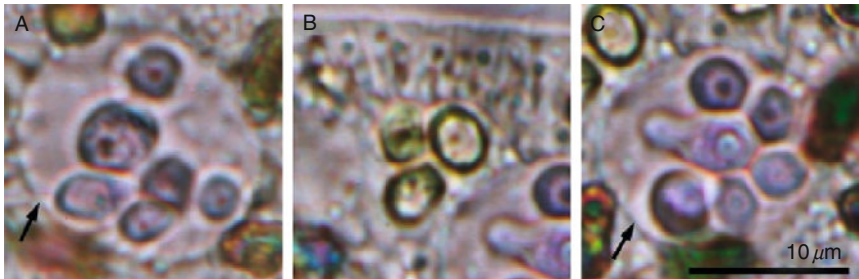


**Figure 2.5** Color changes of bromocresol green (BCG)-labeled yeast cells in DVs of algae-free *P. bursaria* strain OS1w. Algae-free cells and BCG-labeled yeast cells were mixed and the color of the yeast in the host DVs was observed in living cells under a DIC microscope. (A) DV-I: it appears soon after mixing, the yeast cells are blue, indicating that the intravacuolar pH is 6.4–7.0. (B) DV-II: yellow–green yeast cells at 1–2 min after mixing, indicating that the intravacuolar pH is 2.4–3.0. The DV membrane of DV-II is hardly visible under the light microscope. (C) DV-III: blue yeast cells at 3 min after mixing, indicating that the intravacuolar pH is 6.4–7.0. Updated from Kodama and Fujishima (2009c).



At 1–2 min after mixing, yeast cells became yellow–green, as presented in Fig. 2.5B, indicating that the intravacuolar pH decreases to 2.4–3.0. Morphological differentiation of DV-II from DV-I occurred at 0.5–1 min after mixing. These results show that acidosomal fusion to the DV occurs at 0.5–1 min after ingestion. Using Congo-red labeled yeast, we obtained identical results (Kodama and Fujishima, 2005).

Partially digested yellow algae are observed first in DV-IIIb at 2–3 min after mixing. In the late stage of DV-II, BCG-labeled yeast cells became blue, as shown in Fig. 2.5C, indicating that the intravacuolar pH is 6.4–7.0. These results suggest that lysosomal fusion might start before 2–3 min after mixing. Gomori's staining (Gomori, 1952), which is used for detecting intravacuolar acid phosphatase (AcPase) activity, showed that both DV-I and DV-II are AcPase-activity negative, but all substages of DV-III and DV-IV were AcPase-activity positive (Kodama and Fujishima, 2009a, see Section 2.3.3 in this review). These results suggest that lysosomal fusion occurs before 2–3 min after mixing. A schematic representation of DV differentiation of *P. bursaria* is presented in Fig. 2.6.

### 2.3. Presence of four cytological events needed to establish endosymbiosis

Timings for algal escape from the host DV and for protection of themselves from the host's lysosomal fusion were classified. Furthermore, four cytological events that are necessary to establish endosymbiosis were found.

#### 2.3.1. Acquisition of temporal resistance to lysosomal enzymes

In the host cytoplasm, single green *Chlorella* (SGC) is enclosed in a PV membrane derived from the host DV membrane, which provides protection from host lysosomal fusion, as shown in Fig. 2.3B. This indicates that timing of the appearance of SGC should be considered as almost the same as that of the appearance of the PV membrane during the infection process. To determine the timing of the appearance of the SGCs, algae-free *P. bursaria* were pulsed with isolated symbiotic algae for 1.5 min, chased, then fixed at 0.05, 0.5, 1, 1.5, 2, 3, 6, 9, 24, 48, and 72 h after mixing. The percentages of cells with SGC, single digested *Chlorella* (SDC), DV-IIIa or DV-IIIb, and DV-IVa or DV-IVb are portrayed in Fig. 2.7 (Kodama and Fujishima, 2005). All SGCs that existed in the host cytoplasm before 30 min after mixing were digested. One hour after mixing, however, SGCs reappeared in the host cytoplasm. Figure 2.7 depicts that the SGCs that appeared after 0.5 h were derived from DV-IVa or DV-IVb because no green algae were present in other DVs. At 24 h, the SGCs began to multiply by cell division, indicating that these algae had established endosymbiosis (see Section 2.4 in this review). In contrast to results of an earlier study (Meier and Wiessner, 1989), Fig. 2.7 shows that the algal escape from the DV-IVa

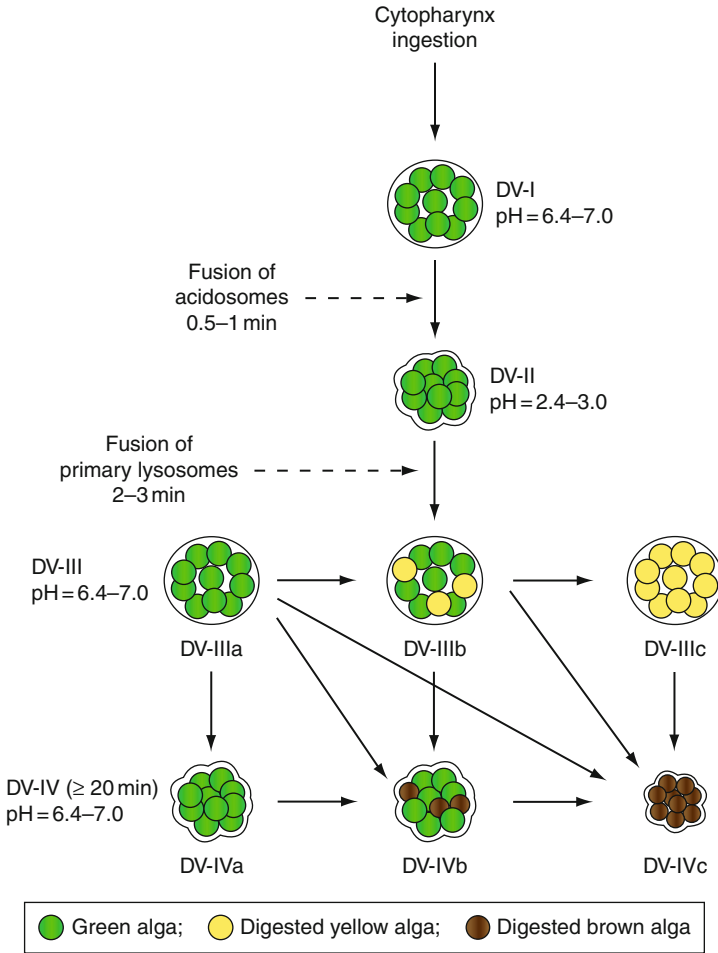


**Figure 2.6** Schematic representation of DV differentiation of *P. bursaria*. When isolated symbiotic *Chlorella* sp. and algae-free paramecia are mixed, one or several algae pass through the host cytopharynx and are pinched off as DV-I. The pH inside DV-I is 6.4-7.0. Acidified and condensed DV-II appeared 0.5-1.0 min after mixing. The pH inside DV-II is 2.4-3.0. Lysosomal fusion occurred at 2.0-3.0 min, leading to swollen DV-IIIa to DV-IIIc. Partially digested yellow algae appeared in DV-IIIb and DV-IIIc. The pH inside DV-III is 6.4-7.0. Condensed DV-IVa to DV-IVc appeared at 20-30 min. The pH inside DV-IV remains at 6.4-7.0. The algae become brown by digestion in DV-IVb and DV-IVc. White circle shows intact green alga. Gray circle shows digested yellow alga. Black circle shows digested brown alga.

or DV-IVb vacuole occurs after acidosomal and lysosomal fusion to the DV. When boiled algae are added to algae-free paramecia, they are all digested in DV-III. Consequently, only the living *Chlorella* can avoid lysosomal digestion in the host DVs.

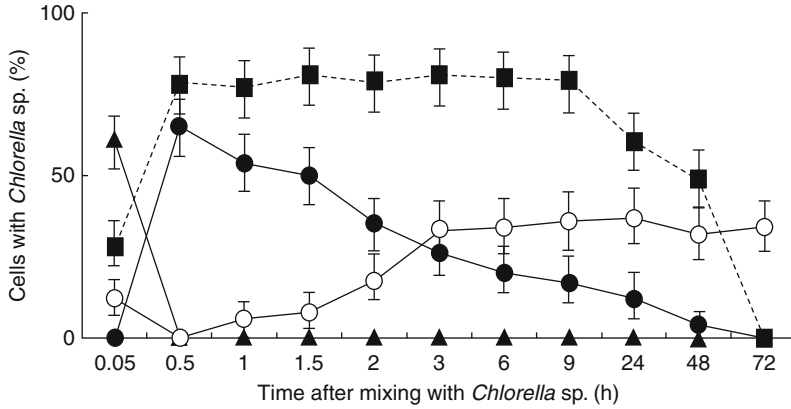


**Figure 2.7** Fate of living *Chlorella* sp. during infection. Isolated symbiotic *Chlorella* sp. and algae-free paramecia were mixed for 1.5 min, washed, chased, and fixed at 0.05, 0.5, 1, 1.5, 2, 3, 6, 9, 24, 48, and 72 h after mixing. The percentages of cells with single green *Chlorella* sp. (SGC), single digested *Chlorella* sp. (SDC), DV-IIIa or DV-IIIb, and DV-IVa or DV-IVb were determined. All SGCs that appeared before 0.5 h after mixing were digested by 0.5 h. After 0.5 h, the percentage of the cells with SGC increased gradually. (▲) Cells with DV-IIIa or DV-IIIb; (●) Cells with DV-IVa or DV-IVb; (○) Cells with SGC; (■) Cells with SDC. For each fixing time interval, 100–300 cells were observed. Bar, 90% confidence limit. From Kodama and Fujishima (2005).

Which DVs are the sources for SGCs? At 30 min after mixing with algae, *Paramecium* cells of five kinds were observed: cell with no alga, cell with digested alga cell with DV-IVa, cell with DV-IVb, and cell with SGC (Fig. 2.8A). The frequency of appearance of these cells was examined by fixing cells at various times after a 1.5 min pulse label with isolated algae (Fig. 2.8B). When DVs or algae of multiple types were present in the same cell, the cell was classified according to the oldest stage, following the scheme presented in Fig. 2.8A. Figure 2.8B shows that the proportion of cells with SGCs was 0% at 0.5 h and that the share increased as time passed. In contrast, the percentage of cells with DV-IVb decreased. At 72 h after mixing, all cells either contained SGCs or were without any algae. The SGCs localized beneath the host cell surface started to divide at and after 24 h of mixing. At 72 h after mixing, about 35% of the cells had SGCs. On the other hand, fewer than 5% of cells contained DV-IVa during the experimental period, if any, which indicates that most SGCs maintained in the host cell appeared from DV-IVb, and the SGCs acquired temporary resistance to the host's lysosomal enzymes in DV-IVb after acidosomal and lysosomal fusion occurred.

What determines the algal fate to survive in DV-IVb fused with lysosomes? We examined the following.

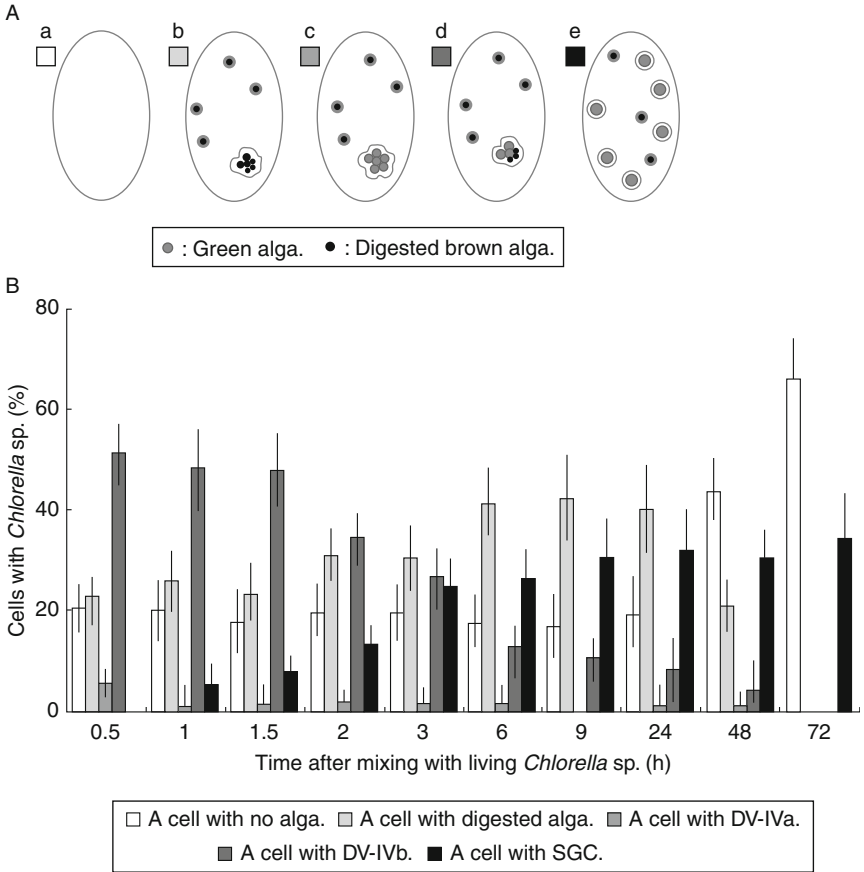


**Figure 2.8** Source of SGCs that can establish endosymbiosis. Algae-free cells were mixed with isolated symbiotic algae for 1.5 min, washed, chased, and fixed at 0.5, 1, 1.5, 2, 3, 6, 9, 24, 48, and 72 h after mixing, as described above. (A) Cells fixed at 0.5 h after mixing with algae can be classified as the following five types: a, a cell with no algae; b, a cell with digested algae; c, a cell with DV-IVa; d, a cell with DV-IVb; e, a cell with SGC. Regarding cells of several types, that is, types b–e seen together, the cells were classified in the order  $b < c < d < e$ . For example, when a cell has DVs with digested algae and SGC, the cell was classified as type e. (B) Percentage of each type of the cells observed. Percentages of cells with SGCs, starting at 0% at 0.5 h increased as time elapsed. In contrast, percentage of cells with DV-IVb decreased. At the same time, the percentage of cells with DV-IVa remained less than 5%. This observation shows clearly that the majority of the SGCs originated from DV-IVb. At each fixing time interval, 100–230 cells were observed. Bar, 95% confidence limit. From Kodama and Fujishima (2005).

**2.3.1.1. Light microscopy of cloned symbiotic *Chlorella vulgaris* cells in the host DV** Different types of algae infecting *P. bursaria* clones exhibit different infection ratios and host dependencies (Nakahara et al., 2003; Nishihara et al., 1999). These differences suggest that different *Chlorella* species or strains used together for infection might result in different algal fates in DV-IVb. To confirm this possibility, symbiotic algae were cloned and the fate of the algae was observed after ingestion in the host DVs. The cloned algae were identified as *C. vulgaris* by observation of their morphological characteristics using light and electron microscopy and by performing a similarity search with the 18S rDNA sequence from the cells (M. Nakahara, unpublished data). Cloned symbiotic algae were mixed with algae-free *P. bursaria* for 1.5 min, then washed and observed 3 h after mixing under a light microscope. Results show that DV-IVb appeared in the host cell, which demonstrates that the different algal fates in DV-IVb are not attributable to differences among algal species or strains.

Figure 2.9 portrays various DV-IVb vacuoles in the host cells 3 h after mixing with cloned symbiotic *C. vulgaris*. Both digested brown and non-digested green algae were present in the same DV, but they showed no specific location, indicating that their different fates of algae are not determined by their positions in the DV. To determine whether the surviving algal cells in the DV-IVb had been protected by their original PV membrane or not, the isolated symbiotic algae were treated with Triton X-100 or Tween 20 detergents before mixing with algae-free cells. No significant difference was found in the ratio of cells with DV-IVb between paramecia mixed with nontreated and treated algae, which shows that the original algal PV membrane, if it is retained before mixing with algae-free cells, is not the cause of algal survival in the host DV (Kodama et al., 2007).

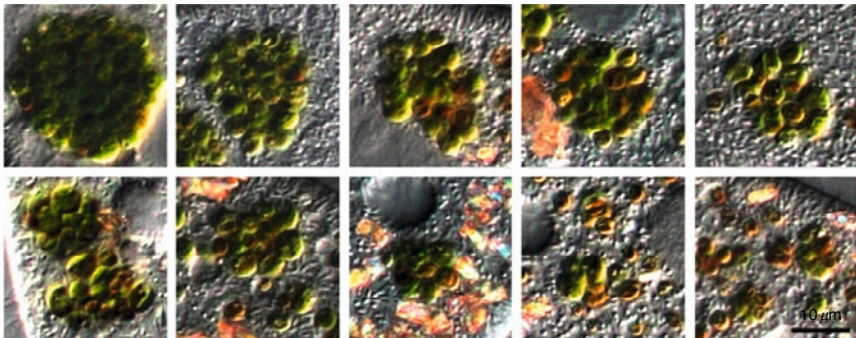


**Figure 2.9** Photomicrographs of various DV-IVb observed 3 h after mixing with algae. Green and brown algae inside the DV-IVb are, respectively, intact algae and digested algae. No relation exists between the algal fates and diameter of DV or algal location in DV-IVb.

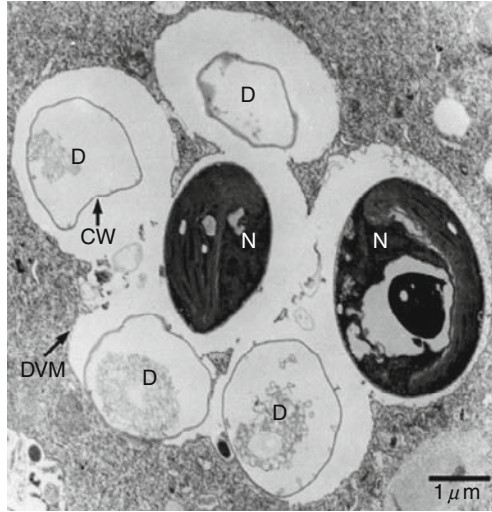


**Figure 2.10** Transmission electron micrograph of a DV-IVb vacuole. At 3 h after mixing with symbiotic *C. vulgaris*, algae-free *P. bursaria* were fixed for transmission electron microscopic observation. Each alga in DV-IVb vacuole adheres to the DV membrane. Electron-translucent digested (D) and electron-dense nondigested (N) algae are present together in the same DV. The nondigested algae are not separated from the digested algae by a membrane representing a PV membrane. DVM, DV membrane; CW, cell wall. From Kodama and Fujishima (2009c).

**2.3.1.2. Transmission electron microscopy of symbiotic *C. vulgaris* cells in the host DV** To confirm the possibility that some algae might have been wrapped with a PV membrane in the DV-IVb before escaping from the DV, the DV-IV was observed using a transmission electron microscope. Figure 2.10 shows DV-IVb, in which the vacuole, intact algae appear as electron-dense cells (Fig. 2.10, N). In contrast, digested algae appear as electron-translucent cells with empty spaces between the cell wall and the cytoplasm (Fig. 2.10, D). Gu et al. (2002) reported that the space between the PV membrane and the algal cell wall is about 25–100 nm wide. Figures 2.2B and 2.3B show a very small distance between the PV membrane and the algal cell. As Fig. 2.10 shows, no membrane resembling a PV membrane was observed around the electron-dense nondigested algae. Therefore, the algal fates are not determined by PV membrane acquisition in the host DV-IVb. The PV membrane might be formed during or after algal escape from the DV-IVb (Kodama et al., 2007).

**2.3.1.3. Effects of cycloheximide and puromycin on algal survival in the host DV during infection** By the treatments with 10–100 μg/ml of cycloheximide, all algae-bearing cells eventually lost the symbiotic algae and

became algae-free cells at 5–9 days after the treatment (Kodama and Fujishima, 2008a). However, no marked effect on cell division of the algae-free cells was found until 3 days after the treatment. These results suggest that cycloheximide inhibited algal protein synthesis but had little effect on host protein synthesis. In contrast, host cell division was inhibited considerably by treatment with 75 and 100  $\mu\text{g}/\text{ml}$  of puromycin. These results coincide well with earlier observations reported by Ayala and Weis (1987) (Kodama et al., 2007).

To determine whether algal or host protein synthesis is needed for algal survival in the host DV, isolated cloned symbiotic *C. vulgaris* strain 1N and algae-free cells were pretreated with cycloheximide or puromycin. Results show that most of the paramecia formed DVs ingesting algae 3 min after mixing with or without cycloheximide treatment. The DV-IVb appeared in the cycloheximide-treated cells; the relative frequency of cells with DV-IVb 3 h after mixing did not differ considerably from that of the control experiment cells (without cycloheximide treatment). On the other hand, DV formation was markedly reduced to about half by puromycin treatment, although DV-IVb appeared and the relative frequency of cells with DV-IVb 3 h after mixing did not differ markedly from that of the control experiment cells (without puromycin treatment). These results show that, in the host DV, neither algal nor host protein synthesis is necessary for algal acquisition of lysosomal enzyme resistance (Kodama et al., 2007).

Karakashian (1975) reported that the greater the number of algae within a single DV, the more likely they are to be capable of preventing the digestion of the vacuole contents, thereby suggesting that algal digestion in the host DV might be related to DV size. To confirm this, we examined the relation between the diameter of the DV containing algae and the presence of digested algae in the DV. *Paramecium* cells were pulse-labeled with isolated symbiotic algae for 1.5 min, washed, and then fixed at 3 h after mixing. The DV-IVs were then classified into three substages as described above: DV-IVa, DV-IVb, and DV-IVc. Then the mean diameter of each DV was measured under a DIC microscope. The mean diameter of DV-IVa (about 23  $\mu\text{m}$ ,  $n > 35$ ) was about twice that of DV-IVb (about 11  $\mu\text{m}$ ,  $n > 128$ ). In contrast, the mean diameter of DV-IVc (about 6.5  $\mu\text{m}$ ,  $n > 64$ ) was the least of the DV-IV types. Therefore, the algae in large DVs are rarely digested, which agrees with the observations of Karakashian (1975) and Kodama and Fujishima (2005) (Kodama et al., 2007). Furthermore, Karakashian and Karakashian (1973) reported that living algae might be able to influence the host cell's digestive processes, and thereby prevent their own digestion. This interference might be affected by secretion of a digestive enzyme inhibitor, or algae might induce a change in the DV membrane so that it can no longer fuse with lysosomes. Therefore, we observed the AcPase activity of the large diameter DV 30 min after mixing with algae. As a result, AcPase activity was present even in such large DVs.

These observations demonstrate that each alga becomes hardly digested for unknown reasons if many algae are ingested in a large DV, irrespective of host lysosomal fusion to such DVs. Consequently, to date, the factor that determines the algal fate, whether it survives or is digested in DV-IV, is not clear; the reason why the large DV can protect algae from digestion remains unknown (Kodama and Fujishima, 2009a; Kodama et al., 2007).

### 2.3.2. Escape from the host DV

At 30 min after mixing with symbiotic algae, some algae start to escape from the DV-IVb because of budding of the membrane into the cytoplasm. This budding is induced not only by living algae but also by the algae that are boiled, fixed with 2.5% (v/v) glutaraldehyde, or fixed with 5.0% (v/v) formaldehyde. Both living and boiled yeasts also escaped from the DVs of *P. bursaria* (Kodama and Fujishima, 2005; Suzaki et al., 2003; Y. Kodama and M. Fujishima, unpublished results). Inorganic polystyrene latex spheres of 3  $\mu\text{m}$  diameter escape too (Y. Kodama and M. Fujishima, unpublished results). However, this budding is not induced when India ink, 0.81- $\mu\text{m}$ -diameter polystyrene latex spheres, or food bacteria *Klebsiella pneumoniae* were ingested into the DVs (Kodama and Fujishima, 2005). These results suggest that *P. bursaria* can recognize the diameter of the contents inside the DVs and that those with 3  $\mu\text{m}$  or greater diameter can escape from the DV. The *Pseudomonas* spp. bacteria ingested by algae-free *P. bursaria* can be maintained in the host PVs, indicating that these organisms can also escape from the host DVs (Görtz, 1982). To date, molecular mechanisms for budding and escape from the DVs remain unknown.

### 2.3.3. Differentiation of the PV membrane from the host DV membrane

To elucidate the timing of the PV from the host DV, algae-free cells were mixed with isolated symbiotic algae for 1.5 min, washed, chased, and fixed at 0.5 min (Fig. 2.11A and B), 1 min (Fig. 2.11C and D), 10 min (Fig. 2.11E and F), 30 min (Fig. 2.11G and H), and 3 h (Fig. 2.11I–L). Figure 2.11A and B shows DV-I. Figure 2.11C and D show DV-II. Figure 2.11E and F shows DV-IIIb, which contain both nondigested green and digested yellow algae. Figure 2.11G and H shows DV-IVb, which contain both nondigested green and digested brown algae. Figure 2.11I and J shows DV-IVb in which a single green alga is just escaping as the result of the budding of the vacuole membrane (red arrowhead). Insets of Fig. 2.11I and J shows enlarged images of the escaping green alga. Figure 2.11K and L images show areas near the host cell surface of paramecia fixed at 3 h: green algae that escaped from the DV-IVb vacuole adhered just under the host cell surface (black arrows). The translocation of SGC beneath the host cell surface and their attachment there begin about 45 min after mixing, at the earliest. Timing of the appearance of



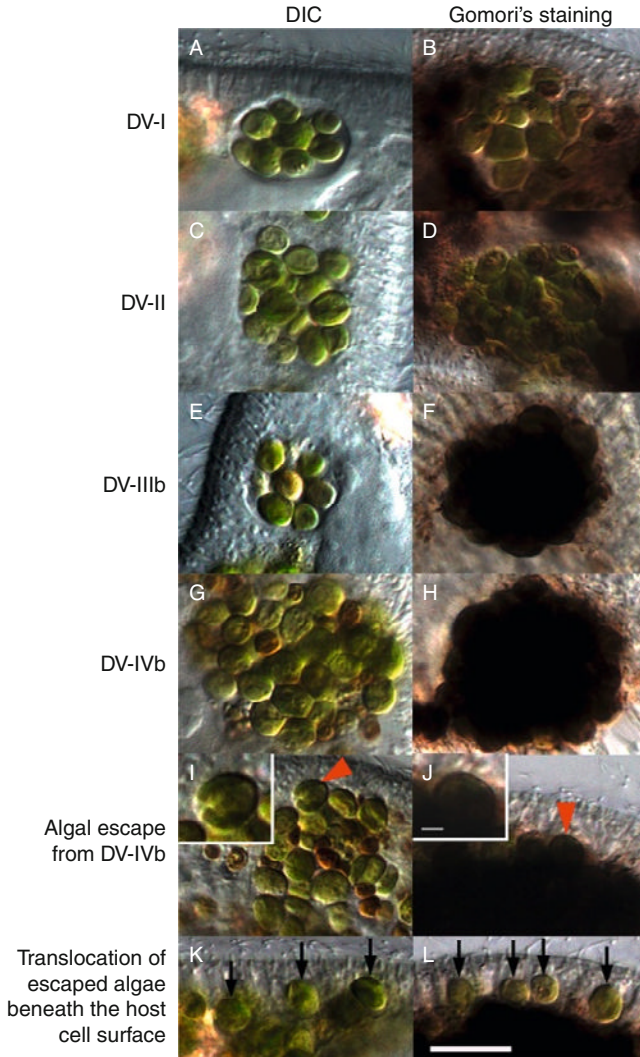


**Figure 2.11** Differential-interference-contrast (DIC) micrographs of infection process of symbiotic *C. vulgaris* cells to algae-free *P. bursaria* cells. Algae-free paramecia were mixed with isolated algae and fixed with 2% glutaraldehyde in 0.1 M cacodylate buffer, pH 7.2 containing 8% sucrose at 0.5 min (A and B), 1 min (C and D), 10 min (E and F), 30 min (G and H), and 3 h (I–L) after mixing. Cells nontreated with Gomori's solution: A, C, E, G, I, and K. Cells treated with Gomori's solution: B, D, F, H, J, and L. For paramecia fixed at 10 min, 30 min, and 3 h after mixing, cells were mixed with isolated algae for 1.5 min, washed with MDS, chased, and fixed. Experiments were repeated more than 10 times, demonstrating the results's reproducibility. DV-I, A and B; DV-II, C and D; DV-IIIb, E and F; DV-IVb, G and H. Panels (I) and (J) show an alga just escaping as the result of budding of the DV-IVb membrane (red arrowhead). Insets of

AcPase activity was examined by staining the pulse-labeled cells with Gomori's solution. Figure 2.11A, C, E, G, I, and K portrays cells that had not been treated with Gomori's solution (control). In Fig. 2.11A (DV-I) and E (DV-IIIb), the DV membranes were clearly visible under a light microscope. In contrast, in Fig. 2.11C (DV-II), G (DV-IVb), and I (DV-IVb), the DV membranes were hardly visible because of contraction of the DVs. In Fig. 2.11E, G, and I, partially digested yellow and brown algae appeared in the DVs. Figure 2.11B, D, F, H, J, and L shows cells stained with Gomori's solution. The AcPase activity detected using Gomori's staining is shown as black granules. Figure 2.11B and D shows that DV-I and DV-II vacuoles were AcPase-activity negative. On the other hand, the AcPase activity appeared in DV-IIIb (Fig. 2.11F) and later stages (Fig. 2.11H and J). The AcPase-activity also appeared in DV-IIIa, DV-IIIc, DV-IVa, and DV-IVc. Black mist-like precipitates were also observed outside the DVs in Fig. 2.11B and D, but decreased in DV-IIIb (Fig. 2.11F) and later stages (Fig. 2.11H, J, and L). These might be primary lysosomes in the host cytoplasm before fusion with DVs. As presented in Fig. 2.8, about 50% of cells 30 min after mixing had DV-IVb vacuoles containing both the green-colored intact algae and partially digested brown algae. Actually, 95.6% of DVs 30 min after mixing were AcPase-activity positive. Therefore, it appears that the DV-IVb vacuoles are AcPase-activity positive, which shows that green-colored algae in DV-IVb vacuoles acquired host lysosomal enzyme resistance in the lysosome-fused DVs as described in Section 2.3.1 of this review. Some of the green-colored alga escapes from the DV-IVb (Fig. 2.11I and J, red arrowheads). Such single green colored alga was covered by thin black layers of Gomori's staining (Fig. 2.11J, red arrowhead), although the SGCs, which were able to escape successfully from the DV-IVb and which localized just under the host cell surface (Fig. 2.11L, arrows) were not covered by the black thin layer. That important difference indicates that the inside of the budded DV membrane enclosing green algae is still AcPase-activity positive, although the inside of the vacuole enclosing an SGC, which is derived from the DV-IVb and localized beneath the host cell surface, is AcPase-activity negative. That fact underscores that differentiation from the host DV membrane to the PV membrane occurs after the appearance of SGCs as the result of budding of the host DV membrane and before translocation of the SGCs beneath the host cell surface. That the first SGC and the first localization of the SGC

---

(I) and (J): enlarged photomicrographs of the escaping alga. (K and L): algae attached immediately beneath the host cell surface (black arrows). DV-I (B) and DV-II (D) are AcPase-activity negative, and DV-IIIb (F) and DV-IVb (H and J) are AcPase-activity positive. The SGCs escaping from the host DVs and which are translocated immediately beneath the host cell surface are AcPase-activity negative (L, black arrows). Bars, 10  $\mu\text{m}$  (L) and 2  $\mu\text{m}$  (inset in J). From Kodama and Fujishima (2009a).

beneath the host cell surface, respectively, occur at 30 and 45 min after mixing suggests that differentiation of the PV membrane occurs within 15 min after the algal escape from the host DV. In fact, that is the first reported evidence elucidating the timing of differentiation of the PV membrane from the DV membrane during the infection process of symbiotic algae to algae-free *P. bursaria* (Kodama and Fujishima, 2009a).

#### 2.3.4. Attachment of PV beneath the host cell surface

Under the *Paramecium* cell surface, thousands of trichocysts are embedded as defensive organelles against predators (Harumoto and Miyake, 1991). Massive discharge of trichocysts in *Paramecium* can be induced by treatment with lysozyme without seriously injuring the cell, but a potent trichocyst discharge inducer, saturated picric acid, fixes the *Paramecium* (Harumoto and Miyake, 1991). The symbiotic algae appear to push the trichocysts aside to become fixed near the host cell surface after escaping from the host DVs. To examine the necessity of trichocysts for algal intracellular localization, algae-free cells and isolated symbiotic algae were mixed for 1.5 min, washed, and then resuspended with the same concentration in MDS. Algal escape from the host DVs begins at 30 min after mixing with algae (Kodama and Fujishima, 2005, 2009a). The pulse-labeled cells were treated with 1 mg/ml lysozyme 30 min after mixing. This concentration of lysozyme can induce full discharge of trichocysts. These cells were fixed at 3 and 24 h after mixing with algae in the presence of the lysozyme. They were then observed to determine whether the algae that had escaped from the host DVs were able to attach beneath the host cell surface of the trichocyst-removed cells.

In the control experiment, at 3 h, green algae attached beneath the host cell surface were observed (Fig. 2.12A and B). These algae apparently moved the trichocysts aside (Fig. 2.12B and C). On the other hand, green algae localized beneath the host cell surface, even in cases where the trichocysts had been removed (Fig. 2.12D–F). In such cells, the density of the algae attached near the host cell surface was higher than that in the trichocyst-bearing cells. Furthermore, regarding the ratio of paramecia with algae localized beneath the host cell surface, about 65% ( $n > 137$ ) of the control cells revealed green algae that had localized beneath the host cell surface, although it increased to about 95% ( $n > 179$ ) in the trichocyst-removed cells by 24 h after mixing. These results demonstrate that the PV membrane does not require trichocysts for the intracellular localization (Kodama and Fujishima, 2009b). Omura and Suzaki (2003) reported that when the algae-free *P. bursaria* cells were fed with *Chlorella*, their trichocysts became detached from the cell surface and finally disappeared, thereby allowing the ingested algae to approach the host cell surface. At the same time, Omura and Suzaki observed the appearance of many small vesicles of about 0.5  $\mu\text{m}$  diameter using transmission electron microscopy and expansion of the cyclosis region near the host cell surface. Their results and ours suggest that

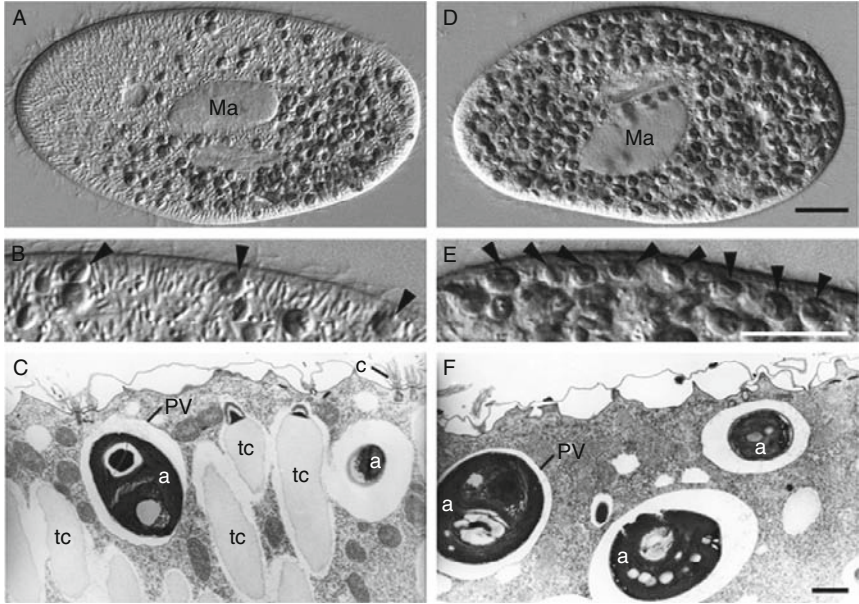


**Figure 2.12** Light and transmission electron micrographs of *P. bursaria*. Strain Yad1w cells that were pulse labeled with symbiotic *C. vulgaris* 1N cells without (A)–(C) or with (D)–(F) treatment of 1 mg/ml lysozyme. (B) and (E) show enlarged dorsal surfaces of living cells at 3 h after mixing with the algae. (A, B, D, and E) DIC micrographs of living cells at 3 h after mixing with the algae. (C and F) Transmission electron micrographs of *P. bursaria* at 3 h after mixing. In a control experiment, the algae moved trichocysts aside (A)–(C). The alga can attach beneath the host cell surface even if trichocysts were removed (D)–(F). Arrowheads in (B) and (E) show symbiotic algae localized immediately beneath the host cell surface. Ma, macronucleus; a, symbiotic *C. vulgaris* localized beneath the host cell surface; PV, perialgal vacuole; tc, trichocyst; c, cilia. Bars, 20  $\mu\text{m}$  (D and E) and 1  $\mu\text{m}$  (F). From Kodama and Fujishima (2009b).

trichocysts are obstacles to rather than prerequisites for algal localization beneath the host cell surface. How and where the symbiotic algae attach to the host cell surface remains unclear (Kodama and Fujishima, 2009b).

## 2.4. Initiation of algal cell division

To determine the timing of initiation of algal cell division during the infection process, algae-free *P. bursaria* were mixed with isolated symbiotic algae for 1.5 min, chased, and fixed at 1, 3, 6, 9, 24, and 48 h after mixing. Subsequently, the green algae per *Paramecium* cell were counted (Kodama and Fujishima, 2005). The average was 9.4 algae/cell at 1 h, decreasing to 4.0 algae/cell at 3 h, and remaining constant thereafter until 9 h. However, the ratio began to increase to 5.3 algae/cell at 24 h. In addition, dividing algae were frequently observed beneath the host cell surface at 24 h both

under light and transmission electron microscopy. The algae begin cell division at about 24 h after mixing with the host cells. On the other hand, *Paramecium* cells apparently did not multiply by binary fission until 72 h after mixing the algae.

We examined the effects of light on algal infection and algal cell division. Algae-free cells were pulse labeled with isolated symbiotic algae from algae-bearing *P. bursaria* cells cultivated under LL conditions for 1.5 min, as described above, and chased with or without light (1500 lux) at  $25 \pm 1$  °C. They were then fixed at 0.05, 0.5, 1, 6, 12, 24, 48, 72, and 96 h after mixing. Results show that the mean number of green algae in a cell showed no significant difference between these two cases for at least 6 h after mixing. However, after 12 h, the mean number of green algae increased gradually in the light, but not in the dark. The cell density of paramecia was almost constant for 4 days in both light and dark conditions. These results demonstrate that light is necessary for algal cell division, but not for algal translocation beneath the host cell surface after escaping from the host DVs (Kodama and Fujishima, 2005).

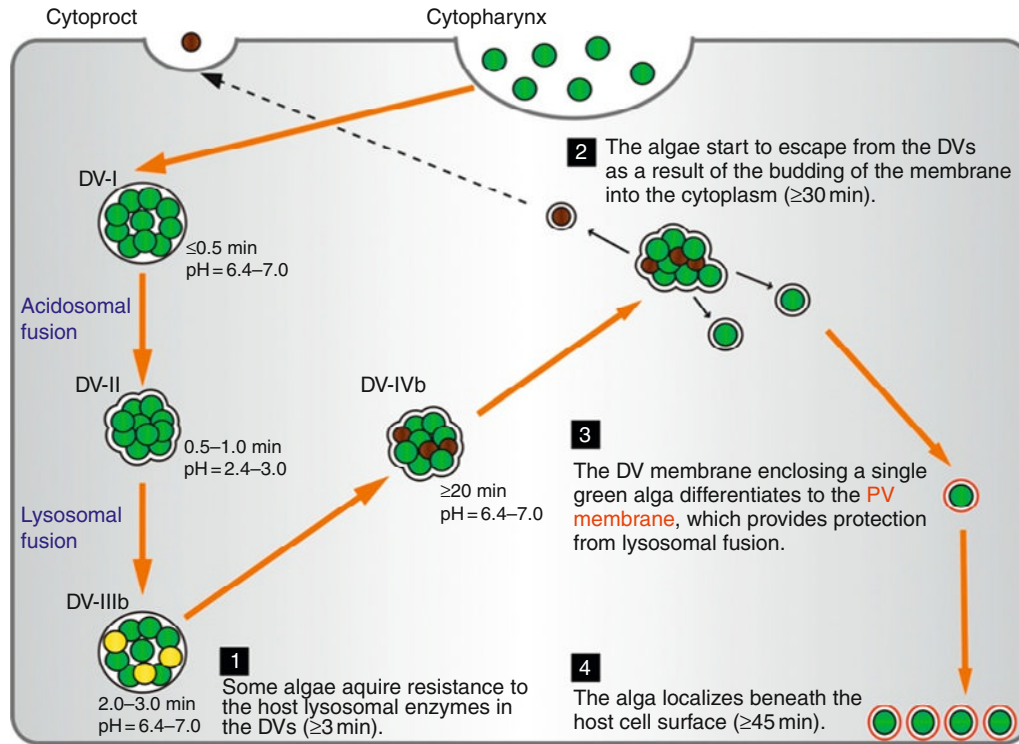
## 2.5. Summary of the infection route

Figure 2.13 presents a schematic representation of the algal infection process and four important cytological events necessary to establish endosymbiosis. Table 2.2 presents various changes of the host cells including the four events in Fig. 2.13 and their timings: they occur during and after algal reinfection.

### 3. DIFFERENT FATES OF INFECTION-CAPABLE AND INFECTION-INCAPABLE *CHLORELLA* SPECIES

Symbiotic *Chlorella* has been differentiated into two algal groups “American” (NC64A as the representative strain) and the “European” (strain, Pbi) using classical approaches and molecular phylogenetic and genetic structural analyses. Recently, Hoshina and Imamura (2009) determined the distribution of the “American” and “European” symbionts by ribosomal DNA sequencing (Fig. 2.14).

Karakashian and Karakashian (1965) and Bomford (1965) reported successful infection of algae-free *P. bursaria* with several strains of free-living algae. However, symbiotic *Chlorella* species derived from *Stentor polymorphus* or *Spongilla fluviatilis* were digested (Bomford, 1965). What is the difference between infection-capable and infection-incapable *Chlorella* spp. to the algae-free cells? Takeda et al. (1998) reported that algal infectivity is dependent on the sugar components of the rigid walls (alkali-insoluble part of the algal cell wall): “infection-capable” *Chlorella* species, including symbiotic



**Figure 2.13** Schematic representation of the algal reinfection process. Using pulse label and chase method, four important cytological events necessary to establish endosymbiosis were clarified. First, 3 min after mixing, some algae acquire temporary resistance to the host lysosomal enzymes in the DVs, even when the digested ones coexist. Second, 30 min after mixing, the algae start to escape from DVs as the result of budding of the membrane into the cytoplasm. Third, within 15 min after the escaping, the DV membrane enclosing SGC differentiated to the PV membrane, which provides protection from lysosomal fusion. Finally, the alga localizes beneath the host cell surface. At about 24 h after mixing, the alga increases by cell division and establishes endosymbiosis.

**Table 2.2** Various changes and their timings which occur during and after algal reinfection

Change	Timing after mixing with symbiotic algae	References
Acidosomal fusion to DVs	0.5–1 min	Kodama and Fujishima (2005)
Lysosomal fusion to DVs	2–3 min	Kodama and Fujishima (2005)
Algal escape from DVs as a result of the budding of the DV membrane	≥ 30 min	Kodama and Fujishima (2005, 2009a)
Differentiation of the DV membrane enclosing an SGC to the PV membrane	≥ 30 min	Kodama and Fujishima (2009a)
Translocation of SGCs beneath the host cell surface	≥ 45 min	Kodama and Fujishima (2005, 2009a)
Initiation of algal cell division	24 h	Kodama and Fujishima (2005)
Shift to the phase of photoaccumulation and mating reactivity rhythm of symbiotic algae	3–4 days	Miwa (2009), Kinoshita et al. (2009)
Acquisition of resistance to hydrogen peroxide (H <sub>2</sub> O <sub>2</sub> )	3–4 days	Kinoshita et al. (2009)

ones, are distinguishable by the presence of glucosamine as a chemical component in their rigid walls, whereas the rigid walls of “infection-incapable” species contain glucose and mannose. Therefore, we examined the algal infectivity and lectin-binding activity of NaOH-treated and -untreated algae.

### 3.1. Difference in algal attachment beneath the host cell surface

Free-living *Chlorella* species such as *C. vulgaris*, *Parachlorella kessleri*, and *C. sorokiniana* are known as infection-capable to algae-free *P. bursaria* cells, as are symbiotic *Chlorella* spp. isolated from algae-bearing *P. bursaria* cells, but *C. ellipsoidea*, *C. saccharophila*, *C. luteoviridis*, *C. zofingiensis*, and *C. mirabilis* are infection-incapable (Takeda et al., 1998). We examined the



**Figure 2.14** Distribution of the “American” (solid symbol) and “European” (empty symbol) *P. bursaria* symbionts, as determined by ribosomal DNA sequences. Two different symbol sizes indicate a record of one to three (smaller) or more than five (larger) samples. Unspecified localities in the USA and Russia, in spite of their vast national territories, are excluded. From Hoshina and Imamura (2009).

infectivity of 14 free-living strains of *Chlorella* and *Parachlorella* species for algae-free *P. bursaria* OS1w cells: *C. vulgaris* C-27, *C. sorokiniana* C-212 and C-43, *P. kessleri* C-208 and C-531, *C. ellipsoidea* C-87 and C-542, *C. saccharophila* C-183 and C-169, *C. fusca* var. *vacuolata* C-104 and C-28, *C. zofingiensis* C-111, and *C. protothecoides* C-150 and C-206 and the symbiotic *Chlorella* sp. strain C-201 derived from *S. fluviatilis*. The infection experiments were conducted by mixing the algae and algae-free *P. bursaria* for 1 h, washing and chasing them, and then fixing them at 1 h and 3 weeks after mixing. The paramecia were classified into four groups depending on the numbers of algae in the cells, that is, 0, 1–5, 6–20, and more than 20; the relative frequencies of these cells are depicted in Fig. 2.15. One hour after mixing, all observed paramecia ingested the algae, although the mean numbers retained in the cells differed among the algal strains used in this study (Fig. 2.15A). *C. sorokiniana* C-212 and *C. kessleri* C-531 were retained in the host cells and increased by cell division. These strains were maintained in the host cells for more than 2 years after mixing. However, *C. sorokiniana* C-43 and *P. kessleri* C-208 were not maintained for more than 4 weeks. A few cells of *P. kessleri* C-208, *C. ellipsoidea* C-542, *C. saccharophila* C-169, *C. fusca* var. *vacuolata* C-104 and C-28, *C. protothecoides* C-206, and *Chlorella* sp. strain C-201 remained in a few paramecia for 3 weeks after mixing (Fig. 2.15B). However, these algae disappeared from the host cells 4 weeks after mixing. Infection-capable algae, *C. sorokiniana* C-212 and *P. kessleri* C-531, localized beneath the host cell surface after escaping from the host DV at 3 weeks after mixing. Dividing algal cells were also observed. However, no examined infection-incapable algal strain localized near the host cell surface or divided. To confirm whether this phenomenon is associated with algal infectivity, algae-free



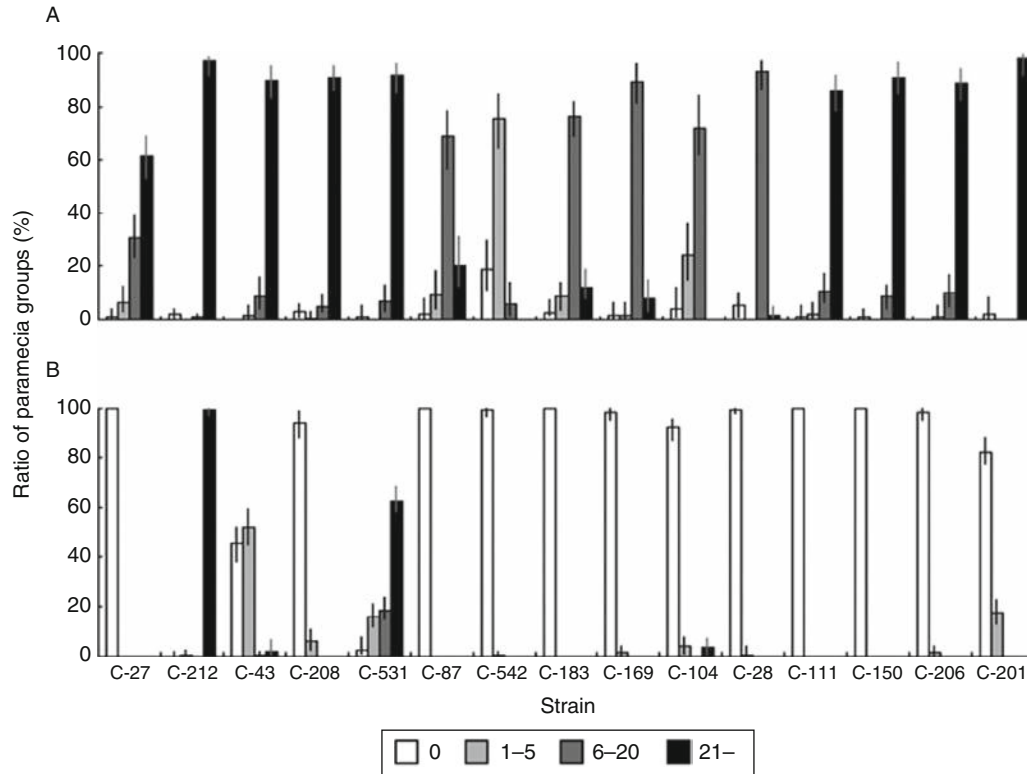


**Figure 2.15** Infectivity of symbiotic and free-living *Chlorella* species to the algae-free *P. bursaria* strain OS1w. (A) and (B) show results at 1 h and 3 weeks after mixing with algae, respectively. *Paramecia* fell into four groups according to the number of algae in the cytoplasm: 0 algae, 1–5 algae, 6–20 algae, and more than 20 algae. For both time intervals, 50–222 cells were observed. Bar in bar graph, 90% confidence limits. X-axis, strains of *Chlorella* species mixed with *paramecia*; Y-axis, percentage of each *paramecia* group. Only algal strains *C. sorokiniana*, C-212 and *C. kessleri* C-531 were maintained in the host cytoplasm. From Kodama and Fujishima (2007).

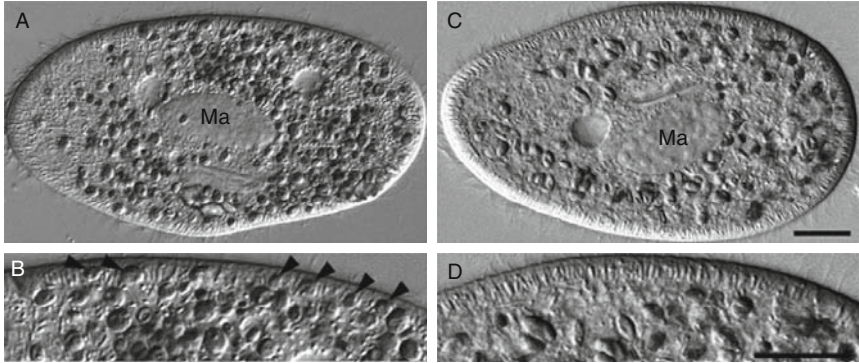


**Figure 2.16** Photomicrographs of *P. bursaria* strain Yad1w cells pulse labeled with symbiotic *C. vulgaris* cells strain 1N isolated from *P. bursaria* strain OS1g1N (A) and with *C. saccharophila* strain C-169 cells (B). Paramecia were observed 3 h after mixing. Symbiotic *C. vulgaris* cells are localized immediately beneath the host cell surface (arrowheads). In contrast, *C. saccharophila* C-169 cells escaped from the host DV, but they failed to localize beneath the host cell surface. Ma, macronucleus. Bars, 20  $\mu$ m.

*P. bursaria* were pulse labeled for 1.5 min with isolated symbiotic algae or infection-incapable *C. saccharophila* C-169 cells, washed, and then observed under a light microscope 3 h after mixing. Results confirmed that the isolated symbiotic algae can be localized beneath the host cell surface after escaping from the host DV (Fig. 2.16A and B), although the infection-incapable algal cells cannot be (Fig. 2.16C and D), which suggests that algal localization beneath the host cell surface might be a prerequisite phenomenon for the algal infection. Although Takeda et al. (1998) reported that all of the algae-free strains that they examined (strains T316w, Kz1w, Sj2w, Ok2w, and Uk2w) were able to establish endosymbiosis with all strains used (*C. vulgaris*, *P. kessleri*, and *C. sorokiniana*). In contrast, the strain OS1w used in this study was only able to establish endosymbiosis with specific strains of *C. vulgaris*, *P. kessleri*, and *C. sorokiniana*. On the other hand, Takeda et al. (1998) reported that the free-living *C. kessleri* C-208 was able to infect *P. bursaria* T316w, Kz1w, Sj2w, Ok2w, and Uk2w. However, the algal strain C-208 showed inability to infect *P. bursaria* OS1w in the present study. These results indicate that the establishment of endosymbiosis is both algae-strain and host-strain specific (Kodama and Fujishima, 2007).

### 3.2. Relation between sugar residues of the algal cell wall and infectivity

To examine the relation between sugar residues of the algal cell wall and infectivity, we examined the binding abilities of Alexa Fluor 488-conjugated WGA, GS-II, and Con A against NaOH-treated and

NaOH-untreated algal cell walls. It is known that WGA binds to *N*-acetylglucosamine and *N*-acetylneuraminic acid residues (Allen et al., 1973; Goldstein et al., 1975; Yamamoto et al., 1981), that GS-II binds to  $\alpha$ - or  $\beta$ - linked *N*-acetyl-D-glucosamine (Ebisu and Goldstein, 1978; Lyer et al., 1976), and that Con A binds selectively to mannose residues (Goldstein et al., 1974; Ogata et al., 1975; Poretz and Goldstein, 1970). In NaOH-untreated algal cell walls, fluorescence labeling with WGA was observed on the cell walls of *C. sorokiniana* C-212 and C-43. *Chlorella* sp. isolated from *P. bursaria* Bwk-16(C<sup>+</sup>) also showed fluorescence, but the fluorescence was present on only 6.9% ( $n > 1000$ ) of the cells. Other examined strains of *Chlorella* species showed no fluorescence. Fluorescence from GS-II was observed only on *C. saccharophila* C-183; not on the other strains examined. The Con A fluorescence was observed on *C. ellipsoidea* C-87 and C-542, *C. saccharophila* C-183 and C-169, *C. fusca* var. *vacuolata* C-104 and C-28, *C. zofingiensis* C-111, *C. protothecoides* C-150 and C-206, and strain C-201 derived from *S. fluviatilis*. *Chlorella* sp. isolated from *P. bursaria* Bwk-16(C<sup>+</sup>) also showed fluorescence, although it was present on only 6.2% ( $n > 1000$ ) of the cells. *C. vulgaris* C-27, *P. kessleri* C-208 and C-531, and *Chlorella* sp. isolated from *P. bursaria* OS1g, Dd1g, KM2g, and OS1g1N were not labeled by any of the lectins. Previous reports in the literature (Nishihara et al., 1996; Reisser et al., 1982; Weis, 1980) have described that symbiotic *Chlorella* spp. cells of *P. bursaria* are agglutinated by Con A if the cells are fixed with glutaraldehyde before mixing with Con A. However, despite glutaraldehyde fixation, Con A neither labeled the symbiotic *Chlorella* spp. cells nor agglutinated them in our experiments. In NaOH-treated algal cell walls, *C. vulgaris* C-27 and *C. sorokiniana* C-43 and C-212 were labeled with WGA fluorescence, although the last strain showed only a few positive cells (2%,  $n > 500$ ). Symbiotic algae obtained from *P. bursaria* OS1g, Dd1g, KM2g, Bwk-16(C<sup>+</sup>), and OS1g1N also showed WGA fluorescence. In addition, GS-II fluorescence was observed on *C. vulgaris* C-27 and *C. sorokiniana* C-212 and C-43; also, a few positive cells were observed for *P. kessleri* C-208 (7.4%,  $n > 161$ ) and C-531 (3.4%,  $n > 238$ ). Furthermore, GS-II also labeled *C. ellipsoidea* C-87 and C-542, *C. saccharophila* C-183 and symbiotic *Chlorella* sp. strain C-201 derived from *S. fluviatilis*, and those from *P. bursaria* OS1g, Dd1g, KM2g, Bwk-16(C<sup>+</sup>), and OS1g1N. Other results showed that Con A labeled *C. ellipsoidea* C-87 and C-542, *C. saccharophila* C-183 and C-169, *C. fusca* var. *vacuolata* C-104, *C. zofingiensis* C-111, *C. protothecoides* C-150 and C-206, *C. vulgaris* C-27, and *C. sorokiniana* C-43 and C-212, though only a few cells of the last strain were labeled (2%,  $n > 500$ ). Finally, Con A also labeled symbiotic *Chlorella* spp. C-201 derived from *S. fluviatilis* and those from *P. bursaria* OS1g, Dd1g, KM2g, Bwk-16(C<sup>+</sup>), and OS1g1N. Consequently, our data show no relation between the infectivity of *Chlorella* species to the algae-free *P. bursaria* and their lectin-binding activity of the cell walls with or without treatment with NaOH, as presented in Table 2.3 (Kodama and Fujishima, 2007).

**Table 2.3** Lectin-binding activity of the NaOH-treated and untreated cell walls of *Chlorella* species and their infectivity for algae-free *P. bursaria*

Species	Strain (alternative name)	Infectivity		Lectin labeling of <sup>a</sup>					
				Nontreated cells			NaOH-treated cells		
		T316w	OS1w	WGA	GS-II	Con A	WGA	GS-II	Con A
<i>C. vulgaris</i>	C-27 <sup>b</sup>	—	—	—	—	—	+	+	+
<i>C. sorokiniana</i>	C-212 (211-8k) <sup>c</sup>	+	+	+	—	—	±	+	±
	C-43 <sup>b</sup>	—	—	+	—	—	+	+	+
<i>Parachlorella kessleri</i> (formerly <i>C. kessleri</i> )	C-208 (211-11g) <sup>c</sup>	+	—	—	—	—	—	±	—
	C-531 (211-11 h) <sup>c</sup>	+	+	—	—	—	—	±	—
<i>C. ellipsoidea</i>	C-87 (211-1a) <sup>c</sup>	—	—	—	—	+	—	+	+
	C-542 (211-1a) <sup>c</sup>	—	—	—	—	+	—	+	+
<i>C. saccharophila</i>	C-183 <sup>b</sup>	—	—	—	+	+	—	+	+
	C-169 <sup>b</sup>	—	—	—	—	+	—	—	+
<i>C. fusca</i> var. <i>vacuolata</i>	C-104 (211-8b) <sup>b</sup>	—	—	—	—	+	—	—	+
	C-28 <sup>b</sup>	—	—	—	—	+	—	—	—
<i>C. zofingiensis</i>	C-111 (211-14) <sup>b</sup>	—	—	—	—	+	—	—	+
<i>C. protothecoides</i>	C-150 (211-11a) <sup>b</sup>	—	—	—	—	+	—	—	+
	C-206 <sup>b</sup>	—	—	—	—	+	—	—	+
Symbiotic <i>Chlorella</i> spp.	C-201 <sup>b</sup>	—	—	—	—	+	—	+	+
	OS1g <sup>b</sup>	+	—	—	—	—	+	+	+
	Dd1g <sup>b</sup>	+	—	—	—	—	+	+	+
	KM2g <sup>b</sup>	+	—	—	—	—	+	+	+
	Bwk-16 (C <sup>+</sup> ) <sup>b</sup>	+	—	±	—	±	+	+	+
	OS1g1N <sup>b</sup>	+	—	—	—	—	+	+	+

<sup>a</sup> Algal cells were labeled with Alexa Fluor 488–conjugated WGA, GS-II, or Con A. +, 100% of cells with fluorescence; ±, < 100%; —, 0%. For each experiment, more than 100 algal cells were observed.

<sup>b</sup> Strain used only by Kodama and Fujishima (2007).

<sup>c</sup> Strain used by Kodama and Fujishima (2007) and Takeda et al. (1998).

WGA, wheat germ agglutinin; GS-II, lectin from *Griffonia simplicifolia*; Con A, concanavalin A. Updated from Kodama and Fujishima (2007).

### 3.3. Effects of WGA on the infectivity of *C. sorokiniana* C-212 to *P. bursaria*

Weis (1980), Reisser et al. (1982), and Nishihara et al. (1996) reported that the infection ratio of algae-free *P. bursaria* decreased if the algae were pretreated with Con A. However, it remains unclear which of the following phenomena was inhibited by Con A: algal resistance to the host lysosomal enzymes in the host DVs, algal escape from the host DVs, algal protection from host lysosomal fusion by enclosing PV membrane, algal localization beneath the host cell surface, or algal cell division. Regarding results of our study, Table 2.3 shows that Con A did not bind either symbiotic or infection-capable free-living algae. Furthermore, *C. sorokiniana* C-212 cells are able to infect algae-free *P. bursaria* cells (Table 2.3) and can be labeled with WGA (Table 2.3 and Fig. 2.17B). To examine the effect of WGA labeling of the cell wall on infection, the algae were treated with 100  $\mu\text{g}/\text{ml}$  of Alexa Fluor 488-conjugated WGA for 3 h under constant darkness. Later, they were mixed with algae-free paramecia for 1 h, washed, chased, and then fixed at 1 and 72 h after mixing. Figure 2.18A shows that many algal cells were ingested by all paramecia at 1 h whether the algae had been labeled with WGA or not. At 72 h, the respective proportions of paramecia containing WGA-labeled and unlabeled algae were not significantly different, but the relative frequency of paramecia with more than 20 algal cells (Fig. 2.18B) showed a significant difference. In both setups, strain C-212 algae were localized immediately beneath the host cell surface. They were able to multiply through binary fission. Although the relative frequency of paramecia with more than 20 algal cells was decreased significantly when the algal cells were labeled with WGA, our data show that lectin labeling of algal cell walls does not inhibit the establishment of endosymbiosis with algae-free *P. bursaria*. Both WGA-labeled and WGA-unlabeled algae were maintained in the host cells for more than 2 years. Therefore, our data show that the infectivity of infection-capable *Chlorella* species for algae-free *P. bursaria* is not based on sugar residues of their cell wall or the

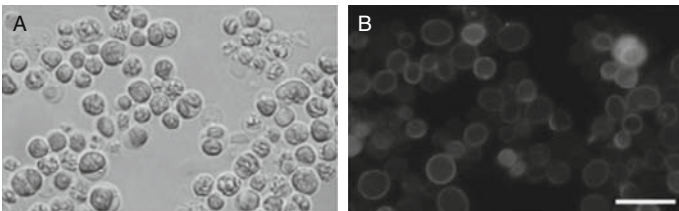


**Figure 2.17** Photomicrographs of *C. sorokiniana* cells strain C-212 treated with Alexa Fluor 488-conjugated WGA: (A) DIC image, (B) fluorescence microscopic image. Fluorescence is apparent on the algal cell wall; Bar, 10  $\mu\text{m}$ .

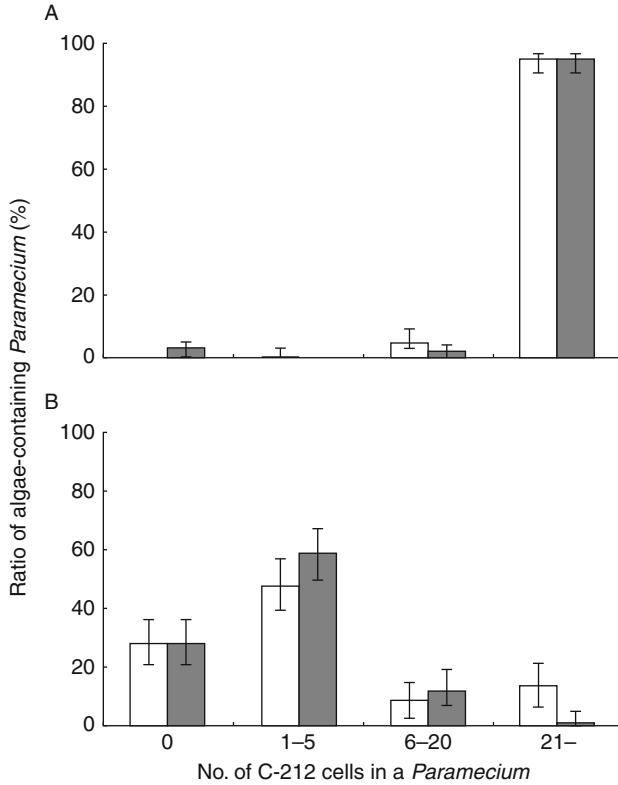


**Figure 2.18** Effect of WGA treatment on the infectivity to the algae-free *P. bursaria* strain OS1w of *C. sorokiniana* strain C-212 algae 1 h (A) and 72 h (B) after mixing with algae-free paramecia. For each time interval, 100–150 cells were observed. White bar, untreated algae; gray bar, WGA-treated algae. Bar in bar graph, 90% confidence limits. Y-axis, ratio of algae-containing *Paramecium*; X-axis, number of C-212 algae ingested by paramecia in four groups (0, 1–5, 6–20, and more than 20 algae). Almost all paramecia ingested many C-212 algae, irrespective of WGA treatment (A). Both WGA-treated and WGA-untreated C-212 cells were maintained in algae-free paramecia (B). From Kodama and Fujishima (2007).

alkali-insoluble part of their cell wall, but on their ability to localize beneath the host cell surface after escaping from the host DVs (Kodama and Fujishima, 2007).

#### 4. FUNCTION OF PV MEMBRANE

The DV and PV membranes are known to show the following qualitative differences: (1) The PV membrane encloses a single algal cell (Gu et al., 2002; Karakashian and Rudzinska, 1981); (2) Because the gap

separating the algal cell wall and the PV membrane is about  $0.05\ \mu\text{m}$ , the PV membrane is hardly visible using a light microscope. Nevertheless, it can be observed readily using a transmission electron microscope (Reisser, 1986); (3) The PV diameter does not vary greatly ( $2.5\text{--}4.5\ \mu\text{m}$ ), except during the division of the enclosed symbiotic alga (Reisser, 1992); (4) The PV does not participate in cyclosis, but it localizes immediately beneath the host cell surface (Kodama and Fujishima, 2005; Reisser, 1986); (5) Particle density and its distribution of the PV membrane show few signs hinting at any endocytotic or exocytotic activity, which can be observed in the DV membrane (Meier et al., 1984).

#### 4.1. Algal proteins necessary for the PV membrane

Cycloheximide is known to inhibit protein synthesis of symbiotic *Chlorella* of the ciliate *P. bursaria* preferentially, but it only slightly inhibits host protein synthesis (Ayala and Weis, 1987). Therefore, algae-free cells can be prepared within 4–6 days after treatment using cycloheximide (Kodama et al., 2007; Weis, 1984). However, the detailed algal removal process has not been observed. As causes for the removal of the symbiotic algae, the following possibilities can be considered: (1) dilution of the number of algal cells by the host's cell division in the presence of cycloheximide and (2) digestion of algal cells by the host's lysosomal fusion to the PV membrane. This phenomenon is expected to be a useful model to examine the features or functions of PV membrane. Therefore, algae-bearing strain OS1g1N cells were treated with  $10\ \mu\text{g}/\text{ml}$  of cycloheximide and observed under light microscopy. Figure 2.19A shows an algae-bearing cell before treatment with cycloheximide (control). Several hundred green symbiotic algae exist in the host cytoplasm; the PV membrane enclosing each symbiotic alga cannot be observed under a light microscope. However, as depicted in Fig. 2.19B, almost the entire PV membrane inside the algae-bearing cells began to swell synchronously at 1 day after the treatment. For that reason, the PV membrane is visible under a light microscope. This indicates that inhibition of the algal protein synthesis induces swelling of the PV membrane. We designated this phenomenon as “synchronous PV-swelling (SPVS).” It was induced in all PVs enclosing symbiotic green algae in the host cell (Kodama and Fujishima, 2008a). The gap separating the algal cell wall and the PV membrane was  $1.26 \pm 0.52\ \mu\text{m}$  (mean  $\pm$  S.D.,  $n > 50$ ). This value shows that the distance between the symbiotic algal cell wall and the PV membrane increased to 25 times wider than the  $0.05\ \mu\text{m}$  original distance determined by Reisser (1986) using transmission electron microscopy. Algal digestion was induced soon after the SPVS (Fig. 2.19B, arrow). Such synchronized symbiotic algal digestion is not usually observed before SPVS. Therefore, this digestion is inferred as a phenomenon that is closely related to SPVS. We observed that the digested algae were

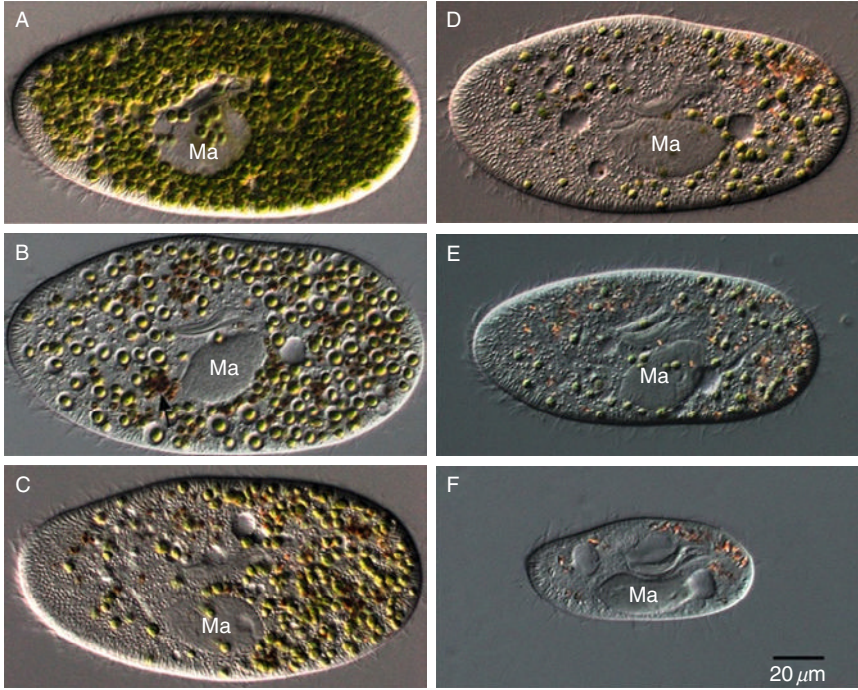


**Figure 2.19** Photomicrographs of algae-bearing OS1g1N cells suspended in fresh culture medium containing  $10 \mu\text{g/ml}$  of cycloheximide at 5000 cells/ml at  $25 \pm 1^\circ\text{C}$  under LL condition. (A) A cell before the treatment. Hundreds of green symbiotic algae exist in the host cytoplasm. (B) A cell 1 day after the treatment. All PVs containing green algae swell synchronously. Furthermore, digested brown algae appear in the host cytoplasm (arrow). (C) A cell 2 days after the treatment. Green algae are numerically reduced and all PV membrane shrinks again. (D) A cell 3 days after the treatment. (E) A cell 5 days after the treatment. All algal cells disappear from the host cytoplasm. The *Paramecium* cells shrink because of starvation, which occurs as the result of the disappearance of symbiotic algae. Ma, macronucleus. From Kodama and Fujishima (2008a).

discharged from the host cytoproct. By day 1 after the treatment with cycloheximide, the mean number of symbiotic green algae per host cell had decreased to about one-sixth of its former value: from 698 to 118.3. The host cell density increased, but it only approximately doubled during the same period, from  $5 \times 10^3$  to  $9.1 \times 10^5$  cells/ml, demonstrating that the cause of the algal removal by treatment with cycloheximide in the LL condition is not the dilution of the algae by host cell division, but algal digestion and discharge from the host cytoproct. Two days after the treatment, the swollen PV condensed and the membrane became hardly visible under the light microscope (Fig. 2.19C). Three days after the treatment, all green algae in some *Paramecium* cells had disappeared. At day 7 after the



treatment, all paramecia were observed to have lost their symbiotic algae completely: they had become algae-free cells (Fig. 2.19F). As presented in Fig. 2.19A–F, the host cell shrank gradually, probably because of starvation induced by loss of the symbiotic algae, or by the lost volume of the algae. Identical results obtained using other algae-bearing *P. bursaria* strains—Dd1g, KM2g, Bwk-16(C<sup>+</sup>), and Yad1g—show that SPVS and following algal digestion are universal phenomena in cells of *P. bursaria* strains. No statistically significant difference was found in the degree of SPVS between the cells treated with 10 or 100  $\mu\text{g/ml}$  cycloheximide. Through treatment at either concentration of cycloheximide, all algae-bearing cells lost the symbiotic algae and became algae-free cells at 3–9 days after treatment.

Schüßler and Schnepf (1992) reported that PV swelling might be induced by treatment of the algae-bearing *P. bursaria* cells with a carboxylic ionophore, monensin. However, unlike SPVS induced by cycloheximide, the PV swelling induced by monensin does not lead to algal digestion in the PVs. They also reported that the PV swelling was observed only under LL condition, not under constant dark (DD) condition. Furthermore, they reported that the PV swelling was inhibited by DCMU, a blocker of electron flow in photosystem II (Kleinig and Sitte, 1986). Therefore, we also examined the necessity of photosynthetic activity for the SPVS. Results show that SPVS was not induced by cycloheximide under DD condition, which is the same as the result obtained through treatment with monensin (Schüßler and Schnepf, 1992). Even if the algae-bearing paramecia were treated with cycloheximide under the LL condition, addition of  $10^{-7}$  M DCMU inhibited SPVS completely. These results show that algal photosynthetic activity is indispensable for induction of SPVS through treatment of cycloheximide and for successive induction of algal digestion in the host cell. Figure 2.20 presents some hypotheses related to induction of SPVS and following algal digestion after treatment of algae-bearing cells with cycloheximide. Based on results obtained from observation of cycloheximide-treated algae-bearing cells, it might be inferred that algal proteins synthesized in the presence of algal photosynthesis serve some important function to prevent expansion of the PV and to maintain the ability of the PV membrane to protect itself from host lysosomal fusion (Kodama and Fujishima, 2008a).

#### 4.2. The PV membrane can provide protection from host lysosomal fusion

Each symbiotic alga localizes near trichocysts beneath the host cell surface. Localization of the algal symbionts near the host cell surface is not a phenomenon that is specific only to *Chlorella*–*P. bursaria* endosymbiosis. Reisser (1986) reported that symbiotic algae and cyanobacteria of *Mayorella viridis*, *Coleps hirtus*, *Coleps spetai*, *Frontonia leucas*, *Malacophrys sphagni*,

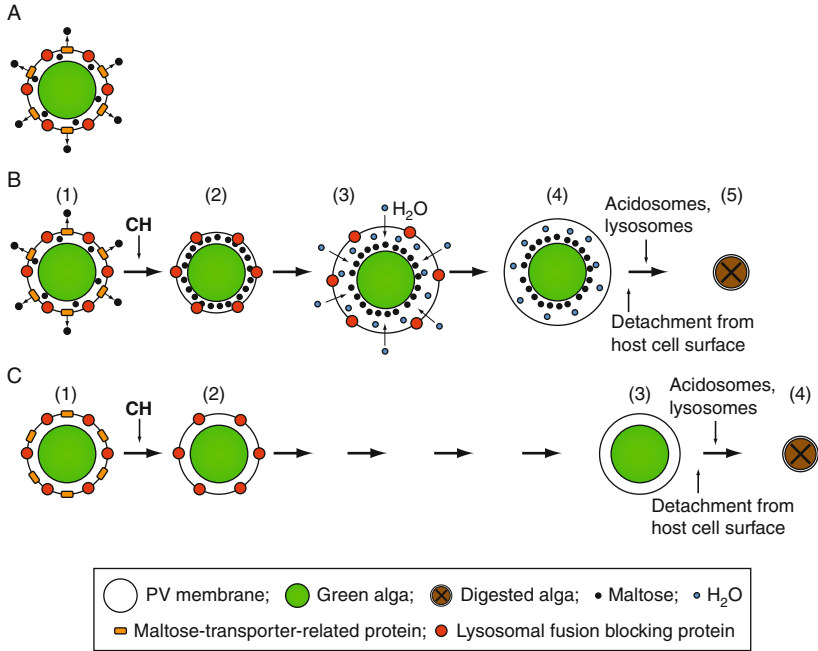


**Figure 2.20** Schematic drawing presenting some hypotheses related to induction of SPVS and digestion of symbiotic alga after treatment of algae-bearing *P. bursaria* cells with 10  $\mu\text{g}/\text{ml}$  cycloheximide under LL or DD conditions. As molecules responsible for functions of the PV membrane, two proteins that are synthesized by the algae, excreted outside the algae and localized on the PV membrane, are postulated. The first is a hypothetical maltose-transporter-related protein (squares on PV membrane) (Willenbrink, 1987) that is synthesized by the alga during photosynthesis and which transports maltose from inside the PV membrane to the outside. Loss of this protein in the LL condition induces accumulation of photosynthesized carbohydrates, mainly maltose. The second is a hypothetical lysosomal fusion-blocking protein (circles on PV membrane) that is synthesized by the algae and which has the ability to block lysosomal fusion to the PV membrane and also the ability to attach to unknown structures immediately beneath the host surface. Consequently, the loss of this protein induces detachment of the PV from the host cell surface and induces fusion with the host lysosomes. The maltose-transporter-related protein disappears rapidly from the PV membrane when the algal protein synthesis is inhibited by cycloheximide. However, the lysosomal fusion blocking protein has a longer turnover time than that of the former. Therefore, this protein remains for some time on the PV membrane when the algal protein synthesis is inhibited by cycloheximide. cycloheximide inhibits algal protein synthesis. Under the LL condition (A), the symbiotic alga synthesizes mainly maltose by photosynthesis in the host cell (Muscatine et al., 1967) and excretes it into a lumen between the cell wall of the algae and the PV membrane. The maltose is then transferred outside of the PV membrane through the maltose-transporter-related protein on the PV membrane. The maltose-transporter-related proteins disappear from the PV membrane (B-2) when the algal protein synthesis is inhibited by treatment with cycloheximide under the LL condition (B). Ayala and Weis (1987) reported that, by treatment with 100  $\mu\text{g}/\text{ml}$  cycloheximide, the rate of carbohydrate secretion by symbiotic algae under LL showed no significant difference between the treated and untreated

*Ophrydium versatile*, *Vorticella* spp., *Climacostomum virens*, *Euplotes daidaleos*, *Halteria bifurcata*, *Stentor polymorphus*, and *Stentor niger* were not situated freely in the host cytoplasm, but they are located individually near the host cell surface. The trichocyst area has been shown to be an AcPase-activity negative area using Gomori's staining (Kodama and Fujishima, 2008a,b, 2009a), indicating that few if any primary lysosomes are present. These observations raise the possibility that the PV membrane might have no capability for protection from lysosomal fusion, but it can avoid lysosomal fusion by binding to the primary lysosome-less trichocyst area of the cell. Although the PV membrane, which originates from the host DV membrane, had been believed to have functions for protection of the symbiotic alga inside the PV from the host's lysosomal fusion (Karakashian and Karakashian, 1973; Karakashian and Rudzinska, 1981; Karakashian et al., 1968; Kodama and Fujishima, 2009a; Meier and Wiessner, 1989; Meier et al., 1984; Reisser, 1981), no report has confirmed the PVs capability of providing protection from host lysosomal fusion. Recently, this problem has been solved by removing the trichocysts using lysozyme to reduce the AcPase-activity negative area, and by exposing the PVs to the AcPase-positive area. Before treatment with lysozyme, the AcPase-activity negative area of trichocyst-bearing algae-free cells are 9.86  $\mu\text{m}$  deep at the anterior surface, 7.34  $\mu\text{m}$  deep at the ventral surface, 5.34  $\mu\text{m}$  deep at the dorsal surface, and 8.00  $\mu\text{m}$  deep at the posterior surface. On the other hand, trichocyst-removed algae-free cells are 5.63  $\mu\text{m}$  deep at the anterior surface, 4.25  $\mu\text{m}$  deep at the ventral surface, 2.79  $\mu\text{m}$  deep at the dorsal surface, and 6.00  $\mu\text{m}$  deep at the posterior surface. Therefore, the lysozyme-treated cells reduced the mean depth of the AcPase-activity negative area. Especially in the dorsal surface of the cells, the mean depth of the AcPase-activity negative area became less than the mean diameter of the algal cell

---

groups. Consequently, the concentration of the carbohydrates including maltose increases inside the PV membrane, and outside water flows into the PV and induces the SPVS (B-3). Later, the lysosomal fusion blocking protein disappears from the swollen PV membrane (B-4). Therefore, the vacuole containing an alga detaches from the host surface; then the host acidosomes fuse to the swollen vacuole and the vacuole contracts by membrane replacement between the acidosomal membrane and the swollen vacuole (Fok et al., 1982; Kodama and Fujishima, 2005). Thereafter, lysosomal fusion occurs to the contracted vacuole and the alga is digested (B-5). As presented in Fig. 2.19C, the PVs that can avoid the lysosomal fusion in the presence of cycloheximide recontracted PV. Such vacuoles might be produced by evasion of lysosomal fusion after acidosomal fusion. Under the DD condition (C-1), cycloheximide treatment induces loss of the maltose-transporter-related protein from the PV membrane (C-2), but no morphological change is induced. Later, the lysosomal fusion blocking protein disappears from the PV membrane (C-3). The vacuole detaches from the host cell surface and fuses with acidosomes and lysosomes; then the algae are digested (C-4). Under the DD condition, the fate of the PV is the same as that of C, irrespective of the presence or absence of cycloheximide. CH, cycloheximide. From Kodama and Fujishima (2008a).

(long axis  $3.70\ \mu\text{m}$ , short axis  $2.96\ \mu\text{m}$ ). To confirm whether the PV membrane functions to provide protection from lysosomal fusion, algae-free cells were mixed with isolated symbiotic algae for 1.5 min, washed, and then resuspended in MDS. At 30 min after mixing with algae, 1 mg/ml lysozyme was added to the cell suspension, fixed at 3 h after mixing, and stained with Gomori's staining. Figure 2.21A portrays an untreated cell with lysozyme and Fig. 2.21B depicts trichocyst-removed cell with lysozyme. Figure 2.21B shows that the algae are not digested even if the algae are exposed to the AcPase-activity positive area. These results demonstrate that the PV membrane, unlike the DV membrane, gives protection from host lysosomal digestion. These results and those obtained through observation of cycloheximide-treated algae-bearing cells indicate that the algal proteins synthesized in the presence of the algal photosynthesis serve important functions to prevent expansion of the PV, to maintain abilities of the PV membrane to attach with unknown structures beneath the host cell surface, and to afford the membrane protection from host lysosomal fusion (Kodama and Fujishima, 2009b).

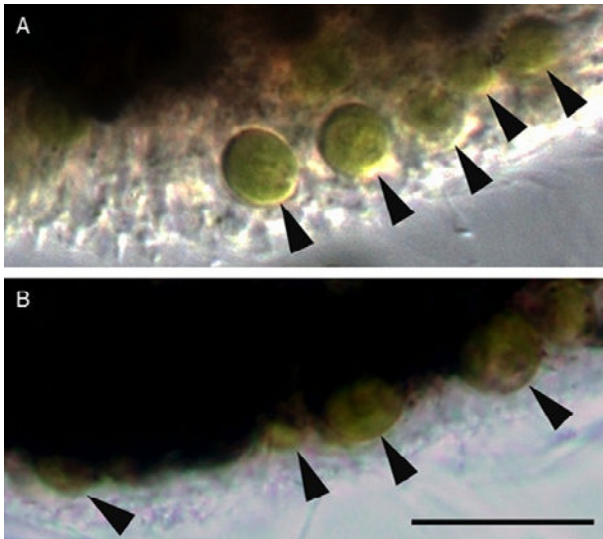


**Figure 2.21** Photomicrographs of dorsal areas of *P. bursaria* cells strain Yad1w stained with Gomori's staining. The algae-free cells were mixed with isolated symbiotic algae strain 1N cells for 1.5 min and resuspended in 1 ml of MDS. Then the cells were suspended in 1 mg/ml lysozyme to remove the host trichocysts, or in 10 mM Na-PB, pH 6.8 as a solvent of lysozyme, at 30 min after mixing with algae. Then, fixed at 3 h after mixing, and stained with Gomori's staining. (A) An untreated cell with lysozyme. (B) Trichocyst-removed cells with lysozyme. Arrowheads show the algae localized beneath the host cell surface. As portrayed in (B), the algae are not digested even if the algae are exposed to the AcPase-activity positive area. Bar,  $20\ \mu\text{m}$ . From Kodama and Fujishima (2009b).

## 5. HOST OR ALGAL CHANGES INDUCED BY INFECTION

Various changes are induced in both host *P. bursaria* and symbiotic algae by algal infection. For example, the host supplies algal cells with nitrogen components and CO<sub>2</sub> (Albers and Wiessner, 1985; Albers et al., 1982; Reisser, 1976, 1980). Within the host, the algae are protected from infection of the *Chlorella* virus (Kawakami and Kawakami, 1978; Reisser et al., 1988; Van Etten et al., 1991; Yamada et al., 2006). In addition, algal carbon dioxide fixation is enhanced by the host extracts; three divalent cations (Ca<sup>2+</sup>, K<sup>2+</sup>, and Mg<sup>2+</sup>) are identified as the active substances (Kamako and Imamura, 2006; Kato and Imamura, 2009). The algae can supply the host with a photosynthetic product, mainly maltose (Brown and Nielsen, 1974; Reisser, 1976, 1986). The algae in the host show a higher rate of photosynthetic oxygen production than in the isolated state, thereby guaranteeing an oxygen supply for the host (Reisser, 1980). Recently, Kato and Imamura (2009) presented a schematic representation of material that was inferred to have been transported, along with metabolic control mechanisms, between the host and symbiotic algae (Fig. 2.22). Algae-bearing *P. bursaria* can

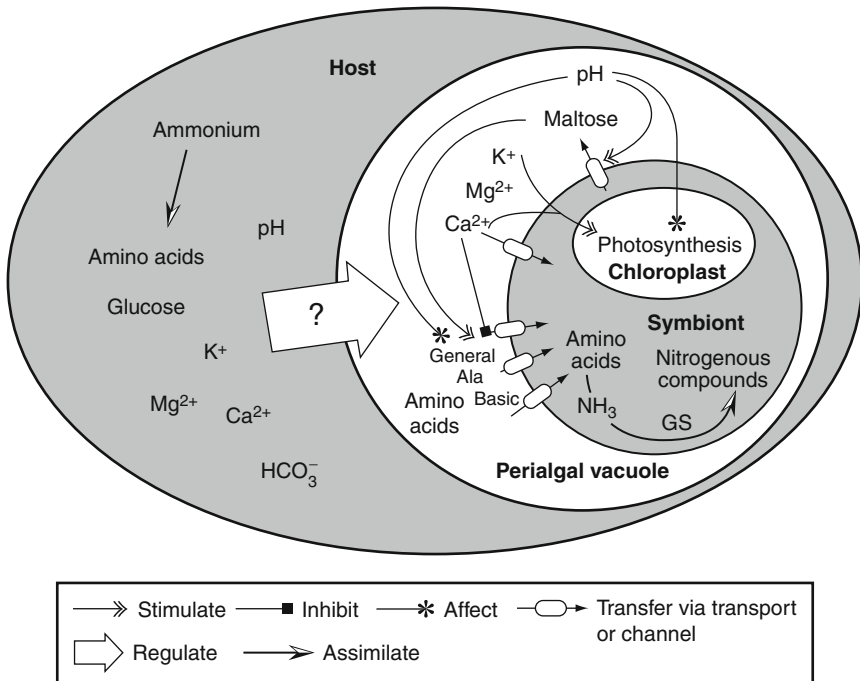


**Figure 2.22** Material supposedly transported, and metabolic control mechanisms, between the host *Parametium* and the symbiotic algae. From Kato and Imamura (2009).

grow better than algae-free cells (Görtz, 1982; Karakashian, 1963, 1975). Algae-bearing cells show a higher survival rate with 0.5 mM nickel chloride ( $\text{NiCl}_2$ ), or at high temperatures ( $42^\circ\text{C}$ ), or in  $150\ \mu\text{M}$  hydrogen peroxide ( $\text{H}_2\text{O}_2$ ) than the algae-free cells (Kinoshita et al., 2009; Miwa, 2009). Figure 2.23 shows that photosynthetic products of symbiotic *Chlorella* are

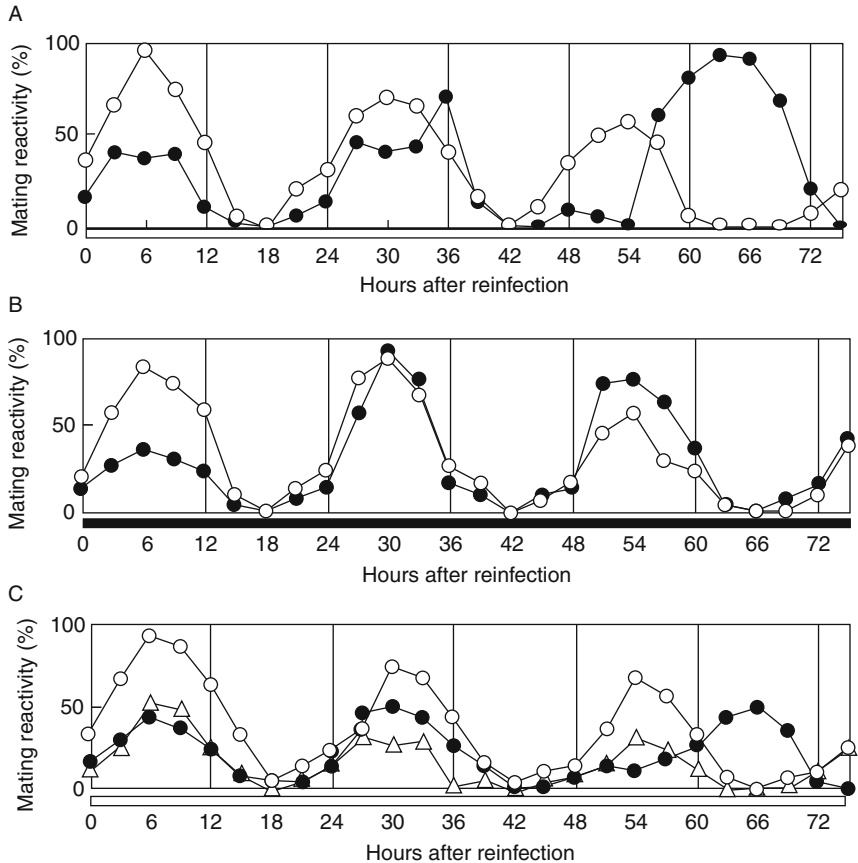


**Figure 2.23** Phase shift of mating reactivity rhythms in symbiotic algae-reinfected cells. Algae-free cells entrained in a LD cycle (12:12 h) were reinfected with *Chlorella* isolated from algae-bearing cells entrained in a reverse LD cycle. They were immediately assayed for mating reactivity rhythms in constant light (LL) (A, C), and in constant darkness (DD) (B). White circles represent control algae-free cells, black circles represent algae-bearing green cells reinfected with reverse-phase *Chlorella*, and triangles represent cells reinfected with reverse-phase *Chlorella*, which were treated with the photosynthesis inhibitor dichlorophenyl dimethylurea (DCMU). They showed the same phase as the original algae-free white cells during the first 2 days, but began to shift depending on the phase of *Chlorella* 3 days after algal reinfection in LL; however, phase shifts were not observed in DD or with DCMU. From Miwa (2009).

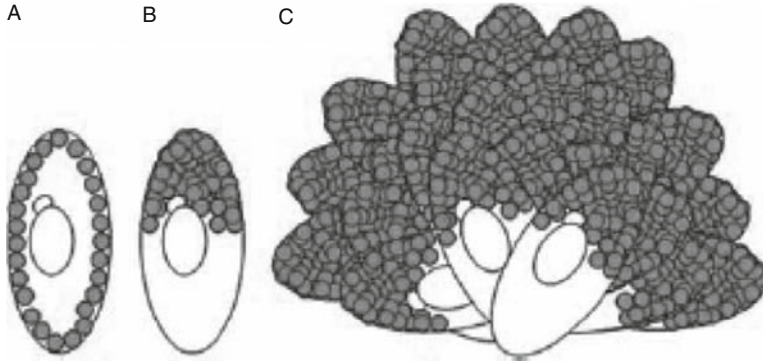


**Figure 2.24** Symbiotic *Chlorella*'s distribution within *P. bursaria* under PAR (A) and UVR (B) exposure; gray circles signify symbiotic algae. Hypothetical assemblage of *P. bursaria* with dislocated symbionts within dense spots ("collective shield") formed under UVR exposure (C). From Sommaruga and Sonntag (2009), an original figure is colored.

related closely to the expression of circadian rhythms in host *P. bursaria* (Miwa, 2009; Miwa et al., 1996; Tanaka and Miwa, 1996, 2000). Recently, Summerer et al. (2009) reported that exposure of artificial UV radiation (UVR) + photosynthetically active radiation (PAR) and "high" PAR ( $160 \text{ mmol m}^{-1} \text{ s}^{-1}$ ) showed an immediate aggregation of algae-bearing *P. bursaria* into several dense "spots" of about 1–3 mm diameter each in a Petri dish. Furthermore, Summerer et al. (2009) reported that *P. bursaria* can achieve protection against UV damage by accumulation, as well as by symbiont dislocation (Fig. 2.24). These facts suggest that symbiotic *Chlorella* might contribute to the host's tolerance to environmental fluctuations (Miwa, 2009).

## 6. CONCLUDING REMARKS

Figure 2.25 shows that in symbiotic or parasitic organisms, the following escape mechanisms from the host lysosomal digestion are known: (1) prevention of acidosomal fusion or lysosomal fusion to the DV, as has been shown for *Legionella pneumophila* (Horwitz and Maxfield, 1984), *Plasmodium falciparum* (Lingelbach and Joiner, 1998), *Salmonella enterica* (Brennan and Cookson, 2000), *Mycobacterium tuberculosis* (Crowle et al., 1991), *Chlamydia trachomatis* (Heinzen et al., 1996), and X-bacteria in *Amoeba proteus* (Kim et al., 1994); (2) escape from the DV into the host cytoplasm, as has been shown for *Listeria monocytogenes* (Cossart and Lecuit, 1998), *Trypanosoma cruzi* (Bogdan and Rollinghoff, 1999), *Shigella flexneri*

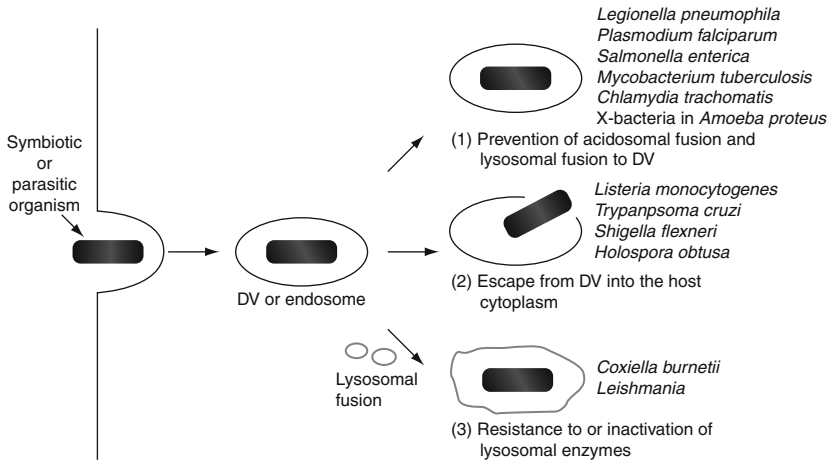


**Figure 2.25** Schematic representation of escape mechanisms from the host's lysosomal digestion of symbiotic or parasitic organisms.

(Sansonetti et al., 1986), and *Holospora obtusa* (Fujishima and Kawai, 1995); and (3) resistance to or inactivation of lysosomal enzymes after lysosomal fusion, as has been shown for infection by *Coxiella burnetii* (Hackstadt and Williams, 1981; Roman et al., 1986) and *Leishmania* (Rittig and Bogdan, 2000). Figure 2.13 presents our data, which indicate that *Chlorella* has a more complicated and novel mechanism to avoid digestion. First, some algae acquire temporary resistance to lysosomal enzymes in DV. Second, the alga escapes from the DV into the cytoplasm. Third, the alga is enwrapped with a PV membrane, which provides protection from the host's lysosomal fusion. Finally, the alga localizes immediately beneath the host cell surface, which is an AcPase-activity negative area. Although molecular analyses of these four events have just begun, the results of such analyses will dramatically promote the study of endosymbiosis control mechanisms in the near future. How can the symbiotic algae acquire temporal resistance to lysosomal enzymes in the host DV-III and DV-IV vacuoles? How can algae escape from the host DV as a result of budding of the DV membrane? What are the substantial differences between the DV and the PV? What is the transportation system of the PV immediately beneath the host cell surface? What is the signal for initiation of algal cell division after localization beneath the host cell surface? Can endosymbiosis be established when the symbiotic algae are not taken up through DVs, but are instead inserted by microinjection? Why, among all of the various *Paramecium* species, can only *P. bursaria* establish endosymbiosis with *Chlorella* species? How can the PV membrane segregate an old cell wall that is discarded after algal cell division, and daughter algal cells? Can a single *Paramecium* cell maintain plural



*Chlorella* species or plural strains of the same *Chlorella* species in a single *P. bursaria* cell? These problems remain to be elucidated to understand the establishment of the secondary symbiosis between *Paramecium* and *Chlorella* cells. Endosymbiosis of *Chlorella* spp. is widespread among freshwater protozoa: *Climacostomum virens* (Reisser, 1984, 1986), *Euplotes daidaleos* (Heckmann et al., 1983), *Vorticella* spp. (Graham and Graham, 1978, 1980), *Stentor polymorphus* (Reisser, 1984, 1986), *Spongilla lacustris* (Frost and Williamson, 1980; Gilbert and Allen, 1973; Williamson, 1979), *Hydra viridis* (Hohman et al., 1982; O'Brien, 1982), and *Mayorella viridis* (Cann, 1981). Whether the symbiotic algae in these cells have identical mechanisms for avoiding host lysosomal digestion of symbiotic algae of *P. bursaria* or not must be examined.

## ACKNOWLEDGMENTS

The authors are indebted to all coworkers at Yamaguchi University. This work was supported by a Japan Society for the Promotion of Science (JSPS) Research Fellowship for Young Scientists granted to Yuuki Kodama, by a grant-in-aid for Scientific Research (B) (no. 17405020) to Masahiro Fujishima from JSPS, and by a Narishige Zoological Science Award of 2009 to Masahiro Fujishima. The authors are also indebted to R. Hoshina and N. Imamura for providing Fig. 2.14, Y. Kato and N. Imamura for providing Fig. 2.22, I. Miwa for providing Fig. 2.23, and R. Sommaruga and B. Sonntag for providing Fig. 2.24. With kind permissions of Springer and Elsevier, these original data could be reused in this chapter.

## REFERENCES

- Albers, D., Wiessner, W., 1985. Nitrogen nutrition of endosymbiotic *Chlorella* spec. Endocyt. Cell Res. 1, 55–64.
- Albers, D., Reisser, W., Wiessner, W., 1982. Studies of the nitrogen supply of endosymbiotic chlorellae in green *Paramecium bursaria*. Plant Sci. Lett. 25, 85–90.
- Allen, A.K., Neuberger, A., Sharon, N., 1973. The purification, composition and specificity of wheat-germ agglutinin. Biochem. J. 131, 155–162.
- Ayala, A., Weis, D.S., 1987. The effect of puromycin and cycloheximide on the infection of alga-free *Paramecium bursaria* by symbiotic *Chlorella*. J. Protozool. 34, 377–381.
- Bogdan, C., Rollinghoff, M., 1999. How do protozoan parasites survive inside macrophages? Parasitol. Today 15, 22.
- Bomford, R., 1965. Infection of alga-free *Paramecium bursaria* with strains of *Chlorella*, *Scenedesmus*, and a yeast. J. Protozool. 12, 221–224.
- Brennan, M., Cookson, B.T., 2000. *Salmonella* induces macrophage death by caspase-1-dependent necrosis. Mol. Microbiol. 38, 31–40.
- Brown, J.A., Nielsen, P.J., 1974. Transfer of photosynthetically produced carbohydrate from endosymbiotic *Chlorellae* to *Paramecium bursaria*. J. Protozool. 21, 569–570.
- Cann, J.P., 1981. An ultrastructural study of *Mayorella viridis* (Leidy) (Amoebida: Paramoebidae), a rhizopod containing zoochlorellae. Arch. Protistenkd. 124, 353–360.
- Cossart, P., Lecuit, M., 1998. Interactions of *Listeria monocytogenes* with mammalian cells during entry and actin-based movement: bacterial factors, cellular ligands and signalling. EMBO J. 17, 3797–3806.

- Crowle, A.J., Dahl, R., Ross, E., May, M.H., 1991. Evidence that vesicles containing living, virulent *Mycobacterium tuberculosis* or *Mycobacterium avium* in cultured human macrophages are not acidic. *Infect. Immun.* 59, 1823–1831.
- Dryl, S., 1959. Antigenic transformation in *Paramecium aurelia* after homologous antiserum treatment during autogamy and conjugation. *J. Protozool.* 6 (Suppl.), 25.
- Ebisu, S., Goldstein, I.J., 1978. *Bandeiraea simplicifolia* lectin II. In: Ginsburg, V. (Ed.), *Complex Carbohydrates, Part C. Vol. 50: Methods in Enzymology*. Academic Press, London, pp. 350–354.
- Fok, A., Lee, Y., Allen, R.D., 1982. The correlation in DV pH and size with the digestive cycle in *Paramecium caudatum*. *J. Protozool.* 29, 409–414.
- Frost, T.M., Williamson, C.E., 1980. *In situ* determination of the effect of symbiotic algae on the growth of the freshwater sponge *Spongilla lacustris*. *Ecology* 61, 1361–1370.
- Fujishima, M., Kawai, M., 1995. Acidification in DV is an early event required for *Holospira* infection of *Paramecium* nucleus. In: Schenk, H.E.A., Herrmann, R.G., Jeon, K.W., Muller, N.E., Schwemmler, W. (Eds.), *Eukaryotism and Symbiosis*. Springer, Berlin, pp. 367–374.
- Gerashchenko, B.I., Nishihara, N., Ohara, T., Tosuji, H., Kosaka, T., Hosoya, H., 2000. Flow cytometry as a strategy to study the endosymbiosis of algae in *Paramecium bursaria*. *Cytometry* 41, 209–215.
- Gilbert, J.J., Allen, H.L., 1973. Chlorophyll and primary productivity of some green freshwater sponges. *Int. Rev. Ges. Hydrobiol.* 58, 633–658.
- Goldstein, I.J., Reichert, C.M., Misaki, A., 1974. Interaction of concanavalin A with model substrates. *Ann. NY Acad. Sci.* 234, 283–296.
- Goldstein, I.J., Hammarstrom, S., Sundblad, G., 1975. Precipitation and carbohydrate-binding specificity studies on wheat germ agglutinin. *Biochim. Biophys. Acta* 405, 53–61.
- Gomori, G., 1952. *Microscopic Histochemistry. Principles and Practice*. University of Chicago Press, Chicago.
- Görtz, H.-D., 1982. Infection of *Paramecium bursaria* with bacteria and yeasts. *J. Cell Sci.* 58, 445–453.
- Graham, L.E., Graham, J.U., 1978. Ultrastructure of endosymbiotic *Chlorella* in a *Vorticella*. *J. Protozool.* 25, 207–210.
- Graham, L.E., Graham, J.U., 1980. Endosymbiotic *Chlorella* (Chlorophyta) in a species of *Vorticella* (Ciliophora). *Trans. Am. Microsc. Soc.* 99, 160–166.
- Gu, F.K., Chen, L., Ni, B., Zhang, X., 2002. A comparative study on the electron microscopic enzyme-cytochemistry of *Paramecium bursaria* from light and dark cultures. *Eur. J. Protistol.* 38, 267–278.
- Hackstadt, T., Williams, J.C., 1981. Biochemical stratagem for obligate parasitism of eukaryotic cells by *Coxiella burnetii*. *Proc. Natl. Acad. Sci. USA* 78, 3240–3244.
- Harumoto, T., Miyake, A., 1991. Defensive function of trichocysts in *Paramecium*. *J. Exp. Zool.* 260, 84–92.
- Heckmann, K., Ten Hagen, R., Görtz, H.-D., 1983. Freshwater *Euplotes* species with a 9 type 1 cirrus pattern depend upon endosymbionts. *J. Protozool.* 30, 284–289.
- Heinzen, R.A., Scidmore, M.A., Rockey, D.D., Hackstadt, T., 1996. Differential interaction with endocytic and exocytic pathways distinguish the parasitophorous vacuoles of *Coxiella burnetii* and *Chlamydia trachomatis*. *Infect. Immun.* 64, 796–809.
- Hohman, T.C., McNeil, P.L., Muscatine, L., 1982. Phagosome-lysosome fusion inhibited algal symbionts of *Hydra viridis*. *J. Cell Biol.* 94, 56–63.
- Horwitz, M.A., Maxfield, F.R., 1984. *Legionella pneumophila* inhibits acidification of its phagosome in human monocytes. *J. Cell Biol.* 99, 1936–1943.
- Hoshina, R., Imamura, N., 2009. Origins of algal symbionts of *Paramecium bursaria*. In: Fujishima, M. (Ed.), *Endosymbionts in Paramecium*. Springer-Verlag, Berlin Heidelberg, pp. 1–29. *Microbiology Monographs* 12.

- Hosoya, H., Kimura, K., Matsuda, S., Kitaura, M., Takahashi, T., 1995. Symbiotic alga-free strains of the green *Paramecium bursaria* produced by herbicide paraquat. *Zool. Sci.* 12, 807–810.
- Jennings, H.S., 1938. Sex reaction types and their interrelations in *Paramecium bursaria* I and II. Clones collected from natural habitats. *Proc. Natl. Acad. Sci. USA* 24, 112–120.
- Kadono, T., Kawano, T., Hosoya, H., Kosaka, T., 2004. Flow cytometric studies of the host-regulated cell cycle in algae symbiotic with green paramecium. *Protoplasma* 223, 133–141.
- Kamako, S.-I., Imamura, N., 2006. Effect of Japanese *Paramecium bursaria* extract on photosynthetic carbon fixation of symbiotic algae. *J. Euk. Microbiol.* 53, 136–141.
- Karakashian, S.J., 1963. Growth of *Paramecium bursaria* as influenced by the presence of algal symbionts. *Physiol. Zool.* 36, 52–68.
- Karakashian, S.J., 1975. Symbiosis in *Paramecium bursaria*. *Symp. Soc. Exp. Biol.* 29, 145–173.
- Karakashian, S.J., Karakashian, M.W., 1965. Evolution and symbiosis in the genus *Chlorella* and related algae. *Evolution* 19, 368–377.
- Karakashian, M.W., Karakashian, S.J., 1973. Intracellular digestion and symbiosis in *Paramecium bursaria*. *Exp. Cell Res.* 81, 111–119.
- Karakashian, S.J., Rudzinska, M.A., 1981. Inhibition of lysosomal fusion with symbiont containing vacuoles in *Paramecium bursaria*. *Exp. Cell Res.* 131, 387–393.
- Karakashian, S.J., Karakashian, M.W., Rudzinska, M.A., 1968. Electron microscopic observations on the symbiosis of *Paramecium bursaria* and its intracellular algae. *J. Protozool.* 15, 113–128.
- Kato, Y., Imamura, N., 2009. Metabolic control between the symbiotic *Chlorella* and the host *Paramecium*. In: Fujishima, M. (Ed.), *Endosymbionts in Paramecium*. Springer-Verlag, Berlin Heidelberg, pp. 57–82. *Microbiology Monographs* 12.
- Kawakami, H., Kawakami, N., 1978. Behavior of a virus in a symbiotic system, *Paramecium bursaria*-zoochlorella. *J. Protozool.* 25, 217–225.
- Kim, K., Na, Y.E., Jeon, K.W., 1994. Bacterial endosymbiont-derived lipopolysaccharides and a protein on symbiosome membranes in newly infected amoebae and their roles in lysosome-symbiosome fusion. *Infect. Immun.* 62, 65–71.
- Kinoshita, H., Oomori, S., Nozaki, M., Miwa, I., 2009. Timing of establishing symbiosis during the re-infection of *Chlorella* sp. in *Paramecium bursaria*. *Jpn. J. Protozool.* 42, 88–89 (in Japanese).
- Kleinig, H., Sitte, P., 1986. *Zellbiologie*, second ed. G. Fischer, Stuttgart.
- Kodama, Y., Fujishima, M., 2005. Symbiotic *Chlorella* sp. of the ciliate *Paramecium bursaria* do not prevent acidification and lysosomal fusion of host digestive vacuoles during infection. *Protoplasma* 225, 191–203.
- Kodama, Y., Fujishima, M., 2007. Infectivity of *Chlorella* species for the ciliate *Paramecium bursaria* is not based on sugar residues of their cell wall components, but based on their ability to localize beneath the host cell membrane after escaping from the host digestive vacuole in the early infection process. *Protoplasma* 231, 55–63.
- Kodama, Y., Fujishima, M., 2008a. Cycloheximide induces synchronous swelling of perialgal vacuoles enclosing symbiotic *Chlorella vulgaris* and digestion of the algae in the ciliate *Paramecium bursaria*. *Protist* 159, 483–494.
- Kodama, Y., Fujishima, M., 2008b. Mechanism of establishment of endosymbiosis between the ciliate *Paramecium bursaria* and the symbiotic *Chlorella* species. *Jpn. J. Protozool.* 41, 117–132 (in Japanese).
- Kodama, Y., Fujishima, M., 2009a. Timing of perialgal vacuole membrane differentiation from digestive vacuole membrane in infection of symbiotic algae *Chlorella vulgaris* of the ciliate *Paramecium bursaria*. *Protist* 160, 65–74.

- Kodama, Y., Fujishima, M., 2009b. Localization of perialgal vacuoles beneath the host cell surface is not a prerequisite phenomenon for protection from the host's lysosomal fusion in the ciliate *Paramecium bursaria*. *Protist* 160, 319–329.
- Kodama, Y., Fujishima, M., 2009c. Infection process of symbiotic *Chlorella* species to *Paramecium bursaria*. In: Fujishima, M. (Ed.), *Endosymbionts in Paramecium*. Springer-Verlag, Berlin Heidelberg, pp. 31–55. *Microbiology Monographs* 12.
- Kodama, Y., Nakahara, M., Fujishima, M., 2007. Symbiotic alga *Chlorella vulgaris* of the ciliate *Paramecium bursaria* shows temporary resistance to host lysosomal enzymes during the early infection process. *Protoplasma* 230, 61–67.
- Lingelbach, K., Joiner, K.A., 1998. The parasitophorous vacuole membrane surrounding *Plasmodium* and *Toxoplasma*: an unusual compartment in infected cells. *J. Cell Sci.* 111, 1467–1475.
- Lyer, P.N., Wilkinson, K.D., Goldstein, L.J., 1976. An *N*-acetyl-D-glycosamine binding lectin from *Bandeiraea simplicifolia* seeds. *Arch. Biochem. Biophys.* 177, 330–333.
- Meier, R., Wiessner, W., 1989. Infection of alga-free *Paramecium bursaria* with symbiotic *Chlorella* sp. isolated from green paramecia. II. A timed study. *J. Cell Sci.* 93, 571–579.
- Meier, R., Lefort-Tran, M., Pouphe, M., Reisser, W., Wiessner, W., 1984. Comparative freeze-fracture study of perialgal and digestive vacuoles in *Paramecium bursaria*. *J. Cell Sci.* 71, 121–140.
- Miwa, I., 2009. Regulation of circadian rhythms of *Paramecium bursaria* by symbiotic *Chlorella* species. In: Fujishima, M. (Ed.), *Endosymbionts in Paramecium*. Springer-Verlag, Berlin Heidelberg, pp. 83–110. *Microbiology Monographs* 12.
- Miwa, I., Fujimori, N., Tanaka, M., 1996. Effects of symbiotic *Chlorella* on the period length and the phase shift of circadian rhythms in *Paramecium bursaria*. *Eur. J. Protistol.* 32, 102–107.
- Muscantine, L., Karakashian, S.J., Karakashian, M.W., 1967. Soluble extracellular products of alga symbiotic with a ciliate, a sponge and a mutant *Hydra*. *Comp. Biochem. Physiol.* 20, 1–12.
- Nakahara, M., Handa, S., Nakano, T., Deguchi, H., 2003. Culture and pyrenoid structure of a symbiotic *Chlorella* species isolated from *Paramecium bursaria*. *Symbiosis* 34, 203–214.
- Nishihara, N., Takahashi, T., Kosaka, T., Hosoya, H., 1996. Characterization of endosymbiotic algae in *Paramecium bursaria*. *Jpn. J. Protozool.* 29, 35 (in Japanese).
- Nishihara, N., Murata-Hori, M., Yamada, T., Kosaka, T., Hosoya, H., 1999. Characteristic variation of cloned endosymbiotic algae in *Paramecium bursaria*. *Jpn. J. Protozool.* 32, 31 (in Japanese).
- O'Brien, T.L., 1982. Inhibition of vacuolar membrane fusion by intracellular symbiotic algae in *Hydra viridis* (Florida Strain). *J. Exp. Zool.* 223, 211–218.
- Ogata, S., Muramatsu, T., Kobata, A., 1975. Fractionation of glycopeptides by affinity column chromatography on concanavalin A-sepharose. *J. Biochem.* 78, 687–696.
- Omura, G., Suzuki, T., 2003. Changes in trichocysts during re-infection of white *Paramecium bursaria* by *Chlorella*. *Jpn. J. Protozool.* 36, 69–70 (in Japanese).
- Pado, R., 1965. Mutual relation of protozoans and symbiotic algae in *Paramecium bursaria* I. The influence of light on the growth of symbionts. *Folia Biol.* 13, 173–182.
- Poretz, R.D., Goldstein, I.J., 1970. An examination of the topography of the saccharide binding sites of concanavalin A and of the forces involved in complexation. *Biochemistry* 9, 2890–2896.
- Reisser, W., 1976. Die stoffwechselfysiologischen Beziehungen zwischen *Paramecium bursaria* Ehrbg. und *Chlorella* spec. in der *Paramecium bursaria*—Symbiose I: der Stickstoff—und der Kohlenstoff-Stoffwechsel. *Arch. Microbiol.* 107, 357–360.
- Reisser, W., 1980. The metabolic interactions between *Paramecium bursaria* Ehrbg. and *Chlorella* spec. in the *Paramecium bursaria*—symbiosis III. The influence of different

- CO<sub>2</sub> concentrations and of glucose on the photosynthetic and respiratory capacity of the symbiotic unit. *Arch. Microbiol.* 125, 291–293.
- Reisser, W., 1981. Host-symbiont interaction in *Paramecium bursaria*: physiological and morphological features and their evolutionary significance. *Ber. Deutsch. Bot. Ges.* 94, 557–563.
- Reisser, W., 1984. The taxonomy of green algae endosymbiotic in ciliates and sponge. *Br. Phycol. J.* 19, 309–318.
- Reisser, W., 1986. Endosymbiotic associations of freshwater protozoa and algae. In: Corliss, J.O., Patterson, D.J. (Eds.), *Progress in Protistology*, Vol. 1. Biopress Ltd., Bristol, pp. 195–214.
- Reisser, W., 1992. Endosymbiotic associations of algae with freshwater protozoa and invertebrates. In: Reisser, W. (Ed.), *Algae and Symbioses: Plants, Animals, Fungi, Viruses, Interactions Explored*, Vol. 1.1. Biopress, Bristol, pp. 1–19.
- Reisser, W., Radunz, A., Wiessner, W., 1982. Participation of algal surface structures in the cell recognition process during infection of aposymbiotic *Paramecium bursaria* with symbiotic chlorellae. *Cytobios* 33, 39–50.
- Reisser, W., Klein, T., Becker, B., 1988. Studies of phycoviruses I. On the ecology of viruses attacking *Chlorellae* exsymbiotic from a European strain of *Paramecium bursaria*. *Arch. Hydrobiol.* 111, 575–583.
- Rittig, M.G., Bogdan, C., 2000. *Leishmania*-host-cell interaction: complexities and alternative views. *Parasitol. Today* 16, 292.
- Roman, M.J., Coriz, P.D., Baca, O.G., 1986. A proposed model to explain persistent infection of host cells with *Coxiella burnetii*. *J. Gen. Microbiol.* 132, 1415–1422.
- Sansonetti, P.J., Ryter, A., Clerc, P., Maurelli, A.T., Mounier, J., 1986. Multiplication of *Shigella flexneri* within HeLa cells: lysis of the phagocytic vacuole and plasmid-mediated contact hemolysis. *Infect. Immun.* 51, 461–469.
- Schüßler, A., Schnepf, E., 1992. Photosynthesis-dependent acidification of perialgal vacuoles in the *Paramecium bursaria/Chlorella* symbiosis: visualization by monensin. *Protoplasma* 166, 218–222.
- Siegel, R., Karakashian, S., 1959. Dissociation and restoration of endocellular symbiosis in *Paramecium bursaria*. *Anat. Rec.* 134, 639.
- Sommaruga, R., Sonntag, B., 2009. Photobiological aspects of the mutualistic association between *Paramecium bursaria* and *Chlorella*. In: Fujishima, M. (Ed.), *Endosymbionts in Paramecium*. Springer-Verlag, Berlin, Heidelberg, pp. 111–130. *Microbiology Monographs* 12.
- Stoebe, B., Maier, U.G., 2002. One, two, three: nature's tool box for building plastids. *Protoplasma* 219, 123–130.
- Summerer, M., Sonntag, B., Hörtnagl, P., Sommaruga, R., 2009. Symbiotic ciliates receive protection against UV damage from their algae: a test with *Paramecium bursaria* and *Chlorella*. *Protist* 160, 233–243.
- Suzaki, T., Omura, G., Görtz, H.-D., 2003. Infection of symbiont-free *Paramecium bursaria* with yeasts. *Jpn. J. Protozool.* 36, 17–18 (in Japanese).
- Takahashi, T., Shirai, Y., Kosaka, T., Hosoya, H., 2007. Arrest of cytoplasmic streaming induces algal proliferation in green paramecia. *PLoS ONE* 2 (12), e1352. doi:10.1371/journal.pone.0001352.
- Takeda, H., Sekiguchi, T., Nunokawa, S., Usuki, I., 1998. Species-specificity of *Chlorella* for establishment of symbiotic association with *Paramecium bursaria*. Does infectivity depend upon sugar components of the cell wall? *Eur. J. Protistol.* 34, 133–137.
- Tanaka, M., Miwa, I., 1996. Significance of photosynthetic products of symbiotic *Chlorella* to establish the endosymbiosis and to express the mating reactivity rhythm in *Paramecium bursaria*. *Zool. Sci.* 13, 685–692.

- Tanaka, M., Miwa, I., 2000. Correlation of photosynthetic products of symbiotic *Chlorella* with the mating reactivity rhythms in a mutant strain of *Paramecium bursaria*. *Zool. Sci.* 17, 735–742.
- Tanaka, M., Murata-Hori, M., Kadono, T., Yamada, T., Kawano, T., Kosaka, T., et al., 2002. Complete elimination of endosymbiotic algae from *Paramecium bursaria* and its confirmation by diagnostic PCR. *Acta Protozool.* 41, 255–261.
- Tonooka, Y., Watanabe, T., 2002. A natural strain of *Paramecium bursaria* lacking symbiotic algae. *Eur. J. Protistol.* 38, 55–58.
- Tonooka, Y., Watanabe, T., 2007. Genetics of the relationship between the ciliate *Paramecium bursaria* and its symbiotic algae. *Inv. Biol.* 126, 287–294.
- Van Etten, J.L., Lane, L.C., Meints, R.H., 1991. Viruses and virus like particles of eukaryotic algae. *Microbiol. Rev.* 55, 586–620.
- Weis, D.S., 1969. Regulation of host and symbiont population size in *Paramecium bursaria*. *Experientia* 15, 664–666.
- Weis, D.S., 1980. Hypothesis: free maltose and algal cell surface sugars are signals in the infection of *Paramecium bursaria* by algae. In: Schwemmler, W., Schenk, E.A. (Eds.), *Endosymbiosis and Cell Biology*, Vol. 1. Walter de Gruyter, Berlin, pp. 105–112.
- Weis, D.S., 1984. The effect of accumulation time of separate cultivation on the frequency of infection of aposymbiotic ciliates by symbiotic algae in *Paramecium bursaria*. *J. Protozool.* 31, 14A.
- Wichterman, R., 1948. The biological effects of X-rays on mating types and conjugation of *Paramecium bursaria*. *Biol. Bull.* 93, 201.
- Willenbrink, J., 1987. Die pflanzliche Vakuole als Speicher. *Naturwissenschaften* 74, 22–29.
- Williamson, C.E., 1979. An ultrastructural investigation of algal symbiosis in white and green *Spongilla lacustris* (L.) (Porifera: Spongillidae). *Trans. Am. Microsc. Soc.* 98, 59–77.
- Yamada, T., Onimatsu, H., Van Etten, J., 2006. *Chlorella* viruses. *Adv. Virus Res.* 66, 293–336.
- Yamamoto, K., Tsuji, T., Matsumoto, I., Osawa, T., 1981. Structural requirements for the binding of oligosaccharides and glycopeptides to immobilized wheat germ agglutinin. *Biochemistry* 29, 5894–5899.

This page intentionally left blank

# MOLECULAR BASIS OF PEROXISOME DIVISION AND PROLIFERATION IN PLANTS

Jianping Hu

## Contents

1. Introduction	80
2. Roles of PEROXIN11 Proteins, Dynamin-Related Proteins, and FISSION1	81
2.1. PEROXIN11 (PEX11) proteins in peroxisome elongation	81
2.2. Dynamin-related proteins (DRPs) and peroxisome fission	85
2.3. FISSION1 as an anchor for DRPs	88
2.4. Interplay between PEX11, FIS1, and DRPs	89
3. Other Proteins and Pathways	89
4. Environmental and Nuclear Regulation of Peroxisome Proliferation	91
4.1. Nuclear regulators of peroxisome proliferation in yeasts and mammals	91
4.2. Environmental factors in plants	92
4.3. Phytochrome A-dependent pathway in light-induced peroxisome proliferation	92
5. Concluding Remarks	93
Acknowledgments	95
References	95

## Abstract

Peroxisomes are multifunctional organelles whose abundance varies depending on the cell type, organism, developmental stage, and environmental and metabolic conditions in which the organism lives. Plant peroxisomes are essential to embryo viability and are involved in numerous biochemical processes in development and in plant interaction with the environment. In the past few years, several classes of peroxisomal proteins required for various steps in peroxisome division and proliferation and a signaling pathway underlying the light induction of peroxisome proliferation have been identified from the model plant species *Arabidopsis thaliana*. Some of the major components of the peroxisome division apparatus have been conserved from plants to yeasts and animals, whereas plant-specific components are also being revealed. Environmental

Department of Energy Plant Research Laboratory, Michigan State University, East Lansing, Michigan, USA



factors and nuclear events that control the process appear to be highly unique in different evolutionary lineages. Future research needs to identify additional members of the peroxisome division/proliferation pathways and to dissect signaling pathways by which various environmental and metabolic cues regulate the abundance of peroxisomes in plants.

**Key Words:** Peroxisome proliferation, PEX11, Dynamin-related proteins, FIS1, Light induction of peroxisome proliferation. © 2010 Elsevier Inc.


## 1. INTRODUCTION

Peroxisomes are eukaryotic organelles that are 0.1–1  $\mu\text{m}$  in diameter, surrounded by a single membrane, and lacking genetic materials. Despite their small size and simple structures, peroxisomes house a battery of enzymes and participate in crucial metabolic pathways (Schrader and Fahimi, 2008). Peroxisomes are essential to human development; deficiencies in peroxisome biogenesis, enzymes, or transporters cause a number of inherited diseases, collectively termed peroxisome disorders (Fidaleo, 2009). Peroxisomes are also central to plant development, as null mutations in a number of proteins required for peroxisome assembly and protein import lead to embryo lethality. In addition to functions such as  $\beta$ -oxidation of fatty acids and degradation of reactive oxygen species, which are common to peroxisomes in all species, plant peroxisomes also mediate the glyoxylate cycle, glycolate recycling during photorespiration, jasmonic acid biosynthesis, metabolism of the proto-auxin, indole-3-butyric acid, generation of signaling molecules, and plant responses to environmental stresses (Kaur et al., 2009; Nyathi and Baker, 2006). To date, about 130 *Arabidopsis* genes have been confirmed to encode peroxisomal proteins (<http://www.peroxisome.msu.edu/>). This number is significantly larger than those identified from human (85 genes) and the yeast *Saccharomyces cerevisiae* (61 genes; summarized by Schrader and Fahimi, 2008), indicating that plant peroxisomes possess a more complex proteome and therefore may carry out more diverse functions compared with peroxisomes from other eukaryotes.

To maintain their functions in development and under adverse conditions, peroxisomes remodel their morphology, number, and protein composition in response to various metabolic and developmental stimuli. Processes giving rise to changes in peroxisome abundance in a cell include (1) *de novo* formation of peroxisomes from the endoplasmic reticulum (ER), (2) division and proliferation from preexisting peroxisomes, (3) inheritance from mother cells after cell division or budding, and (4) pexophagy, an autophagy-related pathway that selectively degrades peroxisomes (Platta and Erdmann, 2007). In plants, very little work has been reported on

*de novo* biogenesis, inheritance, and degradation of peroxisomes, whereas peroxisome division and proliferation have been actively investigated at the cell biological and molecular levels and hence will be the focus of this review. “Division” often refers to the cell cycle-associated duplication (or replication) of peroxisomes. The term “proliferation” is normally used to describe increases in peroxisome abundance in response to external cues, a process that results in the formation of multiple peroxisomes from a preexisting peroxisome within a short period of time (Yan et al., 2005). In this review, the terms “division” and “proliferation” will be used interchangeably, because both events involve a multistep process including peroxisome elongation/growth/tubulation, constriction/segregation, and fission (Fagarasanu et al., 2007; Thoms and Erdmann, 2005).

In recent years, several proteins or protein families involved in the division/proliferation of peroxisomes and the nuclear control of these events have been identified from the model plant species *Arabidopsis thaliana*. These factors were mostly identified through searches for plant homologs of known peroxisomal division proteins from yeast and from forward genetic screens that look for mutants with abnormal peroxisome morphologies or abundance. Studies from *Arabidopsis* support the view that the core components of the peroxisome division and proliferation machineries are largely conserved during evolution, whereas nuclear events that lead to peroxisome proliferation in diverse eukaryotic organisms appear to be largely distinct. However, plant-specific components of the division and proliferation pathways are also being discovered. We recently published a mini review on plant peroxisome division and proliferation, which highlights the latest advances in the field (Kaur and Hu, 2009). Here, I provide a more comprehensive overview of the subject and discuss some examples at more depth. While this review is focusing on the molecular mechanisms of peroxisome division and proliferation in plants, comparisons between different model systems will also be drawn when needed.



## **2. ROLES OF PEROXIN11 PROTEINS, DYNAMIN-RELATED PROTEINS, AND FISSION1**

### **2.1. PEROXIN11 (PEX11) proteins in peroxisome elongation**

#### **2.1.1. PEX11 proteins in nonplant species**

Unlike in plants and mammals, where peroxisomes are essential to organism survival, peroxisomes are dispensable for yeast growth in glucose-containing media and become essential only when yeasts are grown on media solely containing specific carbon or nitrogen sources, for example, oleic acid and methanol (Veenhuis et al., 2000). This feature has enabled yeasts to become an ideal model system to study peroxisome biogenesis (including

proliferation) using mutant analysis. Previous work conducted with yeast peroxisome mutants has led to the identification of a number of proteins involved in peroxisome division and proliferation, among them PEROXIN11 (Pex11p) was the first to be discovered.

The *S. cerevisiae* Pex11p protein is a peripheral membrane protein located at the inner surface of the peroxisome membrane. The *pex11* null mutants contain one or two giant peroxisomes in each cell and fail to grow on medium solely containing oleic acid, because peroxisomes are required to metabolize these substrates. Conversely, overexpressing the *PEX11* gene leads to peroxisomal elongation and an increase in peroxisome number (Erdmann and Blobel, 1995; Marshall et al., 1995). Based on these mutant phenotypes, it is believed that Pex11p mediates the initial step of peroxisome division, that is, peroxisome elongation/tubulation (Fagarasanu et al., 2007). Subsequent work in *S. cerevisiae* led to the identification of two additional peripheral membrane proteins, Pex25p and Pex27p, whose null mutants have few and enlarged peroxisomes and gain-of-function mutants have increased peroxisome abundance (Rottensteiner et al., 2003; Smith et al., 2002; Tam et al., 2003). Pex25p and Pex27p are both much larger than Pex11p, and the C-terminus of each shares weak sequence similarity with the entire Pex11p protein. The *pex25 pex27* double deletion mutants exhibit enhanced mutant phenotypes compared with the single mutants, and the *pex11 pex25 pex27* triple mutants are severely impaired in protein import and completely cease to grow on oleate-containing medium, suggesting that these three proteins are at least partially redundant in function (Tam et al., 2003). It is believed that Pex11p is required for growth mainly under conditions that induce peroxisome proliferation, whereas Pex25p and Pex27p play stronger roles in conditions where peroxisome proliferation is not induced (Rottensteiner et al., 2003; Tam et al., 2003). Although Pex11p, Pex25p, and Pex27p are together referred to as members of the Pex11 family in *S. cerevisiae*, phylogenetic analysis demonstrated that the yeast Pex11p is more closely related to its homologs from other species than with Pex25p and Pex27p, suggesting that the biochemical functions of Pex11p and Pex25p/Pex27p may be distinct (Orth et al., 2007). Filamentous fungi contain three subfamilies of Pex11 (Pex11, Pex11B, and Pex11C), some of which have been shown to be required for the proliferation of peroxisomes and differentiation of the peroxisome derivatives, the Woronin bodies (Escano et al., 2009; Hynes et al., 2008; Kiel et al., 2005, 2006). Interestingly, besides peroxisome proliferation, the *PEX11* gene from the methylotrophic yeast *Hansenula polymorpha* has an additional role in peroxisome segregation during cell division (Krikken et al., 2009).

Three isoforms of PEX11 (PEX11 $\alpha$ , - $\beta$ , and - $\gamma$ ) are found in mammals. All three proteins are integral membrane proteins of the peroxisome, with both the N- and C-termini facing the cytosol, a topology different from the *S. cerevisiae* Pex11p protein (Thoms and Erdmann, 2005). PEX11 $\beta$  is

constitutively expressed; its knockout mutant confers neonatal lethality. In contrast, *PEX11 $\alpha$*  expression is strongly induced by hypolipidemic drugs such as clofibrate, and the PEX11 $\alpha$  protein does not play a major role in development or peroxisome function, because its null mutant has no obvious growth phenotypes. Compared with PEX11 $\alpha$ , PEX11 $\beta$  leads to a stronger peroxisome number increase when overexpressed. Although overexpressing PEX11 $\gamma$  does not cause increases in peroxisome abundance, it does induce enlargement and clustering of peroxisomes (Li et al., 2002a,b). Similarly, *Trypanosoma brucei* has three PEX11-like proteins—that is, Pex11p and two highly identical proteins, GIM5A and GIM5B—that show weak sequence similarity with Pex11p. Consistent with their role in promoting proliferation of peroxisomes (called glycosomes in *Trypanosoma*), loss- and gain-of-function mutants of these genes show phenotypes similar to those of the yeast *pex11* mutants (Lorenz et al., 1998; Voncken et al., 2003). In summary, multiple PEX11-related proteins contribute to peroxisome elongation/tubulation in all the model systems examined so far.

### 2.1.2. PEX11 homologs in *Arabidopsis*

Homology-based searches led to the identification of five PEX11 homologs from both *Arabidopsis* and rice (*Oryza sativa*). In *Arabidopsis*, the PEX11 family can be further divided into three subfamilies, PEX11a, PEX11b, and PEX11c–e. All five PEX11 isoforms were confirmed as being associated with peroxisome membranes using immunolocalization in *Arabidopsis* suspension cultures, and by fluorescence microscopic analysis and protein fractionation in transgenic *Arabidopsis* plants expressing CFP–PEX11 fusion proteins (Lingard and Trelease, 2006; Orth et al., 2007). Protein expression and topological studies using *Arabidopsis* suspension cell cultures demonstrated that all five *Arabidopsis* PEX11 proteins directly target to peroxisomes after they are expressed in the cells. In addition, PEX11b–e have a membrane topology similar to their mammalian homologs, that is, both the N- and C-terminal tails are exposed to the cytosol. An exception is PEX11a, whose C-terminus faces the peroxisomal matrix (Lingard and Trelease, 2006).

Similar to their homologs in other species, *Arabidopsis* PEX11 proteins promote peroxisome division and proliferation, inducing peroxisome elongation or an increase in peroxisome number when overexpressed (Lingard and Trelease, 2006; Orth et al., 2007). Reducing the expression of individual *PEX11* or a subfamily of *PEX11* genes using RNAi results in decreases in peroxisome abundance and defects in peroxisome division. None of the RNAi plants show any growth phenotypes, suggesting that PEX11 isoforms are at least partially redundant in function (Orth et al., 2007). Furthermore, heterologous expression of PEX11c and PEX11e in the *S. cerevisiae pex11* null mutant partially rescued the growth phenotypes on oleic acid medium, providing direct evidence for the conserved role of PEX11 in peroxisome proliferation across diverse species (Orth et al., 2007).

Genes encoding the *Arabidopsis* PEX11 isoforms show distinct expression patterns. For example, *PEX11a* is constitutively expressed at low levels in all tissues, *PEX11e* is strongly expressed in seeds, and *PEX11d* is highly abundant in green leaves. In seedlings, *PEX11b* is strongly induced by light and mediates light-induced peroxisome proliferation (Desai and Hu, 2008; Orth et al., 2007). Among all the model systems in which this protein family has been studied, plants seem to have the largest PEX11 family. PEX11 is also the largest protein family of all the peroxins (proteins involved in peroxisome biogenesis) in *Arabidopsis* ([www.arabidopsis.org](http://www.arabidopsis.org)). Because peroxisome proliferation is essential to plant survival, functionally redundant PEX11 isoforms may have evolved to perform in specific peroxisomal variants and respond to various environmental cues to ensure the optimal amount and proper functioning of these organelles in diverse conditions.

Even though all five *Arabidopsis* PEX11 proteins contribute positively to peroxisome proliferation, biochemical functions may differ among isoforms (Hu, 2007). Evidence supporting this view include (1) *PEX11a* has a membrane topology distinct from the other four isoforms (Lingard and Trelease, 2006), (2) somewhat different peroxisome morphologies were observed after individual PEX11 isoforms were overexpressed in plant cells (Lingard and Trelease, 2006; Orth et al., 2007), and (3) only *PEX11c* and *PEX11e* were able to complement the yeast *pex11* mutant (Orth et al., 2007). To test this hypothesis, we must first determine whether PEX11 isoforms can functionally substitute for each other. Further, to determine the exact contribution of this protein family to peroxisome biogenesis and plant development, mutants in which all five *PEX11* genes are knocked out or silenced need to be generated and analyzed.

### 2.1.3. Possible mechanism for the function of PEX11

The ~24–27-kDa PEX11 protein is the most extensively characterized peroxisome division protein in diverse species, yet its precise biochemical role remains unknown. Based on analyses of proteins extracted from the peroxisomal membrane in *S. cerevisiae* (Erdmann and Blobel, 1995) and purified glycosomes (i.e., peroxisomes) in *T. brucei* (Lorenz et al., 1998), along with a recent proteomic analysis of isolated leaf peroxisomes from *Arabidopsis* (Reumann et al., 2009), we can conclude that PEX11 is one of the most abundant peroxisomal membrane proteins in all species.

Interestingly, PEX11 shares extensive sequence similarity with the lipid-binding domains (LBDs) of peroxisome proliferators PPAR $\alpha$ , - $\beta$ , and - $\gamma$ , members of the animal nuclear hormone receptor superfamily (Barnett et al., 2000; also see Section 4.1). Thus, this protein may be directly involved in remodeling the peroxisomal membrane through phospholipid binding (Fagarasanu et al., 2007). In addition, studies in Chinese hamster ovary (CHO) cells (Kobayashi et al., 2007), *Arabidopsis* cultured cells (Lingard et al., 2008), and tobacco leaves (X. Zhang and J. Hu, unpublished

data) have demonstrated physical interaction or close proximity between PEX11 and proteins involved in the late steps of peroxisome division (see Section 2.4). These data support the notion that, besides inducing membrane elongation/tubulation, PEX11 is also involved, directly or indirectly, in recruiting downstream effector proteins to complete the division process. Other possible functions, such as metabolite transport and fatty acid metabolism, have also been proposed for PEX11 proteins (Thoms and Erdmann, 2005).

A C-terminal dilysine motif (KXKXX) is present in *Arabidopsis* PEX11c–e, mammalian PEX11 $\alpha$ , and the *Trypanosoma* Pex11 protein. This motif was shown in rat to bind to coat protein 1 (COP1) and to recruit the small GTPase adenosine diphosphate (ADP)-ribosylation factor (ARF1), suggesting that PEX11 may mediate peroxisome division by promoting membrane vesiculation (Anton et al., 2000; Passreiter et al., 1998). However, the importance of this domain in peroxisome division was put into question following reports that mutations in the C-terminus of the trypanosome Pex11, which abolished COP binding, did not affect its function (Maier et al., 2000), and that the dilysine motif in *Arabidopsis* PEX11c–e is not required for inducing peroxisome division in *Arabidopsis* cell cultures (Lingard and Trelease, 2006).

Pex11p in *S. cerevisiae* forms homooligomers, resulting in the inhibition of its function in peroxisome division (Marshall et al., 1996). Pex25p and Pex27p also homo- and heterodimerize (Rottensteiner et al., 2003; Tam et al., 2003). Using bimolecular fluorescence complementation (BiFC) assays with *Arabidopsis* cultured cells, Lingard et al. (2008) showed that all five *Arabidopsis* PEX11 isoforms form homo- and heterooligomers. The biological consequences of these dimerization events in plants remain to be determined.

## 2.2. Dynamin-related proteins (DRPs) and peroxisome fission

### 2.2.1. Function of dynamins and DRPs

Dynamins and DRPs constitute a superfamily of large self-assembling GTPases that mediate membrane fission and fusion in biological processes such as endocytosis, vesicle trafficking, cell division, and organelle division and fusion (Praefcke and McMahon, 2004). Both conventional dynamins and DRPs contain a highly conserved N-terminal GTPase domain, a middle domain (MD), and a C-terminal GTPase effector domain (GED) that activates GTPase activity. Most classic dynamins additionally have a pleckstrin homology (PH) domain that is possibly capable of binding to membrane phospholipids, and a proline- and arginine-rich domain (PRD) that is believed to facilitate interaction with some proteins of the actin cytoskeleton (Hong et al., 2003; Thoms and Erdmann, 2005). Dynamins and DRPs act as mechanochemical enzymes or signaling GTPases by

forming oligomeric rings around membranes and enforcing membrane remodeling events in a GTP-driven manner (Gasper et al., 2009; Hoppins et al., 2007; Koch et al., 2004; Osteryoung and Nunnari, 2003; Praefcke and McMahon, 2004).

In nonplant model systems, DRPs known to mediate organelle fission include the mammalian Drp1 (DLP1) and the yeast Dnm1p and Vps1p proteins (Hoepfner et al., 2001; Koch et al., 2003; Kuravi et al., 2006; Li and Gould, 2003; Wilsbach and Payne, 1993). Mutations in these genes lead to fewer and enlarged/elongated peroxisomes that are able to constrict (so-called “beads on a string”), supporting the role for DRPs in the final fission of these organelles. The two yeast DRPs, Vps1p and Dnm1p, are recruited to the membrane through different pathways (see Section 2.3.1). Vps1p is mainly responsible for constitutive peroxisome division, whereas Dnm1p has a stronger role in conditions that induce peroxisome proliferation. Drp1 and Dnm1p are also part of the mitochondrial division machinery, and Vps1p is involved in vacuolar morphogenesis as well (Fagarasanu et al., 2007; Yan et al., 2005).

### 2.2.2. Three DRPs involved in peroxisome fission in *Arabidopsis*

Based on domain structure and sequence similarity, the 16 DRPs from *Arabidopsis* are grouped into six families (Hong et al., 2003). The first *Arabidopsis* DRP identified as active in peroxisome division is DRP3A, which had also been found to play a role in mitochondrial division (Arimura et al., 2004; Logan et al., 2004). A genetic screen performed in plants expressing the peroxisomal marker GFP-PTS1 (*Peroxisome Targeting Signal type 1*, composed of ser-lys-leu) led to the isolation of 24 *drp3A* alleles that are defective in peroxisomal and mitochondrial division to varying degrees (Mano et al., 2004). Carrying out a screen in the YFP-PTS1 background, we identified two additional alleles of DRP3A, substantiating its role as a major regulator of peroxisome division in *Arabidopsis* (Aung and Hu, 2009; Zhang and Hu, 2009). Like DRP3A, the other member of the DRP3 family (DRP3B) is also dual-targeted to peroxisomes and mitochondria; its T-DNA mutant displays impaired fission in mitochondria and (to a lesser extent) peroxisomes (Fujimoto et al., 2009; Zhang and Hu, 2009). DRP3A and DRP3B were found to homo- and heterodimerize in yeast two-hybrid assays (Fujimoto et al., 2009). The *drp3A drp3B* double mutants display a slightly stronger peroxisome phenotype but much more severe phenotypes in plant size and leaf pigmentation compared with the single mutants (Zhang and Hu, 2009).

DRP3A and DRP3B can replace each other in mitochondrial division; however, their roles in peroxisome division seem to differ significantly. More than two dozen *drp3A* alleles, but not a single *drp3B* allele, were isolated from the two GFP/YFP-based peroxisomal morphological mutant screens (Aung and Hu, 2009; Mano et al., 2004; Zhang and Hu, 2009). Further, *drp3A* mutants display stronger peroxisomal phenotypes than *drp3B* (Zhang and Hu, 2009). Lastly, DRP3A was able to rescue the peroxisomal phenotype in the

*drp3B* mutant, but DRP3B could not do the same for the *drp3A* mutant (Fujimoto et al., 2009). In summary, DRP3A has a much stronger contribution to peroxisome division than does DRP3B.

DRP5B (ARC5) was originally identified as a protein required for chloroplast division (Gao et al., 2003). Unexpectedly, we recently found that this protein has an additional role in the division of peroxisomes (X. Zhang and J. Hu, unpublished data). In addition to targeting to chloroplast division rings, GFP-DRP5B also localizes to punctate structures labeled by the peroxisomal marker CFP-PTS1. Besides having enlarged chloroplasts that are impaired in division, *drp5B* mutants also contain highly aggregated and/or enlarged peroxisomes that are unable to divide completely. Finally, the *drp5B* mutants exhibit deficiencies in major peroxisomal functions such as photorespiration and fatty acid  $\beta$ -oxidation. Consistent with the notion that dimer formation is necessary for GTPase activity (Low and Lowe, 2006), DRP5B is also able to self-interact and heterodimerize with DRP3A and DRP3B in both BiFC and coimmunoprecipitation (co-IP) assays (X. Zhang and J. Hu, unpublished data). A recent phylogenetic analysis of dynamin and dynamin-like proteins across diverse species revealed that DRP3A and DRP3B are grouped in the same subclade as the yeast and mammalian DRP proteins involved in peroxisome division (i.e., Dnm1p, Vps1p, and Drp1). In contrast, DRP5B, which is distantly related to DRP3, seems to arise from DRPs involved in cytokinesis. Furthermore, DRP5B and its orthologs are only found in plant and algal genomes (Miyagishima et al., 2008). Taken together, DRP5B is an invention of the plant/algal lineage to mediate the division of their organelles, i.e., chloroplasts and peroxisomes.

Although our results clearly point toward a role for DRP5B in peroxisome division, the contribution of DRP5B may be different from that of DRP3A and DRP3B. First, DRP5B has little sequence similarity with DRP3 and contains an additional PH domain. Second, YFP or GFP fusions of DRP3A and DRP3B were shown to be associated to but not completely colocalized with peroxisomes (Fujimoto et al., 2009; Mano et al., 2004; Zhang and Hu, 2009), yet GFP-DRP5B is evenly distributed on peroxisomes. Future work on the DRPs should include determining the contribution of DRP5B versus DRP3 to peroxisome division by gene complementation experiments and creating *drp3A drp3B drp5B* triple mutants to see whether mutant phenotypes are compounded. We cannot rule out the possibility that other members of the *Arabidopsis* DRP superfamily are also involved in the division of peroxisomes; thus, further analysis of the remaining DRPs in *Arabidopsis* is necessary to ascertain that we have a complete picture of all the DRPs involved in peroxisome division.

Peroxisomes, chloroplasts, and mitochondria act in concert in a number of metabolic processes in plants, such as photorespiration, fatty acid metabolism, and jasmonic acid biosynthesis; their intimate physical association is believed to be required for these coordinated actions (Kaur et al., 2009).



The use of shared fission components such as DRPs may be a mechanism to ensure coordinated divisions among these metabolically linked organelles. Whether such cooperative division events truly occur in plants awaits further investigation.

## 2.3. FISSION1 as an anchor for DRPs

### 2.3.1. FIS1 as a protein responsible for recruiting DRPs to the organelles

It is believed that DRPs do not contain organelle-targeting signals and must be recruited to the organelles from the cytosol by membrane-anchored proteins. In yeast, Dnm1p is recruited to the peroxisome membrane and the outer membrane of mitochondria by the same protein complex, which is composed of the C-terminal tail-anchored protein Fis1p and two WD40 proteins, Mdv1p and Caf4p, which act as linkers at the cytosolic side of the membrane (Hoppins et al., 2007; Motley et al., 2008). The peroxisome targeting of Vps1p, however, is independent of this Fis1p/Caf4p/Mdv1p complex (Motley et al., 2008). Mammals do not seem to have Mdv1p and Caf4p homologs, but they contain a FIS1 homolog, which is required for tethering Drp1 (DLP1) to peroxisomes and mitochondria by interacting with Drp1 through the cytoplasmic tetratricopeptide repeat (TPR) domain (Kobayashi et al., 2007; Koch et al., 2003, 2005; Yoon et al., 2003). The mammalian FIS1 protein homodimerizes, which is necessary for its proper function in organelle fission (Serasinghe and Yoon, 2008). Taken together, FIS1 represents another evolutionarily conserved factor in peroxisome division.

### 2.3.2. Two *Arabidopsis* FIS1 proteins with rate-limiting roles in the fission of peroxisomes and mitochondria

*Arabidopsis* has two FIS1 homologs, FIS1A (BIGYIN) and FIS1B, both of which are dual-targeted to peroxisomes and mitochondria (Zhang and Hu, 2009). The C-terminus of FIS1A/FIS1B and human hFis1 is necessary and sufficient for peroxisomal targeting, with some species-specific features. For example, the sequence downstream from the transmembrane domain is required for peroxisome targeting in mammalian cells but not in plants (Koch et al., 2005; Stojanovski et al., 2004; Zhang and Hu, 2008). Single and double mutants of *FIS1* show slowed growth, reduced number of peroxisomes and mitochondria, and enlarged peroxisomes and mitochondria that are impaired in fission (Scott et al., 2006; Zhang and Hu, 2009). In contrast, ectopic expression of *FIS1A* or *FIS1B* significantly increases the number of peroxisomes and mitochondria (Zhang and Hu, 2008, 2009). These organelle phenotypes resemble those caused by overexpressing hFis1 in human cells (Koch et al., 2005; Yoon et al., 2003), thus reinforcing the role for FIS1 as a rate-limiting factor in initiating organelle fission (Zhang and Hu, 2008).

FIS1A and FIS1B proteins expressed in *Arabidopsis* cultured cells seem to behave differently from those in transgenic plants. For example, they cannot

localize to peroxisomes when expressed alone. In addition, whereas FIS1B is required for cell cycle-associated replication of peroxisomes, FIS1A is not involved in this process (Lingard et al., 2008).

Using BiFC and co-IP assays, we also found FIS1A and FIS1B to self-interact on peroxisomes and mitochondria; however, neither is able to heterodimerize. In addition, these experiments detected interaction between DRP5B and FIS1A but not FIS1B, suggesting that DRP3A, DRP3B, and DRP5B may be recruited to peroxisomes by specific isoforms of FIS1 and possibly other anchor proteins (X. Zhang and J. Hu, unpublished data). It remains to be determined whether these DRPs dissociate from peroxisomes and mitochondria when both *FIS1* genes are knocked out.

#### 2.4. Interplay between PEX11, FIS1, and DRPs

In CHO cells, chemical cross-linking and co-IP assays revealed a peroxisomal heterocomplex, which consists of PEX11 $\beta$ , Drp1 (DLP1), and FIS1, as well as physical interaction between FIS1 and PEX11 $\beta$  (Kobayashi et al., 2007). BiFC experiments with *Arabidopsis* cultured cells showed all five PEX11 proteins to interact with FIS1B (Lingard et al., 2008). Using BiFC and co-IP experiments with tobacco cells expressing tagged PEX11, FIS1, and DRP proteins from *Arabidopsis*, we have shown that members of the *Arabidopsis* PEX11 protein family interact and form complexes with some FIS1 and DRP isoforms on the peroxisome, supporting the existence of a similar protein complex on plant peroxisomes (X. Zhang and J. Hu, unpublished data). All these data collectively suggest that there is an obvious link between proteins involved in the early and late stages of peroxisome division.

In synchronized *Arabidopsis* suspension cell cultures, there is a correlation between peaks of expression of *PEX11c-e*, *FIS1B*, and *DRP3A* and peroxisome elongation and division. This result prompted the hypothesis that oligomerization of PEX11c-e leads to peroxisome elongation and subsequent recruitment of FIS1B, which then recruits DRP3A to complete the fission of peroxisomes (Lingard et al., 2008). In addition, overexpressing PEX11 $\beta$  in human fibroblast cells leads to higher levels of DLP1 (Drp1) that are associated with peroxisomes, suggesting that PEX11 may be involved in the recruitment of DRPs to peroxisomes in a direct or indirect manner (Li and Gould, 2003). The exact functional association between PEX11 and FIS1/DRP remains to be examined.

### 3. OTHER PROTEINS AND PATHWAYS

Recently, the *S. cerevisiae* Rpn11 protein was found to control the fission of both mitochondria and peroxisomes via the Fis1p pathway. Rpn11 is a conserved subunit of the lid subcomplex of the regulatory

particle (RP) on the 26S proteasome, yet its control over organelle division is independent of its proteolytic activity (Hofmann et al., 2009). Virtually nothing is known about the regulators of FIS1 in plants. It will be interesting to see whether the plant Rpn11 protein has a similar role in organelle division.

In yeasts, two additional families of proteins—that is, Pex28p/Pex29p and the Dysferlin domain-containing Pex30p/Pex31p/Pex32p—have been implicated in controlling the separation and size/number of peroxisomes with yet unknown mechanisms (Yan et al., 2005). It is unclear whether these PEX proteins, together with the WD40 linker proteins Mdv1p and Caf4p (see Section 2.3.1), have functional equivalents in plants. Although animals do not contain apparent homologs of Mdv1p and Caf4p, they do use matozoan-specific proteins for peroxisome division. One such protein is Mff (*Mitochondrial fission factor*), which was originally identified from a high-throughput siRNA (small interference RNA) screen in *Drosophila* cells. The mammalian Mff protein is tail-anchored to the membranes of mitochondria and peroxisomes and is required for the division of both organelles. Mff is present in a protein complex different from the FIS1 complex, suggesting that its function is independent of FIS1 (Gandre-Babbe and van der Bliek, 2008). We also identified a plant-specific, dual-targeted protein from *Arabidopsis*. This protein, designated PMD1 (*Peroxisome and Mitochondrial Division 1*), anchors to the membrane of peroxisomes and mitochondria by the C-terminus, causing changes to the morphology and abundance of these two types of organelles in loss- and gain-of-function mutants (K. Aung and J. Hu, unpublished data). It is unknown whether PMD1 functions in the FIS1-dependent or -independent pathway. Isolating proteins that interact with PEX11, FIS1, DRPs, and PMD1 and conducting additional genetic screens for peroxisome division mutants will also be necessary to reveal the plant-specific aspects of peroxisome division.

The metabolic status of the peroxisome also affects the shape and abundance of peroxisomes. Lending support to this view are the findings that some *Arabidopsis*  $\beta$ -oxidation mutants that accumulate acyl-CoAs inside peroxisomes contain fewer but larger peroxisomes (Baker et al., 2006; Graham et al., 2002). In fact, a mechanism underlying the control of peroxisome division by lipid metabolism has been uncovered in the yeast *Yarrowia lipolytica*. In this yeast species, peroxisomes become division competent only after they have obtained the full set of enzymes for lipid metabolism, at which point the  $\beta$ -oxidation enzyme AOX (acyl-CoA oxidase) relocates from matrix to the membrane and binds to the membrane protein Pex16p. This action triggers lipid biosynthesis in the membrane and the subsequent formation of a complex consisting of two peroxisome membrane proteins, Pex10p and Pex19p, and the DRP protein Vps1p, ultimately resulting in peroxisome division (Guo et al., 2003, 2007). However, this mechanism has yet to be found to occur in other yeast species, and thus may be species-specific.



## 4. ENVIRONMENTAL AND NUCLEAR REGULATION OF PEROXISOME PROLIFERATION

### 4.1. Nuclear regulators of peroxisome proliferation in yeasts and mammals

The dynamic behavior of peroxisome abundance is controlled by a suite of endogenous and exogenous cues. Molecular mechanisms by which some of the metabolic cues regulate peroxisome proliferation have been elucidated in yeasts and mammals.

Yeasts are able to utilize a variety of carbon and nitrogen resources. Expression of genes encoding enzymes (e.g.,  $\beta$ -oxidation enzymes) required for the degradation of nonfermentable carbons is generally repressed by fermentable sugars such as glucose; under these conditions, peroxisomes are dispensable for yeast growth. Conversely, the same set of genes is derepressed by nonfermentable carbons and further induced significantly by fatty acids such as oleic acid, under which conditions peroxisomes rapidly proliferate to metabolize these substrates. In *S. cerevisiae*, the transcription factors responsible for oleate-induced changes include the zinc-cluster proteins Pip2p and Oaf1p and the C<sub>2</sub>H<sub>2</sub> zinc-finger protein Adr1p. To activate gene expression, these proteins bind to conserved *cis*-elements in the promoters of the target genes, many of which encode enzymes in fatty acid  $\beta$ -oxidation and proteins involved in peroxisome proliferation. Among these are AOX, the first enzyme in the  $\beta$ -oxidation pathway, and the peroxisome proliferation factors Pex11p and Pex25p. Specifically, Pip2p and Oaf1p form a complex and interact with the oleate response element (ORE), whereas Adr1p binds to the upstream activating site, that is, UAS1 (Gurvitz and Rottensteiner, 2006).

PPAR $\alpha$ , - $\beta$ , and - $\gamma$  are mammalian peroxisome proliferator-activated receptors belonging to the nuclear hormone receptor superfamily. These proteins are activated by a wide range of natural and synthetic compounds and elicit cellular responses such as fatty acid metabolism and peroxisome proliferation (Michalik et al., 2006). When activated by a ligand, such as the hypolipidemic drug clofibrate, these transcription factors form heteroduplexes with the retinoid X receptor (RXR) and bind to the PPAR response element (PPRE) located in the promoters of their target genes. Many of these target genes encode proteins involved in fatty acid metabolism and biogenesis of peroxisomes. Among the three PPARs, PPAR $\alpha$  plays a major role in fatty acid catabolism, whereas PPAR $\beta$  and PPAR $\gamma$  have broader functions (Michalik et al., 2006). PEX11 $\alpha$  from mouse and human both contain a PPRE in the 3'-flanking region that is capable of binding to PPAR $\alpha$ , indicating that PEX11 $\alpha$  is a transcriptional target of PPAR $\alpha$  (Shimizu et al., 2004). However, Li et al. (2002a) found that PEX11 $\alpha$  is

not required for PPAR $\alpha$ -mediated responses; instead, it is required for peroxisome proliferation in response to a nonclassic peroxisome proliferator, 4-phenylbutyrate.

## 4.2. Environmental factors in plants

Homologs of the yeast and mammalian transcriptional factors involved in inducing peroxisome proliferation have not been identified from plant genomes. However, treatment of *Arabidopsis* plants with the peroxisome proliferator clofibrate leads to an increase in the abundance of peroxisomes, along with an upregulation of the *KAT2* gene, which encodes an isoform of the  $\beta$ -oxidation enzyme, 3-ketoacyl-CoA thiolase (Castillo et al., 2008). In addition, tobacco plants expressing the PPAR $\alpha$  protein from *Xenopus laevis* exhibit an increased activity of AOX as well as an increase in peroxisome number (Nila et al., 2006). These results support the idea that some aspects of the clofibrate-regulated peroxisome proliferation pathways may be conserved from animals to plants. Interestingly, *Arabidopsis* leaves treated with jasmonic acid (JA)—a plant hormone whose biosynthesis is completed in the peroxisome—contain fewer peroxisomes, indicating that JA is a negative regulator of peroxisome proliferation (Castillo et al., 2008).

In addition to clofibrate and JA, various stress conditions, imposed by treatments of high light, ozone, isotretinoin, cadmium, and hydrogen peroxide, also cause changes in peroxisome abundance, morphology, movement, and/or activity (de Felipe et al., 1988; Ferreira et al., 1989; Lopez-Huertas et al., 2000; Oksanen et al., 2003; Rodriguez-Serrano et al., 2009). A recent work in *Arabidopsis* described in detail the cellular events taking place after exposure of plants to H<sub>2</sub>O<sub>2</sub> and UV-induced hydroxyl radicals, reporting that peroxisomes produce long extensions (peroxules) and subsequently go through fission (Sinclair et al., 2009). Thus, plant peroxisomes perceive a variety of signals and respond by altering their abundance and morphology, in addition to protein content. The next step in research would be to elucidate the molecular mechanisms underlying these interesting phenomena.

## 4.3. Phytochrome A-dependent pathway in light-induced peroxisome proliferation

A light signaling pathway that regulates peroxisome abundance in plants was partially dissected in our laboratory (Desai and Hu, 2008). Upon light treatment, germinated seedlings make the transition from heterotrophic to autotrophic growth, during which proteins required for photosynthesis and the accompanying photorespiration pathway are actively synthesized and imported into the pertinent organelles. Not surprisingly, we found an increase in peroxisome abundance after treating dark-grown *Arabidopsis*

seedlings containing the peroxisomal marker protein YFP-PTS1 with light. These data suggest that an increase in the number of peroxisomes takes place concomitantly with the enzymatic changes inside these organelles.

The first molecular component discovered in this light-induced peroxisome proliferation pathway is PEX11b, a member of the PEX11 family of peroxisome elongation regulators. The expression of *PEX11b* is strongly upregulated by light, and plants in which the *PEX11b* gene is suppressed by RNAi show reduced responses to light compared with wild-type plants, suggesting that PEX11b plays a pivotal role in this process. A subsequent screening of a number of light signaling mutants in *Arabidopsis* enabled us to identify two regulators of *PEX11b* expression, the far-red light receptor phyA and a bZIP transcription factor, HYH (HY5 Homolog). In *phyA* and *hyh* mutants, light induction of *PEX11b* is strongly reduced and the number of peroxisomes is markedly decreased, whereas overexpressing *PEX11b* complemented the mutant phenotypes. Furthermore, we uncovered a direct link between PEX11b and HYH by demonstrating that the promoter of *PEX11b*, which is enriched in light responsive elements (LREs), interacts with the HYH transcription factor in gel-shift assays. The homolog of HYH, HY5, another master regulator of photomorphogenesis, does not seem to bind to the promoter of *PEX11b* and has little impact on the expression of *PEX11b* (Desai and Hu, 2008).

Based on these data, we proposed the existence of a branch of the phyA-mediated light signaling network, which is composed of the nuclear protein HYH, its transcriptional target *PEX11b*, and possibly other yet unidentified factors. Light-induced peroxisome proliferation is, at least in part, an outcome of *PEX11b* gene activation (Desai and Hu, 2008). Although we need to define this pathway more precisely by identifying other components and the actual *cis*-elements bound by HYH, this work represents the first molecular revelation of a signaling pathway in plant peroxisome proliferation.

## 5. CONCLUDING REMARKS

Through work conducted in the past few years, a model of peroxisome division and proliferation in the reference plant *Arabidopsis* has emerged (Fig. 3.1). Several classes of proteins controlling various steps of peroxisome division/proliferation, and nuclear factors and exogenous cues that have an impact on peroxisome proliferation, have begun to be revealed. Whereas some of the core components of the peroxisome proliferation machinery are largely conserved, environmental and nuclear regulations of the process seem to vary tremendously among different evolutionary lineages.

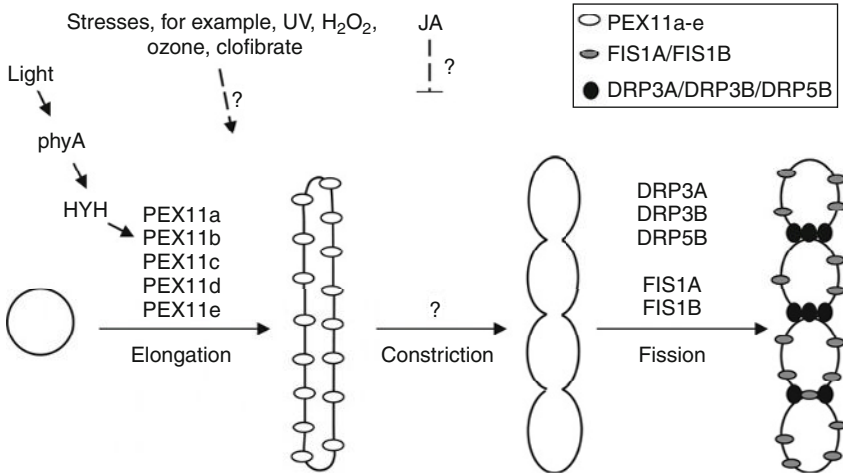


**Figure 3.1** Factors that regulate peroxisome division and proliferation in *Arabidopsis*. Peroxisome division and proliferation from preexisting peroxisomes occur through several partially overlapping steps, including elongation, constriction, and fission. All five isoforms of PEX11 are involved in the initial elongation stage, whereas proteins responsible for membrane constriction are elusive. Peroxisome fission is mediated by at least three dynamin-related proteins—that is, DRP3A, DRP3B, and DRP5B—which are recruited to the peroxisome membranes presumably by the C-terminal tail-anchored proteins FIS1A and FIS1B. Light induces peroxisome proliferation, at least in part, through activation of the *PEX11b* gene via the far-red light receptor phyA and the bZIP transcription factor HYH, the latter of which directly interacts with the *PEX11b* promoter. By yet unknown mechanisms, various stresses and the hypolipidemic drug clofibrate also induce the proliferation of peroxisomes, whereas JA treatment results in a decrease in peroxisome abundance.

Many questions regarding plant peroxisome division/proliferation and dynamics remain to be answered. For example, what is the exact biochemical mechanism by which the PEX11 proteins initiate peroxisome elongation? How do the five *Arabidopsis* PEX11 homologs differ in their function? Which proteins specifically mediate peroxisome constriction? Besides FIS1A and FIS1B, are there other proteins present in the complex that recruits DRPs to peroxisomes? Are there FIS1-independent and plant-specific pathways in peroxisome fission? How is the dual targeting of DRP3A, DRP3B, DRP5B, FIS1A, FIS1B, and PMD1 achieved? Are divisions of peroxisomes, mitochondria, and chloroplasts coordinated? Furthermore, much has to be learned about nuclear proteins regulating the peroxisomal responses to various developmental, metabolic, and environmental stimuli and peroxisomal components that serve as the targets for these nuclear factors. Finally, there are large gaps in our understanding of *de novo* peroxisome biogenesis, peroxisome inheritance after cell division, and how these organelles are degraded in plants. The next few years should

be an exciting time to address these questions using cell biological, genetic, biochemical, *in silico*, and proteomic approaches. Deciphering the dynamic behavior of peroxisomes at the molecular level will be an important step toward a complete understanding of how these essential organelles mediate plant growth and development and plant interaction with the environment.

## ACKNOWLEDGMENTS

I apologize to those whose work I was unable to cite in this review due to space limitations. Work in my lab was supported by grants from the Chemical Sciences, Geosciences and Biosciences Division, Office of Basic Energy Sciences, Office of Science, U.S. Department of Energy (DE-FG02-91ER20021), Michigan State University Intramural Research Grant Program (IRGP), and the National Science Foundation (MCB 0618335). I also thank Navneet Kaur for comments on the manuscript and Karen Bird for editorial assistance.

## REFERENCES

- Anton, M., Passreiter, M., Lay, D., Thai, T.P., Gorgas, K., Just, W.W., 2000. ARF- and coatamer-mediated peroxisomal vesiculation. *Cell Biochem. Biophys.* 32 (Spring), 27–36.
- Arimura, S., Aida, G.P., Fujimoto, M., Nakazono, M., Tsutsumi, N. (2004). *Arabidopsis* dynamin-like protein 2a (ADL2a), like ADL2b, is involved in plant mitochondrial division. *Plant Cell Physiol.* 45, 236–242.
- Aung, K., Hu, J., 2009. The *Arabidopsis* peroxisome division mutant *pdd2* is defective in the *DYNAMIN-RELATED PROTEIN3A (DRP3A)* gene. *Plant Signal. Behav.* 4, 542–544.
- Baker, A., Graham, I.A., Holdsworth, M., Smith, S.M., Theodoulou, F.L., 2006. Chewing the fat: beta-oxidation in signalling and development. *Trends Plant Sci.* 11, 124–132.
- Barnett, P., Tabak, H.F., Hetteema, E.H., 2000. Nuclear receptors arose from pre-existing protein modules during evolution. *Trends Biochem. Sci.* 25, 227–228.
- Castillo, M.C., Sandalio, L.M., Del Rio, L.A., Leon, J., 2008. Peroxisome proliferation, wound-activated responses and expression of peroxisome-associated genes are cross-regulated but uncoupled in *Arabidopsis thaliana*. *Plant Cell Environ.* 31, 492–505.
- de Felipe, M.R., Lucas, M.M., Pozuelo, J.M., 1988. Cytochemical study of catalase and peroxidase in the mesophyll of *Lolium rigidum* plants treated with isoproturon. *J. Plant Physiol.* 132, 67–73.
- Desai, M., Hu, J., 2008. Light induces peroxisome proliferation in *Arabidopsis* seedlings through the photoreceptor phytochrome A, the transcription factor HY5 HOMOLOG, and the peroxisomal protein PEROXIN11b. *Plant Physiol.* 146, 1117–1127.
- Erdmann, R., Blobel, G., 1995. Giant peroxisomes in oleic acid-induced *Saccharomyces cerevisiae* lacking the peroxisomal membrane protein Pmp27p. *J. Cell Biol.* 128, 509–523.
- Escano, C.S., Juvvadi, P.R., Jin, F.J., Takahashi, T., Koyama, Y., Yamashita, S., et al., 2009. Disruption of the *Aopex11-1* gene involved in peroxisome proliferation leads to impaired Woronin body formation in *Aspergillus oryzae*. *Eukaryot. Cell* 8, 296–305.
- Fagarasanu, A., Fagarasanu, M., Rachubinski, R.A., 2007. Maintaining peroxisome populations: a story of division and inheritance. *Annu. Rev. Cell Dev. Biol.* 23, 321–344.
- Ferreira, M.B., Bird, B., Davies, D.D., 1989. The effect of light on the structure and organization of *Lemna* peroxisomes. *J. Exp. Bot.* 40, 1029–1035.



- Fidaleo, M., 2009. Peroxisomes and peroxisomal disorders: the main facts. *Exp. Toxicol. Pathol.* doi:10.1016/j.etp. 2009.08.008.
- Fujimoto, M., Arimura, S., Mano, S., Kondo, M., Saito, C., Ueda, T., et al., 2009. *Arabidopsis* dynamin-related proteins DRP3A and DRP3B are functionally redundant in mitochondrial fission, but have distinct roles in peroxisomal fission. *Plant J.* 58, 388–400.
- Gandre-Babbe, S., van der Blik, A.M., 2008. The novel tail-anchored membrane protein Mff controls mitochondrial and peroxisomal fission in mammalian cells. *Mol. Biol. Cell* 19, 2402–2412.
- Gao, H., Kadirjan-Kalbach, D., Froehlich, J.E., Osteryoung, K.W., 2003. ARC5, a cytosolic dynamin-like protein from plants, is part of the chloroplast division machinery. *Proc. Natl. Acad. Sci. USA* 100, 4328–4333.
- Gasper, R., Meyer, S., Gotthardt, K., Sirajuddin, M., Wittinghofer, A., 2009. It takes two to tango: regulation of G proteins by dimerization. *Nat. Rev. Mol. Cell Biol.* 10, 423–429.
- Graham, I.A., Li, Y., Larson, T.R., 2002. Acyl-CoA measurements in plants suggest a role in regulating various cellular processes. *Biochem. Soc. Trans.* 30, 1095–1099.
- Guo, T., Kit, Y.Y., Nicaud, J.M., Le Dall, M.T., Sears, S.K., Vali, H., et al., 2003. Peroxisome division in the yeast *Yarrowia lipolytica* is regulated by a signal from inside the peroxisome. *J. Cell Biol.* 162, 1255–1266.
- Guo, T., Gregg, C., Boukh-Viner, T., Kyryakov, P., Goldberg, A., Bourque, S., et al., 2007. A signal from inside the peroxisome initiates its division by promoting the remodeling of the peroxisomal membrane. *J. Cell Biol.* 177, 289–303.
- Gurvitz, A., Rottensteiner, H., 2006. The biochemistry of oleate induction: transcriptional upregulation and peroxisome proliferation. *Biochim. Biophys. Acta* 1763, 1392–1402.
- Hoepfner, D., van den Berg, M., Philippsen, P., Tabak, H.F., Hetteema, E.H., 2001. A role for Vps1p, actin, and the Myo2p motor in peroxisome abundance and inheritance in *Saccharomyces cerevisiae*. *J. Cell Biol.* 155, 979–990.
- Hofmann, L., Saunier, R., Cossard, R., Esposito, M., Rinaldi, T., Delehodde, A., 2009. A nonproteolytic proteasome activity controls organelle fission in yeast. *J. Cell Sci.* 122, 3673–3683.
- Hong, Z., Bednarek, S.Y., Blumwald, E., Hwang, I., Jurgens, G., Menzel, D., et al., 2003. A unified nomenclature for *Arabidopsis* dynamin-related large GTPases based on homology and possible functions. *Plant Mol. Biol.* 53, 261–265.
- Hoppins, S., Lackner, L., Nunnari, J., 2007. The machines that divide and fuse mitochondria. *Annu. Rev. Biochem.* 76, 751–780.
- Hu, J., 2007. Plant peroxisome multiplication: highly regulated and still enigmatic. *J. Integr. Plant Biol.* 49, 1112–1118.
- Hynes, M.J., Murray, S.L., Khew, G.S., Davis, M.A., 2008. Genetic analysis of the role of peroxisomes in the utilisation of acetate and fatty acids in *Aspergillus nidulans*. *Genetics* 178, 1355–1369.
- Kaur, N., Hu, J., 2009. Dynamics of peroxisome abundance: a tale of division and proliferation. *Curr. Opin. Plant Biol.* 12, 781–788.
- Kaur, N., Reumann, S., Hu, J., 2009. Peroxisome biogenesis and function. In: *The Arabidopsis Book*. American Society of Plant Biologists, Rockville, MD. doi:10.1199/tab.0123.
- Kiel, J.A., van der Klei, I.J., van der Berg, M.A., Bovenberg, R.A., Veenhuis, M., 2005. Overproduction of a single protein, Pc-Pex11p, results in 2-fold enhanced penicillin production by *Penicillium chrysogenum*. *Fungal Genet. Biol.* 42, 154–164.
- Kiel, J.A., Veenhuis, M., van der Klei, I.J., 2006. *PEX* genes in fungal genomes: common, rare or redundant. *Traffic* 7, 1291–1303.
- Kobayashi, S., Tanaka, A., Fujiki, Y., 2007. Fis1, DLP1, and Pex11p coordinately regulate peroxisome morphogenesis. *Exp. Cell Res.* 313, 1675–1686.

- Koch, A., Thiemann, M., Grabenbauer, M., Yoon, Y., McNiven, M.A., Schrader, M., 2003. Dynamin-like protein 1 is involved in peroxisomal fission. *J. Biol. Chem.* 278, 8597–8605.
- Koch, A., Schneider, G., Luers, G.H., Schrader, M., 2004. Peroxisome elongation and constriction but not fission can occur independently of dynamin-like protein 1. *J. Cell Sci.* 117, 3995–4006.
- Koch, A., Yoon, Y., Bonekamp, N.A., McNiven, M.A., Schrader, M., 2005. A role for Fis1 in both mitochondrial and peroxisomal fission in mammalian cells. *Mol. Biol. Cell* 16, 5077–5086.
- Krikken, A.M., Veenhuis, M., van der Klei, I.J., 2009. *Hansenula polymorpha pex11* cells are affected in peroxisome retention. *FEBS J.* 276, 1429–1439.
- Kuravi, K., Nagotu, S., Krikken, A.M., Sjollem, K., Deckers, M., Erdmann, R., et al., 2006. Dynamin-related proteins Vps1p and Dnm1p control peroxisome abundance in *Saccharomyces cerevisiae*. *J. Cell Sci.* 119, 3994–4001.
- Li, X., Gould, S.J., 2003. The dynamin-like GTPase DLP1 is essential for peroxisome division and is recruited to peroxisomes in part by PEX11. *J. Biol. Chem.* 278, 17012–17020.
- Li, X., Baumgart, E., Dong, G.X., Morrell, J.C., Jimenez-Sanchez, G., Valle, D., et al., 2002a. PEX11 $\alpha$  is required for peroxisome proliferation in response to 4-phenylbutyrate but is dispensable for peroxisome proliferator-activated receptor  $\alpha$ -mediated peroxisome proliferation. *Mol. Cell Biol.* 22, 8226–8240.
- Li, X., Baumgart, E., Morrell, J.C., Jimenez-Sanchez, G., Valle, D., Gould, S.J., 2002b. PEX11  $\beta$  deficiency is lethal and impairs neuronal migration but does not abrogate peroxisome function. *Mol. Cell Biol.* 22, 4358–4365.
- Lingard, M.J., Trelease, R.N., 2006. Five *Arabidopsis* peroxin 11 homologs individually promote peroxisome elongation, duplication or aggregation. *J. Cell Sci.* 119, 1961–1972.
- Lingard, M.J., Gidda, S.K., Bingham, S., Rothstein, S.J., Mullen, R.T., Trelease, R.N., 2008. *Arabidopsis* PEROXIN11c-e, FISSION1b, and DYNAMIN-RELATED PROTEIN3A cooperate in cell cycle-associated replication of peroxisomes. *Plant Cell* 20, 1567–1585.
- Logan, D.C., Scott, I. and Tobin, A.K. (2004). ADL2a, like ADL2b, is involved in the control of higher plant mitochondrial morphology. *J. Exp. Bot.* 55, 783–785.
- Lopez-Huertas, E., Charlton, W.L., Johnson, B., Graham, I.A., Baker, A., 2000. Stress induces peroxisome biogenesis genes. *EMBO J.* 19, 6770–6777.
- Lorenz, P., Maier, A.G., Baumgart, E., Erdmann, R., Clayton, C., 1998. Elongation and clustering of glycosomes in *Trypanosoma brucei* overexpressing the glycosomal Pex11p. *EMBO J.* 17, 3542–3555.
- Low, H.H., Lowe, J., 2006. A bacterial dynamin-like protein. *Nature* 444, 766–769.
- Maier, A.G., Schulreich, S., Bremser, M., Clayton, C., 2000. Binding of coatomer by the PEX11 C-terminus is not required for function. *FEBS Lett.* 484, 82–86.
- Mano, S., Nakamori, C., Kondo, M., Hayashi, M., Nishimura, M., 2004. An *Arabidopsis* dynamin-related protein, DRP3A, controls both peroxisomal and mitochondrial division. *Plant J.* 38, 487–498.
- Marshall, P.A., Krimkevich, Y.I., Lark, R.H., Dyer, J.M., Veenhuis, M., Goodman, J.M., 1995. Pmp27 promotes peroxisomal proliferation. *J. Cell Biol.* 129, 345–355.
- Marshall, P.A., Dyer, J.M., Quick, M.E., Goodman, J.M., 1996. Redox-sensitive homodimerization of Pex11p: a proposed mechanism to regulate peroxisomal division. *J. Cell Biol.* 135, 123–137.
- Michalik, L., Auwerx, J., Berger, J.P., Chatterjee, V.K., Glass, C.K., Gonzalez, F.J., et al., 2006. International Union of Pharmacology. LXI. Peroxisome proliferator-activated receptors. *Pharmacol. Rev.* 58, 726–741.
- Miyagishima, S.Y., Kuwayama, H., Urushihara, H., and Nakanishi, H. (2008). Evolutionary linkage between eukaryotic cytokinesis and chloroplast division by dynamin proteins. *Proc. Natl. Acad. Sci. USA* 105, 15202–15207.

- Motley, A.M., Ward, G.P., Hetteema, E.H., 2008. Dnm1p-dependent peroxisome fission requires Caf4p, Mdv1p and Fis1p. *J. Cell Sci.* 121, 1633–1640.
- Nila, A.G., Sandalio, L.M., Lopez, M.G., Gomez, M., del Rio, L.A., Gomez-Lim, M.A., 2006. Expression of a peroxisome proliferator-activated receptor gene (xPPARalpha) from *Xenopus laevis* in tobacco (*Nicotiana tabacum*) plants. *Planta* 224, 569–581.
- Nyathi, Y., Baker, A., 2006. Plant peroxisomes as a source of signalling molecules. *Biochim. Biophys. Acta* 1763, 1478–1495.
- Oksanen, E., Haikio, E., Sober, J., Karnosky, D.F., 2003. Ozone-induced H<sub>2</sub>O<sub>2</sub> accumulation in field-grown aspen and birch is linked to foliar ultrastructure and peroxisomal activity. *New Phytol.* 161, 791–799.
- Orth, T., Reumann, S., Zhang, X., Fan, J., Wenzel, D., Quan, S., et al., 2007. The PEROXIN11 protein family controls peroxisome proliferation in *Arabidopsis*. *Plant Cell* 19, 333–350.
- Osteryoung, K.W., Nunnari, J., 2003. The division of endosymbiotic organelles. *Science* 302, 1698–1704.
- Passreiter, M., Anton, M., Lay, D., Frank, R., Harter, C., Wieland, F.T., et al., 1998. Peroxisome biogenesis: involvement of ARF and coatamer. *J. Cell Biol.* 141, 373–383.
- Platta, H.W., Erdmann, R., 2007. Peroxisomal dynamics. *Trends Cell Biol.* 17, 474–484.
- Praefcke, G.J., McMahon, H.T., 2004. The dynamin superfamily: universal membrane tubulation and fission molecules? *Nat. Rev. Mol. Cell Biol.* 5, 133–147.
- Reumann, S., Quan, S., Aung, K., Yang, P., Manandhar-Shrestha, K., Holbrook, D., et al., 2009. In-depth proteome analysis of *Arabidopsis* leaf peroxisomes combined with in vivo subcellular targeting verification indicates novel metabolic and regulatory functions of peroxisomes. *Plant Physiol.* 150, 125–143.
- Rodriguez-Serrano, M., Romero-Puertas, M.C., Sparkes, I., Hawes, C., Del Rio, L.A., Sandalio, L.M., 2009. Peroxisome dynamics in *Arabidopsis* plants under oxidative stress induced by cadmium. *Free Radic. Biol. Med.* doi:10.1016/j.freeradbiomed.2009.09.012.
- Rottensteiner, H., Stein, K., Sonnenhol, E., Erdmann, R., 2003. Conserved function of pex11p and the novel pex25p and pex27p in peroxisome biogenesis. *Mol. Biol. Cell* 14, 4316–4328.
- Schrader, M., Fahimi, H.D., 2008. The peroxisome: still a mysterious organelle. *Histochem. Cell Biol.* 129, 421–440.
- Scott, I., Tobin, A.K. and Logan, D.C. (2006). BIGYIN, an orthologue of human and yeast FIS1 genes functions in the control of mitochondrial size and number in *Arabidopsis thaliana*. *J. Exp. Bot.* 57, 1275–1280.
- Serasinghe, M.N., Yoon, Y., 2008. The mitochondrial outer membrane protein hFis1 regulates mitochondrial morphology and fission through self-interaction. *Exp. Cell Res.* 314, 3494–3507.
- Shimizu, M., Takeshita, A., Tsukamoto, T., Gonzalez, F.J., Osumi, T., 2004. Tissue-selective, bidirectional regulation of PEX11alpha and perilipin genes through a common peroxisome proliferator response element. *Mol. Cell Biol.* 24, 1313–1323.
- Sinclair, A.M., Trobacher, C.P., Mathur, N., Greenwood, J.S., Mathur, J., 2009. Peroxule extension over ER defined paths constitutes a rapid subcellular response to hydroxyl stress. *Plant J.* 59, 231–242.
- Smith, J.J., Marelli, M., Christmas, R.H., Vizeacoumar, F.J., Dilworth, D.J., Ideker, T., et al., 2002. Transcriptome profiling to identify genes involved in peroxisome assembly and function. *J. Cell Biol.* 158, 259–271.
- Stojanovski, D., Koutsopoulos, O.S., Okamoto, K., Ryan, M.T., 2004. Levels of human Fis1 at the mitochondrial outer membrane regulate mitochondrial morphology. *J. Cell Sci.* 117, 1201–1210.
- Tam, Y.Y., Torres-Guzman, J.C., Vizeacoumar, F.J., Smith, J.J., Marelli, M., Aitchison, J.D., et al., 2003. Pex11-related proteins in peroxisome dynamics: a role for the novel peroxin

- Pex27p in controlling peroxisome size and number in *Saccharomyces cerevisiae*. *Mol. Biol. Cell* 14, 4089–4102.
- Thoms, S., Erdmann, R., 2005. Dynamin-related proteins and Pex11 proteins in peroxisome division and proliferation. *FEBS J.* 272, 5169–5181.
- Veenhuis, M., Salomons, F.A., Van Der Klei, I.J., 2000. Peroxisome biogenesis and degradation in yeast: a structure/function analysis. *Microsc. Res. Tech.* 51, 584–600.
- Voncken, F., van Hellemond, J.J., Pfisterer, I., Maier, A., Hillmer, S., Clayton, C., 2003. Depletion of GIM5 causes cellular fragility, a decreased glycosome number, and reduced levels of ether-linked phospholipids in trypanosomes. *J. Biol. Chem.* 278, 35299–35310.
- Wilsbach, K., Payne, G.S., 1993. Vps1p, a member of the dynamin GTPase family, is necessary for Golgi membrane protein retention in *Saccharomyces cerevisiae*. *EMBO J.* 12, 3049–3059.
- Yan, M., Rayapuram, N., Subramani, S., 2005. The control of peroxisome number and size during division and proliferation. *Curr. Opin. Cell Biol.* 17, 376–383.
- Yoon, Y., Krueger, E.W., Oswald, B.J., McNiven, M.A., 2003. The mitochondrial protein hFis1 regulates mitochondrial fission in mammalian cells through an interaction with the dynamin-like protein DLP1. *Mol. Cell Biol.* 23, 5409–5420.
- Zhang, X., Hu, J., 2008. FISSION1A and FISSION1B proteins mediate the fission of peroxisomes and mitochondria in *Arabidopsis*. *Mol. Plant* 1, 1036–1047.
- Zhang, X., Hu, J., 2009. Two small protein families, DYNAMIN-RELATED PROTEIN3 and FISSION1, are required for peroxisome fission in *Arabidopsis*. *Plant J.* 57, 146–159.

This page intentionally left blank

# NEW INSIGHTS INTO THE SIGNAL TRANSMISSION FROM TASTE CELLS TO GUSTATORY NERVE FIBERS

Ryusuke Yoshida *and* Yuzo Ninomiya

## Contents

1. Introduction	102
2. Diversity of Taste Bud Cells	103
2.1. Cell types	104
2.2. Expression of taste receptors and their downstream molecules	106
3. Coding of Taste Information	108
3.1. Taste responsiveness of circumvallate taste bud cells	109
3.2. Taste responsiveness of fungiform taste bud cells	112
3.3. Similarity and difference between circumvallate and fungiform taste cells	113
3.4. Cell–cell communication in the taste bud	117
4. Mechanisms for the Signal Transmission from Taste Cells to Gustatory Nerve Fibers	118
4.1. Formation of taste-coding channels	118
4.2. Transmitters in the taste buds	122
4.3. Transmitter release from taste bud cells	123
5. Concluding Remarks	125
Acknowledgments	126
References	126

## Abstract

Taste receptor cells detect chemical compounds in the oral cavity and transfer their messages to gustatory afferent nerve fibers. Considering the coding of taste information, the sensitivity of taste cells and the connection between taste cells and gustatory fibers may be critical in this process. Broadly tuned taste cells and random connections between taste cells and fibers would produce gustatory fibers that have broad sensitivity to multiple taste qualities. Narrowly tuned taste cells and selective connections would yield gustatory nerve fibers that respond to specific taste quality. This review summarizes results showing

Section of Oral Neuroscience, Graduate School of Dental Sciences, Kyushu University, Fukuoka, Japan

molecular and morphological aspects of taste bud cells, physiological responses of taste cells, possible connections between taste cells and gustatory fibers, and transmitter release from taste cells, and discusses how taste qualities are encoded among taste bud cells and how taste information is transmitted from taste cells to gustatory nerve fibers.

**Key Words:** Taste cells, Gustatory nerve fibers, Taste quality, Synapse, Signal transmission. © 2010 Elsevier Inc.

## 1. INTRODUCTION

Sensory information of taste is crucial for evaluating nutritious and poisonous substances in foods. In general, sweet, salty, umami, sour, and bitter are considered to be basic taste qualities. Each of these may be responsible for the detection of nutritious and poisonous contents; sweet for carbohydrate sources of calories, salty for minerals, umami for protein and amino acid content, sour for ripeness of fruits and spoiled foods, and bitter for harmful compounds. The detection of these taste qualities begins with the taste receptors on the apical membrane of taste receptor cells. Activation of taste receptor cells leads to depolarization of the taste receptor cell membrane, transmitter release, and activation of gustatory afferent nerve fibers. At this peripheral stage, how do taste receptor cells encode taste qualities and how do they transfer their signals to gustatory nerve fibers?

Recent studies identified molecular mechanisms for reception and transduction of sweet, bitter, umami, and sour taste (Chandrashekar et al., 2006; Roper, 2007). Each of these receptors is expressed in separate population of taste bud cells and genetic elimination of taste receptor (or receptor cells) leads to total loss of sensitivity to a specific taste quality (Adler et al., 2000; Huang et al., 2006; Nelson et al., 2001; Zhao et al., 2003), suggesting that different taste bud cells define the different taste modalities and that activation of a single type of taste receptor cells is sufficient to encode taste quality, supporting “labeled line model” (Chandrashekar et al., 2006). In this case, taste receptor cells respond to a single taste quality and are innervated selectively by gustatory afferent fibers; thereby each gustatory fiber (called “specialist”) may transmit specific taste information to the brain (Frank et al., 2008). Actually, a huge number of fibers in the mammalian gustatory nerve respond to specific taste quality (Frank, 1973; Hellekant and Ninomiya, 1991; Hellekant et al., 1988; Ninomiya et al., 1982, 1984). In addition, taste bud cells that specifically respond to single taste quality are found in mouse (Caicedo et al., 2002; Yoshida et al., 2006a).

But this model might not account for the existence of taste cells and gustatory nerve fibers that are tuned to multiple taste qualities (Caicedo et al., 2002; Frank, 1973; Hellekant and Ninomiya, 1991; Hellekant et al., 1988;

Ninomiya et al., 1982, 1984; Yoshida et al., 2006a). To broaden the sensitivity of taste cells, individual taste cells would express different sets of taste receptor or taste bud cells would communicate with each other (Roper, 2006). To broaden the sensitivity of gustatory nerve fibers, individual gustatory fibers would integrate taste information derived from multiple types of taste cells or receive inputs from taste cells that are sensitive to multiple taste qualities.

To transfer taste signals, taste bud cells would release transmitters onto gustatory nerve fibers. Several transmitters have been proposed as candidates: serotonin (5-HT), glutamate, acetylcholine, neuropeptide Y, GABA, and adenosine triphosphate (ATP). Among them, release of ATP and 5-HT is well studied (Finger et al., 2005; Huang et al., 2005, 2007; Romanov et al., 2007) and is probably facilitated by action potentials in taste cells (Vandenbeuch and Kinnamon, 2009). Various studies have demonstrated that taste bud cells generate action potentials in response to taste stimuli (Avenet and Lindemann, 1991; B  h   et al., 1990; Cummings et al., 1993; Furue and Yoshii, 1997; Gilbertson et al., 1992; Yoshida et al., 2006a), indicating that these cells transmit taste information to gustatory nerve fibers. However, only a subset of taste cells has conventional synaptic structures, raising the possibility that some nonsynaptic communications may occur between taste cells and gustatory nerve fibers.

To understand signal transduction from taste cells to gustatory nerve fibers, we first review molecular and morphological aspects of taste bud cells. These features may be closely related to physiological properties of taste bud cells because expression patterns of taste receptors may determine response characteristics of taste cells. Next, we summarize recent results on physiological responses of mouse taste cells and discuss how taste qualities are encoded among taste bud cells. Especially, the relationship between cell types and response properties of taste cells will be illustrated. We also discuss the similarity and difference between taste bud cells in the posterior and anterior parts of tongue. Then, we discuss the possible connection between taste cells and gustatory nerve fibers. Presently, there is no direct evidence showing selective or specific connection between taste cells and gustatory fibers. But comparison of responsiveness of taste cells and gustatory fibers and nerve regeneration experiments might give insights on this problem. Finally we review and discuss transmitter release from taste cells, especially ATP release from taste cells.



## 2. DIVERSITY OF TASTE BUD CELLS

The taste bud is a specialized organ for sense of taste. Taste buds of mammals are distributed on the tongue and palate epithelium. On the tongue, three types of papillae, fungiform (anterior part), foliate (sides of



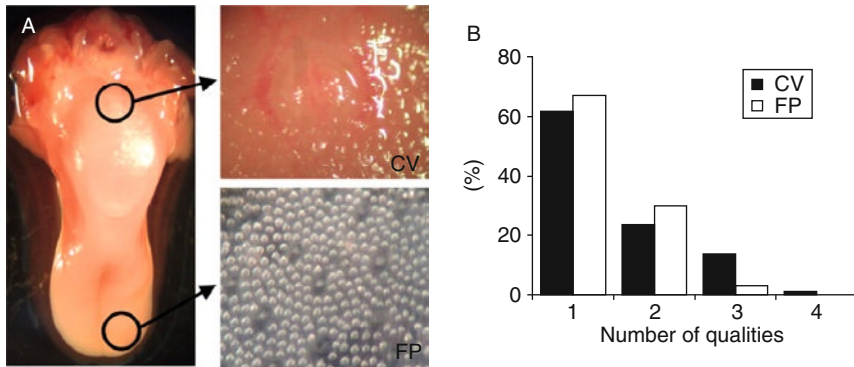


**Figure 4.1** (A) Pictures of mouse tongue, circumvallate (CV), and fungiform (FP) papillae. Fungiform taste buds are shown in tongue epithelium peeled after enzyme treatment (see method in Yoshida et al., 2006a). In mouse, a single circumvallate papilla exists in the center of posterior part of tongue and fungiform papillae are distributed in the anterior part of tongue. (B) Percentage of circumvallate and fungiform taste cells responding to one or more taste qualities. Responses were recorded from taste cells at random. Data for circumvallate taste cells are derived from Caicedo et al. (2002). Data for fungiform taste cells are derived from Yoshida et al. (2006a).

posterior part), and circumvallate (center of posterior part) papillae contain taste buds (Fig. 4.1A). In a single taste bud, there are 50–150 heterogeneous types of cells including taste receptor cells. These cells are oriented perpendicular to the tongue surface in a parallel arrangement and stuck out their apical side to the taste pore, where they contact with chemical compounds in the oral cavity. Taste bud cells have been traditionally classified into several groups by their morphological characteristics, and recently molecular features have been added to these classifications. Such analytical diversity of taste bud cells may represent functional variety in detection of taste information.

## 2.1. Cell types

Taste bud cells have been classified into three groups according to ultrastructural features, dark cells, light cells, and intermediate cells (Delay et al., 1986; Farbman, 1965; Murray, 1971, 1973). Dark cells (Type I cells) are electron-dense cells and have dark protoplasm, apical dense granules, and indented nucleus. Light cells (Type II cells) have light protoplasm and large, round nucleus. Intermediate cells (Type III cells) have similar nucleus as dark cells, but protoplasm of intermediate cells is lighter than that of dark cells. In addition to these three, basal cells (Type IV cells) are located near the base of taste bud and assumed to be progenitor cells.

Among these types of cells, Type III cells have obvious synaptic contacts with nerve fibers (Murray, 1971; Royer and Kinnamon, 1991; Seta and Toyoshima, 1995; Takeda and Hoshino, 1975), suggesting that Type III cells transfer their signals to nerve fibers. Consistent with these morphological data, Type III cells display immunoreactivity for synaptic molecules such as neural cell adhesion molecule (NCAM), synaptosomal-associated protein 25kD (SNAP25), and serotonin (Kim and Roper, 1995; Nelson and Finger, 1993; Yang et al., 2000a; Yee et al., 2001). In addition, expression of aromatic L-amino acid decarboxylase (AADC or DOPA decarboxylase, which is a biosynthetic enzyme common to the pathways for serotonin, dopamine, norepinephrine, and epinephrine), glutamic acid decarboxylase (GAD1 or GAD67, which is a enzyme for biosynthesis of GABA), and synapsin II were confirmed in Type III cells but not Type II cells by single-cell RT-PCR and immunohistochemistry (Defazio et al., 2006; Nakamura et al., 2007). These molecules are well used as markers for Type III cells in taste buds, although each of these molecules may not cover complete population of Type III cells (Table 4.1).

In contrast, Type I and Type II cells are believed not to possess conventional synapses. However, Kinnamon et al. (1988) demonstrated that all three types of mouse taste bud cells formed synaptic connections with sensory nerve fibers. Defazio et al. (2006) demonstrated that 1 of 11 mouse Type II cells have SNAP25. Therefore, small numbers of Type II cells may have synaptic structures. Majority of Type II cells may not possess conventional synapses but they have very close contact with sensory nerve fibers such as subsurface cisternae observed at close apposition between the plasma membrane of Type II cell and nerve processes (Clapp et al., 2004). These structures may provide the sites for signal transmission from Type II

**Table 4.1** Morphological and molecular expression properties of each cell type

	Type I (dark)	Type II (light)	Type III (intermediate)
Apical process	Long apical microvilli	Short apical microvilli	Single thick apical process
Nucleus	Indented nucleus	Large, round nucleus	Indented nucleus
Expression	ecto-ATPase GLAST	T1Rs T2Rs Gustducin TRPM5 PLC $\beta$ 2 IP $_3$ R3	PKD2L1 Serotonin SNAP25 NCAM AADC GAD67

Each marker may not cover all taste cells in each cell type.

taste cells to gustatory nerve fibers. Type I cells have a majority ( $\sim 60\%$ ) in taste bud cells. Type I cells express enzymes for inactivation and uptake of transmitters such as the glutamate–aspartate transporter (GLAST; Lawton et al., 2000) and nucleoside triphosphate diphosphohydrolase-2 (ecto-ATPase; Bartel et al., 2006; Table 4.1), and wrap around other cells (Pumplin et al., 1997). Moreover, Bigiani (2001) demonstrated the existence of mouse taste bud cells with glia-like membrane properties. Considering these data, Type I cells may not contribute directly to detection of taste molecules, but they have supporting roles similar to glia cells in the nervous system.

## 2.2. Expression of taste receptors and their downstream molecules

Recent molecular studies have been revealed taste receptors and their downstream molecules for five basic taste qualities (Chandrashekar et al., 2006; Gilbertson and Boughter, 2003; Lindemann, 2001; Roper, 2007; Sugita, 2006). Sweet, bitter, and umami tastes are mediated by G protein-coupled receptors (GPCR), T1Rs (sweet and umami; Bachmanov et al., 2001; Hoon et al., 1999; Kitagawa et al., 2001; Li et al., 2002; Max et al., 2001; Montmayeur et al., 2001; Nelson et al., 2001, 2002; Sainz et al., 2001), and T2Rs (bitter; Adler et al., 2000; Matsunami et al., 2000). T1R3 combines with T1R2 to form a sweet taste receptor and with T1R1 to form an umami taste receptor (Li et al., 2002; Nelson et al., 2001, 2002). T2Rs are a family of  $\sim 25$  highly divergent GPCRs and some of them have been identified their specific bitter ligands (Behrens and Meyerhof, 2006). Sweet, umami, and bitter tastes are mediated by a common signaling pathway after activation of each receptor. Tastant binding to sweet, umami, and bitter receptors activates heteromeric G protein,  $\alpha$ -gustducin (Wong et al., 1996), and subsequent stimulation of phospholipase C $\beta$ 2 (PLC $\beta$ 2; Zhang et al., 2003). Activation of PLC $\beta$ 2 produces inositol-1,4,5-triphosphate that is a ligand for inositol-1,4,5-triphosphate receptor type 3 (IP $_3$ R3; Hisatsune et al., 2007). Then Ca $^{2+}$  is released from intracellular calcium stores and stimulates transient receptor potential channel M5 (TRPM5; Zhang et al., 2003, 2007). Salty and sour tastes are mediated by channel-type receptors. In case of salt taste, epithelial sodium ion channel (ENaC) is believed to be a receptor because amiloride, an epithelial sodium channel blocker, decreases taste cell, neural, and behavioral responses to NaCl (Avenet and Lindemann, 1988; Heck et al., 1984; Hettinger and Frank, 1990; Ninomiya and Funakoshi, 1988; Shigemura et al., 2008; Spector et al., 1996; Yoshida et al., 2009a). Amiloride-insensitive (AI) components of NaCl responses are suggested to be mediated by transient receptor potential channel V1 (TRPV1) variant (Lyll et al., 2004). In case of sour taste, many candidate receptors have been

proposed such as acid-sensing ion channels (ASICs; Ugawa et al., 2003), hyperpolarization-activated cyclic nucleotide-gated potassium channels (HCNs; Stevens et al., 2001), potassium channels (Lin et al., 2004; Richter et al., 2004a), NPPB-sensitive  $\text{Cl}^-$  channels (Miyamoto et al., 1998), and polycystic kidney disease 1L3 and 2L1 heterodimer (PKD1L3 + PKD2L1; Huang et al., 2006; Ishimaru et al., 2006).

Different morphological features of taste bud cells may correlate with their functional characteristics. As mentioned in the previous section, Type II and Type III cells may be capable of transmitting their signals to gustatory afferent nerve fibers. Therefore, these types of taste cells may possess taste receptors and transduction mechanisms. Immunohistochemical electron microscopic studies have identified the expression of some of these taste-related molecules in the specific type of taste bud cells. Yang et al. (2000b) demonstrated that a subset of Type II cells displays immunoreactivity to antisera directed against gustducin in rat circumvallate papillae. Therefore, gustducin is frequently used as one of Type II cell markers in subsequent studies. Clapp et al. (2004) showed that a large subset of Type II cells displays  $\text{IP}_3\text{R}3$  immunoreactivity within their cytoplasm.  $\text{IP}_3\text{R}3$  is coexpressed with  $\text{PLC}\beta 2$  (Clapp et al., 2001, 2004; Miyoshi et al., 2001) and  $\text{PLC}\beta 2$  is coexpressed with TRPM5 (Perez et al., 2002; Zhang et al., 2003), indicating that Type II cells possess PLC-signaling proteins. Both gustducin and PLC-signaling molecules are expressed in Type II cells. However, these studies demonstrated that the population of  $\text{IP}_3\text{R}3$  immunoreactive cells, TRPM5 immunoreactive cells, and  $\text{PLC}\beta 2$  immunoreactive cells was larger than that of gustducin immunopositive cells. Expression of sweet, umami, and bitter taste receptor was also revealed by histochemical studies. Both T1Rs and T2Rs are coexpressed with gustducin,  $\text{PLC}\beta 2$ , and TRPM5 (Max et al., 2001; Miyoshi et al., 2001; Zhang et al., 2003), but T1Rs are not coexpressed with T2Rs (Nelson et al., 2001) and with SNAP25 (Clapp et al., 2006). Considering these data, Type II cells may be responsible for detection of sweet, umami, and bitter compounds.

Among candidate receptors for sour taste, PKD2L1 is coexpressed with Type III cell markers such as serotonin and NCAM but not with Type I and Type II cell markers such as ecto-ATPase, TRPM5, and  $\text{PLC}\beta 2$  (Kataoka et al., 2008). In addition, PKD2L1-positive cells have conventional synapses (Kataoka et al., 2008). In the circumvallate papillae, PKD2L1 is coexpressed with PKD1L3 but not with T1R3, T2Rs, TRPM5, and  $\text{IP}_3\text{R}3$  (Huang et al., 2006; Ishimaru et al., 2006). These data indicate that Type III cells possess PKD1L3 + PKD2L1, a candidate receptor for sour taste. However, PKD1L3 is not expressed in fungiform taste bud cells (Huang et al., 2006; Ishimaru et al., 2006). Expression of other candidate sour receptors in taste bud cells has been investigated, but cell type of taste cells that express these receptors remains unclear. Immunohistochemical study demonstrated that HCN1/4 is not coexpressed with gustducin (Stevens et al., 2001),

indicating that Type II cells do not express HCN1/4. ASICs are more complicated. Ugawa et al. (2003) demonstrated that ASIC2a/b is expressed in rat taste bud cells, but Richter et al. (2004b) showed expression of ASIC1 and ASIC3 but not ASIC2 and ASIC4 in mouse taste bud cells, indicating species differences in expression of ASICs in the taste bud. Cell type of ASIC-expressing cells remains unclear.

ENaC, an amiloride-sensitive (AS) salt taste receptor, is known to form a heterooligomer, consisting of  $\alpha$ -,  $\beta$ -, and  $\gamma$ -subunit (Garty and Palmer, 1997). Expression of these subunits in taste bud cells has been investigated in rats (Kretz et al., 1999; Li et al., 1994; Lin et al., 1999) and mice (Shigemura et al., 2005) by RT-PCR, *in situ* hybridization, and immunohistochemistry. These studies showed that all three ENaC subunits are abundantly present in fungiform taste cells. However, the relationship between cell type and ENaC expression has not been revealed. In single-cell RT-PCR experiments combined with recording of taste responses of mouse fungiform taste cells, amiloride-sensitive NaCl responsive taste cells do not express both SNAP25 and gustducin for Type II and Type III markers (Yoshida et al., 2009a). A recent patch clamp recording experiment using mice showed that amiloride-sensitive Na<sup>+</sup> channels were expressed in Type I fungiform taste cells, which lack voltage-gated inward currents (Vandenbeuch et al., 2008). Considering these physiological and molecular expression data, it is presumed that ENaCs may be expressed in Type II or Type III cells that do not express gustducin or SNAP25, or Type I cells which can generate action potentials, if such cells exist. TRPV1, a candidate receptor for amiloride-insensitive salt taste, is detected by RT-PCR in taste buds (Liu and Simon, 2001), but cell type of TRPV1-expressing cells is not identified. In summary, Type I cells express enzymes for inactivation or uptake of transmitters. Type II cells express receptor and transduction components for sweet, umami, and bitter tastes but do not possess conventional synapses. Type III cells express candidate sour taste receptors and synapse-related molecules and possess morphological synaptic structures. Table 4.1 summarizes morphological and molecular expression properties of each cell type.

### 3. CODING OF TASTE INFORMATION

How are taste qualities encoded among taste bud cells? To answer this question, we have to know the responsiveness of each individual taste cells. Molecular expression studies suggest that sweet, bitter, sour, salty, and umami tastants would each be recognized by different cells expressing specialized receptors. However, physiological recordings of responses of taste cells indicate that a subset of taste cells is sensitive to multiple taste qualities. Recently, physiological and molecular properties of taste bud cells

have been simultaneously analyzed. These studies may reconcile this discrepancy and provide much insight into coding of taste qualities in taste buds. In addition, taste information encoded by taste cells may be different among the region of tongue, because different response properties between the chorda tympani (CT) nerve innervating the anterior part of tongue (including fungiform and a part of foliate papillae) and the glossopharyngeal (IXth) nerve innervating posterior part of tongue (foliate and circumvallate papillae) have been reported. By comparing circumvallate taste cells with fungiform taste cells, these differences and similarities would be elucidated.

### 3.1. Taste responsiveness of circumvallate taste bud cells

Taste cells are polarized cells that express taste receptors on the apical membrane and are in close contact with gustatory nerve fibers on the basolateral membrane. Apical and basolateral sides are separated by tight junctions at the base of taste pore. Therefore, in general, taste compounds in the oral cavity make contact with only apical membrane of taste cells. To record taste responses from taste cells, polarity of taste cells should be taken into consideration. Taste stimulus should be applied restrictedly to the apical membrane of taste cells. However, if isolated taste cells were used, taste stimulus might affect not only the apical side but also the basolateral membrane of the cells. To overcome this problem, several methods have been developed such as direct electrophysiological recording from apical side (Avenet and Lindemann, 1991), using chamber systems (Furue and Yoshii, 1997; Gilbertson et al., 2001), *in situ*  $\text{Ca}^{2+}$  imaging in slice preparation (Caicedo and Roper, 2001; Caicedo et al., 2002), and electrophysiological recording using isolated taste bud (Miyamoto et al., 1996; Yoshida et al., 2006a). Each of these techniques was applied to examine responses of taste bud cells in one of papillae because there are some difficulties arising from structural differences to examine taste cell responses in both fungiform and circumvallate papillae by same technique. The responsiveness of taste cells of circumvallate taste bud is well studied by using *in situ*  $\text{Ca}^{2+}$  imaging in slice preparation.

Caicedo et al. (2002) recorded calcium transients in taste cells of mouse circumvallate taste buds elicited by taste stimuli representing different taste qualities (saccharin and sucrose for sweet, quinine and cyclohexamide for bitter, NaCl for salty, and citric acid for sour). Bitter, sweet, and sour taste stimuli evoked  $\text{Ca}^{2+}$  changes in taste cells in concentration-dependent manner, and activation thresholds for  $\text{Ca}^{2+}$  transients elicited by these taste stimuli were similar to behavioral thresholds in mice (Lush, 1984, 1989; Lush and Holland, 1988). However, they did not attempt to measure concentration response relationship for NaCl because slice preparation of circumvallate taste buds was flooded by bathing solution containing 150 mM  $\text{Na}^+$ . They also demonstrated the strain difference of  $\text{Ca}^{2+}$  transient elicited by cyclohexamide and sucrose between C57BL/6B and DBA/2J mice. These suggest

that the  $\text{Ca}^{2+}$  transients elicited by taste stimuli represent taste responses of taste cells. Among four basic taste qualities, more than 60% of the responsive cells responded to only one taste quality and the rest responded to multiple taste qualities (Fig. 4.1B). Among responsive taste cells, the numbers of bitter- and sour-sensitive cells are larger than those of sweet- and salt-sensitive cells.

In a more recent study, Tomchik et al. (2007) demonstrated taste responses of identified taste cells in mouse circumvallate taste buds. Two methods were used to identify taste cells. One is sensitivity to bath application of high  $\text{K}^+$  solution (DeFazio et al., 2006). Type III cells (named presynaptic cells) are depolarized by bath application of high  $\text{K}^+$  (50 mM) solution and show  $\text{Ca}^{2+}$  transients evoked by high  $\text{K}^+$  depolarization. Type II cells (named receptor cells) do not show  $\text{Ca}^{2+}$  transients by bath application of high  $\text{K}^+$  solution. The other is the use of transgenic mice.  $\text{PLC}\beta 2$ -GFP and GAD-GFP transgenic mice express GFP in  $\text{PLC}\beta 2$ -positive and GAD-positive cells, respectively (Chattopadhyaya et al., 2004; Kim et al., 2006). Therefore,  $\text{PLC}\beta 2$ -GFP taste cells are Type II and GAD-GFP taste cells are Type III cells. Cyclohexamide, denatonium (bitter), sucrose, SC45647 (sweet), monopotassium glutamate (MPG, umami), acetic acid (sour), and NaCl (salty) were used as taste stimuli and taste responses were recorded from 56 Type II cells and 58 Type III cells. Eighty-two percent (46/56) of Type II cells responded to only one, 14% (8/56) responded to two, and 4% (2/56) responded to three of five basic taste qualities (Fig. 4.2A). On the other hand, 17% (10/58) of Type III cells responded to only one, 24% (14/58) responded to two, 24% (14/58) responded to three, 24% (14/58) responded to four, and 10% (6/58) responded to five of five basic taste qualities (Fig. 4.3A). To quantify the breadth of responsiveness of the taste cells, entropy ( $H$ ) values were calculated (Smith and Travers, 1979; Travers and Smith, 1979).  $H$  values vary continuously from 0.0 for a cell that responds exclusively to one stimulus to 1.0 for a cell that responds equivalently to all the taste stimuli. The mean  $H$  value for Type II cells is  $0.068 \pm 0.02$  (mean  $\pm$  SEM), indicating that Type II cells are specifically tuned to one of five basic taste qualities. The mean  $H$  value for Type III cells is  $0.474 \pm 0.036$  and is significantly higher than that for Type II cells, indicating that Type III cells have more broad sensitivity to five basic taste qualities. Molecular evidences suggest that Type II cells are responsible for sweet, bitter, and umami taste and that Type III cells are responsible for sour taste. Consistent with these data, most of Type II cells (53/56) responded to bitter (36/56), sweet (11/56), or umami (10/56) taste stimulus. Although most of Type III cells (47/58) responded to sour taste stimuli, significant parts of Type III cells responded to sweet (29/58), bitter (51/58), and umami (23/58) compounds. These responses in Type III cells may be explained by cell-cell communication in the taste buds (Roper, 2006; see Section 3.3).

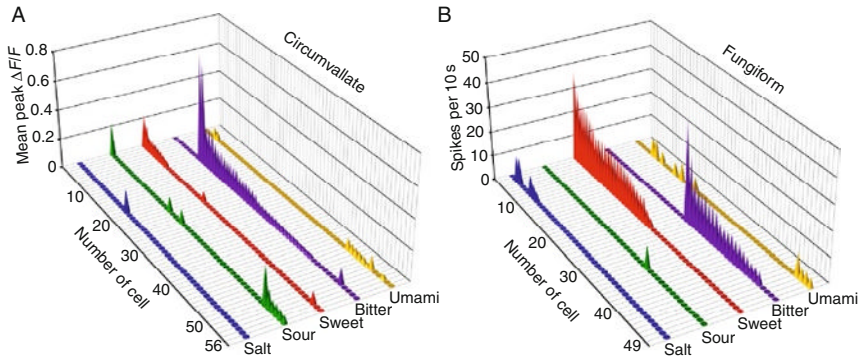


**Figure 4.2** Comparison of responses of Type II taste cells in circumvallate (A) and fungiform (B) taste buds. PLC $\beta$ 2-GFP cells and high K<sup>+</sup>-insensitive cells are treated as Type II cells in circumvallate taste buds. Gustducin-positive cells are treated as Type II cells in fungiform taste buds. Taste stimuli were as following: NaCl (500 or 300 mM) as salty, citric acid (100 mM) or HCl (10 mM) as sour, sucrose (500 mM), SC45647 (100  $\mu$ M), or saccharin (20 mM) as sweet, cyclohexamide (30  $\mu$ M), denatonium (200  $\mu$ M), or quinine (20 mM) as bitter, and monopotassium glutamate (200 mM) + inosine monophosphate (1 mM) or monosodium glutamate (300 mM) as umami. Magnitude of responses was indicated by mean peak  $\Delta F/F$  in calcium imaging (A) or number of spikes per 10 s in spike recording (B). Data for circumvallate taste cells are derived from Tomchik et al. (2007). Data for fungiform taste cells are derived from Yoshida et al. (2009b).

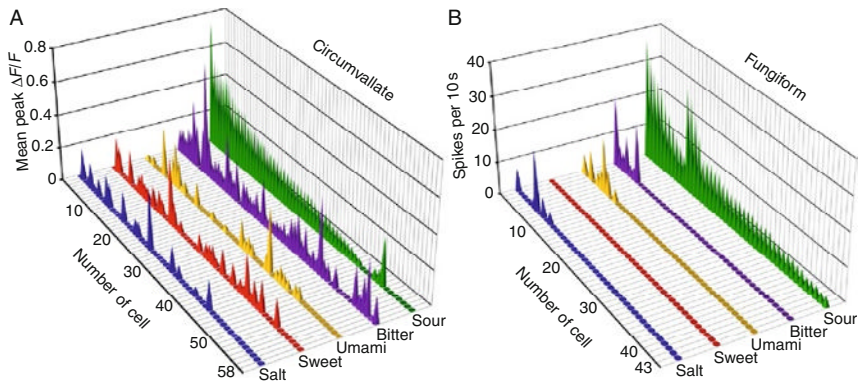


**Figure 4.3** Comparison of responses of Type III taste cells in circumvallate (A) and fungiform (B) taste buds. GAD-GFP cells and high K<sup>+</sup>-sensitive cells are treated as Type III cells in circumvallate taste buds. GAD-GFP cells are treated as Type III cells in fungiform taste buds. Taste stimuli were as following: NaCl (500 or 300 mM) as salty, citric acid (100 mM) or HCl (10 mM) as sour, sucrose (500 mM), SC45647 (100  $\mu$ M) or saccharin (20 mM) as sweet, cyclohexamide (30  $\mu$ M), denatonium (200  $\mu$ M) or quinine (20 mM) as bitter, and monopotassium glutamate (200 mM) + inosine monophosphate (1 mM) or monosodium glutamate (300 mM) as umami. Magnitude of responses was indicated by mean peak  $\Delta F/F$  in calcium imaging (A) or number of spikes per 10 s in spike recording (B). Data for circumvallate taste cells are derived from Tomchik et al. (2007). Data for fungiform taste cells are derived from Yoshida et al. (2009b).



### 3.2. Taste responsiveness of fungiform taste bud cells

It is well known that taste cells generate action potentials in response to various taste stimuli (Avenet and Lindemann, 1991; B  h   et al., 1990; Cummings et al., 1993; Furue and Yoshii, 1997; Gilbertson et al., 1992; Kashiwayanagi et al., 1983; Roper, 1983). Yoshida et al. (2006a,b) investigated response profiles of mouse fungiform taste cells by recording taste-evoked action potentials. The method used in that study allowed taste stimulus application restricted to the apical side of the taste cell membrane and recording of action potentials from the basolateral side of the membrane, similar to procedures used in previous studies in rats (Gilbertson et al., 2001) and mice (Furue and Yoshii, 1997). Four taste stimuli [NaCl (salty), saccharin (sweet), HCl (sour), and quinine (bitter)] were tested to elicit action potentials, and taste responses were recorded from 72 fungiform taste cells. Sixty-seven percent (48/72) of fungiform taste cells responded to one of four taste stimuli, 30% (22/72) responded to two stimuli, and 3% (2/72) responded to three stimuli (Fig. 4.1B), indicating that the majority of taste cells responded specifically to taste stimuli. Classification of mouse fungiform taste cells according to best stimulus showed that 39 of 72 taste cells (54%) responded best to saccharin, 17 cells (24%) responded best to NaCl, 12 cells (17%) responded best to HCl, and 4 cells (6%) responded best to quinine. Therefore, the subpopulation of mouse fungiform taste cells might be as following: sweet best > salt best  $\geq$  sour best > bitter best. By using a hierarchical cluster analysis, fungiform taste cells were classified into four groups similar to the classification according to best stimulus.

A very recent study reported taste responses of Type II and Type III cells in mouse fungiform taste buds (Yoshida et al., 2009b). Taste cells were identified by single-cell RT-PCR after recording of taste responses (Yoshida et al., 2005) or by using gustducin-GFP and GAD-GFP transgenic mice (Tamamaki et al., 2003; Wong et al., 1999). Gustducin and GAD67 were Type II and Type III cell markers, respectively. Five taste stimuli [NaCl, saccharin, HCl, quinine, and monosodium glutamate (MSG; umami)] were applied, and 49 Type II cells and 44 Type III cells responded to at least one of these taste stimuli. Of 49 Type II cells, 25 cells responded best to saccharin (saccharin-best), 20 cells responded best to quinine (quinine-best), and 4 cells responded best to MSG (MSG-best; Fig. 4.2B). There is no NaCl-best cell and HCl-best cell among Type II cells. In addition, no Type II cell responded to both sweet and bitter taste stimuli. Gustducin plays important roles in sweet, bitter, and umami taste transduction (He et al., 2004; Wong et al., 1996). This response profile of gustducin-expressing cells may well correspond with the role of gustducin in taste transduction. Seventy-eight percent (38/49) of taste cells responded to only one, 20% (10/49) responded to two, and 2% (1/49) responded to three of five basic taste stimuli. The mean entropy value for the breadth of

responsiveness of 49 Type II cells was  $0.087 \pm 0.024$  (mean  $\pm$  SEM). The mean entropy value for sweet-best cells ( $0.153 \pm 0.039$ ,  $n = 25$ ) was significantly greater than that for bitter-best cells ( $0.021 \pm 0.021$ ,  $n = 20$ ,  $p < 0.01$ ,  $t$ -test), suggesting that bitter-sensitive cells may be more narrowly tuned to particular taste stimuli than are sweet-sensitive cells. These indicate that Type II cells are specifically tuned to sweet, umami, or bitter taste stimuli. Of 44 Type III cells, all responded to HCl that is consistent with expression pattern of PKD2L1 (Kataoka et al., 2008). Twenty-five percent (11/44) of Type III cells responded to multiple taste stimuli, and 75% (33/44) responded specifically to HCl (Fig. 4.3B). The mean entropy value for the breadth of responsiveness of 44 Type III cells was  $0.123 \pm 0.034$  (mean  $\pm$  SEM). However, the mean entropy value for 11 Type III cells showing multiple taste sensitivity is higher ( $0.491 \pm 0.059$ ) than that for 33 sour-specific Type III cells ( $0.000 \pm 0.000$ ). Therefore, Type III cells may be divided into at least two groups, sour-specific group and broadly tuned group.

As shown earlier, each taste quality (sweet, bitter, umami, and sour) may be discriminated by taste receptor cells. Then, how is sensitivity of each taste cells to taste compounds that belong to similar taste category? Quinine-sensitive Type II cells were tested whether they responded to multiple bitter compounds, such as cyclohexamide, denatonium, caffeine, and sucrose octaacetate (SOA). Among 14 quinine-sensitive Type II cells tested, 11 and 12 cells responded to denatonium and cyclohexamide, respectively. However, these cells did not respond to caffeine or SOA. The mean entropy value for the breadth of responsiveness to three bitter compounds in 14 bitter-sensitive Type II cells was  $0.789 \pm 0.064$ , indicating that bitter-sensitive cells have broad sensitivity to bitter compounds. This is consistent with molecular studies demonstrating that individual taste receptor cells express a large repertoire of bitter-responsive T2Rs (Adler et al., 2000). Similarly, 14 Type III cells were tested their responsiveness to three sour compounds, HCl, citric acid, and acetic acid. Almost all cells responded to all sour stimuli. The mean entropy for the breadth of responsiveness was  $0.894 \pm 0.026$  ( $n = 14$ ), suggesting broad tuning to sour stimuli in Type III cells. Therefore, most of Type II and Type III cells in mouse fungiform taste buds are narrowly tuned to five basic taste qualities, but they have broad sensitivity to taste compounds that elicit similar taste quality.

### 3.3. Similarity and difference between circumvallate and fungiform taste cells

Basic response properties of circumvallate and fungiform taste cells in mice are largely consistent, although taste responses were recorded by using different technique, slice preparation and calcium imaging for circumvallate taste cells versus isolated taste buds and extracellular recording for fungiform

taste cells. In both circumvallate and fungiform taste buds, about 60–70% of taste cells showed specific response to single taste quality and the rest responded to multiple taste qualities if taste responses were recorded from taste cells chosen at random (Caicedo et al., 2002; Yoshida et al., 2006a; Fig. 4.1B). Both circumvallate and fungiform Type II cells responded to sweet, bitter, or umami taste stimuli, and they were specifically tuned to one of five basic taste qualities (Tomchik et al., 2007; Yoshida et al., 2009b; Fig. 4.2). The mean  $H$  value for circumvallate Type II cells is  $0.068 \pm 0.02$ . This value is very close to that for fungiform Type II cells ( $0.087 \pm 0.024$ ). Type III cells in circumvallate and fungiform taste buds responded to sour taste stimuli (Huang et al., 2008a; Tomchik et al., 2007; Yoshida et al., 2009b; Fig. 4.3). These physiological data indicate that Type II cells are responsible for detection of sweet, umami, and bitter compounds and Type III cells contribute to detection of sour taste in both anterior and posterior parts of tongue. These response profiles of Type II and Type III cells are well consistent with molecular expression patterns in these cells. However, there are several major differences between two.

First, fungiform Type III cells tend to respond more specifically to sour taste stimuli than do circumvallate Type III cells. Seventy-five percent (33/44) of fungiform Type III cells responded specifically to HCl, and the rest (11/44) responded to multiple taste stimuli; whereas 17% (10/58) of circumvallate Type III cells responded to only one, and the rest (48/58) responded to more than two basic taste qualities (Fig. 4.3). Consequently, the mean  $H$  value was significantly different between them [ $0.123 \pm 0.034$  (FP) vs.  $0.474 \pm 0.036$  (CV)]. This may be caused by a small population of Type III cells showing multiple taste sensitivities in fungiform taste cells. If fungiform Type III cells responding to multiple taste stimuli were compared with circumvallate Type III cells, the mean  $H$  value was similar between them [ $0.491 \pm 0.059$  (FP) vs.  $0.474 \pm 0.036$  (CV)]. Therefore, these cells may have similar roles in both papillae. However, these multiple sensitive cells may occupy small population in fungiform Type III cells. Interestingly, the number of Type III cells in fungiform taste buds is apparently lower than that in circumvallate taste buds. Using GAD-GFP mice and TRPM5-GFP mice, numbers of GFP-positive cells in single taste bud were counted in both fungiform and circumvallate papillae (Fig. 4.4; Table 4.2). The mean number of GAD-GFP (Type III) cells in a single circumvallate taste bud was about three times larger than that in a single fungiform taste bud. On the other hand, the mean number of TRPM5-GFP (Type II) cells was not so much different between circumvallate and fungiform taste buds, although circumvallate taste buds contained more numbers of TRPM5-GFP cells. These differences may represent small number of multiple sensitive Type III cells in fungiform taste buds. Other possibility may be derived from the identification of Type III cells. In circumvallate taste buds, Type III cells were identified by GFP fluorescence in GAD-GFP transgenic mice and a

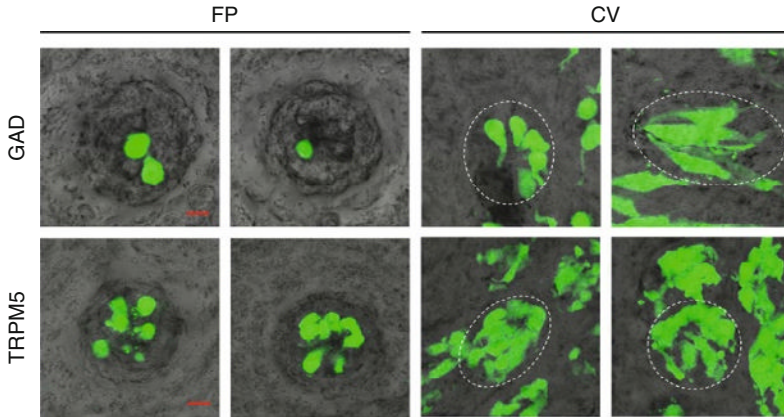


**Figure 4.4** GAD-GFP taste cells and TRPM5-GFP taste cells in mouse fungiform and circumvallate taste buds. Z-series stacks of 20–30 laser confocal scanning microscopy images ( $1.5\ \mu\text{m}$  apart) of a fungiform (FP) and circumvallate (CV) taste bud of GAD-GFP and TRPM5-GFP mice are shown. Green (white in monochrome figure) denotes GFP expression. Dotted lines show the borders of a taste bud. Scale bars are  $10\ \mu\text{m}$ .

**Table 4.2** Number of GFP-positive cells in a fungiform and circumvallate taste bud

	Fungiform	Circumvallate
TRPM5-GFP cell	$8.01 \pm 1.73$ ( $n = 92$ )	$10.57 \pm 1.99$ ( $n = 96$ )
GAD67-GFP cell	$1.64 \pm 0.83$ ( $n = 101$ )	$4.29 \pm 1.29$ ( $n = 111$ )
GAD67/TRPM5	0.205	0.406

Data are indicated by mean  $\pm$  SD.

depolarization by bath application of high  $\text{K}^+$  solution. In contrast, only GAD-GFP taste cells were used as Type III cells in fungiform taste buds. Not only GAD-expressing cells but also other taste bud cells may be depolarized by high  $\text{K}^+$  solution and may respond to multiple taste stimuli. Most GAD-expressing cells coexpressed other Type III cell marker, such as SNAP25 or serotonin, but 20–30% of SNAP25-expressing cells and serotonin-expressing cells did not possess GAD67 (DeFazio et al., 2006; Tomchik et al., 2007). This indicates that GAD-GFP taste cells represent only a subpopulation of Type III cells. To clarify response of Type III cells in fungiform taste buds, further studies are needed.

Second, bitter-best cells in fungiform taste buds may be more broadly tuned to several bitter compounds than bitter-sensitive cells in circumvallate taste buds. Bitter taste receptors, T2Rs, comprise a family of  $\sim 25$  GPCRs (Adler et al., 2000; Matsunami et al., 2000). Each T2R may interact with specific bitter ligands. Heterologous expression studies demonstrated interaction of T2R with specific bitter ligands, such as mouse T2R5 for

cyclohexamide (Chandrashekar et al., 2000; Mueller et al., 2005), human T2R4 and mouse T2R8 for denatonium (Chandrashekar et al., 2000), human T2R16 for  $\beta$ -glucopyranosides (Bufe et al., 2002), human T2R14 for pictotoxinine (Behrens et al., 2004), human T2R38 for phenylthiocarbamide (Bufe et al., 2005; Kim et al., 2003; Mueller et al., 2005), human T2R43 and T2R44 for saccharin, acesulfame K, and aristolochic acid (Kuhn et al., 2004; Pronin et al., 2004). Gene expression analyses in the rat taste buds demonstrated that a single taste receptor cell expresses a large repertoire of T2Rs (Adler et al., 2000), suggesting that each bitter-sensitive taste cell may be capable of detecting multiple bitter compounds. Gene expression analyses of mouse and human circumvallate papillae showed a more limited coexpression of T2Rs (Behrens et al., 2007; Matsunami et al., 2000), suggesting heterogeneous populations of bitter taste cells. In rat circumvallate papillae, most bitter taste cells respond to one or two of five bitter stimuli, quinine, cyclohexamide, denatonium, sucrose octaacetate, and phenylthiocarbamide (Caicedo and Roper, 2001), indicating that most bitter taste cells may be activated by a limited number of bitter compounds. In contrast, most bitter-sensitive cells in mouse fungiform papillae responded to multiple bitter compounds (quinine, cyclohexamide, and denatonium). These cells did not respond to two other bitter compounds (0.5 mM SOA and 10 mM caffeine). One possible explanation for this discrepancy may be different expression patterns of T2Rs between fungiform and circumvallate taste cells. There are little data on the expression patterns of T2Rs in mouse fungiform taste buds; therefore, further studies are needed. Different bitter sensitivities of taste bud cells among the tongue region may be consistent with different sensitivities to bitter compounds between the CT and the IXth nerve (Damak et al., 2006; Danilova and Hellekant, 2003). Denatonium and cyclohexamide evoke a large response in the IXth nerve but only a very slight response in the CT nerve. Caffeine and SOA evoke almost no response in the CT nerve but a slight response in the IXth nerve. Quinine-HCl evokes a large response in both the CT and the IXth nerves. In circumvallate papillae, a large population of bitter-sensitive cells responded specifically to cyclohexamide or denatonium (Caicedo and Roper, 2001), suggesting that these cells may contribute to a large response to these compounds in the IXth nerve. About 30% (23/69) of circumvallate bitter-sensitive cells responded to multiple bitter compounds (Caicedo and Roper, 2001). These cells may be comparable to fungiform bitter-sensitive cells expressing gustducin. In the CT nerve, quinine evokes a larger response than does cyclohexamide or denatonium; however, all these compounds evoked large responses in bitter-sensitive cells expressing gustducin.  $\alpha$ -Gustducin knockout mice showed large residual CT nerve responses to quinine (Wong et al., 1996). Taken together, there is the possibility that quinine-sensitive taste cells that do not express gustducin may exist in fungiform taste buds, and these cells may be more specifically tuned to quinine.

### 3.4. Cell–cell communication in the taste bud

Electrophysiological studies on both circumvallate and fungiform taste cells in mice demonstrated that a significant subset of taste cells, especially Type III cells, responded to multiple taste qualities. Type III cells do not express receptors and transduction mechanisms for sweet, bitter, and umami taste, but some of them apparently respond to these taste compounds. In addition, ultrastructural studies demonstrated that Type III cells, but not Type II cells have synaptic structures. One possible solution for these conundrums is the cell–cell communication in the taste bud (Roper, 2006). In this model, Type II cells that respond to sweet, bitter, or umami taste stimuli transfer their signals to Type III cells.

There are two possible routes for cell–cell communication. One is the gap junctions between taste cells and the other is paracrine secretion of transmitters within the taste bud. Existence of gap junctions between taste bud cells was demonstrated by both dye couplings and electrical couplings in amphibian (Bigiani and Roper, 1993; Yang and Roper, 1987) and mice (Yoshii, 2005), but it is not clear how they function in the taste bud. In a working hypothesis, Type II cells generate second messengers and depolarization in response to taste stimuli, and these messengers and/or depolarization may be transferred to Type III cells via gap junction. However, if this is a case, Type III cells may transmit their information to Type II cells. Many Type III cells responded to sour taste stimuli but Type II cells did not, indicating that taste information could be transmitted from Type II cells to Type III cells but not vice versa. Existence of gap junction between Type II and Type III cells and selective information flow from Type II to Type III cells via gap junctions must be proved in future studies.

Paracrine secretion is a more possible route for the cell–cell communication. In the taste bud, many neurotransmitters and modulators have been identified (see Section 4.2). Among them, ATP may be one of key molecules for information transmission from Type II cells to Type III cells (Huang et al., 2007) as well as from taste cells to gustatory nerve fibers (Finger et al., 2005). When epithelial sheet containing circumvallate or foliate taste buds was stimulated by sapid molecules, ATP release was detected by luciferase assay (Finger et al., 2005), indicating that taste bud cells release ATP in response to taste stimuli. Released ATP may contact with not only gustatory nerve fibers but also taste bud cells because some taste bud cells express purinergic receptors. Purinergic (P2) receptors are divided into two groups: P2X subtypes (P2X<sub>1,2,3,4,5,6,7</sub>) as ionotropic receptors and P2Y subtypes (P2Y<sub>1,2,4,6,11,12,13,14</sub>) as metabotropic receptors (Burnstock, 2007). Among them, histochemical and molecular studies demonstrated the expression of P2Y<sub>1</sub> in rat taste bud cells (Kataoka et al., 2004), P2Y<sub>2</sub>, P2Y<sub>4</sub> in mouse taste bud cells (Bystrova et al., 2006), P2X<sub>2</sub> and P2X<sub>7</sub> in mouse taste bud cells (Hayato et al., 2007). In addition, ATP

and purinergic agonists, such as 2-methylthio-ATP and 3'-O-(4-benzoyl)-ATP, induced calcium and electrical responses in mouse taste bud cells (Baryshnikov et al., 2003; Hayato et al., 2007; Kim et al., 2000). These data indicate that some taste bud cells are able to receive ATP released from themselves or neighboring taste bud cells. One excellent study using bio-sensor technique demonstrated the ATP mediated cell-cell communication in the taste bud (Huang et al., 2007). They used isolated taste bud from mouse circumvallate papillae and serotonin biosensor cells. As mentioned, Type III cells contain serotonin (Yee et al., 2001). Release of serotonin from Type III cells in response to taste stimuli, containing both sweet and bitter tastants, was detected by serotonin biosensor cells that did not respond to taste stimuli (Huang et al., 2005, 2007). This tastants-evoked serotonin release was blocked by broad purinoreceptor antagonist, suramin (Huang et al., 2007), indicating that Type III cells are activated by ATP that is released from neighboring sweet- and bitter-sensitive taste cells then release serotonin. One possible receptor for ATP in Type III cells is P2X<sub>2</sub> because the coexpression of SNAP25 and P2X<sub>2</sub> in mouse fungiform taste buds was demonstrated by immunohistochemistry (Hayato et al., 2007). Other P2 receptors, such as P2Y<sub>1</sub> and P2X<sub>7</sub>, may be involved in this ATP-mediated cell-cell communication.

## 4. MECHANISMS FOR THE SIGNAL TRANSMISSION FROM TASTE CELLS TO GUSTATORY NERVE FIBERS

Taste bud cells that are activated by sapid molecules transmit their signals to gustatory nerve fibers. However, limited number of taste cells (Type III cells but not Type II cells) forms recognizable synapses with gustatory nerve fibers. How do taste cells without synapses transmit their signals to gustatory axons? One possible way is the cell-cell communication among taste buds. But in this way, specific taste information may be lost because presynaptic cells may receive taste information from multiple taste cells that have various taste sensitivities. In this section, we first review and discuss the possible connection between taste cells and gustatory nerve fibers and then underlying mechanisms for signal transmission from taste cells to gustatory axons.

### 4.1. Formation of taste-coding channels

In the previous section, we demonstrated how taste cells encode taste information. Taste cells may be divided into two groups according to their sensitivity to taste stimuli. One is the specialist that responds to specific taste quality and the other is generalist that responds to multiple taste

qualities. In both fungiform and circumvallate taste buds of mice, about 60% of taste cells are specialists and the rest are generalists (Fig. 4.1B). In fungiform taste buds, there are plenty of sweet-sensitive cells and little numbers of bitter-sensitive cells. Are these response profiles conserved among gustatory nerve fibers? To challenge this, responsiveness of mouse fungiform taste cells and CT nerve fibers innervating them was compared (Yoshida et al., 2006a,b). Responses of 72 fungiform taste cells and 105 CT nerve fibers to four basic taste stimuli were recorded at random. Among 72 fungiform taste cells, 39 taste cells (54%) responded best to saccharin, 17 cells (24%) responded best to NaCl, 12 cells (17%) responded best to HCl, and 4 cells (6%) responded best to quinine–HCl (Fig. 4.5A). Among 105 CT nerve fibers, 44 fibers (42%) showed the best response to saccharin, 27 fibers (26%) responded best to NaCl, 24 fibers (23%) responded best to HCl, and 10 fibers (10%) responded best to quinine–HCl (Fig. 4.5A). Thus, relative population of each best taste cell was comparable to that of

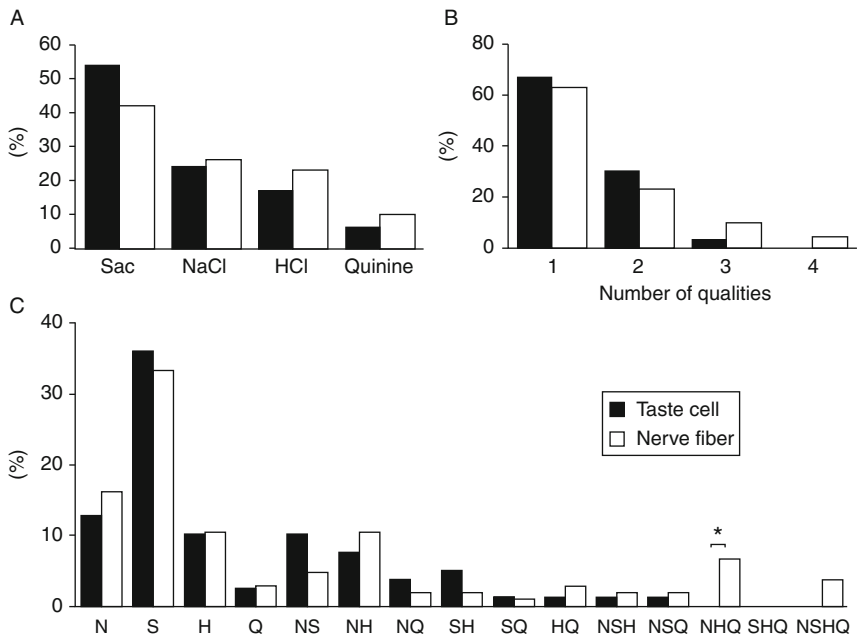


**Figure 4.5** Comparison of response profiles of mouse fungiform taste cells and CT nerve fibers. (A) Percentage of sweet-, salt-, sour-, and bitter-best taste cells and gustatory fibers. (B) Percentage of taste cells and gustatory fibers responding to one or more taste qualities. (C) Percentage of taste cells and gustatory fibers responding to various combinations of the four taste qualities. Black columns show data from fungiform taste cells and white columns show data from CT nerve fibers. S, saccharin; N, NaCl; H, HCl; Q, quinine. \* $p < 0.05$  by  $t$ -test for proportion.



gustatory fibers. In addition, the breadth of responsiveness was very similar between taste cells and gustatory fibers. In fungiform taste buds, 48 cells (67%) responded to one of four taste stimuli, 22 cells (30%) responded to two stimuli, and 2 cells (3%) responded to three stimuli (Fig. 4.5B). These produce the low mean entropy value for the breadth of responsiveness ( $0.158 \pm 0.028$ , mean  $\pm$  SEM). In the CT nerve, 66 fibers (63%) responded to one, 24 (23%) responded to two, 11 (10%) responded to three, and the rest (4 fibers, 4%) responded to four taste stimuli (Fig. 4.5B). These also produce the low mean entropy value ( $0.183 \pm 0.026$ ). If the more moderate response criterion was used, the mean entropy value would become larger. The criteria for the occurrence of a response in that study were the following: Number of spikes was larger than the mean plus two standard deviations of the spontaneous discharge. We reexamine responses of taste cells by using other moderate response criterion ( $>$ the mean + 1 SD). In this case, the mean entropy value for taste cells and CT fibers was  $0.207 \pm 0.029$  ( $n = 78$ ) and  $0.216 \pm 0.027$  ( $n = 105$ ), respectively. These values were not significantly different. When the proportions of nerve fibers responding to various combinations of the four basic taste categories are compared to those of taste cells (Fig. 4.5C), the occurrence of each class of CT fibers with different taste responsiveness to four taste stimuli was mostly quite comparable with that of fungiform taste cells. Only the class which responded to three (NaCl, HCl, and quinine) categories was significantly lower in taste cells than in the fibers. Using a hierarchical cluster analysis, both fungiform taste cells and CT fibers are classified into four groups, each of which was characterized by common taste stimuli that elicit responses. These similarities between taste cells and gustatory axons indicate that the range of responsiveness of taste cells may be close to that of innervating axons. Thus, there is no major modification of taste information sampled by taste cells in signal transmission from taste cells to nerve fibers. To guarantee this, selective connection may be formed between them.

Several nerve regeneration studies demonstrated how synaptic connections are between taste cells and gustatory axon reformed during regeneration or crossregeneration of gustatory nerves. It is well known that there are at least two independent systems for detection of salt taste: amiloride-sensitive and -insensitive system. Existence of these two systems was clearly demonstrated by single unit recordings of CT nerve fibers in rats (Ninomiya and Funakoshi, 1988), mice (Ninomiya, 1996), hamsters (Hettinger and Frank, 1990), rhesus monkey (Hellekant et al., 1997a), and chimpanzees (Hellekant et al., 1997b). In general, amiloride primarily inhibits NaCl (and LiCl) responses of gustatory fibers that selectively respond to sodium and lithium salts (labeled N type), whereas it hardly affects NaCl responses of fibers that show broad sensitivity to electrolytes (labeled E or H type). The IXth nerve contains primarily E-type fibers but only a very few if at all N-type fibers (Formaker and Hill, 1991; Ninomiya et al., 1991).

By cross-union anastomoses between the CT and IXth nerves of mice, the persistence of specific connections between amiloride-sensitive and amiloride-insensitive taste fibers and cells after cross-regeneration was investigated (Ninomiya, 1998). About a half population of NaCl-sensitive CT fibers was AS type and the rest half was AI type. On the other hand, the IXth nerve has almost exclusively the AI type. This relative abundance of the AS and AI types of fibers was not altered by cross-regeneration of the two gustatory nerves into the reverse tongue regions, suggesting that regenerated taste axons selectively recouple with the appropriate type of receptor cell. Subsequent study investigated the process of formation of two differential neural systems for salt taste during the CT nerve regeneration after crush (Yasumatsu et al., 2003). NaCl responses of the CT nerve started to recover from ~3 weeks after the nerve crush, whereas amiloride inhibition of NaCl responses clearly reappeared from ~4 weeks onward. During the course of recovery, N- and E-type fibers were clearly distinguishable on the basis of their amiloride sensitivities, their KCl/NaCl response ratios, and their concentration-response relationships to NaCl. These results suggest that AS and AI systems are independently reformed after the nerve crush. There are three possibilities for the process of nerve regeneration; the regenerated CT nerve fibers would (1) induce AI or AS properties after synapse formation with identical progenitors, (2) innervate AS and AI progenitor cells randomly followed by elimination of mismatched branches, or (3) selectively innervate AS or AI progenitor cells. Among them, the first and the second working hypotheses might require an intermediate type of fibers. However, these fibers have not been observed during the process of recovery of the CT nerve regeneration, indicating that selective innervations of AS and AI taste cells might occur. In the mouse fungiform taste buds, there are two types of NaCl-sensitive taste cells, AS and AI type, which have very similar response properties of N- and E-type fibers, respectively (Yoshida et al., 2009a). These cells may be selectively innervated by each type of fibers. Selective innervation of gustatory axons to taste cells was also demonstrated in sweet taste system (Yasumatsu et al., 2007). The peptide gurmarin inhibits CT nerve responses to sweet compounds by ~50% (Imoto et al., 1991; Miyasaka and Imoto, 1995; Ninomiya and Imoto, 1995; Ninomiya et al., 1997, 1998). In mice, there are two types of sweet-responsive CT fibers: gurmarin-sensitive (GS) and gurmarin-insensitive (GI) types (Ninomiya et al., 1999). After the CT nerve crush, recovery of the GI component preceded recovery of the GS component by about 1 week. During the course of CT regeneration, the GS and GI fibers could be distinguished. These indicate that the two sweet-reception systems may be reconstituted independently during regeneration of the CT nerve. Thus, selective connection may be formed between corresponding classes of taste cells and gustatory axons.

## 4.2. Transmitters in the taste buds

Taste signals must be transmitted from taste cells to gustatory axons. What transmitters are used in this signal transmission? Several transmitters have been proposed as candidates: serotonin (5-HT), glutamate, acetylcholine, neuropeptide Y, GABA, and ATP. Among them, 5-HT is one of the best studied transmitter candidates in taste buds. Early histochemical studies demonstrated the existence of monoamine in taste buds of frog (Hirata and Nada, 1975), rabbit (Nada and Hirata, 1975), and fishes (Nada and Hirata, 1977); then localization of 5-HT was demonstrated in many vertebrates (Fujimoto et al., 1987; Kim and Roper, 1995). As shown in Section 2.1, Type III cells possess 5-HT and its biosynthetic enzyme, AADC (Defazio et al., 2006; Yee et al., 2001). Therefore, Type III cells may use 5-HT as a neurotransmitter. Receptors for 5-HT also have been demonstrated in taste buds. 5-HT<sub>1A</sub> and 5-HT<sub>3</sub> receptors are identified by RT-PCR in taste buds and 5-HT<sub>1A</sub> is immunopositive in a subset of taste bud cells (Kaya et al., 2004). This report also demonstrated that gustatory nerve fibers express 5-HT<sub>3</sub> receptors, suggesting that 5-HT<sub>3</sub> receptor might mediate signal transmission from taste cells to gustatory nerve fibers. However, recent findings indicate that the 5-HT<sub>3A</sub> KO mice show no obvious deficits in taste behavior (Finger et al., 2005). 5-HT could affect the membrane properties of taste cells. An exposure to 5-HT induced an increase in membrane input resistances and a hyperpolarization of *Necturus* receptor cells (Ewald and Roper, 1994). Also in *Necturus* taste cells, voltage-activated calcium currents were potentiated or inhibited by focal application of 5-HT and these effects might be mediated by 5-HT<sub>1A</sub> receptor (Delay et al., 1997). In addition, calcium-activated potassium current and voltage-dependent sodium current in rat taste bud cells were inhibited by application of 5-HT<sub>1A</sub> agonists, such as 1-(1-naphthyl)piperazine and buspirone (Herness and Chen, 2000). Taken together, taste cells (possibly Type III cells) secrete 5-HT onto adjacent taste cells to modulate their activity via 5-HT<sub>1A</sub> receptor. 5-HT may also affect on gustatory nerve fibers, but this effect must be elucidated in further studies.

Regarding the signal transmission from taste cells to gustatory nerve fibers, ATP is the most possible candidate transmitter. Gustatory nerve fibers express ionotropic purinergic receptors, P2X<sub>2</sub> and P2X<sub>3</sub> (Bo et al., 1999), suggesting that ATP may serve as a transmitter in taste system. Gustatory nerve responses of P2X<sub>2</sub> and P2X<sub>3</sub> double-knockout mice to taste stimuli were eliminated despite stimulation by touch, temperature, and menthol solutions elicited robust neural responses (Finger et al., 2005). This report also demonstrated reduced behavioral responses to sweet, umami, and bitter substances in P2X<sub>2</sub>/X<sub>3</sub> double-KO mice. Responses of taste bud cells in P2X<sub>2</sub>/X<sub>3</sub> double-KO mice are not clear; however, these results strongly suggest that ATP serves as a key neurotransmitter linking taste cells to

sensory nerve fibers. Recent study using transgenic mouse expressing a transneuronal tracer, wheat germ agglutinin (WGA), under the control of mouse T1R3 gene promoter demonstrated that WGA protein was detected in the P2X<sub>2</sub>-positive intragemmal fibers surrounding the taste receptor cells and a subpopulation of P2X<sub>2</sub>- or P2X<sub>3</sub>-positive neurons in the geniculate and nodose/petrosal ganglia (Ohmoto et al., 2008). Therefore, taste signal derived from T1R3-positive cells (possibly sweet- and umami-sensitive taste cells) may be transferred to P2X<sub>2</sub>/X<sub>3</sub>-positive gustatory nerve fibers.

### 4.3. Transmitter release from taste bud cells

Are these transmitter candidates released from taste cells by stimulation of sapid molecules? Huang et al. (2005) used Chinese hamster ovary (CHO) cells stably expressing 5-HT receptors as biosensor to monitor 5-HT release from taste bud cells and detected serotonin when taste buds were stimulated by high K<sup>+</sup> solution (depolarization) or sweet, bitter, sour tastants. Finger et al. (2005) showed ATP release from taste buds evoked by taste stimuli in striped tongue epithelium preparations by a standard luciferin–luciferase bioluminescence assay. In addition, a recent study using biosensor cells demonstrated norepinephrine release from taste bud cells by high K<sup>+</sup> solution or sweet, bitter, sour tastants (Huang et al., 2008b). These indicate that 5-HT, ATP, and norepinephrine are released from taste cells in response to taste stimuli. In taste buds, Type III cells that have morphological synapses possess serotonin. Serotonin release evoked by high K<sup>+</sup> or sour stimulation required calcium influx (Huang et al., 2005), indicating that serotonin might be released from Type III cells via conventional synaptic mechanisms. Norepinephrine is coreleased with serotonin (Huang et al., 2008b), suggesting that norepinephrine is released from Type III cells. However, Type II cells do not possess apparent synaptic structures. What transmitter is used in Type II cells and how is it released from Type II cells? ATP is likely to be key.

In 2007, two groups identified ATP release from taste cells by using ATP biosensor cells. Romanov et al. (2007) demonstrated that isolated mouse Type II taste cells that were identified by electrophysiological properties released ATP upon serial depolarization. Hemichannel blockers such as octanol and mimetic peptide GAP26 affected voltage-gated outward currents through ATP-permeable ion channels in Type II cells and ATP release from taste cells was inhibited by application of GAP26. Huang et al. (2007) demonstrated that isolated taste cells released ATP in response to taste (sweet–bitter mixture) stimuli, and these cells did not respond to high K<sup>+</sup> stimulation, indicating that Type II cells release ATP. These ATP releases were blocked by a hemichannel blocker, carbenoxolone. Both studies demonstrated the expression of a hemichannel, pannexin 1, in taste bud cells. Most of pannexin 1-positive cells were also positive to

PLC $\beta$ 2 and TRPM5, indicating that Type II cells express pannexin 1 hemichannel. Thus, Type II cells may be depolarized by taste (sweet, bitter, umami) stimuli and release ATP via pannexin 1 hemichannel. Our recent study more directly demonstrated action potential-dependent ATP release from Type II cells but not Type III cells in response to taste stimuli via hemichannels (Murata et al., 2008, unpublished observation). Using gustducin-GFP and GAD-GFP transgenic mice, action potentials and ATP release were simultaneously assayed in GFP-positive taste cells (Fig. 4.6). As described in previous section, gustducin-GFP (Type II) cells increased firing activities in response to sweet, bitter, or umami taste stimuli and GAD67-GFP (Type III) cells responded to sour taste stimuli. Immediately after recording of taste responses, the electrode solution was collected and subjected to a luciferase assay to quantify ATP. Stimulation of gustducin-GFP taste cells with saccharin, quinine, cyclohexamide, or

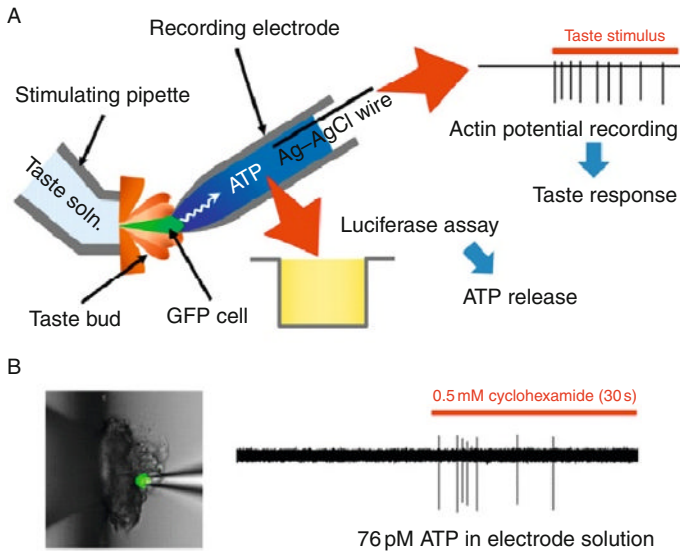


**Figure 4.6** Recording of taste response and ATP release from a taste bud cell. (A) A schematic drawing of recording of taste responses and measurement of released ATP from a GFP taste bud cell. The mucosal side of an isolated taste bud was attached to the stimulating pipette with gentle suction. The receptor membranes of taste cells were stimulated by taste solution for 30 s. Immediately after taste stimulation, electrode solution (10  $\mu$ l) was collected into a 96-well plate and subjected to luciferase assay to measure ATP concentration. (B) A photograph showing a gustducin-GFP taste cell in an isolated taste bud from which taste response was recorded (left). Gustducin is a G protein  $\alpha$ -subunit responsible for sweet, bitter, and umami taste. This GFP-positive cell responded to 0.5 mM cyclohexamide (bitter) with action potentials (right). 76 pM ATP was detected in luciferase assay, indicating that this bitter-sensitive taste cells release ATP in response to bitter taste stimulation.

glutamate increased ATP levels in the electrode solution (Fig. 4.6B), but stimulation of GAD67-GFP taste cells with HCl did not, indicating that Type II cells but not Type III cells release ATP in response to taste stimuli. Amount of ATP released from gustducin-GFP taste cells depended on firing rate; therefore, ATP release was detected in gustducin-GFP taste cells with spontaneous firing. Such ATP release was inhibited by the hemichannel blocker carbenoxolone, indicating that gustducin-GFP taste cells release ATP independent of conventional exocytotic mechanisms. Thus, we hypothesized that action potentials in Type II cells trigger ATP release via hemichannels (maybe pannexin 1 hemichannels). Voltage-gating mechanisms for opening of hemichannels remain to be unsolved.

For transmitter release from taste cells, membrane depolarization and action potentials may be required. As described previously, both Type II and Type III cells generate action potentials in response to taste stimuli (Yoshida et al., 2009b), and action potentials are inhibited by Na<sup>+</sup> channel blocker, tetrodotoxin (TTX; Yoshida et al., 2005). Our preliminary results demonstrate that blocking action potentials by administration of TTX decreased taste-evoked ATP release from Type II cells to one-third of its control, suggesting that action potentials enhance ATP release from taste cells (Y. Murata et al., unpublished observation). A recent report provides the molecular basis for generation of action potentials in taste cells (Gao et al., 2009). Type II taste cells express TTX-sensitive Na<sup>+</sup> channel subunits, SCN2A, SCN3A, and SCN9A, whereas Type III cells express only SCN2A. TTX-sensitive Na<sup>+</sup> channels may be activated by TRPM5 current in Type II cells or PKD, ASIC, or HCN current in Type III cells. Generation of action potentials may lead to opening of hemichannels to release ATP in Type II cells or activation of voltage-gated Ca<sup>2+</sup> channels to release 5-HT and norepinephrine via exocytotic mechanisms in Type III cells. Such potential roles are suggested, but functional significance of action potentials in taste cells remains unclear (Vandenbeuch and Kinnamon, 2009). Future studies may elucidate the role of action potentials in signal transmission from taste cells to gustatory nerve fibers.

## 5. CONCLUDING REMARKS

Taste bud cells exhibit wide varieties in morphological, molecular expression, and physiological properties. From the morphological view, taste bud cells are classified into four groups: Type I–IV cells. Among them, Type II and Type III cells express taste receptors and transduction components, indicating that these cells function as taste receptor cells. Sweet (T1R2/T1R3), bitter (T2Rs), umami (T1R1/T1R3), and sour (PKD1L3/PKD2L2) receptors are expressed in the different set of taste bud cells,

respectively. Such molecular evidences suggest that taste qualities might be discriminated at the taste receptor cell level. However, physiological responses of taste bud cells and gustatory nerve fibers are not so simple. There are at least two types of NaCl-sensitive taste cells and gustatory nerve fibers according to the sensitivity to amiloride (AS and AI type). Sweet-sensitive gustatory fibers are classified into two groups according to sensitivity to gurmarin (GS and GI type). These suggest the existence of multiple receptor systems for salty and sweet taste. In addition, a significant portion of taste bud cells and gustatory nerve fibers respond to multiple taste qualities. Multiple sensitivity in taste bud cells may be caused by cell–cell communication, or expressing multiple taste receptors, or taste receptors that are sensitive to multiple taste qualities. TRPV1 valiant may be one of candidate taste receptors for multiple electrolytes. In any case, gustatory nerve fibers have taste response properties very similar to those of taste bud cells with action potentials. Specific connection between taste cells and gustatory fibers may account for this. But it is not yet known what molecular mechanisms guarantee the specific connection between taste cells and gustatory nerve fibers. Several transmitters are suggested to function in taste bud cells. ATP is one of these candidates and is released from Type II cells that do not possess conventional synapses and respond to sweet, bitter, or umami taste stimuli. Type III cells have synaptic structures and respond to sour taste stimuli release other transmitters such as serotonin and norepinephrine. Therefore, each taste cell may use distinct transmitters, but it is not clear whether transmitters other than ATP contribute to signal transmission from taste cells to gustatory nerve. Action potentials may be required to release transmitters from both Type II and Type III cells, although transduction mechanisms and transmitter releasing mechanisms may be different between Type II and Type III cells. Thus, taste bud cells and gustatory nerve fibers may form coding channels for taste perception. Coding channels for specific taste quality may be devoted to perception of specific taste and those for broad taste qualities may contribute to discrimination of more slight differences between taste compounds.

## **ACKNOWLEDGMENTS**

This work was supported by Japan Society for the Promotion of Science, Grant-in-Aid for Scientific Research (KAKENHI) 18109013, 18077004 (YN), and 21791808 (RY).

## **REFERENCES**

- Adler, E., Hoon, M.A., Mueller, K.L., Chandrashekar, J., Ryba, N.J.P., Zuker, C.S., 2000. A novel family of mammalian taste receptors. *Cell* 100, 693–702.
- Avenet, P., Lindemann, B., 1988. Amiloride-blockable sodium currents in isolated taste receptor cells. *J. Membr. Biol.* 105, 245–255.

- Avenet, P., Lindemann, B., 1991. Non-invasive recording of receptor cell action potentials and sustained currents from single taste buds maintained in the tongue: The response to mucosal NaCl and amiloride. *J. Membr. Biol.* 124, 33–41.
- Bachmanov, A.A., Li, X., Reed, D.R., Ohmen, J.D., Li, S., Chen, Z., et al., 2001. Positional cloning of the mouse saccharin preference (Sac) locus. *Chem. Senses* 26, 925–933.
- Bartel, D.L., Sullivan, S.L., Lavoie, E.G., Sevigny, J., Finger, T.E., 2006. Nucleoside triphosphate diphosphohydrolase-2 is the ecto-ATPase of type I cells in taste buds. *J. Comp. Neurol.* 497, 1–12.
- Baryshnikov, S.G., Rogachevskaja, O.A., Kolesnikov, S.S., 2003. Calcium signaling mediated by P2Y receptors in mouse taste cells. *J. Neurophysiol.* 90, 3283–3294.
- Béché, P., DeSimone, J.A., Avenet, P., Lindemann, B., 1990. Membrane currents in taste cells of rat fungiform papilla: Evidence for two types of Ca currents and inhibition of K currents by saccharin. *J. Gen. Physiol.* 96, 1061–1084.
- Behrens, M., Meyerhof, W., 2006. Bitter taste receptors and human bitter taste perception. *Cell. Mol. Life Sci.* 63, 1501–1509.
- Behrens, M., Brockhoff, A., Kuhn, C., Bufo, B., Winnig, M., Meyerhof, W., 2004. The human taste receptor hTAS2R14 responds to a variety of different bitter compounds. *Biochem. Biophys. Res. Commun.* 319, 479–485.
- Behrens, M., Foerster, S., Staehler, F., Raguse, J.D., Meyerhof, W., 2007. Gustatory expression pattern of the human TAS2R bitter receptor gene family reveals a heterogeneous population of bitter responsive taste receptor cells. *J. Neurosci.* 27, 12630–12640.
- Bigiani, A., 2001. Mouse taste cells with glialike membrane properties. *J. Neurophysiol.* 85, 1552–1560.
- Bigiani, A., Roper, S.D., 1993. Identification of electrophysiologically distinct cell populations in *Necturus* taste buds. *J. Gen. Physiol.* 102, 143–170.
- Bo, X., Alavi, A., Xiang, Z., Oglesby, I., Ford, A., Burnstock, G., 1999. Localization of ATP-gated P2X<sub>2</sub> and P2X<sub>3</sub> receptor immunoreactive nerves in rat taste buds. *Neuroreport* 10, 1107–1111.
- Bufo, B., Hofmann, T., Krautwurst, D., Raguse, J.D., Meyerhof, W., 2002. The human TAS2R16 receptor mediates bitter taste in response to  $\beta$ -glucopyranosides. *Nat. Genet.* 32, 397–401.
- Bufo, B., Breslin, P.A., Kuhn, C., Reed, D.R., Tharp, C.D., Slack, J.P., et al., 2005. The molecular basis of individual differences in phenylthiocarbamide and propylthiouracil bitterness perception. *Curr. Biol.* 15, 322–327.
- Burnstock, G., 2007. Purine and pyrimidine receptors. *Cell. Mol. Life Sci.* 64, 1471–1483.
- Bystrova, M.F., Yatzenko, Y.E., Fedorov, I.V., Rogachevskaja, O.A., Kolesnikov, S.S., 2006. P2Y isoforms operative in mouse taste cells. *Cell Tissue Res.* 323, 377–382.
- Caicedo, A., Roper, S.D., 2001. Taste receptor cells that discriminate between bitter stimuli. *Science* 291, 1557–1560.
- Caicedo, A., Kim, K., Roper, S.D., 2002. Individual mouse taste cells respond to multiple chemical stimuli. *J. Physiol.* 544, 501–509.
- Chandrashekar, J., Mueller, K.L., Hoon, M.A., Adler, E., Feng, L., Guo, W., et al., 2000. T2Rs function as bitter taste receptors. *Cell* 100, 703–711.
- Chandrashekar, J., Hoon, M.A., Ryba, N.J., Zuker, C.S., 2006. The receptors and cells for mammalian taste. *Nature* 444, 288–294.
- Chattopadhyaya, B., Di Cristo, G., Higashiyama, H., Knott, G.W., Kuhlman, S.J., Welker, E., et al., 2004. Experience and activity-dependent maturation of perisomatic GABAergic innervation in primary visual cortex during a postnatal critical period. *J. Neurosci.* 24, 9598–9611.
- Clapp, T.R., Stone, L.M., Margolskee, R.F., Kinnamon, S.C., 2001. Immunocytochemical evidence for co-expression of Type III IP<sub>3</sub> receptor with signaling components of bitter taste transduction. *BMC Neurosci.* 2, 6.



- Clapp, T.R., Yang, R., Stoick, C.L., Kinnamon, S.C., Kinnamon, J.C., 2004. Morphologic characterization of rat taste receptor cells that express components of the phospholipase C signaling pathway. *J. Comp. Neurol.* 468, 311–321.
- Clapp, T.R., Medler, K.F., Damak, S., Margolskee, R.F., Kinnamon, S.C., 2006. Mouse taste cells with G protein-coupled taste receptors lack voltage-gated calcium channels and SNAP-25. *BMC Biol.* 4, 7.
- Cummings, T.A., Powell, J., Kinnamon, S.C., 1993. Sweet taste transduction in hamster taste cells: Evidence for the role of cyclic nucleotides. *J. Neurophysiol.* 70, 2326–2336.
- Damak, S., Rong, M., Yasumatsu, K., Kokrashvili, Z., Perez, C.A., Shigemura, N., et al., 2006. Trpm5 null mice respond to bitter, sweet, and umami compounds. *Chem. Senses* 31, 253–264.
- Danilova, V., Hellekant, G., 2003. Comparison of the responses of the chorda tympani and glossopharyngeal nerves to taste stimuli in C57BL/6J mice. *BMC Neurosci.* 4, 5.
- DeFazio, R.A., Dvoryanchikov, G., Maruyama, Y., Kim, J.W., Pereira, E., Roper, S.D., et al., 2006. Separate populations of receptor cells and presynaptic cells in mouse taste buds. *J. Neurosci.* 26, 3971–3980.
- Delay, R.J., Kinnamon, J.C., Roper, S.D., 1986. Ultrastructure of mouse vallate taste buds: II. Cell types and cell lineage. *J. Comp. Neurol.* 253, 242–252.
- Delay, R.J., Kinnamon, S.C., Roper, S.D., 1997. Serotonin modulates voltage-dependent calcium current in *Necturus* taste cells. *J. Neurophysiol.* 77, 2515–2524.
- Ewald, D.A., Roper, S.D., 1994. Bidirectional synaptic transmission in *Necturus* taste buds. *J. Neurosci.* 14, 3791–3804.
- Farbman, A.I., 1965. Fine structure of the taste bud. *J. Ultrastruct. Res.* 12, 328–350.
- Finger, T.E., Danilova, V., Barrows, J., Bartel, D.L., Vigers, A.J., Stone, L., et al., 2005. ATP signaling is crucial for communication from taste buds to gustatory nerves. *Science* 310, 1495–1499.
- Formaker, B.K., Hill, D.L., 1991. Lack of amiloride sensitivity in SHR and WKY glossopharyngeal taste responses to NaCl. *Physiol. Behav.* 50, 765–769.
- Frank, M., 1973. An analysis of hamster afferent taste nerve response functions. *J. Gen. Physiol.* 61, 588–618.
- Frank, M.E., Lundy, R.F., Contreras, R.J., 2008. Cracking taste codes by tapping into sensory neuron impulse traffic. *Prog. Neurobiol.* 86, 245–263.
- Fujimoto, S., Ueda, H., Kagawa, H., 1987. Immunocytochemistry on the localization of 5-hydroxytryptamine in monkey and rabbit taste buds. *Acta Anat.* 128, 80–83.
- Furue, H., Yoshii, K., 1997. *In situ* tight-seal recordings of taste substance-elicited action currents and voltage-gated Ba currents from single taste bud cells in the peeled epithelium of mouse tongue. *Brain Res.* 776, 133–139.
- Gao, N., Lu, M., Echeverri, F., Laita, B., Kalabat, D., Williams, M.E., et al., 2009. Voltage-gated sodium channels in taste bud cells. *BMC Neurosci.* 10, 20.
- Garty, H., Palmer, L.G., 1997. Epithelial sodium channels: Function, structure, and regulation. *Physiol. Rev.* 77, 359–396.
- Gilbertson, T.A., Boughter, J.D., 2003. Taste transduction: Appetizing times in gustation. *Neuroreport* 14, 905–911.
- Gilbertson, T.A., Avenet, P., Kinnamon, S.C., Roper, S.D., 1992. Proton currents through amiloride-sensitive Na channels in hamster taste cells: Role in acid transduction. *J. Gen. Physiol.* 100, 803–824.
- Gilbertson, T.A., Boughter, J.D., Zhang, H., Smith, D.V., 2001. Distribution of gustatory sensitivities in rat taste cells: Whole-cell responses to apical chemical stimulation. *J. Neurosci.* 21, 4931–4941.
- Hayato, R., Ohtubo, Y., Yoshii, K., 2007. Functional expression of ionotropic purinergic receptors on mouse taste bud cells. *J. Physiol.* 584, 473–488.

- He, W., Yasumatsu, K., Varadarajan, V., Yamada, A., Lem, J., Ninomiya, Y., et al., 2004. Umami taste responses are mediated by alpha-transducin and alpha-gustducin. *J. Neurosci.* 24, 7674–7680.
- Heck, G.L., Mierson, S., DeSimone, J.A., 1984. Salt taste transduction occurs through an amiloride-sensitive sodium transport pathway. *Science* 223, 403–405.
- Hellekant, G., Ninomiya, Y., 1991. On the taste of chimpanzee. *Physiol. Behav.* 49, 927–934.
- Hellekant, G., Dubois, G.E., Roberts, T.W., van de Wel, H., 1988. On the gustatory effect of amiloride in the monkey (*Macaca mulatta*). *Chem. Senses* 13, 89–93.
- Hellekant, G., Danilova, V., Ninomiya, Y., 1997a. Primate sense of taste: Behavioral and single chorda tympani and glossopharyngeal nerve fiber recordings in the rhesus monkey, *Macaca mulatta*. *J. Neurophysiol.* 77, 978–993.
- Hellekant, G., Ninomiya, Y., Danilova, V., 1997b. Taste in chimpanzees II: Single chorda tympani fibers. *Physiol. Behav.* 61, 829–841.
- Herness, M.S., Chen, Y., 2000. Serotonergic agonists inhibit calcium-activated potassium and voltage-dependent sodium currents in rat taste receptor cells. *J. Membr. Biol.* 173, 127–138.
- Hettinger, T.P., Frank, M.E., 1990. Specificity of amiloride inhibition of hamster taste responses. *Brain Res.* 513, 24–34.
- Hirata, K., Nada, O., 1975. A monoamine in the gustatory cell of the frog's taste organ: A fluorescence histochemical and electron microscopic study. *Cell Tissue Res.* 159, 101–108.
- Hisatsune, C., Yasumatsu, K., Takahashi-Iwanaga, H., Ogawa, N., Kuroda, Y., Yoshida, R., et al., 2007. Abnormal taste perception in mice lacking the type 3 inositol 1,4,5-trisphosphate receptor. *J. Biol. Chem.* 282, 37225–37231.
- Hoon, M.A., Adler, E., Lindemeier, J., Battey, J.F., Ryba, N.J., Zuker, C.S., 1999. Putative mammalian taste receptors: A class of taste-specific GPCRs with distinct topographic selectivity. *Cell* 96, 541–551.
- Huang, Y.J., Maruyama, Y., Lu, K.S., Pereira, E., Plonsky, I., Baur, J.E., et al., 2005. Mouse taste buds use serotonin as a neurotransmitter. *J. Neurosci.* 25, 843–847.
- Huang, A.L., Chen, X., Hoon, M.A., Chandrashekar, J., Guo, W., Trankner, D., et al., 2006. The cells and logic for mammalian sour taste detection. *Nature* 442, 934–938.
- Huang, Y.J., Maruyama, Y., Dvoryanchikov, G., Pereira, E., Chaudhari, N., Roper, S.D., 2007. The role of pannexin 1 hemichannels in ATP release and cell–cell communication in mouse taste buds. *Proc. Natl. Acad. Sci. USA* 104, 6436–6441.
- Huang, Y.J., Maruyama, Y., Stimac, R., Roper, S.D., 2008a. Presynaptic (Type III) cells in mouse taste buds sense sour (acid) taste. *J. Physiol.* 586, 2903–2912.
- Huang, Y.J., Maruyama, Y., Roper, S.D., 2008b. Norepinephrine is coreleased with serotonin in mouse taste buds. *J. Neurosci.* 8, 13088–13093.
- Imoto, T., Miyasaka, A., Ishima, R., Akasaka, K., 1991. A novel peptide isolated from the leaves of *Gymnema sylvestre*-1. Characterization and its suppressive effect on the neural responses to sweet taste stimuli in the rat. *Comp. Biochem. Physiol.* 100A, 309–314.
- Ishimaru, Y., Inada, H., Kubota, M., Zhuang, H., Tominaga, M., Matsunami, H., 2006. Transient receptor potential family members PKD1L3 and PKD2L1 form a candidate sour taste receptor. *Proc. Natl. Acad. Sci. USA* 103, 12569–12574.
- Kashiwayanagi, M., Miyake, M., Kurihara, K., 1983. Voltage-dependent  $Ca^{2+}$  channel and  $Na^{+}$  channel in frog taste cells. *Am. J. Physiol.* 244, C82–C88.
- Kataoka, S., Toyono, T., Seta, Y., Ogura, T., Toyoshima, K., 2004. Expression of P2Y<sub>1</sub> receptors in rat taste buds. *Histochem. Cell Biol.* 121, 419–426.
- Kataoka, S., Yang, R., Ishimaru, Y., Matsunami, H., Sevigny, J., Kinnamon, J.C., et al., 2008. The candidate sour taste receptor, PKD2L1, is expressed by type III taste cells in the mouse. *Chem. Senses* 33, 243–254.

- Kaya, N., Shen, T., Lu, S.G., Zhao, F.L., Herness, S., 2004. A paracrine signaling role for serotonin in rat taste buds: Expression and localization of serotonin receptor subtypes. *Am. J. Physiol. Regul. Integr. Comp. Physiol.* 286, R649–R658.
- Kim, D.J., Roper, S.D., 1995. Localization of serotonin in taste buds: A comparative study in four vertebrates. *J. Comp. Neurol.* 353, 364–370.
- Kim, Y.V., Bobkov, Y.V., Kolesnikov, S.S., 2000. Adenosine triphosphate mobilizes cytosolic calcium and modulates ionic currents in mouse taste receptor cells. *Neurosci. Lett.* 290, 165–168.
- Kim, U.K., Jorgenson, E., Coon, H., Leppert, M., Risch, N., Drayna, D., 2003. Positional cloning of the human quantitative trait locus underlying taste sensitivity to phenylthiocarbamide. *Science* 299, 1221–1225.
- Kim, J.W., Roberts, C., Maruyama, Y., Berg, S., Roper, S., Chaudhari, N., 2006. Faithful expression of GFP from the PLC $\beta$ 2 promoter in a functional class of taste receptor cells. *Chem. Senses* 31, 213–219.
- Kinnamon, J.C., Sherman, T.A., Roper, S.D., 1988. Ultrastructure of mouse vallate taste buds: III. Patterns of synaptic connectivity. *J. Comp. Neurol.* 270, 1–10.
- Kitagawa, M., Kusakabe, Y., Miura, H., Ninomiya, Y., Hino, A., 2001. Molecular genetic identification of a candidate receptor gene for sweet taste. *Biochem. Biophys. Res. Commun.* 283, 236–242.
- Kretz, O., Barbry, P., Bock, R., Lindemann, B., 1999. Differential expression of RNA and protein of the three pore-forming subunits of the amiloride-sensitive epithelial sodium channel in taste buds of the rat. *J. Histochem. Cytochem.* 47, 51–64.
- Kuhn, C., Bufe, B., Winnig, M., Hofmann, T., Frank, O., Behrens, M., et al., 2004. Bitter taste receptors for saccharin and acesulfame K. *J. Neurosci.* 24, 10260–10265.
- Lawton, D.M., Furness, D.N., Lindemann, B., Hackney, C.M., 2000. Localization of the glutamate-aspartate transporter, GLAST, in rat taste buds. *Eur. J. Neurosci.* 12, 3163–3171.
- Li, X.J., Blackshaw, S., Snyder, S.H., 1994. Expression and localization of amiloride-sensitive sodium channel indicate a role for non-taste cells in taste perception. *Proc. Natl. Acad. Sci. USA* 91, 1814–1818.
- Li, X., Staszewski, L., Xu, H., Durick, K., Zoller, M., Adler, E., 2002. Human receptors for sweet and umami taste. *Proc. Natl. Acad. Sci. USA* 99, 4692–4696.
- Lin, W., Finger, T.E., Rossier, B.C., Kinnamon, S.C., 1999. Epithelial Na<sup>+</sup> channel subunits in rat taste cells: Localization and regulation by aldosterone. *J. Comp. Neurol.* 405, 406–420.
- Lin, W., Burks, C.A., Hansen, D.R., Kinnamon, S.C., Gilbertson, T.A., 2004. Taste receptor cells express pH-sensitive leak K<sup>+</sup> channels. *J. Neurophysiol.* 92, 2909–2919.
- Lindemann, B., 2001. Receptors and transduction in taste. *Nature* 413, 219–225.
- Liu, L., Simon, S.A., 2001. Acidic stimuli activates two distinct pathways in taste receptor cells from rat fungiform papillae. *Brain Res.* 923, 58–70.
- Lush, I.E., 1984. The genetics of tasting in mice: III. Quinine. *Genet. Res.* 44, 151–160.
- Lush, I.E., 1989. The genetics of tasting in mice. VI. Saccharin, acesulfame, dulcin and sucrose. *Genet. Res.* 53, 95–99.
- Lush, I.E., Holland, G., 1988. The genetics of tasting in mice. V. Glycine and cyclohexamide. *Genet. Res.* 52, 207–212.
- Lyall, V., Heck, G.L., Vinnikova, A.K., Ghosh, S., Phan, T.H., Alam, R.I., et al., 2004. The mammalian amiloride-insensitive non-specific salt taste receptor is a vanilloid receptor-1 variant. *J. Physiol.* 558, 147–159.
- Matsunami, H., Montmayeur, J.P., Buck, L.B., 2000. A candidate of taste receptors in human and mouse. *Nature* 404, 601–604.
- Max, M., Shanker, Y.G., Huang, L., Rong, M., Liu, Z., Campagne, F., et al., 2001. Tas1r3, encoding a new candidate taste receptor, is allelic to the sweet responsiveness locus Sac. *Nat. Genet.* 28, 58–63.

- Miyamoto, T., Miyazaki, T., Okada, Y., Sato, T., 1996. Whole-cell recording from non-dissociated taste cells in mouse taste bud. *J. Neurosci. Methods* 64, 245–252.
- Miyamoto, T., Fujiyama, R., Okada, Y., Sato, T., 1998. Sour transduction involves activation of NPPB-sensitive conductance in mouse taste cells. *J. Neurophysiol.* 80, 1852–1859.
- Miyasaka, A., Imoto, T., 1995. Electrophysiological characterization of the inhibitory effect of a novel peptide gurmardin on the sweet taste response in rats. *Brain Res.* 676, 63–68.
- Miyoshi, M.A., Abe, K., Emori, Y., 2001. IP<sub>3</sub> receptor type 3 and PLC $\beta$ 2 are co-expressed with taste receptors T1R and T2R in rat taste bud cells. *Chem. Senses* 26, 259–265.
- Montmayeur, J.P., Liberles, S.D., Matsunami, H., Buck, L.B., 2001. A candidate taste receptor gene near a sweet taste locus. *Nat. Neurosci.* 4, 492–498.
- Mueller, K.L., Hoon, M.A., Erlenbach, I., Chandrashekar, J., Zuker, C.S., Ryba, N.J., 2005. The receptors and coding logic for bitter taste. *Nature* 434, 225–229.
- Murata, Y., Yoshida, R., Yasuo, T., Yanagawa, Y., Obata, K., Ueno, H., et al., 2008. Firing rate-dependent ATP release from mouse fungiform taste cells with action potentials. *Chem. Senses* 33, S128.
- Murray, R.G., 1971. Ultrastructure of taste receptors. In: Beidler, L.M. (Ed.), *Handbook of Sensory Physiology Vol. 4*. Springer-Verlag, Berlin, pp. 31–50.
- Murray, R., 1973. The ultrastructure of taste buds. In: Friedemann, I. (Ed.), *The Ultrastructure of Sensory Organs*. North-Holland, Amsterdam, pp. 1–81.
- Nada, O., Hirata, K., 1975. The occurrence of the cell type containing a specific monoamine in the taste bud of the rabbit's foliate papilla. *Histochemistry* 43, 237–240.
- Nada, O., Hirata, K., 1977. The monoamine-containing cell in the gustatory epithelium of some vertebrates. *Arch. Histol. Jpn.* 40, 197–206.
- Nakamura, Y., Yanagawa, Y., Obata, K., Watanabe, M., Ueno, H., 2007. GABA is produced in taste bud. *Chem. Senses* 32, J19.
- Nelson, G.M., Finger, T.E., 1993. Immunolocalization of different forms of neural cell adhesion molecule (NCAM) in rat taste buds. *J. Comp. Neurol.* 336, 507–516.
- Nelson, G., Hoon, M.A., Chandrashekar, J., Zhang, Y., Ryba, N.J.P., Zuker, C.S., 2001. Mammalian sweet taste receptors. *Cell* 106, 381–390.
- Nelson, G., Chandrashekar, J., Hoon, M.A., Feng, L., Zhao, G., Ryba, N.J., et al., 2002. An amino-acid taste receptor. *Nature* 416, 199–202.
- Ninomiya, Y., 1996. Salt taste responses of mouse chorda tympani neurons: Evidence for existence of two different amiloride-sensitive receptor components for NaCl with different temperature dependencies. *J. Neurophysiol.* 76, 3550–3554.
- Ninomiya, Y., 1998. Reinnervation of cross-regenerated gustatory nerve fibers into amiloride-sensitive and amiloride-insensitive taste receptor cells. *Proc. Natl. Acad. Sci. USA* 95, 5347–5350.
- Ninomiya, Y., Funakoshi, M., 1988. Amiloride inhibition of responses of rat single chorda tympani fibers to chemical and electrical tongue stimulations. *Brain Res.* 451, 319–325.
- Ninomiya, Y., Imoto, T., 1995. Gurmardin inhibition of sweet taste responses in mice. *Am. J. Physiol.* 268, R1019–R1025.
- Ninomiya, Y., Tonosaki, K., Funakoshi, M., 1982. Gustatory neural response in the mouse. *Brain Res.* 244, 370–373.
- Ninomiya, Y., Mizukoshi, T., Higashi, T., Katsukawa, H., Funakoshi, M., 1984. Gustatory neural responses in three different strains of mice. *Brain Res.* 302, 305–314.
- Ninomiya, Y., Tanimukai, T., Yoshida, S., Funakoshi, M., 1991. Gustatory neural responses in preweanling mice. *Physiol. Behav.* 49, 913–918.
- Ninomiya, Y., Inoue, M., Imoto, T., Nakashima, K., 1997. Lack of gurmardin sensitivity of sweet taste receptors innervated by the glossopharyngeal nerve in C57BL mice. *Am. J. Physiol.* 272, R1002–R1006.

- Ninomiya, Y., Inoue, M., Imoto, T., 1998. Reduction of the suppressive effects of gurmarin on sweet taste responses by addition of  $\beta$ -cyclodextrin. *Chem. Senses* 23, 303–307.
- Ninomiya, Y., Imoto, T., Sugimura, T., 1999. Sweet taste responses of mouse chorda tympani neurons: Existence of gurmarin-sensitive and -insensitive receptor components. *J. Neurophysiol.* 81, 3087–3091.
- Ohmoto, M., Matsumoto, I., Yasuoka, A., Yoshihara, Y., Abe, K., 2008. Genetic tracing of the gustatory and trigeminal neural pathways originating from T1R3-expressing taste receptor cells and solitary chemoreceptor cells. *Mol. Cell. Neurosci.* 38, 505–517.
- Perez, C.A., Huang, L., Rong, M., Kozak, J.A., Preuss, A.K., Zhang, H., et al., 2002. A transient receptor potential channel expressed in taste receptor cells. *Nat. Neurosci.* 5, 1169–1176.
- Pronin, A.N., Tang, H., Connor, J., Keung, W., 2004. Identification of ligands for two human bitter T2R receptors. *Chem. Senses* 29, 583–593.
- Pumplin, D.W., Yu, C., Smith, D.V., 1997. Light and dark cells of rat vallate taste buds are morphologically distinct cell types. *J. Comp. Neurol.* 378, 389–410.
- Richter, T.A., Dvoryanchikov, G.A., Chaudhari, N., Roper, S.D., 2004a. Acid-sensitive two-pore domain potassium (K2P) channels in mouse taste buds. *J. Neurophysiol.* 92, 1928–1936.
- Richter, T.A., Dvoryanchikov, G.A., Roper, S.D., Chaudhari, N., 2004b. Acid-sensing ion channel-2 is not necessary for sour taste in mice. *J. Neurosci.* 24, 4088–4091.
- Romanov, R.A., Rogachevskaja, O.A., Bystrova, M.F., Jiang, P., Margolskee, R.F., Kolesnikov, S.S., 2007. Afferent neurotransmission mediated by hemichannels in mammalian taste cells. *EMBO J.* 26, 657–667.
- Roper, S.D., 1983. Regenerative impulses in taste cells. *Science* 220, 1311–1312.
- Roper, S.D., 2006. Cell communication in taste buds. *Cell. Mol. Life Sci.* 63, 1494–1500.
- Roper, S.D., 2007. Signal transduction and information processing in mammalian taste buds. *Pflügers Arch.* 454, 759–776.
- Royer, S.M., Kinnamon, J.C., 1991. HVEM serial-section analysis of rabbit foliate taste buds: I. Type III cells and their synapses. *J. Comp. Neurol.* 306, 49–72.
- Sainz, E., Korley, J.N., Battey, J.F., Sullivan, S.L., 2001. Identification of a novel member of the T1R family of putative taste receptors. *J. Neurochem.* 77, 896–903.
- Seta, Y., Toyoshima, K., 1995. Three-dimensional structure of the gustatory cell in the mouse fungiform taste buds: A computer-assisted reconstruction from serial ultrathin sections. *Anat. Embryol.* 191, 83–88.
- Shigemura, N., Islam, A.A., Sadamitsu, C., Yoshida, R., Yasumatsu, K., Ninomiya, Y., 2005. Expression of amiloride-sensitive epithelial sodium channels in mouse taste cells after chorda tympani nerve crush. *Chem. Senses* 30, 531–538.
- Shigemura, N., Ohkuri, T., Sadamitsu, C., Yasumatsu, K., Yoshida, R., Beauchamp, G.K., et al., 2008. Amiloride-sensitive NaCl taste responses are associated with genetic variation of ENaC alpha-subunit in mice. *Am. J. Physiol. Regul. Integr. Comp. Physiol.* 294, R66–R75.
- Smith, D.V., Travers, J.B., 1979. A metric for the breadth of tuning of gustatory neurons. *Chem. Senses Flav.* 4, 215–229.
- Spector, A.C., Guagliardo, N.A., St. John, S.J., 1996. Amiloride disrupts NaCl vs KCl discrimination performance: Implications for salt taste coding in rats. *J. Neurosci.* 16, 8115–8122.
- Stevens, D.R., Seifert, R., Bufe, B., Muller, F., Kremmer, E., Gauss, R., et al., 2001. Hyperpolarization-activated channels HCN1 and HCN4 mediate responses to sour stimuli. *Nature* 413, 631–635.
- Sugita, M., 2006. Taste perception and coding in the periphery. *Cell. Mol. Life Sci.* 63, 2000–2015.

- Takeda, M., Hoshino, T., 1975. Fine structure of taste buds in the rat. *Arch. Histol. Jpn.* 37, 395–413.
- Tamamaki, N., Yanagawa, Y., Tomioka, R., Miyazaki, J., Obata, K., Kaneko, T., 2003. Green fluorescent protein expression and colocalization with calretinin, parvalbumin, and somatostatin in the GAD67-GFP knock-in mouse. *J. Comp. Neurol.* 467, 60–79.
- Tomchik, S.M., Berg, S., Kim, J.W., Chaudhari, N., Roper, S.D., 2007. Breadth of tuning and taste coding in mammalian taste buds. *J. Neurosci.* 27, 10840–10848.
- Travers, J.B., Smith, D.V., 1979. Gustatory sensitivities in neurons of the hamster nucleus tractus solitarius. *Sens. Processes* 3, 1–6.
- Ugawa, S., Yamamoto, T., Ueda, T., Ishida, Y., Inagaki, A., Nishigaki, M., et al., 2003. Amiloride-insensitive currents of the acid-sensing ion channel-2a (ASIC2a)/ASIC2b heteromeric sour-taste receptor channel. *J. Neurosci.* 23, 3616–3622.
- Vandenbeuch, A., Kinnamon, S.C., 2009. Why do taste cells generate action potentials? *J. Biol.* 8, 42.
- Vandenbeuch, A., Clapp, T.R., Kinnamon, S.C., 2008. Amiloride-sensitive channels in type I fungiform taste cells in mouse. *BMC Neurosci.* 9, 1.
- Wong, G.T., Gannon, K.S., Margolskee, R.F., 1996. Transduction of bitter and sweet taste by gustducin. *Nature* 381, 796–800.
- Wong, G.T., Ruiz-Avila, L., Margolskee, R.F., 1999. Directing gene expression to gustducin-positive taste receptor cells. *J. Neurosci.* 19, 5802–5809.
- Yang, J., Roper, S.D., 1987. Dye-coupling in taste buds in the mudpuppy, *Necturus maculosus*. *J. Neurosci.* 7, 3561–3565.
- Yang, R., Crowley, H.H., Rock, M.E., Kinnamon, J.C., 2000a. Taste cells with synapses in rat circumvallate papillae display SNAP-25-like immunoreactivity. *J. Comp. Neurol.* 424, 205–215.
- Yang, R., Tabata, S., Crowley, H.H., Margolskee, R.F., Kinnamon, J.C., 2000b. Ultrastructural localization of gustducin immunoreactivity in microvilli of type II taste cells in the rat. *J. Comp. Neurol.* 425, 139–151.
- Yasumatsu, K., Katsukawa, H., Sasamoto, K., Ninomiya, Y., 2003. Recovery of amiloride-sensitive neural coding during regeneration of the gustatory nerve: Behavioral–neural correlation of salt taste discrimination. *J. Neurosci.* 23, 4362–4368.
- Yasumatsu, K., Kusuhara, Y., Shigemura, N., Ninomiya, Y., 2007. Recovery of two independent sweet taste systems during regeneration of the mouse chorda tympani nerve after nerve crush. *Eur. J. Neurosci.* 26, 1521–1529.
- Yee, C.L., Yang, R., Bottger, B., Finger, T.E., Kinnamon, J.C., 2001. “Type III” cells of rat taste buds: Immunohistochemical and ultrastructural studies of neuron-specific enolase, protein gene product 9.5, and serotonin. *J. Comp. Neurol.* 440, 97–108.
- Yoshida, R., Sanematsu, K., Shigemura, N., Yasumatsu, K., Ninomiya, Y., 2005. Taste receptor cells responding with action potentials to taste stimuli and their molecular expression of taste related genes. *Chem. Senses* 30, i19–i20.
- Yoshida, R., Shigemura, N., Sanematsu, K., Yasumatsu, K., Ishizuka, S., Ninomiya, Y., 2006a. Taste responsiveness of fungiform taste cells with action potentials. *J. Neurophysiol.* 96, 3088–3095.
- Yoshida, R., Yasumatsu, K., Shigemura, N., Ninomiya, Y., 2006b. Coding channels for taste perception: Information transmission from taste cells to gustatory nerve fibers. *Arch. Histol. Cytol.* 69, 233–242.
- Yoshida, R., Horio, N., Murata, Y., Yasumatsu, K., Shigemura, N., Ninomiya, Y., 2009a. NaCl responsive taste cells in the mouse fungiform taste buds. *Neuroscience* 159, 795–803.
- Yoshida, R., Miyauchi, A., Yasuo, T., Jyotaki, M., Murata, Y., Yasumatsu, K., et al., 2009b. Discrimination of taste qualities among mouse fungiform taste bud cells. *J. Physiol.* 587, 4425–4439.

- Yoshii, K., 2005. Gap junctions among taste bud cells in mouse fungiform papillae. *Chem. Senses* 30, i35–i36.
- Zhang, Y., Hoon, M.A., Chandrashekar, J., Mueller, K.L., Cook, B., Wu, D., et al., 2003. Coding of sweet, bitter, and umami tastes: Different receptor cells sharing similar signaling pathways. *Cell* 112, 293–301.
- Zhang, Z., Zhao, Z., Margolskee, R., Liman, E., 2007. The transduction channel TRPM5 is gated by intracellular calcium in taste cells. *J. Neurosci.* 27, 5777–5786.
- Zhao, G.Q., Zhang, Y., Hoon, M.A., Chandrashekar, J., Erlenbach, I., Ryba, N.J., Zuker, C.S., 2003. The receptors for mammalian sweet and umami taste. *Cell* 115, 255–266.

# NEW INSIGHTS INTO THE REGULATION OF ION CHANNELS BY INTEGRINS

Andrea Becchetti,\* Serena Pillozzi,<sup>†</sup> Raffaella Morini,\*  
Elisa Nesti,<sup>†</sup> and Annarosa Arcangeli<sup>†</sup>

## Contents

1. Introduction	136
2. Main Structural Features of Integrins and Ion Channels	137
2.1. Integrin receptors	137
2.2. Ion channels	139
3. An Outline of Integrin Signaling	143
4. Integrins and Ion Channels in Normal and Neoplastic Hematopoietic Cells	147
4.1. Integrins	147
4.2. Ion channels	154
4.3. Regulation through formation of molecular complexes and impact on downstream signaling	160
4.4. Implications for oncology	162
5. Integrins and Ion Channels in Cell Migration	163
5.1. Potassium channels	164
5.2. Nicotinic acetylcholine receptors in epithelia	165
6. Integrins and Ion Channels in the Nervous System	166
6.1. Integrin expression in the central nervous system	166
6.2. Integrin-channel interplay in mature neuronal circuits: Control of synaptic function	167
6.3. Integrin-channel interplay in developing neuronal circuits	170
6.4. Integrins, ion channels, and microglia	175
7. Concluding Remarks	176
Acknowledgments	177
References	178

\* Department of Biotechnology and Biosciences, University of Milano-Bicocca, Milano, Italy

<sup>†</sup> Department of Experimental Pathology and Oncology, University of Firenze, Firenze, Italy



## Abstract

By controlling cell adhesion to the extracellular matrix, integrin receptors regulate processes as diverse as cell migration, proliferation, differentiation, apoptosis, and synaptic stability. Because the underlying mechanisms are generally accompanied by changes in transmembrane ion flow, a complex interplay occurs between integrins, ion channels, and other membrane transporters. This reciprocal interaction regulates bidirectional signal transduction across the cell surface and may take place at all levels of control, from transcription to direct conformational coupling. In particular, it is becoming increasingly clear that integrin receptors form macromolecular complexes with ion channels. Besides contributing to the membrane localization of the channel protein, the integrin/channel complex can regulate a variety of downstream signaling pathways, centered on regulatory proteins like tyrosine kinases and small GTPases. In turn, the channel protein usually controls integrin activation and expression. We review some recent advances in the field, with special emphasis on hematology and neuroscience. Some oncological implications are also discussed.

*Key Words:* Cell adhesion, Extracellular matrix, hERG, Leukemia, Lymphoma, Migration, Synaptic plasticity. © 2010 Elsevier Inc.

## 1. INTRODUCTION

The study of the manifold regulatory interactions between ion channels and integrin receptors is a blossoming subfield of cell biology. A Medline search for “integrin” and “ion channels” in the mid-1990s would have retrieved no more than a dozen of papers, whereas now the number of relevant papers is in the order of hundreds and is steadily increasing. The sheer volume of work is not the major difficulty arising when one attempts to present a comprehensive review of the field, however. An even greater obstacle is constituted by the widespread biological implications of these processes, which makes it hard to unify the underlying mechanisms within a broader physiological framework. A few examples will give a flavor of the problem. Cross talk between integrins and ion channels is implicated in the immune response, for example, in lymphocyte activation. It contributes to control motility and migration/pathfinding of fibroblasts, epithelial cells, and most probably neurons and neoplastic cells, at least in certain developmental stages. It also modulates synaptic plasticity and participates in the physiology of smooth muscle and cardiac myocytes (Arcangeli and Becchetti, 2006; Davis et al., 2002; Gall and Lynch, 2004). As we illustrated previously, recent investigations about the interplay between ion transport mechanisms and the integrin-mediated adhesion machinery has revealed a

complex signaling network, with some interesting peculiar features. The membrane proteins involved in these processes can communicate through diffusible messengers, alterations of ion concentration and membrane potential, phosphorylation cascades, direct physical interaction in macromolecular complexes, and indirect transcriptional regulation (Arcangeli and Becchetti, 2006).

The present review aims at updating the reader about some current trends in the field. We have generally (although not exclusively) given privilege to hematology and neuroscience to remain close to our competences and to avoid superposition with other recent treatments (Arcangeli and Becchetti, 2006; Colden-Stanfield, 2008; Davis et al., 2002; Gui et al., 2008). Hematology, in particular, is one of the fields in which these studies have been pursued more thoroughly and for longer time, but comprehensive reviews are lacking. Conversely, the neuroscientific implications have begun to be addressed only recently and we believe these studies are opening a new fruitful field. Nevertheless, we also briefly illustrate some interesting recent developments such as the role of the above mechanisms in epithelial physiology.

The paper is organized as follows. Section 2 provides a quick reference to the main structural and functional features of integrin receptors and some relevant ion channel types. This is followed by a summary of integrin-dependent signaling (Section 3). Section 4 is a thorough survey of the functional implications of integrin-channel cross talk in hematopoietic cells and tumors, which present interesting oncological perspectives. Subsequently, we illustrate what is known about the interplay between integrin receptors and ion channels in cell migration, because of its widespread involvement in a variety of processes, ranging from wound healing to neuronal development. Section 6 is mostly devoted to the nervous system and the last section provides a link between the central nervous system (CNS) and immune system, by describing recent observations about the implications of integrins in the physiology of neuropathic pain and the role of microglia.



## **2. MAIN STRUCTURAL FEATURES OF INTEGRINS AND ION CHANNELS**

### **2.1. Integrin receptors**

Integrin receptors are transmembrane proteins formed by noncovalent association of  $\alpha$  and  $\beta$  subunits. To date, 18  $\alpha$  and 8  $\beta$  subunits are known in mammals. All subunits are type I transmembrane glycoproteins with a short cytoplasmic tail (20–70 amino acids), a membrane-spanning helix and a large multidomain extracellular portion (Hynes, 2002). The  $\beta_4$  subunit is an exception because its cytoplasmic domain contains around 1000 amino

acids (dePereda et al., 1999). Two classes of integrins are distinguished, depending on whether their  $\alpha$  subunit presents an extracellular von Willebrand factor type A. This latter is named  $\alpha A$  or  $\alpha I$  and is homologous to a GTPase domain in which the catalytic site is substituted with a metal ion-dependent adhesion site (MIDAS). MIDAS enables  $\alpha A$  to regulate the dependence of cell adhesion on divalent cations (Michishita et al., 1993).

Integrin subunits can combine to form at least 24 functional heterodimers, each of which binds a specific array of extracellular matrix (ECM) proteins, or cell adhesion molecules (CAMs) that thus act as “counter-receptors”. The conformation of integrins, and thus binding to ECM, is modulated by interaction of the cytoplasmic domain with intracellular signaling and cytoskeletal proteins. Conversely, cell adhesion stimulates a set of scaffolding, cytoskeletal, and regulatory proteins to associate to the cytoplasmic domain, leading to the assembly of the focal adhesion (FA) complexes (Liddington and Ginsberg, 2002; Miranti and Brugge, 2002). Typically, integrins associate with the actin cytoskeleton (except  $\alpha_5\beta_4$ , which preferentially couples to intermediate filaments). The process is often mediated by talin, an intracellular protein which contains specific binding domains for the integrin cytoplasmic tail, the filamentous (F) actin, as well as other proteins that regulate the FA, like FAK (focal adhesion kinase) and phosphatidylinositol 4-phosphate-5-kinase type I $\gamma$  (PIPKI $\gamma$ 90) (Critchley and Gingras, 2008; Wegener and Campbell, 2008). However, the cytoplasmic tails of both  $\alpha$  and  $\beta$  subunits can bind to a variety of other intracellular proteins, such as paxillin,  $\alpha$ -actinin, filamin, melusin, tensin, integrin-linked kinase (ILK), just to name a few (Critchley, 2000; Wegener and Campbell, 2008). As a working hypothesis, when studying the association with ion channels, it is useful to assume that the integrin  $\beta$ -tail is the domain involved (Cherubini et al., 2005). The  $\beta$ -tail contains many protein binding sites, for example, several NPxY sequences (typical targets of phosphotyrosine-binding domains). Moreover, its disordered structure makes it capable of extending over about 8 nm, despite of its shortness (Dunker et al., 2005). Transmembrane segments are thought to be  $\alpha$ -helices and their conformational changes are crucial for transmembrane signal transduction. For structural details we refer to recent literature (Lau et al., 2008a,b; Wegener and Campbell, 2008). From a functional standpoint, experiments using (i) cryomicroscopy, (ii) single particle reconstruction of solubilized  $\alpha_{Ib}/\beta_3$  integrins, (iii) the substituted cysteine accessibility method applied to  $\alpha_{Ib}/\beta_3$ , and (iv) FRET (Förster Resonance Energy Transfer) applied to  $\alpha_1\beta_2$  suggest that the transmembrane domains of the two subunits are bonded when inactive. “Inside-out” activation requires transmembrane domain separation, whereas this does not seem to be necessary for “outside-in” activation (Kim et al., 2003; Luo et al., 2004). Inside-out transduction generally requires the integrin receptor to interact with talin. However, the precise mechanism of activation is still speculative,

because no high-resolution structure is available for the intracellular tail and the transmembrane segment of any subunit. Much more detailed information is available for the extracellular portion of the integrin receptor, because of the thorough studies carried out with NMR and X-ray crystallographic methods (Xiong et al., 2001, 2002). Once again, full structural details about the extracellular domains and the conformational changes that occur on integrin activation are outside the scope of the present review (Arnaout et al., 2005, 2007). We merely remind that the MIDAS domain, which is normally occupied by a divalent cation, rearranges during the transition of the extracellular domain to the “open” conformation, that is, the one with high affinity for the ECM. In this state, MIDAS can bind an acidic residue on the ECM protein, which offers the sixth coordination site for the divalent cations (occupied by water, in the basal state). The  $\beta$  subunits also contain a  $\beta A$  domain, structurally similar to  $\alpha A$ . Its MIDAS is not occupied by a metal cation, but  $\text{Ca}^{2+}$  is typically bound to an adjacent (“ADMIDAS”) site. The ECM proteins that bind integrins usually contain an RGD (Arg-Gly-Asp) sequence which mediates binding. RGD inserts itself between the  $\beta A$  domain and the “propeller” N-terminal domain of the  $\alpha$  subunit. The Asp residue of RGD can bind a MIDAS domain occupied by a metal ion, as it does when it binds  $\alpha A$ .

## 2.2. Ion channels

These are integral membrane proteins whose conformation can shift between a closed and an open state. In the latter, a conductive pathway more or less specific for different ions connects the extra- and intracellular compartments. Channel opening (activation) can depend on membrane potential (voltage-gated channels), intra- or extracellular ligand binding (ligand-gated channels), or mechanical strain (mechanically gated channels), which calls into play channel interaction with the cytoskeleton. In the following sections, we summarize the main features of the channel types that will be mentioned subsequently.

### 2.2.1. Voltage-gated cation channels

Voltage-gated cation channels (VGCs) belong to a large molecular family that comprises  $\text{K}^+$ ,  $\text{Na}^+$ , and  $\text{Ca}^{2+}$  channels. The  $\text{K}^+$  channel types are named  $\text{K}_v1$ – $\text{K}_v12$ , with subtypes named  $\text{K}_v1.1$ , etc. (Gutman et al., 2005). They are formed by four  $\alpha$  subunits which surround a central pore. Both the C- and the N-terminus are intracellular. Each subunit contains six transmembrane domains (S1–S6). S4 is rich of basic amino acid residues, whose side chains are potentially positively charged and are thought to be the main determinant of the voltage sensitivity (Börjesson and Elinder, 2008). The stretch of residues between S5 and S6 faces the extracellular side of the channel pore and is named P(pore)-loop or H5 domain. It provides an

important contribution to ion selectivity (e.g., Yool and Schwarz, 1991). Other conductive properties depend on ion interaction with the pore. Great insight about  $K^+$  channel permeation has come by the first X-ray resolved three-dimensional structure, obtained by MacKinnon's research group for the  $K^+$  channel of the bacterium *Streptomyces lividans* (Doyle et al., 1998). Following this lead, high-resolution structures for other ion channels are being determined (e.g., Jiang et al., 2002). The intracellular domains contain consensus sequences for phosphorylation and the N-terminus determines interaction with regulatory proteins and other subunits. The voltage-gated  $Na^+$  ( $Na_v$ ) and  $Ca^{2+}$  ( $Ca_v$ ) channels share a similar structural pattern, except that the four independent subunits observed in the  $K^+$  channels are substituted by four homologous repeated domains belonging to the same polypeptide. The main function of  $Na_v$  channels is usually initiating action potentials on membrane depolarization, whereas  $Ca_v$  channels control  $Ca^{2+}$  entry during action potentials, exocytosis, muscle contraction, and many other physiological processes. In VGCs, accessory ( $\beta$ ,  $\gamma$ ) subunits may regulate the biophysical channel properties, insertion into the plasma membrane, and interaction with other proteins (Catterall, 1992, 2000).

### 2.2.2. Inward rectifier $K^+$ channels

The inward rectifying  $K^+$  ( $K_{IR}$ ) channels are related to the VGC family. They are formed by four subunits, each containing only two transmembrane domains (M1 and M2) homologous, respectively, to S5 and S6 and linked by a P-loop (Nichols and Lopatin, 1997). The term inward rectification refers to the fact that these channels preferentially conduct inward currents (i.e.,  $K^+$  flowing into the cytosol), because outward currents are blocked by intracellular  $Mg^{2+}$  and organic cations, particularly polyamines. Among these, those possessing more positive charges, like spermine and spermidine, are more efficient (Lu, 2004).  $K_{IR}$  channels contribute to regulate the cellular excitability in neurons and muscle, the cardiac action potential repolarization,  $K^+$  buffering by astrocytes (Kofuji and Newman, 2004), and a variety of other functions in both developing and mature tissues.

### 2.2.3. Transient receptor potential (TRP) channels

These are homo- or heterotetramers of subunits related to the VGC superfamily, with six transmembrane domains, a P-loop, and cytoplasmic N- and C-terminus. They are generally permeable to cations, but the permeability ratios between  $Ca^{2+}$  and monovalent cations vary considerably between subtypes. The channel activation mechanisms are also very diverse and make these channels important sensors of local environment signals. Basing on sequence homology, six mammalian subfamilies have been described: TRPA, TRPC, TRPM, TRPV, TRPP, and TRPML (Venkatachalam and Montell, 2007). TRP channels are widely distributed

in mammalian tissues and are implicated in different functions and dysfunctions that are presently the object of intense study (Nilius et al., 2007). TRP channels are also widely expressed in the nervous system. Apart from their established role as peripheral temperature sensors, growing evidence attributes to them important developmental functions. In particular,  $\text{Ca}^{2+}$  influx through TRP channels provides an important contribution to regulate axon guidance and neuronal survival in response to paracrine signals (Talavera et al., 2008).

#### 2.2.4. Ion channels gated by neurotransmitters

Neurotransmitters can activate ion channels (*ionotropic receptors*) or receptors that activate intracellular signaling pathways (*metabotropic receptors*). Recent work points to functional relations between integrin receptors and ionotropic receptors, particularly neuronal nicotinic receptors (nAChRs), glutamate receptors (GluRs), and purinergic receptors, which we briefly describe.

**2.2.4.1. Neuronal nicotinic acetylcholine receptors** The nAChR is a pentameric channel originally found to be expressed on the postsynaptic membranes of the neuromuscular junction. Twelve neuronal subunits are presently known:  $\alpha_2$ – $\alpha_{10}$  and  $\beta_2$ – $\beta_4$ ;  $\alpha_9$  and  $\alpha_{10}$  are mainly expressed in the cochlea whereas the role of the other subunits in the brain is matter of debate (Gotti and Clementi, 2004). Interestingly, growing evidence shows that “neuronal” nAChR subunits are frequently expressed in nonneuronal tissue and cancer cells (Schuller, 2009; Wessler and Kirkpatrick, 2008). In the CNS, both homo- and heteropentameric receptors are known to be expressed. The former are probably mostly  $(\alpha_7)_5$ , whereas the spectrum of heteropentamers is much wider and differs between species. A common form, at least in rodents’ brain, is  $(\alpha_4)_2(\beta_2)_3$  while in the peripheral nervous system  $\alpha_3$  and  $\beta_4$  subunits are widespread (Gotti and Clementi, 2004). Heteromeric receptors fully activate when two (or three, depending on subunit stoichiometry) ACh molecules bind to the specific extracellular pockets, which are mostly (but not exclusively) formed by residues belonging to the  $\alpha$  subunits. Five ligand molecules can contribute to the activation of homomeric nAChRs. All neuronal nAChRs are permeable to  $\text{Na}^+$ ,  $\text{K}^+$ , and  $\text{Ca}^{2+}$ . The permeability to the latter is particularly pronounced in  $\alpha_7$ -containing receptors. In peripheral ganglia, nAChRs mediate postsynaptic transmission. In the brain, pre-, post-, and nonsynaptic nAChR expression is observed in different regions and cells. In general, cholinergic transmission in the brain controls the level of arousal with implications for learning and for the transitions between sleep and waking phases (Dani and Bertrand, 2007; Lendvai and Vizi, 2008). The functional roles in nonneuronal tissue are still debated. The neuronal nAChRs present inward rectification produced by mechanisms similar to those observed in  $\text{K}_{\text{IR}}$  channels,

that is, voltage-dependent block caused by intracellular organic cations, such as polyamines (Haghighi and Cooper, 1998).

**2.2.4.2. Iontropic glutamate receptors** Glutamate is the main excitatory transmitter in the CNS. Iontropic GluRs are also expressed in nonexcitable cells, like astrocytes, lymphocytes, and endocrine cells, in which their roles are still unclear (Nedergaard et al., 2002). Three families of ionotropic GluRs have been identified to date, which can be distinguished by relatively specific agonists: *N*-methyl-D-aspartate (NMDA),  $\alpha$ -amino-3-hydroxy-5-methyl-4-isoxazole propionic acid (AMPA), and kainate (KA) (Mayer, 2005; Mayer and Armstrong, 2004). Channels activated by AMPA and KA are also named non-NMDA receptors, which quickly activate in the presence of glutamate, and then desensitize within about 30 ms. In most central neurons, non-NMDA receptors produce the early component of excitatory postsynaptic currents. They are usually permeable to  $\text{Na}^+$  and  $\text{K}^+$ , but not  $\text{Ca}^{2+}$ . The NMDA receptors require extracellular glycine for opening in the presence of the agonist. Because their kinetics is slower than that of non-NMDA receptors, they determine the slow component of the excitatory postsynaptic currents. At negative  $V_m$ , NMDA GluRs are inhibited by extracellular  $\text{Mg}^{2+}$ . Hence, when glutamate is released onto a resting neuron, these receptors scarcely activate, unless the membrane is sufficiently depolarized by other depolarizing channel types. The NMDA receptors are permeable to  $\text{Ca}^{2+}$  as well as to  $\text{Na}^+$  and  $\text{K}^+$ . The functional properties of NMDA receptors bring about two important physiological consequences.

First, when glutamate release is strong enough to produce sufficient postsynaptic depolarization, significant  $\text{Ca}^{2+}$  influx is caused by NMDA receptor activation. The ensuing stimulation of intracellular pathways produces long-lasting synaptic remodeling, a process thought to be implicated in learning and memory. A major example is long-term potentiation (LTP), which was first observed in the hippocampus (Bliss and Lomø, 1973) and subsequently found in other cerebral regions. Brief high-frequency trains of stimuli on any of the principal fiber pathways within the hippocampus (i.e., either the perforant, or the mossy fiber, or the Schaffer collateral pathway) increases the amplitude of the excitatory postsynaptic potentials in the corresponding target neurons. Potentiation may last for weeks and depends on a  $\text{Ca}^{2+}$ -dependent enhancement of GluR function and expression. NMDA receptors have a particularly important role in the early phases of LTP in the Schaffer collateral and perforant pathways. In these, LTP is associative in the sense that both pre- and postsynaptic cells must be active to produce significant depolarization in pre- and postsynaptic terminals. Sufficient postsynaptic depolarization relieves the voltage-dependent block of extracellular  $\text{Mg}^{2+}$  on NMDA receptors, leading to significant  $\text{Ca}^{2+}$  influx, which stimulates the long-term changes in synaptic efficacy (Kandel et al., 2000).

Second, abnormal tonic levels of extracellular glutamate induced by hyperexcitation or other reasons may have neurotoxic effects. A steady  $\text{Ca}^{2+}$  influx damages the cells through multiple mechanisms that converge on production of reactive oxygen species, altered mitochondrial function, and activation of the caspase and proteolytic cascades that lead to apoptosis. The increased  $\text{Na}^+$  entry caused by overactivation of non-NMDA receptors can also be harmful because of altered control of cell volume (Mattson and Bazan, 2006).

**2.2.4.3. Ionotropic purinergic receptors**  $\text{P}_2$ -type purinergic receptors are subdivided into ionotropic  $\text{P}_{2X}$  receptors and metabotropic  $\text{P}_{2Y}$  receptors, which are structurally unrelated. Seven subunits of  $\text{P}_{2X}$  receptors have been identified ( $\text{P}_{2X1}$ – $\text{P}_{2X7}$ ), which can form homo- or heterotrimeric channels activated by extracellular ligands, typically ATP. No subunit-specific antagonists are known to date.  $\text{P}_{2X}$  receptors have intracellular N- and C-terminus and two transmembrane domains connected by a long extracellular loop and involved in subunit association. The extracellular domains form the ligand-binding site and contain modulatory sites. The C-terminal portion is the most variable, ranging from a length of 27 residues for  $\text{P}_{2X6}$  to 239 residues for  $\text{P}_{2X7}$ , and is thought to control the rate of channel desensitization and receptor trafficking. Both the N- and C-terminus are targets for posttranscriptional and translational regulation and mediate protein–protein interaction. The open channel is permeable to  $\text{Na}^+$  and  $\text{K}^+$  and presents a relatively high permeability to  $\text{Ca}^{2+}$ . Besides their roles in the adult and developing nervous system,  $\text{P}_{2X}$  receptors exert physiological functions in the respiratory, gastrointestinal, cardiovascular, genitourinary, and other systems (Illes and Alexandre, 2004; Köles et al., 2007; North, 2002).

### 3. AN OUTLINE OF INTEGRIN SIGNALING

Integrins are enzymatically inactive receptors that link the ECM to intracellular components to elicit signal transduction. This process (“outside-in signaling”) is required for polymerization of the actin cytoskeleton during cell adhesion and controls downstream functions such as cell migration, proliferation, survival, and differentiation. To the best of our knowledge, the first evidence for an ECM-mediated intracellular signaling was provided in the late 1980s. In quiescent fibroblast or in monocytes, gene transcription was found to be induced upon interaction with the ECM (Dike and Farmer, 1988; Eierman et al., 1989). Presently, the list of papers describing the many facets of integrin-mediated signaling pathways is immense. Integrins seem to be linked to almost all of the known signaling pathways, including induction of cytosolic kinases, stimulation of



the phosphoinositide metabolism, activation of Ras/MAPK and PKC pathways, and regulation of Rho GTPases (Defilippi et al., 2006; Giancotti and Tarone, 2003; Miranti and Brugge, 2002; Schwartz and Ginsberg, 2002). These signals greatly overlap and are properly integrated with those activated by growth factor and cytokine receptors, which makes physiological sense, because cells must integrate multiple stimuli from ECM, growth factors, hormones, and mechanical stress to organize appropriate responses.

As mentioned above, upon binding to the matrix, integrins undergo a conformational change and interact with signaling proteins to convey information to other cytosolic targets and to the nucleus. Protein tyrosine phosphorylation is a primary response to integrin stimulation and a preferential way to propagate signals throughout the cell. In particular, FAK, the Src family kinases (SFKs), and ILK are pivotal elements in transducing integrin engagement into cell signaling.

FAK is an evolutionary conserved scaffold protein that can bind cytoskeletal and signaling molecules, thus triggering several distinct pathways. On integrin activation, FAK undergoes phosphorylation on Tyr397, which induces the formation of a high-affinity interaction site for the SH2 domain of the SFKs, the p85 regulatory subunit of the phosphatidylinositol 3-kinase (PI-3K) and phospholipase C- $\gamma$ . The subsequent phosphorylation of Tyr925 promotes FAK association with the Grb2 adaptor, which provides a link to MAPK (Parsons, 2003).

The SFK family comprises several members, all sharing similar biochemical and functional features. In the inactive conformation, the molecule is "closed" because of phosphorylation of its Tyr530 residue. On stimulation, this amino acid residue is dephosphorylated, which opens up the protein and makes it available for autophosphorylation in the kinase domain (Tyr 419) and interaction with downstream effectors (Yeatman, 2004). The balance between phosphorylation and dephosphorylation of Tyr 530 depends on the relative activity of the Csk kinase and several protein phosphatases (PTPases) like PTP $\alpha$  and SHP1/2. The major substrate of v-Src and v-Crk is p130Cas (Crk-associated substrate), a scaffold protein capable of associating with multiple signaling partners. In fact, upon integrin-mediated adhesion, FAK, Src, and p130Cas form a multimeric signaling complex crucially involved in organizing FAs and actin cytoskeleton and generating downstream signaling, which ultimately regulates complex processes such as motility and invasion. During migration, lamellipodia and filopodia protrude from the cell leading edge and form new dynamic adhesion sites, which rapidly form and disassemble. Tyrosine phosphorylation is required for FA turnover and FAK, Src, and p130Cas are all necessary for efficient disassembly of FAs (Ridley et al., 2003). For example, aberrant activation of Src kinases, as well as transformation by oncogenic v-Src, leads to FA disassembly and loss of cell spreading. An additional mechanism by

which Src and FAK control FA organization and cell motility is through the regulation of the small GTPase Rho. Integrin activation transiently decreases the RhoA activity, which relieves the contractile forces at the sites of integrin engagement. This results in FA disruption and promotes lamellipodial extension during cell migration (BurrIDGE and Wennerberg, 2004).

Prosurvival signals emanating from the ECM also proceed via FAK and Src to activate the small GTPases Rho and Rac, as well as JNK and Erk1/2 MAPK (Defilippi et al., 2006). Another important pathway, which can transduce the prosurvival signals triggered by integrins, is centered on ILK and converges onto the phosphorylation of Akt. ILK is a serine/threonine protein kinase discovered in 1996 in a yeast two-hybrid screen, using the cytoplasmic tail of  $\beta_1$  integrin as bait (Hannigan et al., 1996). Subsequently, it turned out to be expressed in several cell types, with a preferential location in FAs. ILK has a tripartite structure that reflects its multifunctionality. Its N-terminal domain contains four ankyrin repeats and binds to several intracellular proteins; the central pleckstrin homology (PH)-like domain binds to phosphoinositides; the C-terminal domain has kinase function but also interacts with integrins and other proteins of the FA complex, thus providing connection with the actin cytoskeleton (McDonald et al., 2008). ILK is central to the regulation of signal transduction and functions as a hub around which several signaling pathways are coordinated. It should be noted that the role of ILK in cell signaling has been studied in transformed or tumorigenic cells, or both. Therefore, caution should be exerted in assuming that the pathways controlled by ILK in nontransformed cells are the same as those identified in cancer cells. ILK activity is stimulated by integrins and soluble mediators, while its expression is upregulated by hypoxia (Lee et al., 2006). When activated, ILK regulates different downstream effectors, and particularly the phosphorylation of Akt (at Ser473) and of glycogen synthase kinase 3 (GSK3) (Delcomenne et al., 1998; McDonald et al., 2008). By promoting Akt phosphorylation, ILK stimulates the signals that regulate cell survival, including the pathways that involve caspase activation and stimulation of nuclear factor  $\kappa$ B (NF- $\kappa$ B) (Hannigan et al., 2005; Legate et al., 2006). The ILK-centered prosurvival signals exert a predominant role in the complex interplay between hematopoietic precursor cells (HPCs) and the bone marrow (BM) microenvironment. As further discussed in Section 4, the BM stroma protects the HPCs and ultimately controls the whole hematopoietic process (Walenda et al., 2009). This local environmental protection is also relevant in the chemoresistance induced by the BM stroma on leukemic blasts (Konopleva et al., 2002). It is brought about through a complex interplay between different components of the ECM, integrin receptors, the stroma-derived factor SDF-1 $\alpha$ , and its receptor CXCR4. Both CXCR4 and integrin signaling are implicated in adhesion and survival, and hence chemoresistance, of leukemias. According

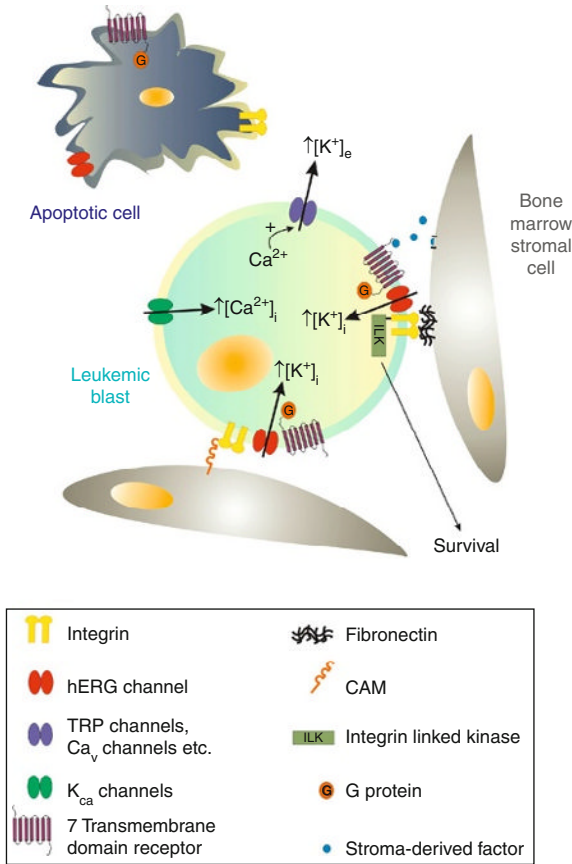


**Figure 5.1** Blasts adhesion to the BM stroma: integrin-dependent binding. The adhesion of BM stroma to leukemic blasts, by the binding between integrins and CAM or fibronectin molecules, confers protection to apoptosis and contributes to neoplastic cell proliferation. This integrin-dependent mechanism involves different components as channels and receptors. Integrins can interact with ion channels to form a bimolecular complex; the following association with either a growth factor or a chemokine receptor creates a supramolecular complex which can activate intracellular signaling pathways. For example, the interaction with a seven-transmembrane receptor, like CXCR4, in the presence of stroma-derived factors can produce ILK activation which promotes survival and confers chemoresistance to leukemia cells. Other channels are involved in malignant transformation (TRP, K<sub>Ca</sub> channels, etc.). CAM, cell–cell adhesion molecule; ILK, integrin-linked kinase; BM, bone marrow.

to the model proposed by Jin et al. (2008) in chronic myelogenous leukemias (CMLs), interaction between SDF1  $\alpha$  and CXCR4 in the BM microenvironment could trigger integrin engagement and activation of ILK, which would further promote survival of leukemia cells (Fig. 5.1).

This model introduces us to another aspect of integrin signaling. In addition to the canonical integrin-triggered pathways described above, the growth factor receptors, particularly receptor tyrosine kinases (RPTKs) and cytokine receptors, are integrin partners in assembling the transduction machinery required for proliferation, survival, and migration. Integrins stimulate direct phosphorylation and partial activation of several RPTKs, even in the absence of any growth factor ligand. In the case of the EGF receptor (EGFR), integrin-dependent activation leads to phosphorylation of EGFR on a specific subset of tyrosine residues, only partially overlapping to those phosphorylated by EGF. Consistently, the integrin-dependent EGFR activation induces cell survival as well as lamellipodia formation, whereas is not sufficient for cell migration (Defilippi et al., 2006).

## 4. INTEGRINS AND ION CHANNELS IN NORMAL AND NEOPLASTIC HEMATOPOIETIC CELLS

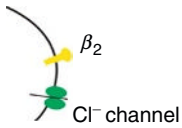
### 4.1. Integrins

BM is a very peculiar microenvironment where both hematopoietic and nonhematopoietic (stromal) cells cooperate to sustain one of the most active homeostatic processes of living bodies, hematopoiesis. In one day, this process can replenish more than  $7 \times 10^9$  blood cells (leukocytes, erythrocytes, and platelets) per kg of body weight. The BM hematopoietic cells comprise hematopoietic stem cells (HSCs), which undergo self-renewal in selected areas of the BM, the HSC niches, and HPC, with more restricted lineage potential (Table 5.1). The BM stroma is constituted by both stromal cells (fibroblasts, endothelial cells, macrophages, osteoblasts) and ECM proteins. Besides providing structural support, it strongly contributes to sustain hematopoiesis through signals triggered by adhesion-dependent and soluble factors. HSC and HPC are mostly sessile within the BM but become able to migrate between the hematopoietic tissues during fetal development. They also retain capacity to circulate in the peripheral blood (PB) during the adult life, although at barely detectable levels. In this dynamic scenario, integrins exert a pivotal role by mediating most of the functional interactions between hematopoietic cells and the BM microenvironment (Soligo et al., 1990; Voura et al., 1997). The regulated expression of specific integrin subunits as well as their localization in selected areas of the BM confirm that these molecules have different regulatory roles in hematopoiesis (Soligo et al., 1990).

#### 4.1.1. Hematopoietic stem cells and progenitors

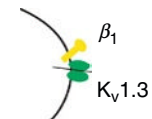
Few data are available regarding the integrin expression profile in HSCs, except that the  $\beta_1$  integrin subunit is expressed at high levels in quiescent HSCs and mediates their adhesion in the HSC niches (Arai et al., 2004). It is

**Table 5.1** Integrins and ion channels in normal hematopoietic cells

Cell type (phenotype)	Integrin	Function	Ion channel (iuphar)	Function	Interplay integrin/ ion channel
HSC (Lin <sup>-</sup> CD34 <sup>+</sup> CD133 <sup>+</sup> CD38 <sup>-</sup> )	$\beta_1$	Adhesion to BM			
	$\beta_3$	Quiescence			
	$\alpha_v\beta_3$	Adhesion to osteoblasts			
	$\alpha_2$	Capacity for long-term hemopoiesis			
	$\alpha_{11b}\beta_3$	Hemopoietic development			
HPC (Lin <sup>-</sup> CD34 <sup>+</sup> )	$\alpha_4\beta_1^I$	Adhesion to BM; migration; exit to PB; control of cell cycle	K <sub>IR</sub> 4.3	Generation of committed progenitors	
	$\alpha_5\beta_1^{II}$	Adhesion to BM	K <sub>IR</sub> 1.1	Generation of committed progenitors	
	$\alpha_9\beta_1$	Release in and from the BM niche	K <sub>v</sub> 11.1 <sup>a</sup>	Proliferation	
	$\beta_2$ $\beta_3$				
Neutrophils	$\alpha_4\beta_1$	Adhesion to VCAM-1; migration; extravasation from circulation to sites of injury or infection	TRPC6	Migration	

Macrophage  
Lymphocytes  
T

$\alpha_M\beta_2^{III}$	Adhesion to ICAM-1-2	TRPM2	Cation influx
$\alpha_L\beta_2^{IV}$	Adhesion to ICAM-1-5	TRPV1,2,5,6	Store operated $Ca^{2+}$ entry
$\alpha_X\beta_2$	Adhesion to fibrinogen	BK	Antimicrobial activity
$\beta_2$	Triggering of $Cl^-$ efflux; migration; recruitment to inflammatory sites	$Cl^-$ -SAC	Cell volume homeostasis; chemotaxis; shape change; migration
		CaCCs $ClC_{1-5}$ $K_{IR}^b$	
$\alpha_{1-6}\beta_1$	Migration; antigen presentation; TCR signaling; cross of vascular endothelium; formation of the p-SMAC at the IS	CRAC	T cell activation; regulation of the signaling events triggered on antigen presentation
$\alpha_M\beta_2^{III}$		$K_v1.3$	Clustering of associated proteins at the IS
$\alpha_L\beta_2$ $\alpha_X\beta_2$		$K_{Ca}3.1^c$ Orai1	Store-operated $Ca^{2+}$ influx; proliferation; cytokine production.



(continued)

**Table 5.1** (continued)

Cell type (phenotype)	Integrin	Function	Ion channel (iuphar)	Function	Interplay integrin/ ion channel
B	$\alpha_D\beta_2$		TRPM7	Cell growth	
	$\alpha_4\beta_7$		Cl(swell)	Proliferation	
	$\alpha_E\beta_7$		$I_{ir}$	$Ca^{2+}$ influx	
			$I_{dr}$	$Ca^{2+}$ influx	
	$\alpha_4\beta_1$	Proliferation; binding to fibrinogen	K <sub>v</sub> 1.3	Proliferation	
	$\beta_2$				
	$\alpha_v\beta_3$	EBV-induced proliferation and invasion	K <sub>Ca</sub> 3.1 <sup>c</sup>	Proliferation	
	$\alpha_4\beta_7$	Adhesion to FN and VCAM-1; migration	CRAC	$Ca^{2+}$ entry	
			$Ca^{2+}$ NSCC	Adhesion to ICAM-1 and VCAM-1	
Platelets	$\alpha_{IIb}\beta_3$	Aggregation	TRPC1	$Ca^{2+}$ entry	
			TRPC6	Cation entry	
Erythrocytes			K <sub>Ca</sub> 3.1	Cell volume homeostasis	

Following the common name of integrins and ion channels reported in the table: I, VLA-4; II, VLA-5; III, Mac-1; IV, LFA-1.

Abbreviations: PB, peripheral blood; BM, bone marrow; p-SMAC, peripheral supramolecular activation cluster; IS, immunological synapse.

<sup>a</sup> hERG1.

<sup>b</sup> IRK1.

<sup>c</sup> TREK-1.

worth recalling that the capacity of entering a quiescent state is indispensable for the maintenance and self-renewal of HSCs. Moreover, the HSC population capable of strong adherence to osteoblasts is characterized by high expression of  $\beta_3$  integrin. In these cells,  $\beta_3$  associates with  $\alpha_v$  to assure strong adhesion to the niche' osteoblasts and hence the quiescence and maintenance of stemness properties (Umehoto et al., 2006). Conversely, the HSCs endowed with a high capacity to induce long-term hemopoiesis are characterized by upregulation of the  $\alpha_2$  integrin subunit (Wagers and Weissman, 2006). Finally, another integrin type found to be expressed in mouse embryonic and neonatal HSCs is  $\alpha_{IIb}\beta_3$  (Mikkola et al., 2003).

The situation in HCPs is more heterogeneous and plastic. Under steady-state conditions, that is, when HCPs are firmly adherent to the BM stroma, cells express multiple integrins ( $\alpha_4\beta_1$ ,  $\alpha_5\beta_1$ ,  $\alpha_L\beta_2$ , and  $\alpha_M\beta_2$ ), along with L-selectin, PECAM-1, and CD44. The main determinants of HPC adhesion to the BM stroma are  $\alpha_4\beta_1$  and  $\alpha_5\beta_1$  integrins, whose counter-receptors are either FN or the cell surface ligand VCAM-1. Cytokines are also essential to promote HPC release into the PB, through their modulatory role on adhesion receptor expression. When floating in the PB, HPCs acquire properties different from those typical of the BM-residing HPCs, including a different integrin expression pattern. Indeed,  $\alpha_4$  is a marker to distinguish the BM HPC from the PB HPC. This difference also implies that the two HPC populations have different ability to adhere to stromal elements. The following section summarizes the functional profile of integrins expressed in normal mature hemopoietic cells, by mentioning a few selected examples. The complete pattern is reported in Table 5.1.

#### 4.1.2. Leukocytes: Neutrophils and macrophages

The role of integrins in the regulation of leukocyte trafficking, transendothelial migration, and activation is well known and further highlighted by several human conditions in which defects in integrin expression or function occur (Ley and Reutgershan, 2006). Common integrins expressed on leukocytes include  $\alpha_L\beta_2$ ,  $\alpha_M\beta_2$ ,  $\alpha_X\beta_2$ , and  $\alpha_4\beta_1$ , with counter-receptors on vascular endothelial cells being ICAM-1-5 and VCAM-1. Circulating leukocytes generally keep their integrins in a nonadhesive state in which the ectodomains are held in a bent or folded conformation that impairs the ligand binding capacity. When needed, integrin avidity is modulated by stimulation with chemoattractants or cytokines, which quickly lead to integrin activation and clustering. This process establishes firm cell adhesion to the vascular endothelium and triggers the following transendothelial migration into the underlying tissues (Rose et al., 2007). Both the adhesive and the signaling functions of integrins are tightly regulated. The rapid activation serves to establish adhesion, while the temporally and spatially regulated signal transduction controls efficient migration across the endothelium.



### 4.1.3. Lymphocytes

All lymphocyte populations express integrin receptors (Table 5.1). Here, we briefly review those expressed by T cell subsets, with particular emphasis to their functional significance. T cells express at least 12 of the 24 known integrin heterodimers, the expression pattern depending on the subset and maturation state of the cell (von Andrian and Mackay, 2000). All of the four leukocyte-specific  $\beta_2$  integrins ( $\alpha_L\beta_2$ ,  $\alpha_M\beta_2$ ,  $\alpha_X\beta_2$ ,  $\alpha_D\beta_2$ ) are found on T cells,  $\alpha_L\beta_2$  being the most abundant and widespread. T cells also express  $\beta_7$  ( $\alpha_4\beta_7$  and  $\alpha_E\beta_7$ ) and  $\beta_1$  ( $\alpha_{1-6}\beta_1$ ). These integrins play a prominent role in T cell migration to peripheral lymph nodes and inflammatory sites, and in antigen presentation and cytotoxic killing. As in the case of leukocytes, integrins are normally inactive, but exposure to proper cytokines or chemokines or engagement of other receptors produces rapid activation. A major functional challenge faced by the T cell is to make the transition from a circulating cell to an actively migrating T cell able to cross the vascular endothelium of the blood vessel. This process is orchestrated by  $\alpha_L\beta_2$ ,  $\alpha_4\beta_1$ , and  $\alpha_4\beta_7$ . SDF-1 (also named CXCL12) switches the  $\alpha_4$  integrin to a high-avidity state, resulting in T cell arrest on the endothelium (Grabovsky et al., 2000). Subsequently, to permit T cell migration through the perivascular basement membrane as well as the long collagen fibrils to the source of inflammation, the  $\beta_1$  integrins are clustered at both the leading edge and uropod of the T cell (Dustin and De Fougères, 2001).

Another important integrin-dependent aspect in T lymphocyte function is formation of the so-called *immunological synapse* (IS; Lin et al., 2005b). For naïve T cells to achieve competent activation, they must bind to the dendritic cells (DCs) that express surface cognate antigens recognized by the T cell receptor (TCR). When a T cell interacts with such DCs, a series of spatial and temporal molecular reorganization events occurs, which lead to the formation of an IS, that is, a microscopically distinct structure at the contact site. The IS is a “bullseye”-type structure, in which the TCR itself and TCR-related signaling kinases and adapters localize to the center of the bullseye, to form the central supramolecular activation cluster (c-SMAC). In parallel, integrins (mainly the  $\beta_2$ - and  $\beta_1$ -containing integrins) and the integrin-associated protein talin localize to an outer ring-like structure that surrounds the center, named peripheral SMAC (p-SMAC). Although integrin receptors can transduce signals that promote TCR signaling and specific T cell differentiation events, their precise function in the IS, besides facilitating cell-cell adhesion, remains unclear. As will be detailed later, a necessary step for T cell activation following TCR engagement is stimulation of  $\text{Ca}^{2+}$  entry through the plasma membrane. TCR activation increases phospholipase C- $\gamma$  activity, with ensuing production of inositol 1,4,5-triphosphate and  $\text{Ca}^{2+}$  release from the endoplasmic reticulum. Activation of store-operated,  $\text{Ca}^{2+}$  release-activated  $\text{Ca}^{2+}$  (CRAC) channels on the plasma membrane is also promoted.

Finally, naïve and effector/memory T cells possess different trafficking patterns, mirrored by differential integrin expression. For example, circulating human CD4 memory T cells maintain a different balance of  $\alpha_4\beta_1$  and  $\alpha_4\beta_7$  integrin expression, depending on function (Denucci et al., 2009). T cells with high levels of  $\alpha_4\beta_7$  but low levels of the  $\beta_1$  subunit migrate preferentially into mucosal tissues, whereas T cells with high  $\alpha_4\beta_1$  levels but low  $\beta_7$  expression preferentially migrate through peripheral nonmucosal tissues such as skin. The factors that control the differential expression of integrins on activated T cells within the local lymphoid environments are beginning to be elucidated. From our standpoint it is specially intriguing that these T cell subsets also present a different pattern of ion channel expression (see below).

#### 4.1.4. Platelets

The  $\alpha_{IIb}\beta_3$  is the main integrin expressed in platelets, where it is essential for platelet aggregation. The ligands for  $\alpha_{IIb}\beta_3$  are the multivalent adhesive proteins fibrinogen and von Willebrand factor. In resting platelets,  $\alpha_{IIb}\beta_3$  is in a low activation state, whereas it rapidly undergoes a conformational change upon stimulation with various agonists. This activates platelet aggregation. Moreover, fibrinogen binding to  $\alpha_{IIb}\beta_3$  triggers a complex signaling pathway which regulates the extent of irreversible platelet aggregation and clot retraction (Payrastre et al., 2000).

#### 4.1.5. Neoplastic hematopoietic cells

All the main classes of adhesion receptors are expressed on the blast cells of *leukemia* patients. We will concentrate on those integrins whose main role is mediating (i) interaction of leukemic blasts with the BM stroma; (ii) leukemic cell release from the BM with subsequent homing into extramedullary sites; (iii) adhesive interactions that may affect the proliferation and survival of leukemic cells (Liesveld, 1997).

Peculiar mechanisms are emerging in specific leukemia subsets. In *acute leukemias* (both myeloid, AML, and lymphoid, ALL), blasts adhere to the BM stroma via the binding of  $\alpha_4\beta_1$  to FN and VCAM-1 on stromal cells. Adhesion seems to influence chemosensitivity, in that it may confer protection from chemotherapy-induced apoptosis. Therefore,  $\alpha_4\beta_1$  integrin could be a useful therapeutic target. Consistently, a clinical study shows that increased expression of  $\alpha_4\beta_1$ , and even more, increased binding of soluble VCAM-1 via  $\alpha_4\beta_1$  were significantly associated with longer overall survival in AML (Becker et al., 2009). On the other hand, in *chronic myeloid leukemias* (CML), an interesting interaction between  $\beta_1$  integrins and CXCR4 was observed and its relevance for leukemia cell survival and chemoresistance clearly shown (see Section 3).

Other observations point to the relevance of the entire integrin-dependent signaling network in leukemia progression. For example, aberrant

FAK expression is frequent in AML cells and FAK activity enhance migration of leukemic cells from the BM to the PB (Recher et al., 2004). The survival of AML cells within the BM is sustained by another integrin-related protein, ILK. In all probability, the effect depends on the fact that ILK, after interacting with  $\beta_1$  integrins, phosphorylates Akt in a PI-3K-dependent manner, with ensuing regulation of prosurvival signals (Tabe et al., 2007).

*Chronic lymphocytic leukemias* (CLL) are characterized by a reduced level of  $\alpha_1\beta_2$  compared to normal lymphocytes. Moreover, in CCL,  $\alpha_1\beta_2$  is insensitive to the chemokine-mediated activation that usually leads to increase the GTP-loading of the GTPase Rap1. This accounts for the reduced capacity of CCL cells to adhere and home to peripheral lymphoid organs (Hartmann et al., 2009). On the other hand, CCL cells maintain a good expression of  $\alpha_4\beta_1$ , which also presents clinical relevance because it affects both treatment-free and overall survival (Nückel et al., 2009). In *mantle cell lymphoma*, neoplastic cells express high levels of  $\alpha_4\beta_1$ , which in these cells mediates the B-cell trafficking and homing to lymphoid tissues (Kurtova et al., 2009). *Myeloma* cells express both the  $\beta_1$  and  $\alpha_4$  integrin subunits, CD44, ICAM-1, CD138 (syndecan-1), and CXCR4 as the major adhesion molecules. CAMs are involved in homing the malignant plasma cells to the BM in the production of growth factors and the recirculation of these tumor cells in the advanced stages of disease (Cook et al., 1997). Moreover,  $\alpha_4\beta_1$  plays a critical role in the cell adhesion-mediated drug resistance of myeloma cells (Kobune et al., 2007; Noborio-Hatano et al., 2009).

## 4.2. Ion channels

### 4.2.1. Hematopoietic stem cells and progenitor cells

While no study is available on ion channel expression in true HSCs,  $K_{IR}$  currents were observed in primitive HPCs ( $CD34^+ CD38^-$ ) stimulated with the combination of interleukin-3 (IL-3) and stem cell factor (SCF; Shirihai et al., 1996). The biophysical features of whole cell currents suggested that several  $K_{IR}$  channel types were coexpressed. In fact, later work showed that both strongly rectifying ( $K_{IR}$  4.3) and weakly rectifying ( $K_{IR}$  1.1) channels are present in these cells. The expression of both  $K_{IR}$  types seems essential for the generation of committed progenitors *in vitro*, as inhibition of the expression of either suppresses the generation of progenitor cells from IL-3 and SCF-stimulated umbilical cord blood (CB)  $CD34^+ CD38^-$  cells (Shirihai et al., 1998). More recently, the transcripts encoding  $K_v11.1$  channels were detected in circulating  $CD34^+$  cells upon cell cycle induction by IL3 (interleukin 3), GM-CSF (granulocyte-macrophage colony-stimulating factor), G-CSF (granulocyte colony-stimulating factor), and SCF (Pillozzi et al., 2002). As illustrated in more detail in Section 4.3,  $K_v11.1$  (commonly named hERG1) associates with the  $\beta_1$  integrin in CB  $CD34^+$  cells. This interaction is essential for proper BM engraftment of

these HPCs. Recently, the  $K_v11.1$  (*hERG1*) transcript was also observed in  $CD34^+/CD38^-/CD128$  (high) leukemic cells (Li et al., 2008).

#### 4.2.2. Leukocytes

In neutrophils, the transcripts from different TRP members (TRPC6, TRPM2, TRPV1, TRPV2, TRPV5, and TRPV6) were detected by RT-PCR (Heiner et al., 2003). However, a biophysical and pharmacological characterization has been only carried out for TRPM2. These currents turned out to be evoked by ADP-ribose and  $NAD^+$ , and contribute to activate neutrophils in response to chemoattractants, producing a positive feedback signal during the oxidative burst (Heiner et al., 2003). A  $Ca^{2+}$ -activated BK-type  $K^+$  channels was also recently observed in neutrophils. Its activity appears to be essential for normal antimicrobial activity (Essin et al., 2009).

Other work points to the necessity of characterizing the profile of  $Cl^-$  channel and transporter expression in neutrophils.  $Cl^-$  efflux is, at least in part, dependent on  $\beta_2$  integrin-mediated adherence of neutrophils to fibronectin (FN), suggesting that adhesion molecules may play a direct role in eliciting signals that activate  $Cl^-$  release from these cells during spreading and activation of the respiratory burst (Menegazzi et al., 1999). Several types of  $Cl^-$  channels have been well characterized in human neutrophils: stretch-activated channels ( $Cl^-^{SAC}$ ), calcium-activated channels (CaCCs), voltage-independent and voltage-dependent channels ( $ClC_{1-5}$ ), and protein kinase C-regulated channels (Volk et al., 2008).

In macrophages, the best characterized ionic conductance is the  $K_{IR}$  channel cloned from the macrophage-like cell line J5774 (Kubo et al., 1993). This channel type has been further described in primary human and murine macrophages and in several macrophage-like cell lines (for review, see Gallin, 1991).

#### 4.2.3. Lymphocytes

For more than 25 years it has been widely recognized that a coordinated influx of  $Ca^{2+}$  is essential to trigger T cell activation. During these years, patch clamp analysis, molecular and genetic manipulation as well as functional studies with specific blockers have led to the demonstration that a unique contingent of ion channels orchestrate the triggering, duration and intensity of the  $Ca^{2+}$  signals that control T cell activation. Pioneering work performed in the early 1980s showed that voltage-gated  $K^+$  channels are expressed in T cells and regulate mitosis (Chandy et al., 1984; DeCoursey et al., 1984; Fukushima and Hagiwara, 1985; Fukushima et al., 1984; Matteson and Deutsch, 1984). Subsequent work led to clarify the differential channel expression in T lymphocyte populations and its implications for the regulation of T cell activation (Cahalan et al., 1985; Krasznai, 2005; Wulff et al., 2003). These cells turned out to express delayed rectifying

$K_v1.3$   $K^+$  channels and intermediate conductance  $K_{Ca}3.1$   $Ca^{2+}$ -dependent  $K^+$  channels (Douglass et al., 1990; Logsdon et al., 1997; Wulff et al., 2000) as well as Orai1 (which forms the CRAC channel once assembled with the stromal interacting protein 1, STIM-1; Zhang et al., 2006), TRPM7, and  $Cl_{swell}$  channels (Cahalan and Chandy, 2009). The concerted action of these ion channels performs vital roles for the T cell activation and effector functions. In general,  $K^+$  channel-dependent hyperpolarization facilitates the  $Ca^{2+}$  influx induced by antigen binding. The consequent stimulation of intracellular  $Ca^{2+}$ - and PKC-dependent pathways triggers proliferation (Chandy et al., 2004). Moreover,  $K_v1.3$  localizes on the plasma membrane of T cells as part of a signaling complex that includes the  $\beta_1$  integrin, a PDZ-domain protein called hDlg (or SAP97), an auxiliary channel subunit  $K_v\beta_2$ , and the adapter proteins ZIP and  $p56^{lck}$  (Lck) (Beeton et al., 2006; Chandy et al., 2004), which further stresses its relevance for T cell activation (see below). The functional network that controls intracellular  $Ca^{2+}$  and hence activation of lymphocytes operates at different levels. We will focus on what happens at the IS formed when T cells encounter specific antigen-presenting cells. Both  $K_v1.3$  and  $K_{Ca}3.1$  are recruited to the IS during antigen presentation, while STIM1 and Orai1 relocate at the DC interface within 5 min of contact, resulting in a localized  $Ca^{2+}$  influx into the synaptic region of the T cell. It is possible that the recruitment of CRAC channels to the IS where receptors, adhesion molecules, and other stimulatory molecules accumulate, is important for long-term  $Ca^{2+}$ -dependent regulation of the signaling events triggered on antigen presentation. Moreover, as  $K_v1.3$  is part of the large signaling complex described above, its localization in the IS promotes the clustering of the associated proteins at the synapse. As is typical of membrane complexes such as these, colocalization of these proteins at the IS probably provides a sophisticated mechanism to couple external stimuli with different intracellular signaling cascade. The possible contribution of local changes in the concentration of ions different from  $Ca^{2+}$  is poorly understood, but should not be neglected as elevated extracellular  $K^+$  has been reported to activate the  $\beta_1$  integrin and to induce integrin-mediated adhesion in T cells (Levite et al., 2000). Finally, the close proximity of  $K_v1.3$  to its partners within the signaling complex may provide a mechanism for regulation of the channel itself. In summary,  $K_v1.3$  likely serves as a scaffold that couples the TCR complex to  $\beta_1$  integrin and to an array of intracellular signals that collectively modulate T cell activation (Cahalan and Chandy, 2009). Another intriguing aspect of the  $K_v1.3$  physiology is that, following activation, effector/memory T (TEM) cells express higher levels of the  $K_v1.3$  and lower levels of  $K_{Ca}3.1$ , compared to naïve and central memory T cells (TCM). Upon repeated *in vitro* antigenic stimulation, naïve cells differentiated into  $K_v1.3^{high}$   $K_{Ca}3.1^{low}$  TEM cells. Therefore, the balance of these channel types constitutes a specific functional marker of activated TEM lymphocytes. Besides scientific interest,

these observations present pharmacological relevance. The potent  $K_v1.3$ -blocking peptide ShK, extracted from the sea anemone *Stichodactyla helianthus*, suppresses TEM cell proliferation without affecting naïve or TCM lymphocytes. Thus, inhibition of  $K_v1.3$  could be exploited in clinical treatment of autoimmune diseases (Wulff et al., 2003).

A similar picture also applies to B lymphocytes. It has in fact been reported that  $IgD^+ CD27^+$  naïve B cells upregulate  $K_{Ca}3.1$  during activation, and their proliferation is suppressed by specifically blocking  $K_{Ca}3.1$  but not  $K_v1.3$ . In contrast, class-switched  $IgD^- CD27^+$  memory B cells express high levels of  $K_v1.3$  and their mitogen-driven proliferation is suppressed by the  $K_v1.3$  inhibitor ShK (Wulff et al., 2004). The complete set of ion channels expressed in T and B lymphocytes and their physiological roles are reported in Table 5.1. More details are found in specialized reviews (Cahalan and Chandy, 2009; Oh-hora and Rao, 2008).

#### 4.2.4. Platelets

Platelets control  $Ca^{2+}$  homeostasis mainly through TRPC1 and TRPC6 channels. The mechanism is still controversial, but TRPC6 seems to be involved in receptor-activated, diacylglycerol-mediated cation entry, while TRPC1 is apparently involved in store-operated  $Ca^{2+}$  entry. As reminded above, store-dependent  $Ca^{2+}$  influx in nonexcitable cells often occurs via the coupling of the intracellular store  $Ca^{2+}$  sensor STIM-1 with plasma membrane CRAC channels (Zhang et al., 2006). Genetic evidence indicates an important role for STIM-1 in platelet function (Tolhurst et al., 2008), and TRPC1 is apparently the only ion channel coupled to STIM-1 to mediate store-dependent  $Ca^{2+}$  entry in the platelet (López et al., 2006).

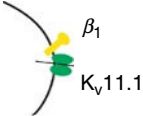
#### 4.2.5. Erythrocytes

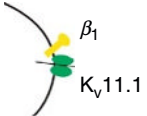
In human erythrocytes three different types of ion channels have been described so far (Table 5.1). The most relevant, the Gardos channel, is a  $Ca^{2+}$ -activated  $K^+$  channel ( $K_{Ca}3.1$ ). It is considered the major regulator of erythrocyte volume because, by mediating  $K^+$  efflux, controls dehydration and shrinkage (Brugnara, 1997; Gardos, 1958; Grygorczyk and Schwarz, 1983).

#### 4.2.6. Neoplastic hematopoietic cells

A detailed analysis of the  $K^+$  channel transcripts in primary leukemias as well as several hematopoietic cell lines has been carried out by different groups (Arcangeli et al., 2009; Pillozzi et al., 2002; Smith et al., 2002).  $K^+$  currents seem often to be necessary during proliferation, although the specific channel involved depends on cell type (Arcangeli et al., 2009; Table 5.2). Novel insights into this picture are provided by the discovery that the  $K_v11.1$  transcript is also expressed in leukemia stem cells (identified as  $CD34^+/CD38^-/CD123$  (high)), that is, in the stem cell population that

**Table 5.2** Integrins and ion channels in neoplastic hematopoietic cells

	Integrin	Function	Ion channel	Function	Interplay integrin/ion channel
Myeloid leukemia					
Acute	$\alpha_4\beta_1^I$	Adhesion to FN and VCAM-1; correlation with improved overall survival	4-AP sensitive $K^+$ channels	Cell signaling	
	$\alpha_5\beta_1^{II}$ $\alpha_M\beta_2^{III}$	Adhesion to FN Correlation with unfavorable prognosis	$K_{DR}$ $K_{IR}^a$	Differentiation	
	$\alpha_v\beta_3$	Migration	$K_{Ca}1.1^b$ $K_v11.1^c$	Differentiation Proliferation; migration; correlation with shorter overall survival	
Chronic	$\alpha_4\beta_1^I$ $\alpha_5\beta_1^{II}$ $\beta_2$	Adhesion to FN and VCAM-1; proliferation Adhesion to FN; proliferation	CRAC AQP5 TRPV5, TRPV6	Proliferation	
Lymphoid leukemia					
Acute	$\alpha_6$ $\alpha_4\beta_1^I$	Marker for detection of MRD Proliferation	$K_v1.3$ $K_v11.1^c$	Proliferation; protection from chemotherapy-induced apoptosis	

	$\alpha_5\beta_1^{\text{II}}$		K <sub>v</sub> 12.2 K <sub>Ca</sub> 2.2 TRPV5, TRPV6 TRESK Na <sub>v</sub> 1.5	Ca <sup>2+</sup> homeostasis	
Chronic	$\alpha_3\beta_1$ $\alpha_4\beta_1^{\text{I}}$	Adhesion to FN and VCAM-1; migration			
	$\alpha_5\beta_1^{\text{II}}$ $\alpha_1\beta_2^{\text{IV}}$	Adhesion to FN Adhesion to peripheral lymphoid organs; migration			
Lymphoma	$\alpha_4\beta_7$ $\alpha_4$	Adhesion to BM	K <sub>v</sub> 1.3	Maintenance of the membrane potential	
	$\alpha_4\beta_1^{\text{I}}$	Adhesion to BM; homing to lymphoid tissues	K <sub>v</sub> 11.1 <sup>c</sup>	Proliferation	
	$\alpha_1\beta_2^{\text{IV}}$ $\alpha_4\beta_7$	Leukemic dissemination	K <sub>Ca</sub> 2.3 K <sub>Ca</sub> 3.1 <sup>b</sup>	Cell cycle	
Myeloma	$\alpha_4\beta_1^{\text{I}}$	Adhesion to BM; drug resistance; homing to the BM; production of GF	VDAC	Apoptosis	
			AQP1	Correlation with BM angiogenesis	
			Cl swell		

Following the common name of integrins and ion channels reported in the table: I, VLA-4; II, VLA-5; III, Mac-1; IV, LFA-1.

Abbreviations: PB, peripheral blood; BM, bone marrow; MRD, minimal residual disease; GF, growth factor.

<sup>a</sup> IRK1.

<sup>b</sup> TREK-1.

<sup>c</sup> hERG1.



is critical for perpetuation of the leukemia disease (Li et al., 2008). The data reported in this paper generally support the notion that  $K_v11.1$  channels are implicated in the regulation of leukemia cell proliferation and cell cycle.

A completely novel player is represented by a member of the family of Aquaporins (AQP), namely AQP5 (Chae et al., 2008). AQP5 turned out to be overexpressed in CML cells. They promote cell proliferation and inhibit apoptosis, perhaps through an effect on cell volume control. In addition, the AQP5 expression increased with the emergence of imatinib mesylate resistance (Chae et al., 2008).

K562 cells, that is, a human cell line obtained from a patient with CML in blast crisis, were also shown to coexpress transient TRPV5 and TRPV6, the two channel proteins that physically interact in these cells (Semenova et al., 2009). The same two channels were also detected in the lymphoblastic leukemia Jurkat cell line. Their expression pattern and high  $Ca^{2+}$  permeability indicate an important role in controlling  $Ca^{2+}$  homeostasis and probably in malignant transformation of blood cells (Vasil'eva et al., 2008). Another emerging channel in oncology is represented by the TWIK-related spinal cord  $K^+$  (TRESK) channels, belonging to the double-pore domain  $K^+$  channel family, which resulted to be expressed in the Jurkat cell line (Pottosin et al., 2008). Some studies also report altered expression of ion channels and transporters in primary lymphomas. For example, upregulation of *KCNN3* ( $K_{Ca2.3}$ ) was observed in germinal center B-like diffuse large B cell lymphoma (DLBCL), whereas *KCNA3* ( $K_v1.3$ ) was upregulated in activated B-like DLBCL (Alizadeh et al., 2000). Moreover, in the lymphoma cell line Daudi, expression of  $K_{Ca3.1}$  has been described and its activity may account for cell malignant growth and proliferation (Wang et al., 2007).

### 4.3. Regulation through formation of molecular complexes and impact on downstream signaling

How do integrins interact with ion channels in hematopoietic cells? In general, such a functional connection is reciprocal, integrins activate ion channels (outside to in signaling) and ion channels regulate integrins (inside to out signaling). This bidirectional cross talk mainly relies on cytoplasmic messengers ( $Ca^{2+}$ , pH, protein kinases) commuting between the two proteins (Arcangeli and Becchetti, 2006). We here focus our attention on another mechanism of integrin/ion channels interaction that has been only cursorily treated in previous reviews. Growing evidence indicates that certain integrin and ion channel types can interact directly as the two proteins coassemble onto the plasma membrane to form a supramolecular complex. This constitutes a platform for triggering and orchestrating downstream cell signals. As far as we are aware, the first evidence of assembly between integrins and ion channels was obtained in hematopoietic cells by

Levite et al. (2000), who found that the  $\beta_1$  integrin subunit associate with  $K_v1.3$  channels in T lymphocytes. This leads to activate the integrin adhesive properties and prompts cell migration. Shortly afterward, a physical link between  $K_v1.3$  channels and  $\beta_1$  integrins was described in melanoma cells (Artym and Petty, 2002).

The  $\beta_1$  integrin subunit was also found to associate with another  $K_v$  channel, the  $K_v11.1$  channel, in leukemia cells (Cherubini et al., 2002). This observation was subsequently extended to other cancer cells, with the aid of membrane immunoprecipitation methods. Three types of  $\beta_1/K_v11.1$  macromolecular complexes have been described so far. (1) A bimolecular complex, limited to  $\beta_1$  and  $K_v11.1$ . Once formed, this complex recruits cytosolic signaling proteins, like FAK, which activate in an integrin- and ion channel-dependent manner. Similar observations were carried out in normal epithelial cells transfected with the  $K_v11.1$  channel (Cherubini et al., 2005) and in transformed epithelial cells like colon and gastric adenocarcinomas. Tests with specific inhibitors suggest that formation of such a complex regulates the cancer cell motility and invasive properties (Lastraioli et al., 2004) as well as the secretion of angiogenic factors (Crociani et al., submitted). (2) A trimolecular complex, in which a third membrane protein, a growth factor receptor, associates with the integrin/channel dimer. Such a complex was demonstrated to occur in AML and in human cytokine-stimulated HPC. In these cases, the adjunctive partner was the VEGF receptor 1 (Flt-1) (Pillozzi et al., 2007a) and the  $K_v11.1$  was almost exclusively constituted by the truncated hERG1B isoform, which is highly expressed in leukemia cells (Crociani et al., 2003). However, work in transfected human embryonic kidney (HEK293) cells suggests that hERG1B does not coimmunoprecipitate with the  $\beta_1$  integrin. In AML cells, it is Flt-1 that coimmunoprecipitates with hERG1B and also provides linkage to  $\beta_1$ , probably through an integrin protein domain different from the one used by the full length  $K_v11.1$  forms. The trimeric complex stimulates cell signaling through the Flt-1-dependent pathways, which nonetheless also depend on  $K_v11.1$  activation, as shown by selectively inhibiting the latter. (3) In ALL these membrane complexes can also contain, as a third element, a seven-spanning domain membrane receptor, in particular a chemokine receptor (Pillozzi et al., 2007b). Differently from the AML complex described above, this type of trimeric complex also turned out to assemble in the absence of any stimulation. It was hypothesized that, in B-ALL cells, the integrin receptor is the central member of the complex, which interacts with both the chemokine receptor, as documented in other experimental systems (Hartmann et al., 2005; Tabe et al., 2007), and the ion channel. Whether this double interaction involves different integrinic domains remains to be established. What is, however, important from a functional point of view is that the above multiprotein complex stimulates signaling through ILK, and its formation controls cell survival and chemoresistance in ALL.

It was previously showed that integrin-dependent activation of  $K_v11.1$  modulates cell differentiation, in both neuroblastoma and preosteoclastic leukemia cells. In the latter, inhibiting the  $K_v11.1$  activation induced by FN prevents the acquisition of the osteoclast phenotype typically triggered by cell adhesion (Hofmann et al., 2001). More light on the functional consequences of the integrin/channel interaction was shed by the subsequent demonstration that cross talk between integrins and  $K_v11.1$  relies on direct interaction of the two proteins on the plasma membranes, which is necessary to stimulate the downstream signals. In AML cells, the  $\beta_1$ /Flt-1/ $K_v11.1$  complex regulates both leukemia cell proliferation inside the BM and migration to the PB and extramedullary sites. The channel activity is indeed relevant in both processes, since they were inhibited when  $K_v11.1$  channel activity was specifically blocked (Pillozzi et al., 2007a). Complex formation in AML cells triggered p-tyr on Flt-1 and the activation of downstream MAPK and PI3K/pAkt pathways. Moreover,  $K_v11.1$  activity was necessary for the modulation of these signals. Therefore, it can be concluded that the biological effects depend on cell signals that are triggered by the contribution of membrane complex formation and channel activity, although it is presently unclear whether  $K_v11.1$  activity is only necessary for the complex assembly or it has independent effects on downstream signaling.

Altogether, it emerges that the association of integrin receptors with  $K_v11.1$  is a common occurrence in leukemia cells. The membrane complex can also comprise other protein partners, typically growth factor or chemokine receptors. Such a multiprotein structure serves as a molecular platform which recruits other proteins and second messengers, thus constituting a signaling site able to trigger and sustain the intracellular messages involved in cell proliferation and migration.

#### 4.4. Implications for oncology

What is the significance of the interaction between integrins and ion channels, and particularly of the  $\beta_1$ / $K_v11.1$  complex, in oncology? The presence of the complex on leukemia blasts identified a subgroup of AML patients with a worst prognosis (Pillozzi et al., 2007a). Moreover, in childhood ALL, formation of the  $\beta_1$ / $K_v11.1$ /CXCR4 complex leads to overcome drug resistance (Pillozzi et al., 2007b). As stated above, the BM microenvironment provides a “sanctuary” in which subpopulations of leukemia cells can evade the chemotherapy-induced death and acquire a drug-resistant phenotype. Protection involves a complex interplay between stroma-produced cytokines and adhesion molecules on leukemia cells (Matsunaga et al., 2003). Hence, when ALL cell lines are cultured on human BM stromal cells, the apoptotic effect of chemotherapeutic drugs like doxorubicin, prednisone, vincristin, and methotrexate are strongly inhibited. In this condition, addition of specific  $K_v11.1$  blockers bypasses

the resistance to these drugs, promptly restoring a significant level of apoptosis in leukemia cells (Pillozzi et al., unpublished results). Because the  $\beta_1/K_v11.1/CXCR4$  complex in ALL cells activates ILK, with ensuing switch-on of the MAPK and PI3K/pAKT pathways, and because blocking  $K_v11.1$  inhibits both pathways, it is again conceivable that  $K_v11.1$  channels constitute a pivotal regulation point for the integrin- and chemokine receptor-dependent signaling and hence chemoresistance.

Another mechanism relying on integrin/ $K_v11.1$  interaction that may indirectly affect leukemia therapy was recently observed in HPCs, that is,  $CD34^+$  cells. Previous studies demonstrated that treatment of CB  $CD34^+$  cells with high energy shock waves (HESW) significantly improves their *in vitro* expansion and engraftment in immunodeficient NOD/SCID mice (Berger et al., 2005). We found that HESW exposure increases the CB  $CD34^+$  cell adhesion without affecting the expansion of CAMs and CXCR4. HESW does not affect cell migration of the cell distribution between the cell cycle phases, but increases the percentage of CB  $CD34^+$  cells that express high levels of  $K_v11.1$  protein, with consequent hyperpolarization of the HESW-treated  $CD34^+$  cells. Specific inhibition of  $K_v11.1$  produces the expected cell depolarization, with parallel inhibition of cell adhesion. We conclude that treatment of  $CD34^+$  cells with HESW stimulates their adhesive properties and may facilitate their homing in a transplant setting. The effect seems partly mediated by  $K_v11.1$  activity (Timeus F. personal communication).

## 5. INTEGRINS AND ION CHANNELS IN CELL MIGRATION

A most interesting recent development in cell physiology regards the comprehension of several mechanisms by which integrins and different channel types interact in controlling cell migration. These processes are a fundamental component of embryogenesis and tissue remodeling in the adult. Moreover, they accompany many processes of pathological relevance, such as inflammation, wound healing, and metastatic spread. Migrating cells protrude actin-containing lamellipodia from their leading edge. Subsequently, the actin cytoskeleton connects to the substratum through focal contacts, which contain integrins. Finally, the bulk of the trailing cell is drawn forward (traction phase; Bray, 2001). Cell migration is modulated by chemical stimuli, which can regulate random migration (chemokinesis) or directional migration (chemotaxis; Gee, 1984). The latter process requires particularly precise coordination between the subsequent adhesion and release steps and cytoskeletal contraction along the direction of migration. As typical mediators of cell interaction with the environment, it is not surprising that integrins play major roles in eukaryotic cell migration.

## 5.1. Potassium channels

Studies carried out in the last 15 years have led to recognize that several types of  $\text{Ca}^{2+}$ -activated and voltage-dependent  $\text{K}^+$  channels are implicated in the cell migration machinery. This rapidly growing field has been reviewed recently (Schwab et al., 2007, 2008) and will not be discussed in detail here. In brief,  $\text{K}^+$  channel activation is believed to modulate cell crawling through different mechanisms. By changing  $V_m$ ,  $\text{K}^+$  channels alter the driving force for other ions, and especially  $\text{Ca}^{2+}$ , which controls migration at several levels (Schwab et al., 2008).  $\text{K}^+$  flux must also accompany the anion fluxes during the local volume alterations coupled with the cell shape changes that occur in migration (Sontheimer, 2008). Moreover, cell volume controls the actin cytoskeleton (Pedersen et al., 2001). Finally,  $\text{K}^+$  channels form complexes and thereby modulate several proteins involved in cell movement, such as FAK (Rezzonico et al., 2003; Wei et al., 2008), cortactin (Tian et al., 2006; Williams et al., 2007), and integrins themselves, on which we focus our discussion.

Detailed studies have been carried out on the related  $\alpha_4\beta_1$  and  $\alpha_9\beta_1$  integrins. Both of them stimulate motility and inhibit cell spreading, but the mechanisms underlying these effects are different (Vandenberg, 2008). In T cells, phosphorylation of  $\alpha_4\beta_1$  integrin stimulates lamellipodial protrusion, whereas dephosphorylation at the trailing edge facilitates retraction. This process is mediated by binding of paxillin to the integrin C-terminus, which activates the small G protein Rac (Goldfinger et al., 2003; Han et al., 2003; Liu et al., 1999; Ridley et al., 2003; Rose et al., 2007). The  $\alpha_9$  containing integrins are also known to bind paxillin (Liu et al., 2001; Young et al., 2001), but recent work shows they control cell migration through a mechanism that involves  $\text{K}_{\text{IR}}$  channels (deHart et al., 2008). Previous work by the same research group demonstrated that interaction between spermidine/spermine  $N^1$ -acetyltransferase and the cytoplasmic domain of  $\alpha_9$  integrin is necessary and sufficient for the migration mediated by  $\alpha_9\beta_1$  to occur in Chinese hamster ovary cells (Chen et al., 2004). This enzyme is thought to be the rate limiting for the conversion of spermine and spermidine to polyamines containing a lesser number of positive charges (such as putrescine). These latter bind with lower affinity to acidic targets in proteins and are further metabolized or excreted by the cell (Pegg, 2008). deHart et al. (2008) have shown that functional acetyltransferase is necessary for cell migration and that a decrease of intracellular spermine and spermidine triggers the  $\alpha_9\beta_1$ -dependent migration. Other studies in intestinal cells had previously indicated that the migration of epithelial cells depends on polyamines, probably through activation of Rac1 (Ray et al., 2003). However, the work by deHart et al. (2008) in engineered cell lines adds the important observation that the stimulation of  $\alpha_9$ -mediated migration through the

polyamine catabolism is likely to depend on activation of a typical polyamine target, namely the  $K_{IR}$  4.2 channel. In fact, blocking the activity or expression of  $K_{IR}$  4.2 inhibits the  $\alpha_9$ -dependent cell migration in cell lines as well as microvascular endothelial cells. What is more,  $K_{IR}$  4.2 was also found to colocalize with  $\alpha_9\beta_1$  integrin in FA complexes at the leading edge of crawling cells, which points to a complex regulatory network through which integrins and ion channels can communicate, in analogy to what has been described in leukemia cells. Whether the involvement of a specific  $K_{IR}$  channel has a special functional meaning in these cells or the precise way of increasing  $K^+$  currents is relatively indifferent for the downstream processes constitute an important point that remains to be elucidated.

## 5.2. Nicotinic acetylcholine receptors in epithelia

As reminded earlier, the “neuronal” nAChR subunits are also expressed in a variety of nonneuronal tissues. Their functions are manifold and only partially understood, but relatively ample evidence shows that cholinergic agonists can exert paracrine roles that include stimulation of chemotaxis through activation of nAChRs themselves (Chernyavsky et al., 2004; Wessler and Kirkpatrick, 2008). Here, we focus on the studies carried out on keratinocytes, while some related observations concerning the regulation of neurite extension are reviewed in a later section.

As other nonneuronal cell types, epithelial keratinocytes release ACh, which acts as an autocrine and paracrine factor that stimulates expression and activity of muscarinic and nicotinic ACh receptors. In particular, stimulation of nAChRs controls keratinocyte migration, a process that determines wound repair. During this process, keratinocytes extend their lamellipodia and then crawl perpendicularly to the wound axis. Work on galvanotropism (migration directed by steady electric currents) has suggested that cell migration could depend on accumulation of ion channels at the leading edge. When seeded in an electric field of a magnitude similar to the one present near wounds in mammalian skin (Barker et al., 1982), keratinocytes tend to migrate parallel to the lines of the electric field, toward the cathode (Nishimura et al., 1996). Basing on similar work in other physiological systems, it had been previously proposed that a high density of depolarizing ion channels at the leading membrane could elicit events that stimulate extension of cell protrusions (Poo, 1981). Subsequent work has confirmed that certain channel types, and particularly nAChRs, tend to cluster at the leading edge of cells undergoing galvanotaxis (e.g., Luther and Peng, 1985; Peng et al., 1993). The mechanisms whereby acetylcholine receptors contribute to the regulation of oriented cell migration have been investigated in detail in human keratinocytes. Chemotaxis toward the cholinergic agonist seems to depend mostly on activation of homomeric

( $\alpha_7$ ) nAChRs. This process is preceded by redistribution of the  $\alpha_7$  nAChR subunit to the cell's leading edge, where the nAChR colocalizes with  $\beta_1$  integrins (Chernyavsky et al., 2004). The M1 muscarinic receptor was also found to cluster at the leading edge and inhibition of either the ionotropic or the metabotropic receptor inhibits migration. Both ionotropic and metabotropic ACh receptors thus converge in controlling the Ras/Raf/MEK1/ERK pathway, whose final effect is upregulation of  $\alpha_2$  and  $\alpha_3$  integrin subunits, which stabilize the leading lamellipodium (Chernyavsky et al., 2005). This, as well as subsequent work, led these authors to propose the following regulatory scheme (see Fig. 6 in Chernyavsky et al., 2009). Activation of  $\alpha_7$  nAChR stimulates expression of the  $\alpha_2$  integrin gene through the Raf/MEK/ERK cascade, cooperatively activated by a  $\text{Ca}^{2+}$ -independent mechanism (mediated by Ras) and a  $\text{Ca}^{2+}$ -dependent pathway mediated by CaMKII and PKC. In parallel, engagement of the nAChR leads to phosphorylation of Jak2, thus leading to cytoskeletal reorganization mediated by the PI-3K/ROK cascade.

As noted earlier, although structurally unrelated to  $\text{K}_{\text{IR}}$  channels, nAChRs also present inward rectification caused by voltage-dependent channel block produced by intracellular polyamines. Therefore, a fruitful topic for further study may be the possible implication of the polyamine metabolism in the epithelial cells whose migration is controlled by nAChR activation.

## 6. INTEGRINS AND ION CHANNELS IN THE NERVOUS SYSTEM

### 6.1. Integrin expression in the central nervous system

The roles of integrin receptors during the development of the nervous system and the implications for synaptic function and epileptogenesis have been reviewed elsewhere (Clegg et al., 2003; Denda and Reichardt, 2007; Dityatev et al., 2006; Gall and Lynch, 2004; Morini and Becchetti, 2008; Schmid and Anton, 2003; Tarone et al., 2000). Here, we first provide a brief summary of the distribution and roles of integrin receptors in immature and adult brains for reader's reference. In the following sections, we focus on some advances particularly relevant from the cell signaling viewpoint.

Integrin expression during cerebral development is generally mutable, because it must match the expression of the different ECM environments established in different stages. Some receptor forms, however, persist in the adult, in which *in situ* hybridization studies reveal highly specific regional patterns of expression, at least in rodents (Pinkstaff et al., 1998). The  $\beta_1$ ,  $\beta_3$ ,  $\beta_5$ , and  $\beta_8$  subunits are expressed by neurons throughout the developing

cerebral wall and persist in the adult, particularly in the hippocampal and cortical synapses. The  $\beta_8$  subunit is also expressed by glial cells. On the other hand,  $\beta_2$  and  $\beta_4$  expression is limited to the adult hippocampus, whereas  $\beta_6$  is found in both adult cerebral cortex and hippocampus (Cousin et al., 1997; Nishimura et al., 1998). As to the  $\alpha$  integrins,  $\alpha_1$ ,  $\alpha_3$ , and  $\alpha_4$  are widely distributed in the developing rat brain, whereas in the adult they are confined to a few specific layers in the hippocampus, cerebellum, and neocortex. In contrast,  $\alpha_5$  and  $\alpha_7$  integrins are only detected in the adult, especially on neocortical cell bodies and apical dendrites (Pinkstaff et al., 1999). Expression of  $\alpha_8$  is detected in cortical neuron dendrites since E16. Electron microscopy studies indicate that it is associated with the postsynaptic densities of the dendritic spines of hippocampal pyramidal neurons and granule cells. Finally,  $\alpha_v$  is typically observed in the radial glial fibers of the developing cerebral cortex and persists in neurons and astrocytes of the mature cortex.

Several studies have addressed the function of different integrin types during cortical development (e.g., Belvindrah et al., 2007; Graus-Porta et al., 2001; Schmid and Anton, 2003; Schmid et al., 2005). Murine strains knocked out for different integrins, such as  $\beta_1$  (Belvindrah et al., 2007; Graus-Porta et al., 2001),  $\alpha_v$ , and  $\alpha_6$  (Schmid and Anton, 2003), present different patterns of cortical malformation. Full review of this literature is beyond our purposes, considering that the cellular physiology of these processes and consequently the regulatory relations with channels and transporters during neuronal development are largely unknown.

## 6.2. Integrin-channel interplay in mature neuronal circuits: Control of synaptic function

In mature neuronal circuits, the balance between synaptic stability and plasticity depends on membrane interaction with the ECM. As illustrated above, many integrins are localized specifically at synapses (particularly  $\alpha_3$ ,  $\alpha_5$ ,  $\alpha_8$ ,  $\alpha_v$  and  $\beta_1$ ,  $\beta_3$ ,  $\beta_8$ ). Nonetheless, until about a decade ago, the integrin-mediated interactions between neurons and the ECM in the adult nervous system were tacitly considered to be much less dynamic than those occurring during development. They were thus believed to contribute to the neural tissue stability, but give little contribution to synaptogenesis and the physiology of mature synapses. The situation changed in the late 1990s, where different lines of evidence pointed to a degree of flexibility in the neuronal interactions with the ECM, with implications for synaptic plasticity, neuronal regeneration, and epileptogenesis (e.g., Condic, 2001; Grotewiel et al., 1998; Pinkstaff et al., 1998; Stäubli et al., 1998). In fact, integrin ligands containing RGD motifs were soon found to be able to produce changes in neuronal excitability and  $\text{Ca}^{2+}$  fluxes within minutes (Wildering et al., 2002).



Glutamate receptors, in particular, turned out to be a target of integrin-dependent regulation (Chavis and Westbrook, 2001; Gall and Lynch, 2004). This has clear implications for synaptic plasticity, as suggested by early work indicating that interfering with the integrin-mediated adhesion to ECM tends to block LTP in adult rat hippocampal slices (Stäubli et al., 1990, 1998). The notion was confirmed by subsequent studies that took avail of the snake toxins that preferentially inhibit the  $\beta_1$ - and  $\beta_3$ -mediated adhesion (Chun et al., 2001) and of antibodies against the  $\alpha_3$  integrin (Kramar et al., 2002). Differently from RGD peptides, these more specific agents allow to dissect the dynamics of integrin effects. They generally point to the relevance of  $\alpha_3\beta_1$  and  $\alpha_5\beta_1$  integrins for hippocampal LTP and suggest that LTP comprises several integrin-dependent consolidation stages. Studies with murine strains knocked-out for integrin subunits confirm that several integrins have a part in the neuronal cell physiology. Reduced expression of  $\alpha_3$  leads to incapacity of maintaining LTP, whereas simultaneous deletion of  $\alpha_3$  and  $\alpha_5$  leads to defective paired-pulse facilitation. Finally, decrease of  $\alpha_3$ ,  $\alpha_5$ , and  $\alpha_8$  leads to defective LTP and spatial memory in water maze (Chan et al., 2003). On the other hand, specific deletion of  $\alpha_3$  in forebrain excitatory neurons produces defective LTP at hippocampal Schaffer collateral CA1 synapses, with no basal anomaly in synaptic transmission and paired-pulse facilitation. In this case, the spatial tasks dependent on hippocampus function were normal, with the exception of nonmatch-to-place working memory (Chan et al., 2007). These effects were similar to those observed in  $\beta_1$ -integrin conditional knockout mice (Chan et al., 2006), which indicate that  $\alpha_3\beta_1$  integrin (and its interaction with laminin (LM)) gives a prominent contribution to determine this aspect of memory in central synapses.

How integrins enhance and stabilize LTP is unclear. The  $\beta_1$  subunit is thought to control the actin polymerization in dendritic spines that accompanies the early stages of LTP stabilization (Kramar et al., 2006), but conclusive evidence about these issues is not available to date. Considering that LTP depends on gene expression, which is partly mediated by cytosolic  $\text{Ca}^{2+}$  increase, current working hypotheses are based on knowledge gained in other cell types and reviewed in the other sections of the present paper. Because synaptic potentiation involves upregulation of excitatory synaptic ion channels, we focus below on what is known about the interplay between integrins and the neuronal glutamate receptors. Considering the high permeability to  $\text{Ca}^{2+}$  of the NMDA receptors, these results also suggest general mechanisms for integrins to modulate the  $\text{Ca}^{2+}$ -dependent signaling.

Finally, we notice that other lines of evidence suggest that synaptic stability may also be controlled by direct interaction of ion channels with the ECM proteins. This mechanism was indicated by work carried out on the *Torpedo* electric organ (Sunderland et al., 2000). Further work with

electric organs as well as cultured murine motor nerve terminals showed that LM  $\beta 2$  directly binds to the extracellular portion of the pore forming  $\text{Ca}_v(\alpha)$  subunit in *Torpedo* and that interaction between LM and the  $\text{Ca}^{2+}$  channel is necessary for proper assembly of the active presynaptic zones in motor neuron terminals (Nishimune et al., 2004; Sunderland et al., 2000).

### 6.2.1. Synaptic plasticity in the hippocampus

A relatively large literature is available about the interplay of integrins and ionotropic GluRs in immature (Chavis and Westbrook, 2001) and mature hippocampus (Gall and Lynch, 2004). In hippocampal slices and synaptoneurosomes from mature rats, integrin activation with RGD-containing peptides potentiates the NMDA receptors (Lin et al., 2003). The effect depends on strong activation of FAK and the associated protein Pyk2, with ensuing SFK-dependent phosphorylation of both NR2A and NR2B channel subunits (Bernard-Trifilo et al., 2005).

The integrin-dependent modulation of excitatory transmission in hippocampal slices from adult rats also depends on activation of AMPA receptors, as shown by perfusing these slices with RGD-containing peptides. The response is inhibited by a mixture of anti-integrin antibodies, which cover the spectrum of integrins expressed in this region (Kramar et al., 2003). This work provided further interesting signaling insight. Integrin activation led to phosphorylation of both CaMKII and the GluR1 subunit of AMPA receptors. To inhibit these phosphorylation steps, it turned out to be sufficient to block the NMDA receptors. Conversely, the synaptic potentiation due to AMPA receptor stimulation was only blocked when specific inhibitors of NMDA receptors and of SFK were applied together. Therefore, it seems that integrin binding activates two intracellular pathways. The first is not dependent on Src and stimulates the NMDA receptors, with consequent phosphorylation of CaMKII and GluR1 (which leads to AMPA receptor potentiation). The second is mediated by SFK activation and also modulates the AMPA receptors. The studies mentioned above on  $\beta_1$  integrin knockout mice support the idea that integrins control AMPA receptors, at least in the hippocampus. In these animal models, the fast excitatory transmission at CA3–CA1 synapses is strongly reduced, probably because of defective postsynaptic AMPA receptors (Chan et al., 2006). It is clear that the interplay of integrins and AMPA receptors is complex and includes feedback from channel activation to integrin expression, as is also increasingly recognized in other experimental systems. The AMPA channel activity stimulates the membrane expression of  $\alpha_5$  and  $\beta_1$  subunits, which in turn stimulate, once activated, intracellular kinase-dependent signaling cascades (Lin et al., 2005a).

It is also worth mentioning that interference in LTP consolidation is also produced by using compounds that inhibit ECM proteases such as tissue

plasminogen activator (Baranes et al., 1998), metalloproteases (Nagy et al., 2006), and neuropsin (kallikrein-related peptidase 8; Tamura et al., 2006). Increasing evidence indicates that the cellular effects induced by ECM proteases are often mediated by integrin receptors (Ishikawa et al., 2008; Michaluk et al., 2009). These observations provide a conceptual link with the cellular mechanisms induced by the tumor microenvironment.

### 6.2.2. Recent clues about the neocortex

To determine the potential cognitive implication of integrin-dependent plasticity, it will also be necessary to analyze these processes in selected neocortical regions, about which very little is known. Biochemical and imaging work on dissociated rat neocortical neurons highlight integrin-dependent signaling mechanisms partly similar to those observed in the hippocampus. Integrin activation was found to stimulate  $\text{Ca}^{2+}$  influx, probably through NMDA receptors. This was accompanied by activation of SFK and MAPK, with ensuing phosphorylation and nuclear translocation of ERK1/2 (Watson et al., 2007). Nevertheless, in these neurons, the integrin-dependent activation of the ERK1/2 kinase pathway does not seem to depend on any typical mediator of integrin signaling, such as FAK phosphorylation or alteration of the  $\text{Ca}^{2+}$ -calmodulin-dependent protein kinase II (CaMKII). These findings further complicate the picture of integrin-dependent signaling, because they suggest that, in the adult brain, the signaling pathways recruited by cell adhesion to the ECM differ between cerebral regions and neuronal types.

The integrin-induced  $\text{Ca}^{2+}$  fluxes have also been recently studied in neuron-enriched primary neocortical cultures (Lin et al., 2008). In these cells, activating  $\alpha_5\beta_1$  integrins quickly stimulates a prolonged increase in  $[\text{Ca}^{2+}]_i$ . The response depends on voltage-gated  $\text{Ca}^{2+}$  channels and NMDA receptors, but complete inhibition is only obtained when the voltage-gated  $\text{Na}^+$  channels, the AMPA receptors, and tyrosine kinases are blocked. These and other results (e.g., Hilgenberg and Smith, 2004) suggest that interaction of cultured neocortical neurons with the ECM recruits tyrosine kinase pathways and stimulates  $\text{Ca}^{2+}$  influx through different pathways both voltage dependent and independent, such as voltage-gated  $\text{Ca}^{2+}$  channels, NMDA receptors,  $\text{Ca}^{2+}$  release from intracellular stores, etc. The mechanistic details and the general significance of these results are still matter of debate.

### 6.3. Integrin-channel interplay in developing neuronal circuits

The nervous system develops in subsequent stages, all of which depend on ion channel function, often regulated by cell adhesion to the ECM. After rounds of cell division of neural stem cells, specific signals determine exit

from cell cycle. At this stage, both VGCs and ligand-gated channels control neuronal progenitor proliferation and exit from cell cycle, as they do in many (perhaps all) other cell types. Derangement of ion fluxes in this phase is also relevant for neoplastic processes, as has been reviewed above and elsewhere (Arcangeli et al., 2009; Cayre et al., 2009; Lang et al., 2005). Subsequently, neurons migrate radially or tangentially to reach their final destination. This process is under complex regulation by ECM proteins, cell-cell adhesion molecules (CAMs), and diffusible factors (Spitzer, 2006; Zheng and Poo, 2007) (Fig. 5.2). In former sections, we have outlined the current state of knowledge about ion channel roles in cell migration. Those mechanisms suggest fruitful lines of research for neuronal migration as well, about which not much is known to date. When neurons have reached their final location, differentiation occurs, which implies expression of the full complement of VGCs, neurotransmitter synthesis, and expression of neurotransmitter receptors. Moreover, axons must be properly addressed to target tissues for synapse formation on other neurons, vessels, muscle, etc. This implies the existence of sensitive mechanisms for regulating growth cone guidance and dendritic outgrowth, which are briefly illustrated below.

Similar  $\text{Ca}^{2+}$ -dependent signals regulate both dendrite extension during the late stages of neuronal differentiation and the growth cone pathfinding that leads axons to their final postsynaptic targets. Extracellular cues trigger  $\text{Ca}^{2+}$  influx through a variety of membrane channels. Growth cone extension requires a permissive range of  $[\text{Ca}^{2+}]_i$ , whereas the frequency of  $\text{Ca}^{2+}$  waves and spikes controls the rate of axonal elongation. More localized  $\text{Ca}^{2+}$  transients regulate cone steering in response to extracellular signals (Gomez and Zheng, 2006; Kater et al., 1988).  $\text{Ca}^{2+}$  exerts its effects by modulating the many well-known  $\text{Ca}^{2+}$ -sensitive signaling pathways that converge on cytoskeletal elements and associated regulators such as myosin, Rho, gelsolin, ROCK, and others (Zheng and Poo, 2007). These signals must involve integrins, because of the necessity of coordinating the adhesion points' turnover, that is, assembly at the front and disassembly at the rear of moving cells, a particularly delicate process in the long neuronal processes.

During the 1980s, it had become clear that axonal growth *in vivo* and neurite extension *in vitro* are regulated by the coordinated action of three main kinds of factors: soluble neurotrophic compounds, ECM components, and a variety of CAMs (Bixby and Harris, 1991). In the early 1990s, several *in vitro* approaches were applied to the study of the underlying cellular processes and the role of ion fluxes began to emerge. In agreement with the recognition of the importance of  $\text{Ca}^{2+}$  signals in these processes, neurite growth in response to CAMs such as N-Cadherin, L1, and N-CAM was found to depend, at least in part, on activation of voltage-sensitive  $\text{Ca}^{2+}$  channels (Bixby et al., 1994; Doherty et al., 1991; Williams et al., 1992). LM was also found to elicit cytosolic  $\text{Ca}^{2+}$  transients in chick ciliary ganglion neurons (Bixby et al., 1994). Parallel studies on the integrin-dependent

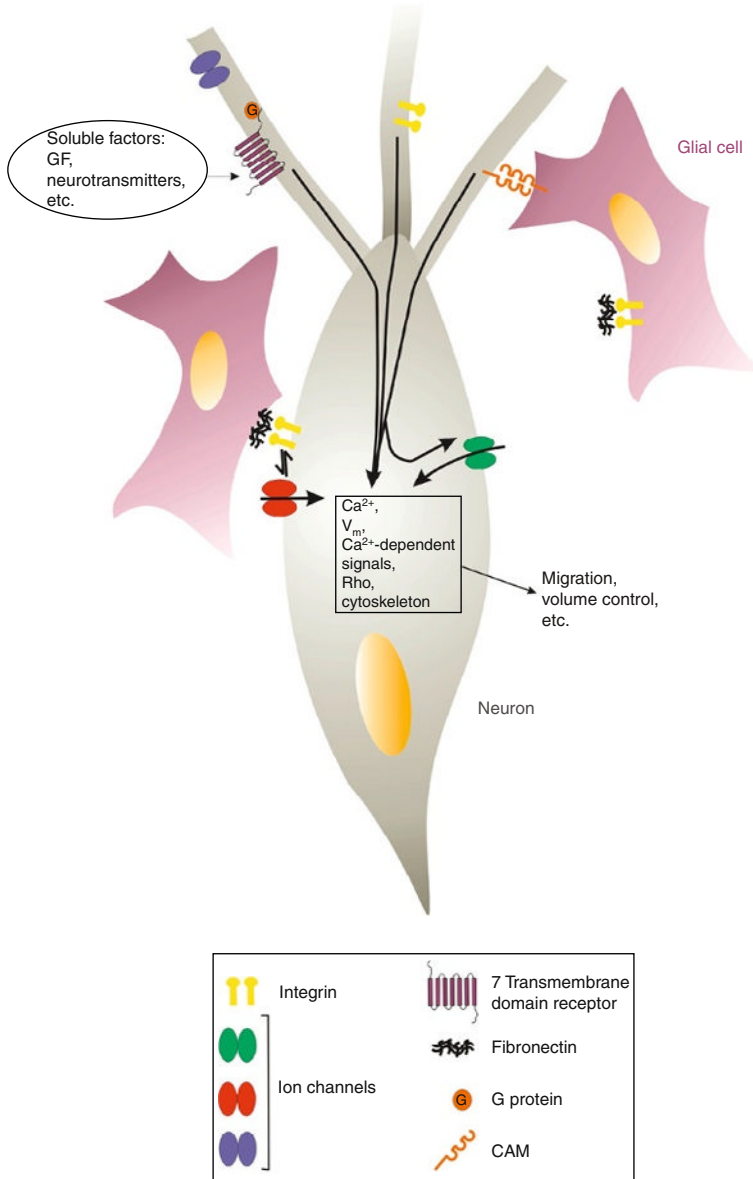


**Figure 5.2** Migration-related signals in neurons. Neuronal migration and neurite extension take place during development of the nervous system and, in later stages, during synaptic maturation and plastic changes as well as during tissue remodeling after damage. The mechanisms occurring at axon growth cones and neurite tips are thought to be similar. Neurons respond to three main types of different external guidance or differentiation signals: diffusible messengers (e.g., neurotransmitters or neuropeptides), ECM proteins such as fibronectin and laminin and neuronal or glial CAMs. Extracellular signals are transduced by specific membrane receptor types (as indicated) which

adhesion to the ECM led to observe that neurite outgrowth in neuroblastoma cells grown onto FN, vitronectin (VN), or LM depends on activation of  $K^+$  channels (Arcangeli et al., 1993, 1996), that were subsequently recognized to belong to the  $K_v11$  subfamily (Bianchi et al., 1998). The contribution of  $K^+$  channels to neurite extension has not been much followed up, because most of these studies have subsequently concentrated on the contribution of  $K^+$  channels to cell proliferation and differentiation in experimentally simpler cell types. On the other hand, the implication of  $Ca^{2+}$  channels in neurite extension is supported by many studies, indicating that cytosolic  $Ca^{2+}$  controls the physiology of neuron extension. Detailed mechanistic insight has been reached, for instance, in the case of the  $\alpha_5\beta_1$ -mediated neurite outgrowth, triggered by GM1 gangliosides. Gangliosides are glycosphingolipids containing sialic acid. The ganliotetraose family prevails in the nervous system. GM1 is the monosialosyl form of this family and modulates many membrane proteins, including integrins and proteins implicated in  $Ca^{2+}$  signaling, often by direct association (Ledeen and Wu, 1992, 2002; Mocchetti, 2005). Downstream signals can also be activated by cross-linking the membrane-associated GM1 with other proteins, by using multivalent molecules such as antibodies, the B subunit of cholera toxin, and lectins. This mechanism was first described in rat lymphocytes (Dixon et al., 1987) and subsequently observed in other cell types, including neuroblastoma (e.g., Carlson et al., 1994; Quattrini et al., 2001) and primary neurons (Milani et al., 1992; Wu et al., 1996). Further studies in neuroblastoma showed that such a stimulation of  $Ca^{2+}$  influx leads to neurite extension (Fang et al., 2000; Masco et al., 1991; O'Hanlon et al., 2003) and depends on voltage-independent channels (Fang et al., 2002) that have been recently recognized to be TRPC5 (Wu et al., 2007). Cross-linking of GM1 to  $\alpha_5\beta_1$  integrin leads to activation of TRPC5. The GM1/integrin complex triggers phosphorylation of the integrin-associated FAK, with ensuing stimulation of phospholipase  $C\gamma$  and PI-3K.  $Ca^{2+}$  influx through TRPC5 is necessary to trigger neurite extension in neuroblastoma as well as dissociated cerebellar granule neurons (Wu et al., 2007). Interestingly, TRPC5 expression in the cell body sharply declined as differentiation proceeded in both neuroblastoma and cerebellar neurons. These results imply that TRPC channels are necessary to trigger the early phases of neuritogenesis. Moreover, the stimulus depends on integrin engagement

---

channel these messages into common signaling pathways that interact with ion channels in complex ways. The combination of (i) alterations in  $V_m$  and  $[Ca^{2+}]_i$ , (ii) physical interaction between ion channels and other signaling elements, and (iii) the stimulation of the biochemical cascades discussed in the text brings about sophisticated control of cell adhesion, cytoskeletal function, cell volume, in different cellular compartments (e.g., the anterior and the rear front, during cell movement). CAM, cell-cell adhesion molecule; GF, growth factors;  $V_m$ , membrane potential.

and subsequent FAK phosphorylation. That FAK is implicated in neurite outgrowth is also suggested by work in other experimental models (Ivankovic-Dikic et al., 2000). Therefore, the functional implication of integrin-mediated signaling in TRPC5-dependent neuritogenesis seems convincing. Because, however, in the work described above integrin was activated by GM1 cross-linking, it remains to be determined which extracellular physiological signal may activate this mechanism. A possible candidate suggested by Ledeen and colleagues is the galectin family, some of which members are expressed in the nervous system and can bind and cross-link membrane-associated gangliosides (Gabiuss et al., 2002; Taylor and Drickamer, 2007).

Knowledge about the control of integrin function by  $\text{Ca}^{2+}$  is much less complete than that concerning the  $\text{Ca}^{2+}$ -dependent regulation of the actin cytoskeleton, although it is likely that the mechanisms determined in other experimental systems should broadly apply to the nervous system as well. In fact, Rho GTPases are implicated in regulating the adhesion contacts formed by growth cones (Woo and Gomez, 2006). It is thus conceivable that the  $\text{Ca}^{2+}$  signals discussed above may also control the dynamics of neurite adhesion to the substrate. Disassembly is instead controlled by the microtubule dynamics and work in fibroblasts suggests that this is mainly regulated by dynamin and FAK, and not Rho (Broussard et al., 2008; Ezratty et al., 2005). In analogy with what has been observed in other cell types (Arcangeli and Becchetti, 2006), the adhesion machinery could feedback and regulate  $\text{Ca}^{2+}$  signaling in growth cones as well. Some evidence along this line is available not for integrins but for the CAMs expressed on cultured dorsal root ganglion neurons, which steer growth cones by local stimulation of  $\text{Ca}^{2+}$  release from intracellular stores (Ooashi et al., 2005). The expression of CAMs also changes depending on the pattern of neuronal discharge (Hanson and Landmesser, 2004; Itoh et al., 1995). Nevertheless, the link between neuronal activity and the expression of membrane receptors that respond to fixed or diffusible guidance cues is still largely unexplored and we predict interesting future developments.

Not much either is known about the interplay of integrins and ion channels in growth cone pathfinding. A thoroughly studied example of growth cone guidance by ECM proteins was actually found not to be mediated by integrin receptors. Sann et al. (2008) recently studied the interaction between the LM  $\beta_2$  expressed in the skin and the  $\text{Ca}_v2.2$  channels expressed on the growth cones of sensory Rohon-Beard neurons, in *Xenopus laevis*. In the skin, a stop signal must induce sensory axons to cease growing when they arrive. LM  $\beta_2$  is an obvious candidate, because it is known to induce motor axons to stop growing, *in vitro* (Porter et al., 1995). In fact, sensory spinal *Xenopus* neurons grown on LM  $\beta_2$  present significant decrease in neurite outgrowth, compared to the controls. When encountering an LM coated surface, these neurons produce transient intracellular

$\text{Ca}^{2+}$  elevations and pause. Blocking the LM-dependent  $\text{Ca}^{2+}$  influx through  $\text{Ca}_v2.2$  channels expressed in these growth cones prevents the block of axonal growth. That  $\text{Ca}^{2+}$  influx from the extracellular environment (through mechanosensitive channels) blocks neurite outgrowth in *Xenopus* spinal neurons grown onto FN and LM coated surfaces was also reported by Jacques-Fricke et al. (2006). What is particularly interesting from our standpoint is that the stop signal is not mediated by LM binding to integrin receptors. In analogy to what has been observed in the neuromuscular junction preparations mentioned earlier (Nishimune et al., 2004), data indicate that LM regulates the growth cones by forming a complex with the voltage-dependent  $\text{Ca}^{2+}$  channel (Sann et al., 2008).

#### 6.4. Integrins, ion channels, and microglia

One of the issues emerging from recent literature is that multiple ion channel types cooperate in producing the diverse biological effects ensuing from cell adhesion to the ECM. An important future task will thus be to obtain an integrated physiological picture, at least for a few cell types. In this light, microglia provides a nice experimental model. Work carried out by independent research groups points to the involvement of  $\text{K}_v1.3$  and  $\text{P}_{2X}$  channel interaction with integrin receptors in microglial activation. Previous work *in vitro*, carried out on cultured HEK cells, showed that  $\text{P}_{2X}$  receptors can form a membrane complex with  $\beta_2$  integrin that connects extracellular LM with the cytoskeleton (Kim et al., 2001). Nonetheless, the functional association between purinergic ionotropic receptors and integrins has not been much attended to until Tsuda et al. (2003) found that upregulation of  $\text{P}_{2X4}$  in spinal microglia is necessary for the development of neuropathic pain after injury. Consistently, the FN-dependent tactile allodynia is blocked in mice lacking  $\text{P}_{2X4}$  (Tsuda et al., 2008). Moreover, the increase in  $\text{P}_{2X4}$  expression in turn depends on integrin activation (particularly  $\beta_1$ ). This is suggested by both *in vitro* and *in vivo* experiments. For example, in the spinal cord of injured rats, blocking  $\beta_1$  and  $\beta_3$  integrins with echistatin prevents  $\text{P}_{2X4}$  upregulation (Tsuda et al., 2008). *In vivo*, integrin activation is probably caused by increased FN release in injured sites (Nasu-Tada et al., 2006).

However, the resting microglia also expresses  $\text{K}_v1.3$  channels. In analogy with what happens in T cells,  $\text{K}^+$  channel activity seem to be necessary for microglial activation (Fordyce et al., 2005). In culture rat cortical microglia, inhibition of  $\text{K}_v1.3$  inhibits the microglial migration induced by different stimuli and the neuronal death induced by microglia. Moreover, the anti-inflammatory and neuroprotective agent minocycline prevents the allodynia induced by peripheral nerve injury. In fact, minocycline reduces the microglial expression of  $\text{K}_v1.3$  and  $\beta_1$  integrin (but not  $\beta_2$ ; Nutile-McMenemy et al., 2007). Although the mechanistic details of these



responses have still to be elucidated, the authors speculate that minocycline could act upstream of the migration stimulating pathway, by acting on a  $K_v1.3/\beta_1$  integrin interaction, as is also suggested by the fact that these proteins form macromolecular complexes in other cell types (Artym and Petty, 2002; Levite et al., 2000).

By combining the above evidence, although still somewhat fragmentary, a broader picture is slowly emerging. Damaged sites in the CNS increase the expression of ECM proteins. The consequent stimulation of microglia depends on the interplay between  $K_v$  channels and integrin receptors. This interaction is likely to control downstream signals analogous to those described in other cell types. Besides regulating cell motility, proliferation, and activation, these signals also upregulate  $P_{2X}$  channels, which is necessary for proper physiological response, such as the development of neuropathic pain. On the other hand, very recent evidence suggests that the development of hyperalgesia in sensory neurons depends on integrin-dependent stimulation of TRP-type channels (Alessandri-Haber et al., 2008; Jeske et al., 2009).

## 7. CONCLUDING REMARKS

During the last two decades, the analysis of complex systems has become a flourishing field at the borderline between mathematics, informatics, and the physical sciences. Biological organisms are certainly the complex systems for antonomasia and pose many fascinating scientific questions. Nevertheless, the implication of the above studies for biology is still limited, because of the considerable experimental and theoretical difficulties. No doubt, reaching a full understanding of at least a few accessible biological systems will ultimately require a thorough appreciation of their complex and interconnected nature. In this light, we believe that the multifaceted regulatory interplay between integrin receptors and ion channels offers a fertile research field for investigators looking for experimental challenges which may open broader biological perspectives.

By controlling cell adhesion to the ECM, integrin receptors regulate processes as diverse as cell proliferation, differentiation and apoptosis, cell migration in a developmental or regenerative context, and the stability of mature neural circuits. Disparate as they are, these biological functions are underlied by mechanisms which often comprise changes in transmembrane ion flow. Recent and less recent literature has thus pointed to complex physical and functional interplay between integrins, ion channels, and other membrane transporters. This interaction regulates bidirectional signal transduction across the cell surface and may take place at all levels of control, from transcription to direct conformational coupling. The functional link

between integrins and membrane channels, however it is brought about, is thus a central coordinator of an array of intra- and intercellular regulatory networks which produce their effects in parallel. Further, it is increasingly clear that those regulatory pivots may also recruit other membrane receptors, such as CAMs, metabotropic receptors, growth factor receptors, etc.

A telling example is the integrin–channel cross talk that occurs during the immune response, which determines, for instance, the lymphocyte activation occurring at the IS. As we remarked earlier, hematology is one of the first disciplines in which these studies have been pursued in depth. Therefore, thorough studies in selected experimental models are now available, although a comprehensive physiopathological picture is still lacking. It is particularly interesting to notice that the mechanisms thus revealed provide valuable hints to those implicated in BM control of HSCs, and hence to hemopoiesis overall. By citing some recent evidence along these lines, we have sought to convince the reader that the cooperation of ECM receptors and ion transport has relevant oncological implications as regards the explanation of how the tumor microenvironment controls neoplastic proliferation and how cell–cell contact induces tumor chemoresistance. The latter issue frequently represents the major hindrance to cancer therapy and we believe the viewpoint here outlined may suggest fruitful lines of research for clarifying some of the underlying mechanisms.

Moreover, ion channels and integrin receptors participate in the control of cell movement, whose implications for migration/pathfinding have been mostly addressed in fibroblasts, epithelial cells, and neurones. The combination of neurite extension control and the modulation of certain neurotransmitter receptors indicates that the integrin–channel interplay may have general relevance for synaptic plasticity. Nevertheless, the neuroscientific implications of these mechanisms are among the most neglected in the field, with the exception of the regulation of glutamate receptors in hippocampal preparations. Logic as well as some of the evidence we have illustrated suggest that most of the above mechanisms are likely involved in the modulation of the stability of neuronal circuits. Other studies in the CNS point to oncological implications. In particular, the dependence of glial cell migration on ion channel activity is crucial for proper balance of migration and cell volume control during glioma cell spread. In this case, however, very little is known about the implications of ECM receptors, which presents another potential field for fruitful studies.

## **ACKNOWLEDGMENTS**

The authors' work is supported by the Italian Association of Cancer Research (AIRC), the Association for International Cancer Research (AICR), the Italian Ministry for University and Scientific Research, the Associazione Genitori Noi per Voi, the Istituto Toscano

Tumori, the Ente Cassa di Risparmio di Firenze (to the Dipartimento di Patologia e Oncologia Sperimentali, University of Firenze, and to CeSAL, University of Firenze), and the University of Milano-Bicocca (FAR).

## REFERENCES

- Alessandri-Haber, N., Dina, O.A., Joseph, E.K., Reichling, D.B., Levine, J.D., 2008. Interaction of transient receptor potential vanilloid 4, integrin, and SRC tyrosine kinase in mechanical hyperalgesia. *J. Neurosci.* 28, 1046–1057.
- Alizadeh, A.A., Eisen, M.B., Davis, R.E., Ma, C., Lossos, I.S., Rosenwald, A., et al., 2000. Distinct types of diffuse large B-cell lymphoma identified by gene expression profiling. *Nature* 403, 503–511.
- Arai, F., Hirao, A., Ohmura, M., Sato, H., Matsuoka, S., Takubo, K., et al., 2004. Tie2/angiopoietin-1 signaling regulates hematopoietic stem cell quiescence in the bone marrow niche. *Cell* 118, 149–161.
- Arcangeli, A., Becchetti, A., 2006. Complex functional interaction between integrin receptors and ion channels. *Trends Cell Biol.* 16, 631–639.
- Arcangeli, A., Becchetti, A., Mannini, A., Mugnai, G., De Filippi, P., Tarone, G., et al., 1993. Integrin-mediated neurite outgrowth in neuroblastoma cells depends on the activation of potassium channels. *J. Cell Biol.* 122, 1131–1143.
- Arcangeli, A., Faravelli, L., Bianchi, L., Rosati, B., Gritti, A., Vescovi, A., et al., 1996. Soluble or bound laminin elicit in human neuroblastoma cells short- or long-term potentiation of a  $K^+$  inwardly rectifying current: relevance to neuritogenesis. *Cell Adhes. Commun.* 4, 369–385.
- Arcangeli, A., Crociani, O., Lastraioli, E., Masi, A., Pillozzi, S., Becchetti, A., 2009. Targeting ion channels in cancer: a novel frontier in antineoplastic therapy. *Curr. Med. Chem.* 16, 66–93.
- Arnaout, M.A., Mahalingam, B., Xiong, J.P., 2005. Integrin structure, allostery and bidirectional signalling. *Annu. Rev. Cell Dev. Biol.* 21, 381–410.
- Arnaout, M.A., Goodman, S.L., Xiong, J.P., 2007. Structure and mechanics of integrin-based cell adhesion. *Curr. Opin. Cell Biol.* 19, 295–507.
- Artym, V.V., Petty, H.R., 2002. Molecular proximity of Kv1.3 voltage-gated potassium channels and beta(1)-integrins on the plasma membrane of melanoma cells: effects of cell adherence and channel blockers. *J. Gen. Physiol.* 120, 29–37.
- Baranes, D., Lederfein, D., Huang, H., Chen, M.M., Bailey, C.H., Kandel, E.R., 1998. Tissue plasminogen activator contributes to the late phase of LTP and to synaptic growth in the hippocampal mossy fiber pathway. *Neuron* 21, 813–825.
- Barker, A.T., Jaffe, L.F., Vanable, J.W., 1982. The glabrous epidermis of cavies contains a powerful battery. *Am. J. Physiol.* 242, R358–R366.
- Becker, P.S., Kopecky, K.J., Wilks, A.N., Chien, S., Harlan, J.M., Willman, C.L., et al., 2009. Very late antigen-4 function of myeloblasts correlates with improved overall survival for patients with acute myeloid leukemia. *Blood* 113, 866–874.
- Beeton, C., Wulff, H., Standifer, N.E., Azam, P., Mullen, K.M., Pennington, M.W., et al., 2006. Kv1.3 channels are a therapeutic target for T cell-mediated autoimmune diseases. *Proc. Natl. Acad. Sci. USA* 103, 17414–17419.
- Belvindrah, R., Graus-Porta, D., Goebbels, S., Nave, K.A., Muller, U., 2007. Beta1 integrins in radial glia but not in migrating neurons are essential for the formation of cell layers in the cerebral cortex. *J. Neurosci.* 27, 13854–13865.
- Berger, M., Frairia, R., Piacibello, W., Sanavio, F., Palmero, A., Venturi, C., et al., 2005. Feasibility of cord blood stem cell manipulation with high-energy shock waves: an *in vitro* and *in vivo* study. *Exp. Hematol.* 33, 1371–1387.

- Bernard-Trifilo, J.A., Kramar, A.E., Torp, R., Lin, C.-Y., Pineda, E.A., Lynch, G., et al., 2005. Integrin signaling cascades are operational in adult hippocampal synapses and modulate NMDA receptor physiology. *J. Neurochem.* 93, 834–849.
- Bianchi, L., Wible, B., Arcangeli, A., Tagliatela, M., Morra, F., Castaldo, P., et al., 1998. Herg encodes a  $K^+$  current highly conserved in tumors of different histogenesis: a selective advantage for cancer cells? *Cancer Res.* 58, 815–822.
- Bixby, J.L., Harris, W.A., 1991. Molecular mechanisms of axon growth and guidance. *Annu. Rev. Cell Biol.* 7, 117–159.
- Bixby, J.L., Grunwald, G.B., Bookman, R.J., 1994.  $Ca^{2+}$  influx and neurite growth in response to purified N-Cadherin and laminin. *J. Cell Biol.* 127, 1461–1475.
- Bliss, T.V.P., Lomø, T., 1973. Long-lasting potentiation of synaptic transmission in the dentate gyrus of the anesthetized rabbit following stimulation of the perforant path. *J. Physiol. (London)* 232, 331–356.
- Böriesson, S.J., Elinder, F., 2008. Structure function and modification of the voltage sensor in voltage-gated ion channels. *Cell Biochem. Biophys.* 52, 149–174.
- Bray, D., 2001. *Cell Movements: From Molecules to Motility*, second ed. Garland Science, New York.
- Broussard, J.A., Webb, D.J., Kaverina, I., 2008. Asymmetric focal adhesion disassembly in motile cells. *Curr. Opin. Cell Biol.* 20, 85–90.
- Brugnara, C., 1997. Erythrocyte membrane transport physiology. *Curr. Opin. Hematol.* 4, 122–127.
- Burridge, K., Wennerberg, K., 2004. Rho and Rac take center stage. *Cell* 116, 167–179.
- Cahalan, M.D., Chandy, K.G., 2009. The functional network of ion channels in T lymphocytes. *Immunol. Rev.* 231, 59–87.
- Cahalan, M.D., Chandy, K.G., DeCoursey, T.E., Gupta, S., 1985. A voltage-gated potassium channel in human T lymphocytes. *J. Physiol. (London)* 358, 197–237.
- Carlson, R.O., Masco, D., Brooker, G., Spiegel, S., 1994. Endogenous ganglioside GM1 modulates L-type calcium channel activity in N18 neuroblastoma cells. *J. Neurosci.* 14, 2272–2281.
- Catterall, W.A., 1992. Cellular and molecular biology of voltage-gated sodium channels. *Physiol. Rev.* 72, S15–S48.
- Catterall, W.A., 2000. Structure and regulation of voltage-gated calcium channels. *Annu. Rev. Cell Dev. Biol.* 16, 521–555.
- Cayre, M., Canoll, P., Goldman, J.E., 2009. Cell migration in the normal and pathological postnatal mammalian brain. *Prog. Neurobiol.* 88, 41–63.
- Chae, Y.K., Kang, S.K., Kim, M.S., Woo, J., Lee, J., Chang, S., et al., 2008. Human AQP5 plays a role in the progression of chronic myelogenous leukemia (CML). *PLoS ONE* 3, e2594.
- Chan, C.S., Weeber, E.J., Kurup, S., Sweatt, J.D., Davis, R.L., 2003. Integrin requirement for hippocampal synaptic plasticity and spatial memory. *J. Neurosci.* 23, 7107–7116.
- Chan, C.S., Weeber, E.J., Kurup, S., Fuchs, E., Sweatt, J.D., Davis, R.L., 2006. Beta1-integrins are required for hippocampal AMPA receptor dependent synaptic transmission, synaptic plasticity, and working memory. *J. Neurosci.* 26, 223–232.
- Chan, C.S., Levenson, J.M., Mukhopadhyay, P.S., Zong, L., Bradley, A., Sweatt, J.D., et al., 2007. Alpha3-integrins are required for hippocampal long-term potentiation and working memory. *Learn. Mem.* 14, 606–615.
- Chandy, K.G., DeCoursey, T.E., Cahalan, M.D., McLaughlin, C., Gupta, S., 1984. Voltage-gated potassium channels are required for human T lymphocyte activation. *J. Exp. Med.* 160, 369–385.
- Chandy, K.G., Wulff, H., Beeton, C., Pennington, M., Gutman, G.A., Cahalan, M.D., 2004.  $K^+$  channels as targets for specific immunomodulation. *Trends Pharmacol. Sci.* 25, 280–289.

- Chavis, P., Westbrook, G., 2001. Integrins mediate functional pre- and postsynaptic maturation at a hippocampal synapse. *Nature* 411, 317–321.
- Chen, C., Young, B.A., Coleman, C.S., Pegg, A.E., Sheppard, D., 2004. Spermidine/spermine N1-acetyltransferase specifically binds to the integrin  $\alpha 9$  subunit cytoplasmic domain and enhances cell migration. *J. Cell Biol.* 167, 161–170.
- Chernyavsky, A.I., Arredondo, J., Marubio, L.M., Grando, S.A., 2004. Differential regulation of keratinocyte chemokinesis and chemotaxis through distinct nicotinic receptors subtypes. *J. Cell Sci.* 117, 5665–5679.
- Chernyavsky, A.I., Arredondo, J., Karlsson, E., Wessler, I., Grando, S.A., 2005. The Ras/Raf-1/MEK1/ERK signaling pathway coupled to integrin expression mediates cholinergic regulation of keratinocyte directional migration. *J. Biol. Chem.* 280, 39220–39228.
- Chernyavsky, A.I., Arredondo, J., Qian, J., Galitovskiy, V., Grando, S.A., 2009. Coupling of ionic events to protein kinase signalling cascades upon activation of  $\alpha 7$  nicotinic receptor. Cooperative regulation of  $\alpha 2$ -integrin expression and Rho-kinase activity. *J. Biol. Chem.* 284, 22140–22148.
- Cherubini, A., Pillozzi, S., Hofmann, G., Crociani, O., Guasti, L., Lastraioli, E., et al., 2002. HERG K<sup>+</sup> channels and beta1 integrins interact through the assembly of a macromolecular complex. *Ann. N. Y. Acad. Sci.* 973, 559–561.
- Cherubini, A., Hofmann, G., Pillozzi, S., Guasti, L., Crociani, O., Cilia, E., et al., 2005. hERG1 channels are physically linked to beta1 integrins and modulate adhesion-dependent signalling. *Mol. Biol. Cell* 16, 2972–2983.
- Chun, D., Gall, C.M., Bi, X., Lynch, G., 2001. Evidence that integrins contribute to multiple stages in the consolidation of long term potentiation in rat hippocampus. *Neuroscience* 105, 815–829.
- Clegg, D.O., Wingerd, K.L., Hikita, S.T., Tolhurst, E.C., 2003. Integrins in the development, function and disfunction of the nervous system. *Front. Biosci.* 8, d723–d750.
- Colden-Stanfield, M., 2002. Clustering of very late antigen-4 integrins modulates K(+) currents to alter Ca(2+)-mediated monocyte function. *Am. J. Physiol. Cell Physiol.* 283, C990–C1000.
- Condic, M.L., 2001. Adult neuronal regeneration induced by transgenic integrin expression. *J. Neurosci.* 21, 4782–4788.
- Cook, G., Dumber, M., Franklin, I.M., 1997. The role of adhesion molecules in multiple myeloma. *Acta Haematol.* 97, 81–99.
- Cousin, B., Leloup, C., Penicaud, L., Price, J., 1997. Developmental changes in integrin  $\beta$ -subunits in rat cerebral cortex. *Neurosci. Lett.* 234, 161–165.
- Critchley, D.R., 2000. Focal adhesions—the cytoskeletal connections. *Curr. Opin. Cell Biol.* 12, 133–139.
- Critchley, D.R., Gingras, A.R., 2008. Talin at a glance. *J. Cell Sci.* 121, 1345–1347.
- Crociani, O., Guasti, L., Balzi, M., Becchetti, A., Wanke, E., Olivotto, M., et al., 2003. Cell cycle-dependent expression of HERG1 and HERG1B isoforms in tumor cells. *J. Biol. Chem.* 278, 2947–2955.
- Dani, J.A., Bertrand, D., 2007. Nicotinic acetylcholine receptors and nicotinic cholinergic mechanisms of the central nervous system. *Annu. Rev. Pharmacol. Toxicol.* 47, 699–729.
- Davis, M.J., Wu, X., Nurkiewicz, T.R., Kawasaki, J., Gui, P., Hill, M.A., et al., 2002. Regulation of ion channels by integrins. *Cell Biochem. Biophys.* 36, 41–66.
- DeCoursey, T.E., Chandy, K.G., Gupta, S., Cahalan, M.D., 1984. Voltage-gated K<sup>+</sup> channels in human T lymphocytes: a role in mitogenesis? *Nature* 307, 465–468.
- Defilippi, P., Di Stefano, P., Cabodi, S., 2006. p130Cas: a versatile scaffold in signaling networks. *Trends Cell Biol.* 16, 257–263.

- deHart, G.-W., Jin, T., McCloskey, D.E., Pegg, A.E., Sheppard, D., 2008. The  $\alpha 9\beta 1$  integrin enhances cell migration by polyamine-mediated modulation of an inward-rectifier potassium channel. *Proc. Natl. Acad. Sci. USA* 105, 7188–7193.
- Delcommenne, M., Tan, C., Gray, V., Rue, L., Woodgett, J., Dedhar, S., 1998. Phosphoinositide-3-OH kinase-dependent regulation of glycogen synthase kinase 3 and protein kinase B/AKT by the integrin-linked kinase. *Proc. Natl. Acad. Sci. USA* 95, 11211–11216.
- Denda, S., Reichardt, L.S., 2007. Studies on integrins in the nervous system. *Methods Enzymol.* 426, 203–221.
- Denucci, C.C., Mitchell, J.S., Shimizu, Y., 2009. Integrin function in T-cell homing to lymphoid and nonlymphoid sites: getting there and staying there. *Crit. Rev. Immunol.* 29, 87–109.
- dePereda, J.M., Wiche, G., Liddington, R.C., 1999. Crystal structure of a tandem pair of fibronectin type III domains from the cytoplasmic tail of integrin  $\alpha 6\beta 4$ . *EMBO J.* 18, 4087–4095.
- Dike, L.E., Farmer, S.R., 1998. Cell adhesion induces expression of growth-associated genes in suspension-arrested fibroblasts. *Proc. Natl. Acad. Sci. USA* 85, 6792–6796.
- Dityatev, A., Frischknecht, R., Seidenbecher, C.I., 2006. Extracellular matrix and synaptic functions. *Results Probl. Cell Differ.* 43, 69–97.
- Dixon, S.J., Stewart, D., Grinstein, S., Spiegel, S., 1987. Transmembrane signalling by the B subunit of cholera toxin: increased cytoplasmic free calcium in rat lymphocytes. *J. Cell Biol.* 105, 1153–1161.
- Doherty, P., Ashton, S.V., Moore, S.E., Walsh, S.F., 1991. Morphoregulatory activities of N-CAM and N-cadherin can be accounted for by G protein-dependent activation of L- and N-type neuronal calcium channels. *Cell* 67, 21–34.
- Douglass, J., Osborne, P.B., Cai, Y.C., Wilkinson, M., Christie, M.J., Adelman, J.P., 1990. Characterization and functional expression of a rat genomic DNA clone encoding a lymphocyte potassium channel. *J. Immunol.* 144, 4841–4850.
- Doyle, D.A., Cabral, J.M., Pfuetzner, R.A., Kuo, A., Gulbis, J.M., Cohen, L.S., et al., 1998. The structure of the potassium channel: molecular basis of  $K^+$  conduction and selectivity. *Science* 280, 69–77.
- Dunker, A.K., Cortese, M.S., Romero, P., Iakoncheva, L.M., Uversky, V.N., 2005. Flexible nets. The roles of intrinsic disorder in protein interaction networks. *FEBS J.* 272, 5129–5148.
- Dustin, M.L., de Fougères, A.R., 2001. Reprogramming T cells: the role of extracellular matrix in coordination of T cell activation and migration. *Curr. Opin. Immunol.* 13, 286–290.
- Eierman, D.F., Johnson, C.E., Haskill, J.S., 1989. Human monocyte inflammatory mediator gene expression is selectively regulated by adherence substrates. *J. Immunol.* 142, 1970–1976.
- Essin, K., Gollasch, M., Rolle, S., Weissgerber, P., Sausbier, M., Bohn, E., et al., 2009. BK channels in innate immune functions of neutrophils and macrophages. *Blood* 113, 1326–1331.
- Ezratty, E.J., Partridge, M.A., Gundersen, G.G., 2005. Microtubule-induced focal adhesion disassembly is mediated by dynamin and focal adhesion kinase. *Nat. Cell Biol.* 7, 581–590.
- Fang, Y., Wu, G., Xie, X., Lu, Z.-H., Ledeen, R.W., 2000. Endogenous GM1 ganglioside of the plasma membrane promotes neuritogenesis by two mechanisms. *Neurochem. Res.* 25, 931–940.
- Fang, Y., Xie, X., Ledeen, R.W., Wu, G., 2002. Characterization of cholera toxin B subunit-induced  $Ca^{2+}$  influx in neuroblastoma cells: evidence for a voltage independent GM1-associated  $Ca^{2+}$  channel. *J. Neurosci. Res.* 57, 1–10.

- Fordyce, C.B., Jagasia, R., Zhu, X., Schlichter, L.C., 2005. Microglia Kv1.3 channels contribute to their ability to kill neurons. *J. Neurosci.* 25, 7139–7149.
- Fukushima, Y., Hagiwara, S., 1985. Currents carried by monovalent cations through calcium channels in mouse neoplastic B lymphocytes. *J. Physiol. (London)* 358, 255–284.
- Fukushima, Y., Hagiwara, S., Henkart, M., 1984. Potassium current in clonal cytotoxic T lymphocytes from the mouse. *J. Physiol. (London)* 351, 645–656.
- Gabius, H.J., Andre, S., Kaltner, H., Siebert, H.C., 2002. The sugar code: functional lectinomics. *Biochem. Biophys. Acta* 1572, 165–177.
- Gall, C.M., Lynch, G., 2004. Integrins, synaptic plasticity, and epileptogenesis. *Adv. Exp. Med. Biol.* 548, 12–33.
- Gallin, E.K., 1991. Ion channels in leukocytes. *Physiol. Rev.* 71, 775–811.
- Gardos, G., 1958. The function of calcium in the potassium permeability of human erythrocytes. *Biochem. Biophys. Acta* 30, 653–654.
- Gee, A.P., 1984. Advantages and limitations of methods for measuring cellular chemotaxis and chemokinesis. *Mol. Cell. Biochem.* 62, 5–11.
- Giancotti, F.G., Tarone, G., 2003. Positional control of cell fate through joint integrin/receptor protein kinase signaling. *Annu. Rev. Cell Dev. Biol.* 19, 173–206.
- Goldfinger, L.E., Han, J., Kiosses, W.B., Howe, A.K., Ginsberg, M.H., 2003. Spatial restriction of alpha4 integrin phosphorylation regulates lamellipodial stability and alpha4-beta1 dependent cell migration. *J. Cell Biol.* 162, 731–741.
- Gomez, T.M., Zheng, J.Q., 2006. The molecular basis for calcium-dependent axon path-finding. *Nat. Rev. Neurosci.* 7, 115–125.
- Gotti, C., Clementi, F., 2004. Neuronal nicotinic receptors: from structure to pathology. *Prog. Neurobiol.* 74, 363–396.
- Grabovsky, V., Feigelson, S., Chen, C., Bleijs, D.A., Peled, A., Cinamon, G., et al., 2000. Subsecond induction of alpha4 integrin clustering by immobilized chemokines stimulates leukocyte tethering and rolling on endothelial vascular cell adhesion molecule 1 under flow conditions. *J. Exp. Med.* 192, 495–506.
- Graus-Porta, D., Blaess, S., Senften, M., Littlewood-Evans, A., Damsky, C., Huang, Z., et al., 2001.  $\beta$ 1-class integrin regulate the development of laminae and folia in the cerebral and cerebellar cortex. *Neuron* 31, 367–379.
- Grotewiel, M.S., Beck, C.D., Wu, K.H., Zhu, X.R., Davis, R.L., 1998. Integrin-mediated short-term memory in *Drosophila*. *Nature* 391, 455–460.
- Grygorczyk, R., Schwarz, W., 1983. Properties of the  $\text{Ca}^{2+}$ -activated  $\text{K}^{+}$  conductance of human red cells as revealed by the patch-clamp technique. *Cell Calcium* 4, 499–510.
- Gui, P., Chao, J.-T., Wu, X., Yang, Y., Davis, G.E., Davis, M.J., 2008. Coordinated regulation of vascular  $\text{Ca}^{2+}$  and  $\text{K}^{+}$  channels by integrin signaling. Epub: [www.landbioscience.com/curie/chapter/4042](http://www.landbioscience.com/curie/chapter/4042). In: Becchetti, A., Arcangeli, A. (Eds.), *Integrin Receptors and Ion Channels: Molecular Complexes and Signaling*. Landes Bioscience (in press).
- Gutman, G.A., Chandy, K.G., Grissmer, S., Lazdunski, M., McKinnon, D., Pardo, L.A., et al., 2005. International Union of Pharmacology. LIII. Nomenclature and molecular relationships of voltage-gated potassium channels. *Pharmacol. Rev.* 57, 473–508.
- Haghighi, A.P., Cooper, E., 1998. Neuronal nicotinic acetylcholine receptors are blocked by intracellular spermine in a voltage-dependent manner. *J. Neurosci.* 18, 3050–4092.
- Han, J., Rose, D.M., Woodside, D.G., Goldfinger, M.E., Ginsberg, M.H., 2003. Integrin alpha 4 beta 1-dependent T cell migration requires both phosphorylation and dephosphorylation of the alpha 4 cytoplasmic domain to regulate the reversible binding of paxillin. *J. Biol. Chem.* 278, 34845–34853.
- Hannigan, G.E., Leung-Hageteijn, C., Fitz-Gibbon, L., Coppolino, M.G., Radeva, G., Filmus, J., et al., 1996. Regulation of cell adhesion and anchorage-dependent growth by a new beta 1-integrin-linked protein kinase. *Nature* 379, 91–96.

- Hannigan, G., Troussard, A.A., Dedhar, S., 2005. Integrin-linked kinase: a cancer therapeutic target unique among its ILK. *Nat. Rev. Cancer* 5, 51–63.
- Hanson, M.G., Landmesser, L.T., 2004. Normal patterns of spontaneous activity are required for correct motor axon guidance and the expression of specific guidance molecules. *Neuron* 43, 687–701.
- Hartmann, T.N., Burger, J.A., Glodek, A., Fujii, N., Burger, M., 2005. CXCR4 chemokine receptor and integrin signaling co-operate in mediating adhesion and chemoresistance in small cell lung cancer (SCLC) cells. *Oncogene* 24, 4462–4471.
- Hartmann, T.N., Grabovsky, V., Wang, W., Desch, P., Rubenzer, G., Wollner, S., et al., 2009. Circulating B-cell chronic lymphocytic leukemia cells display impaired migration to lymph nodes and bone marrow. *Cancer Res.* 69, 3121–3130.
- Heiner, I., Eisfeld, J., Halaszovich, C.R., Wehage, E., Jüngling, E., Zitt, C., et al., 2003. Expression profile of the transient receptor potential (TRP) family in neutrophil granulocytes: evidence for currents through long TRP channel 2 induced by ADP-ribose and NAD. *Biochem. J.* 371, 1045–1053.
- Hilgenberg, L.G., Smith, M.A., 2004. Agrin signaling in cortical neurons is mediated by a tyrosine kinase-dependent increase in intracellular  $Ca^{2+}$  that engages both CaMKII and MAPK signal pathways. *J. Neurobiol.* 61, 289–300.
- Hofmann, G., Bernabei, P.A., Crociani, O., Cherubini, A., Guasti, L., Pillozzi, S., et al., 2001. HERG  $K^+$  channels activation during beta(1) integrin-mediated adhesion to fibronectin induces an up-regulation of alpha(v)beta(3) integrin in the preosteoclastic leukemia cell line FLG 29.1. *J. Biol. Chem.* 276, 4923–4931.
- Hynes, R.O., 2002. Integrins: bidirectional, allosteric signaling machines. *Cell* 110, 673–687.
- Illes, P., Alexandre, R.J., 2004. Molecular physiology of P2 receptors in the central nervous system. *Eur. J. Pharmacol.* 483, 5–17.
- Ishikawa, Y., Horii, Y., Tamura, H., Shiosaka, S., 2008. Neuropsin (KLK8)-dependent and -independent synaptic tagging in the Schaffer-collateral pathway of mouse hippocampus. *J. Neurosci.* 28, 843–849.
- Itoh, K., Stevens, B., Schachner, M., Fields, R.D., 1995. Regulated expression of the neural cell adhesion molecule L1 by specific patterns of neural impulses. *Science* 270, 1369–1372.
- Ivankovic-Dikic, I., Gronroos, E., Blaukat, A., Barth, B.-U., Dikic, I., 2000. Pyk2 and FAK regulate neurite outgrowth induced by growth factors and integrins. *Nat. Cell Biol.* 2, 574–581.
- Jacques-Fricke, B.T., Seow, Y., Gottlieb, P.A., Sachs, F., Gomez, T.M., 2006.  $Ca^{2+}$  influx through mechanosensitive channels inhibits neurite outgrowth in opposition to other influx pathways and release from intracellular stores. *J. Neurosci.* 26, 5656–5664.
- Jeske, N.A., Patwardhan, A.M., Henry, M.A., Milam, S.B., 2009. Fibronectin stimulates TRPV1 translocation in primary sensory neurons. *J. Neurochem.* 108, 591–600.
- Jiang, Y., Lee, A., Chen, J., Cadene, M., Chait, B.T., MacKinnon, R., 2002. Crystal structure and mechanism of a calcium gated potassium channel. *Nature* 417, 515–522.
- Jin, L., Tabe, Y., Konoplev, S., Xu, Y., Leysath, C.E., Lu, H., et al., 2008. CXCR4 up-regulation by imatinib induces chronic myelogenous leukemia (CML) cell migration to bone marrow stroma and promotes survival of quiescent CML cells. *Mol. Cancer Ther.* 7, 48–58.
- Kandel, E.R., Schwartz, J.H., Jessell, T.M. (Eds.), 2000. *Principles of Neural Science*, fourth ed. McGraw-Hill, New York.
- Kater, S.B., Mattson, M.P., Cohan, C., Connor, J., 1988. Calcium regulation of the neuronal growth cone. *Trends Neurosci.* 11, 315–321.
- Kim, M., Jiang, L.-H., Wilson, H.L., North, R.A., Suprenant, A., 2001. Proteomic and functional evidence for a P2X7 receptor signalling complex. *EMBO J.* 20, 6347–6358.



- Kim, M., Carman, C.V., Springer, T.A., 2003. Bidirectional transmembrane signaling by cytoplasmic domain separation in integrins. *Science* 301, 1720–1725.
- Kobune, M., Chiba, H., Kato, J., Kato, K., Nakamura, K., Kawano, Y., et al., 2007. Wnt3/RhoA/ROCK signaling pathway is involved in adhesion-mediated drug resistance of multiple myeloma in an autocrine mechanism. *Mol. Cancer Ther.* 6, 1774–1784.
- Kofuji, P., Newman, E.A., 2004. Potassium buffering in the central nervous system. *Neuroscience* 129, 1045–1056.
- Köles, L., Fürst, S., Illes, P., 2007. Purine ionotropic (P2X) receptors. *Curr. Pharm. Des.* 13, 2368–2384.
- Konopleva, M., Konoplev, S., Hu, W., Zaritskey, A.Y., Afanasiev, B.V., Andreeff, M., 2002. Stromal cells prevent apoptosis of AML cells by up-regulation of anti-apoptotic proteins. *Leukemia* 16, 1713–1724.
- Kramar, E.A., Bernard, J.A., Gall, C.M., Lynch, G., 2002. Alpha3 integrin receptors contribute to the consolidation of long-term potentiation. *Neuroscience* 110, 29–39.
- Kramar, E.A., Bernard, J.A., Gall, C.M., Lynch, G., 2003. Integrins modulate fast synaptic transmission at hippocampal synapses. *J. Biol. Chem.* 278, 10722–10730.
- Kramar, E.A., Lin, B., Rex, C.S., Gall, C.M., Lynch, G., 2006. Integrin-driven actin polymerization consolidates long-term potentiation. *Proc. Natl. Acad. Sci. USA* 103, 5579–5584.
- Krasznai, Z., 2005. Ion channels in T cells: from molecular pharmacology to therapy. *Arch. Immunol. Ther. Exp. (Warsz.)* 53, 127–135.
- Kubo, Y., Baldwin, T.J., Jan, Y.N., Jan, L.Y., 1993. Primary structure and functional expression of a mouse inward rectifier potassium channel. *Nature* 362, 127–133.
- Kurtova, A.V., Tamayo, A.T., Ford, R.J., Burger, J.A., 2009. Mantle cell lymphoma cells express high levels of CXCR4, CXCR5, and VLA-4 (CD49d): importance for interactions with the stromal microenvironment and specific targeting. *Blood* 113, 4604–4613.
- Lang, F., Föller, M., Lang, K.S., Lang, P.A., Ritter, M., Gulbins, E., et al., 2005. Ion channels in cell proliferation and apoptotic cell death. *J. Membr. Biol.* 205, 147–157.
- Lastrioli, E., Guasti, L., Crociani, O., Polvani, S., Hofmann, G., Witchel, H., et al., 2004. *herg1* gene and HERG1 protein are overexpressed in colorectal cancers and regulate cell invasion of tumor cells. *Cancer Res.* 64, 606–611.
- Lau, T.L., Partridge, A.W., Ginsberg, M.H., Ulmer, T.S., 2008a. Structure of the integrin  $\beta 3$  transmembrane segment in phospholipid bicelles and detergent micelles. *Biochemistry* 47, 4008–4016.
- Lau, T.L., Dua, V., Ulmer, T.S., 2008b. Structure of the integrin  $\alpha$ IIb transmembrane segment. *J. Biol. Chem.* 283, 16162–16168.
- Ledeen, R.W., Wu, G., 1992. Ganglioside function in the neuron. *Trends Glycosci. Glycotechnol.* 4, 174–187.
- Ledeen, R.W., Wu, G., 2002. Ganglioside function in calcium homeostasis and signalling. *Neurochem. Res.* 27, 637–647.
- Lee, S.P., Youn, S.W., Cho, H.J., Li, L., Kim, T.Y., Yook, H.S., et al., 2006. Integrin-linked kinase, a hypoxia-responsive molecule, controls postnatal vasculogenesis by recruitment of endothelial progenitor cells to ischemic tissue. *Circulation* 114, 150–159.
- Legate, K.R., Montañez, E., Kudlacek, O., Fässler, R., 2006. ILK, PINCH and parvin: the tIPP of integrin signaling. *Nat. Rev. Mol. Cell Biol.* 7, 20–31.
- Lendvai, B., Vizi, E.S., 2008. Nonsynaptic chemical transmission through nicotinic acetylcholine receptors. *Physiol. Rev.* 88, 333–340.
- Levite, M., Cahalon, L., Peretz, A., Hershkoviz, R., Sobko, A., Ariel, A., et al., 2000. Extracellular K(+) and opening of voltage-gated potassium channels activate T cell integrin function: physical and functional association between Kv1.3 channels and beta1 integrins. *J. Exp. Med.* 191, 1167–1176.
- Ley, K., Reuterman, J., 2006. Leucocyte-endothelial interactions in health and disease. *Handb. Exp. Pharmacol.* 176, 97–133.

- Li, H., Liu, L., Guo, L., Zhang, J., Du, W., Li, X., et al., 2008. HERG K<sup>+</sup> channel expression in CD34<sup>+</sup>/CD38<sup>-</sup>/CD123(high) cells and primary leukemia cells and analysis of its regulation in leukemia cells. *Int. J. Hematol.* 87, 387–392.
- Liddington, R.C., Ginsberg, M.H., 2002. Integrin activation takes shape. *J. Cell Biol.* 158, 833–839.
- Liesveld, J.L., 1997. Expression and function of adhesion receptors in acute myelogenous leukemia: parallels with normal erythroid and myeloid progenitors. *Acta Haematol.* 97, 53–62.
- Lin, B., Arai, A.C., Lynch, G., Gall, C.M., 2003. Integrins regulate NMDA receptor-mediated synaptic currents. *J. Neurophysiol.* 89, 2874–2878.
- Lin, C.-Y., Lynch, G., Gall, C.M., 2005a. AMPA receptor stimulation increases  $\alpha 5\beta 1$  integrin surface expression, adhesive function and signaling. *J. Neurochem.* 94, 531–546.
- Lin, J., Miller, M.J., Shaw, A.S., 2005b. The c-SMAC: sorting it all out (or in). *J. Cell Biol.* 170, 177–182.
- Lin, C.-Y., Hilgenberg, L.G., Smith, M.A., Lynch, G., Gall, C.M., 2008. Integrin regulation of cytoplasmic calcium in excitatory neurons depends upon glutamate receptors and release from intracellular stores. *Mol. Cell. Neurosci.* 37, 770–780.
- Liu, S., Thomas, S.M., Woodside, D.G., Rose, D.M., Kiosses, W.B., Pfaff, M., et al., 1999. Binding of paxillin to  $\alpha 4$  integrins modifies integrin-dependent biological responses. *Nature* 402, 676–681.
- Liu, S., Slepak, M., Ginsberg, M.H., 2001. Binding of paxillin to the  $\alpha 9$  integrin cytoplasmic domain inhibits cell spreading. *J. Biol. Chem.* 276, 37086–37092.
- Logsdon, N.J., Kang, J., Togo, J.A., Christian, E.P., Aiyar, J., 1997. A novel gene, hKCa4, encodes the calcium-activated potassium channel in human T lymphocytes. *J. Biol. Chem.* 272, 32723–32726.
- López, J.J., Salido, G.M., Pariente, J.A., Rosado, J.A., 2006. Interaction of STIM1 with endogenously expressed human canonical TRP1 upon depletion of intracellular Ca<sup>2+</sup> stores. *J. Biol. Chem.* 281, 28254–28264.
- Lu, Z., 2004. Mechanism of rectification in inward-rectifier K<sup>+</sup> channels. *Annu. Rev. Physiol.* 66, 103–129.
- Luo, B.H., Springer, T.A., Takagi, J.A., 2004. A specific interface between integrin transmembrane helices and affinity for ligand. *PLoS Biol.* 2, 776–786.
- Luther, P.W., Peng, H.B., 1985. Membrane-related specializations associated with acetylcholine receptor aggregates induced by electric fields. *J. Cell Biol.* 100, 235–244.
- Masco, D., Van de Walle, M., Spiegel, S., 1991. Interaction of ganglioside GM1 with the B subunit of cholera toxin modulates growth and differentiation of neuroblastoma N18 cells. *J. Neurosci.* 11, 2443–2452.
- Matsunaga, T., Takemoto, N., Sato, T., Takimoto, R., Tanaka, I., Fujimi, A., et al., 2003. Interaction between leukemic cell VLA-4 and stromal fibronectin is a decisive factor for minimal residual disease of acute myelogenous leukemia. *Nat. Med.* 9, 1158–1165.
- Matteson, D.R., Deutsch, C.K., 1984. channels in T lymphocytes: a patch clamp study using monoclonal antibody adhesion. *Nature* 307, 468–471.
- Mattson, M.P., Bazan, N.G., 2006. Apoptosis and necrosis. In: Siegel, G.J., Albers, R.W., Brady, S.T., Price, D.L. (Eds.), *Basic Neurochemistry*, seventh ed. Elsevier Academic Press, Burlington, pp. 603–615.
- Mayer, M.L., 2005. Glutamate receptor ion channels. *Curr. Opin. Neurobiol.* 15, 282–288.
- Mayer, M.L., Armstrong, N., 2004. Structure and function of glutamate receptor ion channels. *Annu. Rev. Physiol.* 66, 161–181.
- McDonald, P.C., Fielding, A.B., Dedhar, S., 2008. Integrin-linked kinase—essential roles in physiology and cancer biology. *J. Cell Sci.* 121, 3121–3132.
- Menegazzi, R., Busetto, S., Decliva, E., Cramer, R., Dri, P., Patriarca, P., 1999. Triggering of chloride ion efflux from human neutrophils as a novel function of leukocyte beta 2

- integrins: relationship with spreading and activation of the respiratory burst. *J. Immunol.* 162, 423–434.
- Michaluk, P., Mikasova, L., Groc, L., Frischknecht, R., Choquet, D., Kaczmarek, L., 2009. Matrix metalloproteinase-9 controls NMDA receptor surface diffusion through integrin  $\beta 1$  signaling. *J. Neurosci.* 29, 6007–6012.
- Michishita, M., Videm, V., Arnaout, M.A., 1993. A novel divalent cation-binding site in the A domain of the beta2 integrin CR3 (CD11b/Cd18) is essential for ligand binding. *Cell* 72, 857–867.
- Mikkola, H.K., Fujiwara, Y., Schlaeger, T.M., Traver, D., Orkin, S.H., 2003. Expression of CD41 marks the initiation of definitive hematopoiesis in the mouse embryo. *Blood* 101, 508–516.
- Milani, D., Minozzi, M.-C., Petrelli, L., Guidolin, D., Skaper, S.D., Spoerri, P.E., 1992. Interaction of ganglioside GM1 with the B subunit of cholera toxin modulates free calcium in sensory neurons. *J. Neurosci. Res.* 33, 446–475.
- Miranti, C.K., Brugge, J.S., 2002. Sensing the environment. A historical perspective of integrin signal transduction. *Nat. Cell Biol.* 4, E83–E90.
- Mocchetti, I., 2005. Exogenous gangliosides, neuronal plasticity and repair, and the neurotrophins. *Cell. Mol. Life Sci.* 62, 2283–2294.
- Morini, R., Becchetti, A., 2008. Integrin receptors and ligand-gated channels. In: Becchetti, A., Arcangeli, A. (Eds.), *Integrin Receptors and Ion Channels: Molecular Complexes and Signaling*. Landes Bioscience (in press). Epub: [www.landesbioscience.com/curie/chapter/4014](http://www.landesbioscience.com/curie/chapter/4014).
- Nagy, V., Bozdagi, O., Matynia, A., Balcerzyk, M., Okulski, P., Dzwonek, J., et al., 2006. Matrix metalloproteinase-9 is required for hippocampal late-phase long-term potentiation and memory. *J. Neurosci.* 26, 1923–1934.
- Nasu-Tada, K., Koizumi, S., Tsuda, M., Kunifusa, E., Inoue, K., 2006. Possible involvement of increase in spinal fibronectin following peripheral nerve injury in upregulation of microglial P2X4, a key molecule for mechanical allodynia. *Glia* 53, 769–775.
- Nedergaard, M., Takano, T., Hansen, A.J., 2002. Beyond the role of glutamate as a neurotransmitter. *Nat. Rev. Neurosci.* 3, 748–753.
- Nichols, C.G., Lopatin, A.N., 1997. Inward rectifier potassium channels. *Annu. Rev. Physiol.* 59, 171–191.
- Nilius, B., Owsianik, G., Voets, Y., Peters, J.A., 2007. Transient receptor potential cation channels in disease. *Physiol. Rev.* 87, 165–217.
- Nishimune, H., Sanes, J.R., Carlson, S.S., 2004. A synaptic laminin-calcium channel interaction organizes active zones in motor nerve terminal. *Nature* 432, 580–587.
- Nishimura, K.Y., Isseroff, R.R., Nuccitelli, R., 1996. Human keratinocytes migrate to the negative pole in direct current electric fields comparable to those measured in mammalian wounds. *J. Cell Sci.* 109, 199–207.
- Nishimura, S.L., Boylen, K.P., Einheber, S., Milner, T.A., Ramos, D.M., Pytela, R., 1998. Synaptic and glial localization of the integrin  $\alpha$ v $\beta$ 8 in mouse and rat brain. *Brain Res.* 791, 271–282.
- Noborio-Hatano, K., Kikuchi, J., Takatoku, M., Shimizu, R., Wada, T., Ueda, M., et al., 2009. Bortezomib overcomes cell-adhesion-mediated drug resistance through down-regulation of VLA-4 expression in multiple myeloma. *Oncogene* 28, 231–242.
- North, R.A., 2002. Molecular physiology of P2X receptors. *Physiol. Rev.* 82, 1013–1067.
- Nüchel, H., Switala, M., Collins, C.H., Sellmann, L., Grosse-Wilde, H., Dührsen, U., et al., 2009. High CD49d protein and mRNA expression predicts poor outcome in chronic lymphocytic leukemia. *Clin. Immunol.* 131, 472–480.
- Nutile-McMenemy, N., Elfenbein, A., Deleo, J.A., 2007. Minocycline decreases *in vitro* microglial motility, beta1-integrin, and Kv1.3 channel expression. *J. Neurochem.* 103, 2035–2046.

- O'Hanlon, G.M., Hirst, T.R., Willison, H.J., 2003. Ganglioside GM1 binding toxins and human neuropathy-associated IgM antibodies differentially promote neuritogenesis in a PC12 assay. *Neurosci. Res.* 47, 383–390.
- Oh-hora, M., Rao, A., 2008. Calcium signaling in lymphocytes. *Curr. Opin. Immunol.* 20, 250–258.
- Ooashi, N., Futatsugi, A., Yoshihara, F., Mikoshiba, K., Kamiguchi, H., 2005. Cell adhesion molecules regulate  $Ca^{2+}$ -mediated steering of growth cones via cyclic AMP and ryanodine receptor type 3. *J. Cell Biol.* 170, 1159–1167.
- Parsons, J.T., 2003. Focal adhesion kinase: the first ten years. *J. Cell Sci.* 116, 1409–1416.
- Payrastré, B., Missy, K., Trumel, C., Bodin, S., Plantavid, M., Chap, H., 2000. The integrin  $\alpha$  IIb/ $\beta$  3 in human platelet signal transduction. *Biochem. Pharmacol.* 60, 1069–1074.
- Pedersen, S.F., Hoffmann, E.K., Mills, J.W., 2001. The cytoskeleton and cell volume regulation. *Comp. Biochem. Physiol.* 130, 385–399.
- Pegg, A.E., 2008. Spermidine/spermine-N(1)-acetyltransferase: a key metabolic regulator. *Am. J. Physiol. Endocrinol. Metab.* 294, E995–E1010.
- Peng, H.B., Baker, L.P., Dai, Z., 1993. A role of tyrosine phosphorylation in the formation of acetylcholine receptor clusters induced by electric fields in cultured *Xenopus* muscle cells. *J. Cell Biol.* 120, 197–204.
- Pillozzi, S., Brizzi, M.F., Balzi, M., Crociani, O., Cherubini, A., Guasti, L., et al., 2002. HERG potassium channels are constitutively expressed in primary human acute myeloid leukemias and regulate cell proliferation of normal and leukemic hemopoietic progenitors. *Leukemia* 16, 1791–1798.
- Pillozzi, S., Brizzi, M.F., Bernabei, P.A., Bartolozzi, B., Caporale, R., Basile, V., et al., 2007a. VEGFR-1 (FLT-1),  $\beta$ 1 integrin, and hERG  $K^+$  can form a macromolecular signaling complex in acute myeloid leukemia: role in cell migration and clinical outcome. *Blood* 110, 1238–1250.
- Pillozzi, S., Accordi, B., Veltroni, M., Masselli, M., Pancrazzi, E., Gaipa, G., et al., 2007b. Expression and role of hERG1 channels in pediatric acute lymphoblastic leukaemias: shortcoming of drug resistance by hERG1 channel inhibitors in stroma-supported leukaemia cell cultures *in vitro*. *Blood* 110, 222A.
- Pillozzi, S., Masselli, M., De Lorenzo, E., Accordi, B., Cilia, E., Crociani, O., Amedei, A., et al., 2009. Chemotherapy resistance in acute lymphoblastic leukemia requires hERG1 channels and is overcome by hERG1 blockers. Submitted to *J Clin Inv*.
- Pinkstaff, J.K., Lynch, G., Gall, C., 1998. Localization and seizure-regulation of integrin  $\beta$ 1 mRNA in adult rat brain. *Mol. Brain Res.* 55, 265–276.
- Pinkstaff, J.K., Detterich, J., Lynch, G., Gall, C., 1999. Integrin subunit gene expression is regionally differentiated in adult brain. *J. Neurosci.* 19, 1541–1556.
- Poo, M.M., 1981. In situ electrophoresis of membrane components. *Annu. Rev. Biophys. Bioeng.* 10, 245–276.
- Porter, B.E., Weis, J., Sanes, J.R., 1995. A motoneuron-selective stop signal in the synaptic protein S-lamimin. *Neuron.* 14, 549–559.
- Pottosin, I.I., Bonales-Alatorre, E., Valencia-Cruz, G., Mendoza-Magaña, M.L., Dobrovinskaya, O.R., 2008. TRESK-like potassium channels in leukemic T cells. *Pflügers Arch.* 456, 1037–1048.
- Quattrini, A., Lorenzetti, I., Sciorati, G., Corbo, M., Previtali, S.C., Feltri, M.L., et al., 2001. Human IgM anti GM1 autoantibodies modulate intracellular calcium homeostasis in neuroblastoma cells. *J. Neuroimmunol.* 114, 213–219.
- Ray, R.M., McCormack, S.A., Covington, C., Viar, M.J., Zheng, Y., Johnson, L.R., 2003. The requirement for polyamines for intestinal epithelial cell migration is mediated through Rac1. *J. Biol. Chem.* 278, 13039–13046.
- Recher, C., Ysebaert, L., Beyne-Rauzy, O., Mansat-De Mas, V., Ruidavets, J.B., Cariven, P., et al., 2004. Expression of focal adhesion kinase in acute myeloid leukemia

- is associated with enhanced blast migration, increased cellularity, and poor prognosis. *Cancer Res.* 64, 3191–3197.
- Rezzonico, R., Cayatte, C., Bourget-Ponzio, I., Romey, G., Belhacene, M., Loubat, A., et al., 2003. Focal adhesion kinase pp 125FAK interacts with the large conductance calcium-activated hSlo potassium channel in human osteoblasts: potential role in mechanotransduction. *J. Bone Miner. Res.* 18, 1863–1871.
- Ridley, A.E., Schwartz, M.A., Burridge, K., Firtel, R.A., Ginsberg, M.H., Borisy, G., et al., 2003. Cell migration: integrating signals from front to back. *Science* 302, 1704–1709.
- Rose, D.M., Alon, R., Ginsberg, M.H., 2007. Integrin modulation and signaling in leukocyte adhesion and migration. *Immunol. Rev.* 218, 126–134.
- Sann, S.B., Xu, L., Nishimune, H., Sanes, J.R., Spitzer, N.C., 2008. Neurite outgrowth and *in vivo* sensory innervation mediated by a Cav2.2-laminin  $\beta 2$  stop signal. *J. Neurosci.* 28, 2366–2374.
- Schmid, R.S., Anton, E.S., 2003. Role of integrins in the development of the cerebral cortex. *Cereb. Cortex* 13, 219–224.
- Schmid, R.S., Jo, R., Shelton, S., Kreidberg, J.A., Anton, E.S., 2005. Reelin, integrin and DAB1 interaction during embryonic cerebral cortical development. *Cereb. Cortex* 15, 1632–1636.
- Schuller, H.M., 2009. Is cancer triggered by altered signalling of nicotinic acetylcholine receptors? *Nat. Rev. Cancer* 9, 195–205.
- Schwab, A., Nechyporuk-Zloy, V., Fabian, A., Stock, C., 2007. Cells move when ions and water flow. *Pflügers Arch.* 453, 421–432.
- Schwab, A., Hanley, P., Fabian, A., Stock, C., 2008. Potassium channels keep mobile cells on the go. *Physiology* 23, 212–220.
- Schwartz, M.A., Ginsberg, M.H., 2002. Networks and crosstalk: integrin signalling spreads. *Nat. Cell Biol.* 4, E65–E68.
- Semenova, S.B., Vassilieva, I.O., Fomina, A.F., Runov, A.L., Negulyaev, Y.A., 2009. Endogenous expression of TRPV5 and TRPV6 calcium channels in human leukemia K562 cells. *Am. J. Physiol. Cell Physiol.* 296, C1098–C1104.
- Shirihai, O., Merchav, S., Attali, B., Dagan, D., 1996. K<sup>+</sup> channel antisense oligodeoxynucleotides inhibit cytokine-induced expansion of human hemopoietic progenitors. *Pflügers Arch.* 431, 632–638.
- Shirihai, O., Attali, B., Dagan, D., Merchav, S., 1998. Expression of two inward rectifier potassium channels is essential for differentiation of primitive human hematopoietic progenitor cells. *J. Cell. Physiol.* 177, 197–205.
- Smith, G.A., Tsui, H.W., Newell, E.W., Jiang, X., Zhu, X.P., Tsui, F.W., et al., 2002. Functional up-regulation of HERG K<sup>+</sup> channels in neoplastic hematopoietic cells. *J. Biol. Chem.* 277, 18528–18534.
- Soligo, D., Schirò, R., Luksch, R., Manara, G., Quirici, N., Parravicini, C., et al., 1990. Expression of integrins in human bone marrow. *Br. J. Haematol.* 76, 323–332.
- Sontheimer, H., 2008. An unexpected role for ion channels in brain tumor metastasis. *Exp. Biol. Med.* 233, 779–791.
- Spitzer, N.C., 2006. Electrical activity in early neuronal development. *Nature* 444, 707–712.
- Stäubli, U., Vanderklish, P., Lynch, G., 1990. An inhibitor of integrin receptors blocks long-term potentiation. *Behav. Neural Biol.* 53, 1–5.
- Stäubli, U., Chun, D., Lynch, G., 1998. Time-dependent reversal of long-term potentiation by an integrin antagonist. *J. Neurosci.* 18, 3460–3469.
- Sunderland, W.J., Son, Y.J., Miner, J.H., Sanes, J.R., Carlson, S.S., 2000. The presynaptic calcium channel is part of a transmembrane complex linking a synaptic laminin ( $\alpha 4 \beta 2 \gamma 1$ ) with non-erythroid spectrin. *J. Neurosci.* 20, 1009–1019.

- Tabe, Y., Jin, L., Tsutsumi-Ishii, Y., Xu, Y., McQueen, T., Priebe, W., et al., 2007. Activation of integrin-linked kinase is a critical prosurvival pathway induced in leukemic cells by bone marrow-derived stromal cells. *Cancer Res.* 67, 684–694.
- Talavera, K., Nilius, B., Voets, T., 2008. Neuronal TRP channels: thermometers, pathfinders and life-savers. *Trends Neurosci.* 31, 287–295.
- Tamura, H., Ishikawa, Y., Hino, N., Maeda, M., Yoshida, S., Kaku, S., et al., 2006. Neuropsin is essential for early processes of memory acquisition and Schaffer collateral long-term potentiation by previous synaptic activity. *J. Neurosci.* 25, 7221–7231.
- Tarone, G., Hirsch, E., Brancaccio, M., De Acetis, M., Barberis, L., Balzac, F., et al., 2000. Integrin function and regulation in development. *Int. J. Dev. Biol.* 44, 725–731.
- Taylor, M.E., Drickamer, K., 2007. Paradigms for glycan-binding receptors in cell-adhesion. *Curr. Opin. Cell Biol.* 19, 572–577.
- Tian, L., Chen, L., McClafferty, H., Sailer, C.A., Ruth, P., Knaus, H.G., et al., 2006. A noncanonical SH3 domain binding motif links BK channels to the actin cytoskeleton via the SH3 adapter cortactin. *FASEB J.* 20, 2588–2590.
- Tolhurst, G., Carter, R.N., Amisten, S., Holdich, J.P., Erlinge, D., Mahaut-Smith, M.P., 2008. Expression profiling and electrophysiological studies suggest a major role for Orail in the store-operated  $Ca^{2+}$  influx pathway of platelets and megakaryocytes. *Platelets* 19, 308–313.
- Tsuda, M., Shigemoto-Mogami, Y., Koizumi, S., Mizokoshi, A., Kohsaka, S., Salter, M.W., et al., 2003. P2X4 receptors induced in spinal microglia gate tactile allodynia after nerve injury. *Nature* 424, 778–783.
- Tsuda, M., Toyomitsu, E., Komatsu, T., Masuda, T., Kunifusa, E., Nasu-Tada, K., et al., 2008. Fibronectin/integrin system is involved in P2X(4) receptor upregulation in the spinal cord and neuropathic pain after nerve injury. *Glia* 56, 579–585.
- Uemoto, T., Yamato, M., Shiratsuchi, Y., Terasawa, M., Yang, J., Nishida, K., et al., 2007. Expression of integrin beta3 is correlated to the properties of quiescent hemopoietic stem cells possessing the side population phenotype. *J. Immunol.* 177, 7733–7739.
- Vandenberg, C.A., 2008. Integrins step up the pace of cell migration through polyamines and potassium channels. *Proc. Natl. Acad. Sci. USA* 105, 7109–7110.
- Vasil'eva, I.O., Neguliaev, Iu.A., Marakhova, I.I., Semenova, S.B., 2008. TRPV5 and TRPV6 calcium channels in human T cells. *Tsitologiya* 50, 953–957.
- Venkatachalam, K., Montell, C., 2007. TRP channels. *Annu. Rev. Biochem.* 76, 387–417.
- Volk, A.P., Heise, C.K., Hougen, J.L., Artman, C.M., Volk, K.A., Wessels, D., et al., 2008. CLC-3 and IC1swell are required for normal neutrophil chemotaxis and shape change. *J. Biol. Chem.* 283, 34315–34326.
- von Andrian, U.H., Mackay, C.R., 2000. T-cell function and migration. Two sides of the same coin. *N. Engl. J. Med.* 343, 1020–1034.
- Voura, E.B., Billia, F., Iscove, N.N., Hawley, R.G., 1997. Expression mapping of adhesion receptor genes during differentiation of individual hematopoietic precursors. *Exp. Hematol.* 25, 1172–1179.
- Wagers, A.J., Weissman, I.L., 2006. Differential expression of alpha2 integrin separates long-term and short-term reconstituting Lin-/loThy1.1(lo)c-kit+ Sca-1+ hematopoietic stem cells. *Stem Cells* 24, 1087–1094.
- Walenda, T., Bork, S., Horn, P., Wein, F., Saffrich, R., Diehlmann, A., et al., 2009. Co-culture with mesenchymal stromal cells increases proliferation and maintenance of hematopoietic progenitor cells. *J. Cell. Mol. Med.* (May 11; Epub ahead of print).
- Wang, J., Xu, Y.Q., Liang, Y.Y., Gongora, R., Warnock, D.G., Ma, H.P., 2007. An intermediate-conductance  $Ca^{2+}$ -activated  $K^{+}$  channel mediates B lymphoma cell cycle progression induced by serum. *Pflügers Arch.* 454, 945–956.
- Watson, P.M., Humphries, M.J., Relton, J., Rothwell, N.J., Verkhratsky, A., Gibson, R. M., 2007. Integrin-binding RGD peptides induce rapid intracellular calcium increases and MAPK signaling in cortical neurons. *Mol. Cell. Neurosci.* 34, 147–154.

- Wegener, K.L., Campbell, I.D., 2008. Transmembrane and cytoplasmic domains in integrin activation and protein-protein interactions. *Mol. Membr. Biol.* 25, 376–387.
- Wei, J.-F., Wei, L., Zhou, X., Lu, Z.-Y., Francis, K., Hu, X.-Y., et al., 2008. Formation of Kv2.1-FAK complex as a mechanism of FAK activation, cell polarization and enhanced motility. *J. Cell. Physiol.* 217, 544–557.
- Wessler, I., Kirkpatrick, C.J., 2008. Acetylcholine beyond neurons: the non-neuronal cholinergic system in humans. *Br. J. Pharmacol.* 154, 1558–1571.
- Wildering, W.C., Hermann, P.M., Bulloch, A.G.M., 2002. Rapid neuromodulatory actions of integrin ligands. *J. Neurosci.* 22, 2419–2426.
- Williams, E., Doherty, P., Turner, G., Reid, R.A., Hamperly, J.J., Walsh, F.S., 1992. Calcium influx into neurons can solely account for cell contact-dependent neurite outgrowth stimulated by transfected L1. *J. Cell Biol.* 119, 883–892.
- Williams, M.R., Markey, J.C., Doczi, M.A., Morielli, A.D., 2007. An essential role for cortactin in the modulation of the potassium channel Kv1.2. *Proc. Natl. Acad. Sci. USA* 104, 17412–17417.
- Woo, S., Gomez, T.M., 2006. Rac1 and RhoA promote neurite outgrowth through formation and stabilization of growth cone point contacts. *J. Neurosci.* 26, 1418–1428.
- Wu, G., Lu, Z.-H., Nakamura, K., Spray, D.C., Ledeen, R.W., 1996. Trophic effect of cholera toxin B subunit in cultured cerebellar granule neurons: modulation of intracellular calcium by GM1 ganglioside. *J. Neurosci. Res.* 44, 243–254.
- Wu, G., Lu, Z.-H., Obukhov, A.G., Nowicky, M.C., Ledeen, R.W., 2007. Induction of calcium influx through TRPC5 channels by cross-linking of GM1 ganglioside associated with  $\alpha 5 \beta 1$  integrin initiates neurite outgrowth. *J. Neurosci.* 27, 7447–7458.
- Wulff, H., Miller, M.J., Hansel, W., Grissmer, S., Cahalan, M.D., Chandy, K.G., 2000. Design of a potent and selective inhibitor of the intermediate-conductance  $\text{Ca}^{2+}$ -activated  $\text{K}^{+}$  channel, IKCa1: a potential immunosuppressant. *Proc. Natl. Acad. Sci. USA* 97, 8151–8156.
- Wulff, H., Beeton, C., Chandy, K.G., 2003. Potassium channels as therapeutic targets for autoimmune disorders. *Curr. Opin. Drug Discov. Dev.* 6, 640–647.
- Wulff, H., Knaus, H.G., Pennington, M., Chandy, K.G., 2004.  $\text{K}^{+}$  channel expression during B cell differentiation: implications for immunomodulation and autoimmunity. *J. Immunol.* 173, 776–786.
- Xiong, J.P., Stehle, T., Diefenbach, B., Zhang, R., Dunker, R., Scott, D.L., et al., 2001. Crystal structure of the extracellular segment of integrin  $\alpha\text{V}\beta 3$ . *Science* 294, 339–345.
- Xiong, J.P., Stehle, T., Zhang, R., Joachimiak, A., Frech, M., Goodman, S.L., et al., 2002. Crystal structure of the extracellular segment of integrin  $\alpha\text{V}\beta 3$  in complex with an Arg-Gly-Asp ligand. *Science* 296, 151–155.
- Yeaman, T.J., 2004. A renaissance for SRC. *Nat. Rev. Cancer* 4, 470–480.
- Yool, A.J., Schwarz, T.L., 1991. Alteration of ionic selectivity of a  $\text{K}^{+}$  channel by mutation of the H5 region. *Nature* 349, 700–704.
- Young, B.A., Taooka, Y., Liu, S., Askins, K.J., Yokosaki, Y., Thomas, S.M., et al., 2001. The cytoplasmic domain of the integrin  $\alpha 9$  subunit requires the adaptor protein paxillin to inhibit cell spreading but promotes cell migration in a paxillin-independent manner. *Mol. Biol. Cell* 12, 3214–3225.
- Zhang, S.L., Yeromin, A.V., Zhang, X.H., Yu, Y., Safrina, O., Penna, A., et al., 2006. Genome-wide RNAi screen of  $\text{Ca}(2+)$  influx identifies genes that regulate  $\text{Ca}(2+)$  release-activated  $\text{Ca}(2+)$  channel activity. *Proc. Natl. Acad. Sci. USA* 103, 9357–9362.
- Zheng, J.Q., Poo, M.M., 2007. Calcium signalling in neuronal motility. *Annu. Rev. Cell Dev. Biol.* 23, 375–404.

# Index

## A

- Acetylcholine, 103
- Acid-sensing ion channels (ASIC), 107
- Adenosine triphosphate (ATP), 103
- Arabidopsis
  - division and proliferation, 94
  - dynammin-related proteins (DRPs), 86–88
  - PEROXIN11 (PEX11) proteins, 83–84

## C

- Chinese hamster ovary (CHO) cells
  - PEROXIN11 (PEX11) proteins, 84–85
  - PEX11 $\beta$ , Drp1 (DLP1), and FIS1 heterocomplex, 89
- Chlorella spp., symbiosis
  - infection-capability
    - algal attachment, 54–57
    - sugar residues and infectivity relationship, 57–59
    - WGA effects, 60–61
  - infection induced changes
    - mating reactivity rhythms, 69–70
    - photosynthesis rate, 68
    - survival rate, 69
  - infection route to paramecium
    - acidosomal and lysosomal fusion, 38–40
    - algal cell division initiation, 51–52
    - changes and timings of, 53–54
    - classification, digestive vacuole (DV), 37–38
    - cytological events, 40–51
    - process, 53
- Chronic lymphocytic leukemias (CLL), 154
- Circumvallate cells, taste buds
  - apical and basolateral membrane, 109
  - calcium transients, 109–110
  - K<sup>+</sup> solution, 110
  - stimuli recording methods, 109
  - Type II and III responses, 111
  - vs.* fungiform cells
    - bitter taste-sensitiveness, 115–116
    - GAD-GFP and TRPM5-GFP cells population, 114–115
    - sour taste stimuli, 114
- Claudin family
  - coregulation, 20–21
  - electrophysiological properties, 11
  - expression patterns

- eye, 14–16
- inner ear, 14
- kidney, 11–14
- skin, 16
- interactions, TJ strands
  - CD9, 20
  - dynamic behavior, 18
  - ephrin-B1, 20
  - homo and heteropolymerization, 16–17
  - MAGUK family and MUPP1, 19
  - OAP-1, 19
  - physiological importance, 17
- paracellular pathway, 2
- phenotypes
  - claudin 1, 21–22
  - claudin 3 and 4, 22
  - claudin 5, 22–23
  - claudin 6, 22
  - claudin 7, 23
  - claudin 9, 24–25
  - claudin 15, 23
  - claudin 16, 23–24
  - claudin 19, 24
  - claudin 11 and 14, 25–26
- structure
  - conserved amino acid sequence, 4–9
  - cytoplasmatic tail, 10–11
  - extracellular loop (ECL1 and ECL2), 9–10
- Crohn's disease, 18

## D

- Digestive vacuole (DV), paramecium
  - acidosomal and lysosomal fusion timing
    - differentiation, 40–41
    - pH changes, 38–40
  - classification, 37–38
  - perialgal vacuole (PV) membrane
    - differentiation, 47–50
- Dynammin-related proteins (DRPs)
  - functions, 85–86
  - peroxisome fission in Arabidopsis, 86–88

## E

- Endosymbiosis. *See also* Secondary symbiosis, paramecium and chlorella cells
  - acid phosphatase (AcPase) reaction, 36
  - algae-free *P. bursaria*, 34–35



Epithelial sodium ion channel (ENaC), 108  
Ethylnitrosourea (ENU) mutagenesis, 24

## F

FISSION1 (FIS1) proteins  
DRPs recruitment to organelles, 88  
role, peroxisomes and mitochondrial fission, 88–89  
Fungiform cells, taste buds  
action potentials, 112  
sensitive Type II cells, 113  
Type II and III cells, 112–113  
*vs.* circumvallate cells  
bitter taste-sensitiveness, 115–116  
GAD-GFP and TRPM5-GFP cells  
population, 114–115  
sour taste stimuli, 114

## G

Glutamate, 103  
G protein-coupled receptors (GPCR), 106  
Gustatory nerve fibers  
taste-coding channels formation  
cell groups, 118  
CT nerve fibers, 119–120  
nerve regeneration, 120–121  
transmitters  
action potentials, 125  
ATP, 122–123  
hemichannel blocker, 123–124  
serotonin (5-HT), 122  
taste stimuli, 123  
transgenic mice studies, 124–125

## H

High energy shock waves (HESW), 163

## I

Integrins  
cell migration  
nicotinic acetylcholine receptors, epithelia, 165–166  
potassium channels, 164–165  
process, 163  
hematopoietic stem cells and progenitors, 147–151  
leukocytes, 151  
lymphocytes  
immunological synapse, 152  
leukocyte-specific  $\beta_2$  integrins, 152  
T-cells, 153  
neoplastic hematopoietic cells, 153–154, 158–159  
nervous system  
 $\alpha$  and  $\beta$  expression, 166–167

mature neuronal circuits, 167–170  
microglia, 175–176  
neuronal circuits, 170–175  
oncology implications, 162–163  
platelets, 153  
receptors  
cytoplasmic tails, 138  
functional heterodimers, 138–139  
MIDAS domain, 139  
transmembrane proteins, 137–138  
regulation and downstream signaling  
 $K_v11.1$  activation, 162  
 $\beta_1/K_v11.1$  complex, 161  
signalling, outline of  
bone marrow stroma, 145–146  
EGF receptor (EGFR), 147  
ILK, 145  
pathways, 143–144  
protein tyrosine phosphorylation, 144  
receptor tyrosine kinases (RPTKs), 147  
SFKs and FAK, 144–145

## Ion channels

cell migration  
nicotinic acetylcholine receptors, epithelia, 165–166  
potassium channels, 164–165  
process, 163  
erythrocytes, 157  
hematopoietic stem cells and progenitor cells, 148–150, 154–155  
inward rectifying  $K^+$  (KIR) channels, 140  
leukocytes, 155  
lymphocytes, 155–157  
neoplastic hematopoietic cells, 157–160  
nervous system  
 $\alpha$  and  $\beta$  expression, 166–167  
mature neuronal circuits, 167–170  
microglia, 175–176  
neuronal circuits, 170–175  
neurotransmitters  
ionotropic glutamate receptors, 142–143  
neuronal nicotinic acetylcholine receptors (nAChR), 141–142  
purinergic receptors, ionotropic, 143  
oncology implications, 162–163  
platelets, 157  
regulation and downstream signaling  
 $K_v11.1$  activation, 162  
 $\beta_1/K_v11.1$  complex, 161  
transient receptor potential (TRP), 140–141  
voltage-gated cation channels (VGCs), 139–140

## J

Jasmonic acid (JA), 92

**L**

Leukocytes, 151, 155  
 Long-term potentiation (LTP), 142, 168  
 LTP. *See* Long-term potentiation  
 Lymphocytes, 152–153, 155–157

**M**

Metal ion-dependent adhesion site (MIDAS), 138  
 MIDAS. *See* Metal ion-dependent adhesion site  
 Mitochondrial fission factor (Mff), 90  
 Multi-PDZ domain protein 1 (MUPP1), 19–20

**N**

Neonatal ichthyosis and sclerosing cholangitis (NISCH) syndrome, 21–22  
 Neoplastic hematopoietic cells, 153–154, 157–160  
 Nervous system  
   integrin expression, 166–167  
   mature neuronal circuits  
     hippocampus, synaptic plasticity, 169–170  
     LTP, 168  
     neocortex, 170  
     neuron and ECM, 167  
     synaptic stability, 168–169  
   microglia, 175–176  
   neuronal circuits development  
     Ca<sup>2+</sup>-dependent signal, 171  
     downstream signals, 173  
     growth cone, 174  
     integrin function control, 174  
     ion channel function, 170–171  
     migration-related signals, neurons, 172  
     neurite extension, 171–173  
     neuroblastoma, 173  
     TRPC5, 173–174  
     *Xenopus* spinal neurons, 174–175  
 Neuronal nicotinic acetylcholine receptors (nAChR), 141–142  
 Neuropeptide Y, 103

**P**

*Paramecium bursaria*  
   algae-bearing cells, 34–35  
   different fates of chlorella species  
     algal attachment, 54–57  
     algal infectivity, 52–54  
     sugar residues and infectivity relationship, 57–59  
     WGA effects, 60–61  
   infection induced changes  
     mating reactivity rhythms, 69–70  
     photosynthesis rate, 68  
     survival rate, 69  
   infection route, algae

    acidosomal and lysosomal fusion, 38–40  
     algal cell division initiation, 51–52  
     cytological events, 40–51  
     digestive vacuole classification, 37–38  
     process, 53  
     lysosomal escape mechanisms of, 70–72  
     perialgal vacuole (PV) membrane functions  
     algal proteins, 62–64  
     protection from lysosomal fusion, 64–67  
 Perialgal vacuole (PV) membrane functions  
   algal proteins, 62–64  
   protection from lysosomal fusion, 64–67  
 PEROXIN11 (PEX11) proteins role  
   in Arabidopsis, 83–84  
   functional mechanism, 84–85  
   in nonplant species  
     isoforms, 83–84  
     mutant phenotypes, 82–83  
 Peroxisome  
   definition, division and proliferation, 81  
   dynamin-related proteins (DRPs)  
     functions, 85–86  
     peroxisome fission in Arabidopsis, 86–88  
   environmental factors regulation, 92  
 FISSION1 proteins  
   DRPs recruitment to organelles, 88  
   role, peroxisomes and mitochondrial fission, 88–89  
   heterocomplex, 89  
   nuclear regulation, 91–92  
 PEROXIN11 (PEX11) proteins role  
   in Arabidopsis, 83–84  
   functional mechanism, 84–85  
   in nonplant species, 81–83  
   phytochrome A-dependent pathway, 92–93  
 PMD1 protein, 90  
 Rpn11 protein, 89–90  
 Phytochrome A-dependent pathway, 92–93  
 Pleckstrin homology (PH) domain, 85  
 PMD1 protein, 90  
 Pulse-labeling and chasing method, 37–38

**R**

Rpn11 protein, 89–90

**S**

Secondary symbiosis, paramecium and chlorella cells  
   different fates of chlorella species  
     attachment, 54–57  
     infectivity, 52–54  
     sugar residues and infectivity relationship, 57–59  
     WGA effects, 60–61  
 endosymbiosis  
   acid phosphatase (AcPase) reaction, 36  
   algae-free *P. bursaria*, 34–35

Secondary symbiosis, paramecium and chlorella cells (*cont.*)  
 escape mechanisms, lysosomal enzymes  
   inactivation, 70–72  
 infection induced changes  
   mating reactivity rhythms, 69–70  
   photosynthesis rate, 68  
   survival rate, 69  
 infection route  
   acidosomal and lysosomal fusion, 38–40  
   algal cell division initiation, 51–52  
   changes and timings of, 53  
   classification, digestive vacuole (DV), 37–38  
   cytological events, 40–51  
   process, 53  
   perialgal vacuole (PV) membrane functions  
     algal proteins, 62–64  
     protection from lysosomal fusion, 64–67  
 Serotonin (5-HT), 103, 122  
 SFKs. *See* Src family kinases  
 Src family kinases (SFKs), 144–145

## T

Taste bud cells  
 cell type  
   classification, 104  
   morphological and molecular expression  
   properties, 105  
   Type I and Type II, 105–106  
   Type III, 105  
 coding information  
   cell–cell communication, 117–118  
   circumvallate cells, 109–111  
   fungiform cells, 112–113  
   similarity and differences of, 112–116  
 diversity, 103–104  
 molecular mechanisms, 102  
 receptors and downstream molecules  
   amiloride-insensitive (AI), 106–107

epithelial sodium ion channel (ENaC), 108  
 G protein–coupled receptors (GPCR), 106  
 morphological features, 107  
 PKD2L1, 107–108  
 PLC  $\beta$ 2, 106  
 T2Rs, 106  
 sensory information, 102  
 transmitters, 103  
 Tight junctions (TJs)  
   claudin family  
     conserved TJ proteins, 4–6  
     coregulation, 20–21  
     electrophysiological properties, 11  
     expression pattern, 11–16  
     phenotypes, 7–8, 21–26  
     structure, 4–11  
     TJ strands interactions, 16–20  
   integral proteins, 4  
   semipermeability, 3  
   strands, 2–3  
 Transient receptor potential (TRP) channels,  
 140–141

## V

Velocardiofacial syndrome (VCFS), 22–23  
 VGCs. *See* Voltage-gated cation channels  
 Voltage-gated cation channels (VGCs), 139–140

## W

Williams-Beuren syndrome (WBS), 22

## Y

Yeast cells, 39

## Z

Zonula occludens, 2–3